THE ROLE OF THE PROLINE RICH HOMEODOMAIN IN THE REGULATION OF PROLIFERATION, SURVIVAL AND MIGRATION OF BREAST CELLS

By

DANIEL STEPHEN ROBERTS

A thesis submitted to the University of Birmingham for the degree of Doctor of Philosophy.

Department of Immunity and Infection

College of Medicinal and Dental Sciences

The University of Birmingham

December 2013

Word count: 47,059

Abstract

This thesis demonstrates that the Proline Rich Homeodomain transcription factor (PRH/HHEX) plays an important role in regulating the proliferation and migratory behaviour of breast cells. In tumourigenic MCF-7 breast cells, shRNA knockdown of PRH results in a pro-invasive and pro-proliferative phenotype. Key genes regulated by PRH in MCF-7 cells include *TP53*, endoglin (*ENG*) and e-cadherin (*CDH1*), which regulate migration/invasion in breast cells. Significantly, exogenous PRH functions as an inhibitor of cell proliferation/survival and migration/invasion in all breast cell types examined. Furthermore, the effects of exogenous PRH on cell proliferation/survival are dependent on the DNA binding activity of PRH. This work provides an explanation for the finding that *PRH* expression is associated with increased overall survival in breast cancer patients. In contrast with this work, MCF-7 xenograft experiments reveal that expression of exogenous PRH in MCF-7 cells is oncogenic. Furthermore, shRNA knockdown experiments in MDA-MB-231 cells show that endogenous PRH increases proliferation of these cells. This thesis therefore demonstrates that the role of PRH can differ dramatically between breast cell types and between *ex vivo* and *in vivo* conditions.

Acknowledgements

Firstly I would like to thank my supervisor Dr. Padma-Sheela Jayaraman, for giving me the opportunity to be her Ph.D. student, as well as her continued advice and support during my time in the lab and writing this thesis. I would also like to thank Dr. Kevin Gaston for his useful advice and discussions. I would like to thank Dr. Rachael Kershaw for useful discussions, as well as help with immunofluorescence, migration and invasion assays, as well as qPCR. I would also like to thank Dr. Peter Noy for help with qPCR, cell culture and ChIP assays, as well as teaching me general laboratory techniques when I first started in the laboratory. I would also like the thank the other members of the Jayaraman laboratory which I have encountered during my Ph.D., including Laura V. Ballesteros, who assisted me with migration assays, and Dr. Anshuman Shukla, who assisted me with protein purification (and Angry Birds!). I would also like to thank Gaston lab members Dr. Anyaporn Sawasdichai and Yusra Siddiqui for their assistance. I would like to thank Professor Roy Bicknell, for allowing us to perform animal experiments under his Home Office licence, as well as allowing us to use his reagents when required. I would also like to thank members of the first and third floor labs, who have filled my lunches completing/cheating the Sun/Times/Guardian crosswords. I would like to thank the Medical Research Council and Breast Cancer Campaign, for funding my stipend and my research. I would like to give special thanks to my Dad, who has supported me from the day I was born, and encouraged me to aim high and to always try my hardest.

Table of contents

List of figures

List of tables

List of Abbreviations

Abbreviation	Description
ABL	Abelson murine leukaemia viral oncogene homolog 1
ALDH1	Alcohol dehydrogenase 1
ALDH2	Alcohol dehydrogenase 2
ALT	Alternative lengthening of telomeres
AML	Acute myeloid leukaemia
AP-1	Activator protein 1
APC	Allophycocyanin
APS	Ammonium persulphate
ATF	Activating transcription factor
BCR	Breakpoint cluster region
BRAF	Serine/threonine protein kinase B-Raf
BRCA1	Breast cancer type 1 susceptability protein
BRCA2	Breast cancer type 2 susceptability protein
BrdU	Bromodeoxyuridine
BSA	Bovine serum albumin
CD	Cluster of differentiation
CDH1	E-Cadherin
cDNA	Complementary DNA
ChIP	Chromatin Immunoprecipitation
CIC	Cancer initiating cell
CIP	Calf intestinal phosphatase
CK2	Protein kinase CK2 (also known as Caesin kinase 2)
co-SMAD	Common-mediator SMAD
CREB	cAMP response binding element protein
DAB	Diaminobenzidine
DMAT	Dimethylamino-4,5,6,7-tetrabromo-1H-benzimidazole
DMEM	Dulbecco's Modified Eagle Medium
DMSO	Dimethyl sulphoxide
DNA	Deoxyribonucleic acid
DTT	Dithiothreitol
ECM	Extracellular matrix
EDTA	Ethylenediaminetetraacetic acid
EGF	Epidermal growth factor
EGFR	Epidermal growth factor receptor
eIF-4E	Eukaryotic translation initiation factor 4E
EMT	Epithelial-to-mesenchymal transition
ENCODE	Encyclopedia of DNA elements
ENG	Endoglin
ER	Oestrogen receptor
ERCC1	DNA repair excision protein ERCC1
ESM1	Endothelial cell-specific molecule 1

Abbreviation	Description
ETS	E-twenty six
F12	Nutrient Mixture F-12 (Ham's)
FACS	Fluorescense activated cell sorting
FBS	Foetal bovine serum
FDA	Food and drug administration
FITC	Fluorescein isothiocyanate
FOXN1	Forkhead box protein N1
FRT	Flippase recombination target
FSC	Forward scatter
GAPDH	Glyceraldehyde 3-phosphate dehydrogenase
GATA3	GATA binding protein 3
GFP	Green fluorescense protein
GOBO	Gene Expression-Based Outcome for Breast Cancer Online
GPDH1	Glycerol-3-phosphate dehydrogenase 1
GRB7	Growth factor receptor bound protein 7
GSA	Gene Set Analysis
GSC	Goosecoid
GST	Glutathione S-transferase
GTF	General transcription factor
HAT	Histone acetyltransferase
HDAC	Histone deacetylase
HEK	Human embryonic kidney
HER2	Human epidermal growth factor receptor 2
HHEX	Haematopoietically-expressed homeobox protein
HIF-1α	Hypoxia-induceable factor 1-alpha
HIV	Human immunodeficiency virus
HMEC	Human mammary epithelial cell
HMT	Histone methyltransferase
HNF-1A	Hepatocyte nuclear factor 1 alpha
HNF3α	Hepatocyte nuclear factor 3 alpha
hnRNP	Heterogeneous nuclear ribonuclease
HRP	Horse radish peroxidase
HUVEC	Human umbilical vein endothelial cells
ID1	Inhibitor of differentiation 1 (also known as Inhibitor of DNA binding 1)
IPTG	Isopropyl β-D-1-thiogalactopyranoside
ITR	Inverted tandem repeat
JAK	Janus kinase
JDP	Jun dimerisation proteins
KDR	Kinase insert domain receptor
LB	Lysogeny broth
LBX1	Ladybird Homeobox 1
LMO2	LIM domain only 2
MAD	Mothers against decapentaplegic protein
MAPK	Mitogen activated protein kinase
MBD	Methyl-CpG-binding domain

Abbreviation	Description
MCF	Michigan Cancer Foundation
MCMV	Murine cytomegalovirus
MDM2	Mouse double minute homolog 2
MET	Mesenchymal-to-epithelial transition
MMP	Matrix metalloproteinase
MOI	Multiplicity of infection
MTT	3-(4,5-dimethylthiazol-2-yl)-2,5-diphenyltetrazolium bromide
NCOA1	Nuclear receptor coactivator 1
NF-Kb	Nuclear factor kappa-light-chain-enhancer of activated B cells
NR1	Neuropilin 1
NR2	Neuropilin 2
NTCP	Sodium-dependent bile acid co-transporter
NTP	Nucleoside triphosphate
NUP98	Nuclear pore complex protein 98kDa
PAG	Polyagarose gel
PAGE	Polyagarose gel electrophoresis
PBS	Phosphate buffered saline
PBS-T	PBS-tween
PCI	Phenol:Chloroform:Isoamylalcohol
PCR	Polymerase chain rection
PI	Propidium iodide
PIGF	Phosphatidylinisitol-glycan biosynthesis class F protein
PML	Promyelocytic leukemia protein
PR	Progesterone receptor
PRH	Proline-Rich Homeodomain
PRRX1	Paired mesoderm homeobox protein 1
PTEN	Phosphatase and tensin homologue
PVDF	Polyvinylidene fluoride
qPCR	Quantitative PCR
Rb	Retinoblastoma protein
RIPA	Radioimmunoprecipitation assay
RISC	RNA induced sliencing complex
RNA	Ribonucleic acid
RNAa	RNA activation
ROS	Reactive oxygen species
RPMI	Roswell Park Memorial Institute
RSC	Chromatin structure remodelling complex
R-SMAD	Receptor regulated SMAD
SATB1	Special AT-rich binding protein 1
SDS	Sodium dodecyl sulphate
SELEX	systematic evolution of ligands by exponential enrichment
SEMA-3A	Semaphorin-3A
shRNA	Small hairpin RNA
siRNA	Small interfeting RNA
SMA	Small body size protein

Abbreviation	Description
SMAD	(Portmanteau of of Drosophila proteins MAD and SMA)
SSC	Side scatter
STAT	Signal Transducer and Activator of Transcription
SWI/SNF	SWItch/Sucrose NonFermentable
T2D	Type II Diabetes
TBB	Tetrabromobenzotriazole
TBP	TATA box binding protein
TEMED	tetramethylethylelediamine
TGF-β	Transforming growth factor beta
TIAF1	TGF-β induced anti-apoptotic factor 1
TLE	Transducin-like enhancer
TNBC	Triple negative breast cancer
TNF	Tumour necrosis factor
TRAF4	TNF-receptor associated factor 4
TRITC	Tetramethylrhodamine isothiocyanate
UCSC	University of California, Santa Cruz
uPAR	Urokinase receptor
UV	Ultraviolet
VEGF	Vascular endothelial growth factor
VEGFR-1	Vascular endothelial growth factor receptor 1
VEGFR-2	Vascular endothelial growth factor receptor 2
VSP	VEGF signalling pathway
WPRE	Woodchuck Hepatitis Post-Transcriptional Regulatory Element
XBP1	X-box binding protein 1
Z-VAD-FMK	Z-Val-Ala-Asp-fluoromethylketone

INTRODUCTION

1. Introduction

1.1 Transcriptional regulation and cancer

1.1.1 Transcription and gene regulation

The human genome contains approximately 20,000-25,000 protein coding sequences (Baltimore, 2001, Collins et al., 2004). This was surprising, as it was initially thought that complex organisms such as humans would contain substantially more genes than relatively simple organisms; for example, the nematode worm (*Caenorhabditis elegans*) genome contains nearly 20,000 genes (Consortium, 1998). One way in which complex organisms can arise from a relatively limited gene set is by generating greater complexity in the control of transcription of these genes (Levine and Tjian, 2003).

Transcription is the process by which the DNA genetic code is copied into a single stranded RNA molecule. This is carried out by four DNA-dependent RNA polymerases in eukaryotic cells. When the RNA is used as a template to synthesise protein it is known as messenger RNA (mRNA) and this is transcribed by RNA polymerase II. The mRNA is used as a template for the production of protein in a process called translation (Geiduschek and Tocchini-Valentini, 1988, Roeder, 1996, Ringel et al., 2011).

The process of transcription starts with pre-initiation. This is where the promoter (the sequence upstream of the region coding for the protein molecule) is recognised by RNA polymerase II. The RNA polymerase II holo-enzyme pre-initiation complex (which is

composed of RNA polymerase II and many accessory general transcription factors (GTFs)), binds to the core promoter sequence around 30-100 base pairs upstream of the transcription start site (TSS) (reviewed in Fuda et al., 2009). The most characterised of these is a core sequence of 5'-TATAAA-3' 25-30 bases upstream of the transcription start site (known as the TATA box) (Lifton et al., 1978). This is bound by the GTF known as TFIID (Starr and Hawley, 1991). The DNA double strands are then unwound by another GTF, TFIIH, which has helicase activity (Kim et al., 2000). RNA polymerase II binds to the promoter and commences transcription, however this interaction is mediated by a number of co-activators and co-repressors associated with the holoenzyme complex, which respectively increase or decrease the rate of transcription and initiation (Roeder, 1996). The RNA polymerase then elongates the RNA, until the polymerase reaches the end of the gene, where the process is terminated. This occurs by the addition of adenosines on the 3' end of the mRNA, in a process called polyadenylation. This allows the recruitment of termination factor proteins, destabilising the DNA:RNA interaction (reviewed in Kuehner et al., 2011).

In addition to promoter sequences, other DNA sequence elements, such as enhancers, silencers and initiators, are bound by other sequence-specific transcription factors. These DNA sequence elements are typically located up to 50 kilobases upsteam or downstream of the gene. These help to determine the rate of transcription and initiation for the gene in question, and to ensure that the expression of the gene is appropriate for the cellular context (reviewed in Smallwood and Ren, 2013).

Transcription factors are often characterised by containing domains which enable sequence specific DNA binding. These domains include basic helix-loop-helix domains, leucine zippers,

zinc fingers and homeodomains (reviewed in Mitchell and Tjian, 1989). To prevent transcription factors from permanently binding to DNA and activating/repressing transcription, they are regulated by various mechanisms. This includes ligand binding (for example androgen receptor, which is activated by testosterone), phosphorylation (such as the STAT proteins), and proteasomal processing (such as NF-κB) (Weigel and Moore, 2007, Gilmore, 2006).

Transcription factors also alter the rate of transcription and initiation by recruiting chromatin modifying or binding proteins to the vicinity of the gene. This alteration in the chromatin environment is vital for transcription because nuclear DNA is not freely available to the RNA polymerase pre-initation complex. Rather, nuclear DNA is condensed and wrapped round a histone protein octamer, forming chromatin (Richmond and Finch, 1984). Each octamer:DNA complex is called a nucleosome and these occur approximately every 200 DNA base pairs (around 150 base pairs are wrapped around the histones, plus there is an approximate 50 base pair "linker") (Richmond and Finch, 1984). The histones are basic proteins, and their positive charge allows them to associate with the negatively charged DNA (reviewed in Szerlong and Hansen, 2010).

Examples of chromatin modifying or binding proteins that alter the chromatin environment are histone modifying enzymes, such as histone acetyltransferases (HATs), histone deacetylases (HDACs) and histone methyltransferases (HMTs) (reviewed in Bannister and Kouzarides, 2011). Some modifications of histones allow dissociation of the histone:DNA interactions, and therefore makes the DNA more accessible to transcription factors (such as acetylation of lysine 9 on histone 3) (Brownell and Allis, 1996). Histone modifications also

allow chromatin binding-proteins to interact with chromatin, via protein domains such as bromodomains (e.g. CREB binding protein) and chromodomains (e.g. the Polycomb group of proteins) (Filippakopoulos and Knapp, 2012, Sanchez and Zhou, 2009, Boyer et al., 2006). Chromatin structure can also be remodelled by protein complexes, such as the SWI/SNF and chromatin structure remodelling (RSC) complexes. These complexes alter the position of nucleosomes on the DNA, destabilising the DNA:histone interaction, and thus enable the transcriptional machinery to interact with the DNA (Flaus and Owen-Hughes, 2003, Tang et al., 2010). In addition there are proteins that modify DNA, and thereby alter chromatin structure. DNA methyltransferases methylate cytosine in CpG dinucleotides, which leads to binding of methyl-CpG-binding domain proteins (MBDs). This in turn leads to transcriptional silencing of the target gene (Brenner et al., 2004, Kulis and Esteller, 2010).

It has recently been discovered that small RNAs can also regulate transcription. It is well established that small and micro RNAs transcribed in the genome can lead to a decrease in gene expression via RNA interference. This is through the destruction of specific mRNA molecules by the RNA-induced silencing complex (RISC), which are targeted by complementary RNAs (reviewed in Hannon, 2002). However small RNAs targeting the promoter sequences has been shown to increase expression of certain genes, such as E-cadherin and VEGF (Vascular endothelial growth factor), in a phenomenon termed RNA activation (RNAa) (Li et al., 2006). This process is dependent on the Argonaute 2 protein, a protein which is involved in RNA interference, as well as heterogeneous nuclear ribonucleases (hnRNPs) A1, A2/B1 and C1/C2 (Jia et al., 2012). H3K9 trimethylation (a marker for gene silencing) is also lost at target sites (Li et al., 2006). However, the precise mechanism of how this occurs in not fully understood (reviewed in Portnoy et al., 2011). In

conclusion, although many factors influence the rate of transcription and initiation, transcription factors are key players in determining the expression level of target genes.

1.1.2 Transcription factors and cancer

Genes involved in transcriptional regulation are the second most common class of genes that are mutated in cancer, after genes encoding protein kinases (Futreal et al., 2004). One example of a transcription factor gene which is frequently mutated in cancer is *MYC*. *MYC* codes for Myc protein, which through dimerization with its partner Max can bind to Enhancer-box sequences (E-boxes), via their helix-loop-helix domains (Blackwood and Eisenman, 1991). *MYC* is commonly translocated in Burkitt's lymphoma to a transcriptionally active region, hence causing upregulation of Myc/Max target genes, which promote cell growth and proliferation (Li et al., 2003).

Another group of transcription factors often misregulated in cancer are the Hox proteins. Many of these proteins are important in development, specifying positional identity along the anterior-posterior axis (Grier et al., 2005). The *HOXA9* gene is frequently translocated in human AML patients, and fused to the *NUP98* gene. The *HOXA9-NUP98* fusion gene codes for a fusion protein with the homeodomain of Hoxa9 and the transcriptional activation activity of NUP98. (Cillo et al., 1999). This leads to the upregulation of genes associated with cell proliferation and survival, including cyclin d2 and *ID1* (Ghannam et al., 2004).

1.1.3 Cancer

Cancer is commonly defined as a group of diseases, whereby a group of cells divide uncontrollably and spread throughout the body. There have been over 200 different types of cancers recorded in humans (CRUK, 2013). Cancer is the cause of around 13% of all deaths worldwide, and is on the increase as global life expectancy increases (Jemal et al., 2011). Most deaths from cancer (90%) are due to the cancer metastasis; the colonisation of tissues which are far away from the primary tumour (Mehlen and Puisieux, 2006).

For normal cells to become cancerous, they must acquire certain properties, or "hallmarks" of cancer (Hanahan and Weinberg, 2000). Some of these hallmarks are to do with cell proliferation, such as sustaining proliferative signalling, resisting cell death and evading growth suppressors. Most, if not all, tumours inactivate "tumour-suppressor genes", such as those encoding the p53 and Rb proteins, which act to supress cell proliferation and promote apoptosis (Weinberg, 1991). Both p53 and Rb influence transcription and the cell cycle. P53 is an oligiomeric DNA binding transcription factor, whereas Rb is a co-repressor of transcription. Tumours also up-regulate "proto-oncogenes", which are genes which code for proteins that increase cell growth and proliferation, or evade apoptosis, such as *MYC* (He et al., 1998). Tumour cells can also become insensitive to extracellular growth signals, by either expressing permanently active forms of proteins in downstream signalling pathways (such as BRAF in melanomas), or by upregulating ligand expression themselves, and signalling in a paracrine and/or autocrine manner (such as VEGF expression) (Davies et al., 2002, Fiedler et al., 1997).

Another hallmark of a tumour cell is that it is immortal, and can undergo an unlimited number of cell divisions. This is partly because cancer cells lengthen their repetitive sequences present at the telomeres that are required for cell division, either by upregulating the enzyme telomerase, or by the ALT (alternative lengthening of telomeres) mechanism (Henson et al., 2002, Kim et al., 1994). In normal cells, various DNA repair pathways are used to preserve the integrity of the genome, and to keep the mutation rate very low. However, in tumour cells, many of these DNA repair pathways are perturbed. For example, mutation of the genes encoding DNA repair proteins BRCA1 and BRCA2 is often seen in hereditary breast cancer, and mutation of the *ERCC1* gene is often seen in non-small cell carcinoma (Olaussen et al., 2006, Farmer et al., 2005).

Once a cell becomes immortal, the tumour will grow to less than $1mm^3$ in size unless additional nutrients and oxygen are supplied and waste products and carbon dioxide are removed (Folkman, 1990). Therefore, for this to occur, tumours must create their own blood vessels (angiogenesis) (Hanahan and Folkman, 1996). Tumours typically upregulate pro-angiogenic factors, such as increased vascular endothelial growth factor (VEGF), for this to occur (Ferrara et al., 2004). This process is further referred to later in this chapter.

For tumours to become cancers, they must break away from their site of origin and move to a secondary organ. For this to happen cells must detach from the primary tumour, by losing their cell-to-cell contacts and cell-to-ECM (extracellular matrix) contacts, in a process called the epithelial-to-mesenchymal transition (EMT). The tumour cells then enter the circulatory or lymphatic systems, in a process known as intravasation, and they are transported to secondary sites. The cells then undergo extravasation - that is escape from the vessel lumen

- and then it is thought they undergo a conversion from a migratory mesenchymal morphology to a more epithelial morphology (mesenchymal-to-epithelial transition (MET)), although this has not yet been proven (Kalluri and Weinberg, 2009). This then allows the tumour to form at the secondary site (Fidler, 2003). The English surgeon Stephen Paget discovered in 1889 that cancers do not metastasise to random places in the body, suggesting the metastatic tumour cells have a specific affinity for certain organs (Paget, 1889). For example, hepatocellular carcinomas tend to metastasise to the lungs, abdominal lymph nodes and the bone (Katyal et al., 2000). This led to Paget putting forward the "seed and soil" theory, that the environment in which the tumour is in also has an effect on tumour colonisation and growth, as well as the aberrations present in the tumour cell itself (Paget, 1889). Some progress has been made into what genes allow tumours to metastasise to certain sites, for example, ST6GALNAC5 expression enhances metastasis to the brain (Bos et al., 2009). However, whilst there has been progress over the last ten years, the mechanisms which determine why cancers metastasise to certain sites in the body still requires further investigation (Chaffer and Weinberg, 2011).

It has long been understood that the immune system plays a role in preventing tumour progression, in that the immune system can target and destroy transformed cells, and hence prevent tumour growth (reviewed by Hanahan and Weinberg, 2000). However, the immune system can also have pro-tumourgenic effects. For example, mice which are deficient in tumour necrosis factor (TNF), or NF-κB, both proteins associated with inflammation, showed decreased tumourgenesis (Moore et al., 1999, Maeda et al., 2005).

1.1.4 Epithelial-mesenchymal transition

The epithelial-mesenchymal transition (EMT) is thought to play a role in cancer progression, as it promotes tumour cell invasiveness through the basement membrane and into the bloodstream, thus allowing the cancer to metastasise (Chaffer and Weinberg, 2011). EMT is a process that also occurs during development, and is critical for the generation of tissues and organs. It involves the loss of tight, gap and adherens junctions, cytoskeletal reorganisation, loss of apical polarity and the acquisition of spindle shaped cell morphology (figure 1.1) (Thiery and Sleeman, 2006). EMT during development is involved in several processes; including gastrulation (formation of the mesoderm from the embryonic epithelium) and neural crest delamination, where the neural crest cells migrate throughout the embryo and differentiate in various tissues and organs (Theveneau and Mayor, 2012, Thiery and Sleeman, 2006). EMT is characterised by the loss of epithelial marker proteins, such as E-Cadherin, and increased expression of mesenchymal markers such as N-Cadherin, Vimentin, and the transcription factors Slug, Twist and Snail (Kalluri and Weinberg, 2009) (see figure 1.1).

EMT can be induced by several mechanisms. Hypoxia was found to induce EMT in many breast cancer cell lines, via the uPAR and notch signalling pathways, and this leads to a more invasive and migratory phenotype (Chen et al., 2009b, Lester et al., 2007). The EMT process in cancer cells can itself influence the external environment, further contributing to cancer progression. For example, Twist-induced EMT in luminal MCF-7 breast tumour cell line xenograft experiments showed increased angiogenesis, which was due to VEGF secretion (Mironchik et al., 2005).

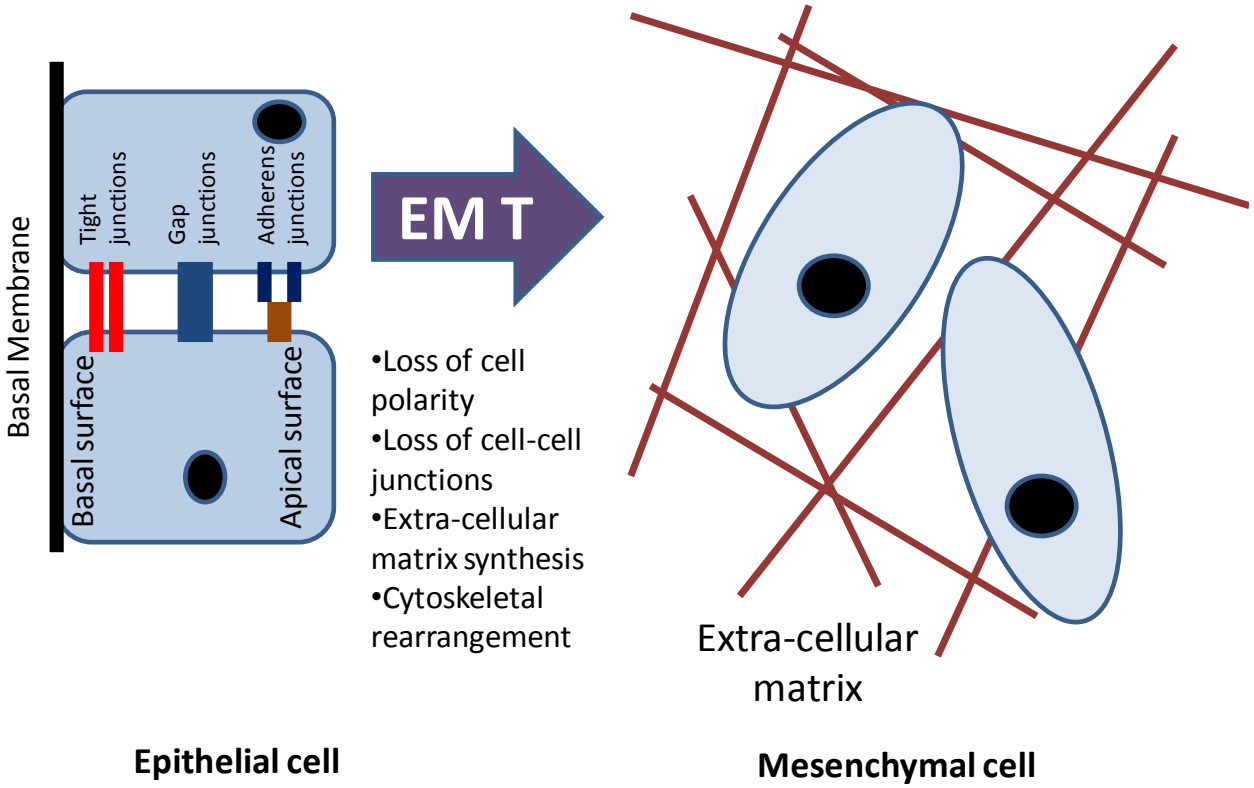

Figure 1.1: Epithelial-to-mesenchymal transition.

Figure 1.2: Diagram of the human breast. Taken from Cancer Research UK website.

1.1.5 Breast cancer

Breast cancer is the most common cancer in the world, with 1.4 million people being diagnosed globally in 2008 (GLOBOCAN). Breast cancer primarily affects women; although men can get breast cancer (49,564 women were diagnosed with breast cancer in the UK in 2010, compared with 397 men (Cancer Research UK)). The breasts are apocrine glands, which produce milk to feed an infant child. The breast consists of many alveoli, which contain milk secreting lactocytes. These alveoli form clusters together, making up a lobule (Hassiotou and Geddes, 2013). During lactation, lobules secrete milk into the milk ducts, which are connected to the nipple (Ramsay et al., 2005) (see figure 1.2). Breast cancers typically show similar histochemistry to the milk ducts (ductal carcinoma) or the breast lobules (lobular carcinoma).

1.1.6 Types of breast cancer

Breast cancer can be sub-classified into many different sub-types, such as lobular and ductal as described above. Breast cancer is also histopathically distinguished by grade, grade 1 being the most differentiated cancers (with the best prognosis), whilst grade 3 cancers are poorly differentiated (and have the worst prognosis) (Richardson, 1957). Breast cancers are also distinguished by stage, with stage IA showing no evidence of tumour metastasis towards the lymph nodes, whilst stage IV cancer shows metastasis distant from the original tumour (Woodward et al., 2003).

Breast cancer can also be distinguished dependent on which receptors are present in the cell. The three most important receptors are Oestrogen Receptor (ER), Progesterone Receptor (PR) and Human Epidermal Growth Factor Receptor 2 (HER2). The presence or absence of these receptors has a substantive effect on prognosis and on the treatment of the cancer.

ERs are ligand-activated transcription factors. ER in its transcriptionally inactive state is present in the cytoplasm of the cell. When a suitable ligand (such as 17β-oestradiol) binds to ER, this causes ER to dimerise and translocate to the nucleus, causing it to be transcriptionally active (Htun et al., 1999). ER then binds to DNA with other transcriptional activators, such as nuclear receptor coactivator 1 (NCOA1) which then turn off transcription of target genes (Hall and McDonnell, 2005). ER is upregulated in around 70% of breast tumours (Shakur Mohibi, 2011). ER activity can be targeted using ER antagonists, such as tamoxifen and aromatase inhibitors. Aromatase is an enzyme which converts testosterone to oestradiol, and thus inhibition of aromatase leads to decreased oestrogen and decreased activation of ERs (reviewed in Wood et al., 2003).

PR is also a ligand-activated transcription factor, which is regulated in a similar way to ER. Binding of the ligand progestin causes dimerization of PR, as well as translocation of PR from the nucleus to the cytoplasm (Mockus and Horwitz, 1983). PR regulates transcription of genes involved in regulation of cell growth and migration, including *VEGFA* (Yin et al., 2012, Tamm et al., 2009). PR is upregulated in around 60-70% of breast carcinomas (Kammori et al., 2005). Breast tumours which are positive for both ER and PR are much more likely to

respond to anti-hormornal therapies, such as tamoxifen, than ER+/PR- breast tumours (Osborne et al., 1980).

HER2 is a plasma-membrane bound tyrosine kinase, and is a member of the epidermal growth factor receptor (EGFR) family. Ligand binding to HER2 leads to homodimerisation or heterodimerisation with other receptors of the EGFR family. This then results in the activation of genes associated with cell survival and proliferation, via signaling pathways such as the mitogen-activated protein kinase (MAPK) pathway, and the JAK/STAT pathway (Roy and Perez, 2009, Olayioye, 2001). Amplification of *HER2* has been detected in 25-30% of breast cancers, and patients with *HER2* amplifications have more aggressive cancers (Slamon et al., 1989). HER2 positive breast cancers are currently treated with the monoclonal antibody trastuzumab, which prevents dimerization of the HER2 receptor, as well as targets HER2-positive cells for destruction by the immune system (Cho et al., 2003, Clynes et al., 2000).

Breast cancers which are negative for ER, PR and *HER2* amplification are commonly referred to as “triple-negative breast cancers” (TNBCs), and will not respond to hormone or HER2 specific treatments. TNBCs tend to be diagnosed in women who are younger compared to other breast cancers, and are more likely to recur before 5 years (Bauer et al., 2007, Dent et al., 2007).

Breast cancers can also be classified into 5 clusters based on their gene expression; luminal A, luminal B, basal, *HER2* amplified and normal-like breast cancers (Sørlie et al., 2001). Luminal A breast cancers show the highest expression of luminal-specific genes, such as

Breast Cancer type	Luminal	Basal	HER2 amplified	"Normal-like"
Genes which are typically highly expressed	*ESR1* *GATA3* *XBP1* prolactin receptor *HNF3α*	laminin gamma 2 keratin 5 keratin 7 integrin beta 4 caveolin 2 *MMP-14*	*HER2* *GRB7* *TRAF4* flotillin 2 *TIAF1*	*CD36* *GPDH1* *ALDH2* integrin alpha 7

Table 1.1: Genes associated with breast cancer subtypes. Genes typically upregulated in various breast cancer subtypes (Data from Sørlie et al., 2001, Perou et al., 2000).

ESR1 (which codes for ERα protein), GATA binding protein 3 (*GATA3*) and X-box binding protein 1 (*XBP1*) (Sørlie et al., 2001). Luminal B subtypes express these luminal enriched-genes, but at a much lower level (Sørlie et al., 2001). The luminal breast cancers broadly correlate with ER+ breast cancers, as *ESR1* is a luminal-specific gene. The basal breast cancer subtype is characterised by high transcript levels of laminin γ2, keratins 5 and 17 and integrin-β4, and low mRNA expression of *ESR1* and genes associated with it (Perou et al., 2000). Basal-breast cancer is sometimes used as an analogous term for TNBC, however these terms are not synonyms, not all basal breast cancers are TNBC or *vice versa* (Seal and Chia, 2010). *HER2* amplified breast cancers are characterised by amplified expression of genes in the 17q22.24 region, including *HER2*, growth factor receptor bound protein 7 (*GRB7*), as well as TNF-receptor associated factor 4 (*TRAF4*) (Sørlie et al., 2001). HER2 tumours are typically characterised by low expression of ER and genes associated with ER expression, much like basal breast tumours (Perou et al., 2000). "Normal-like" breast cancers typically have low expression of genes associated with luminal epithelial cells, and

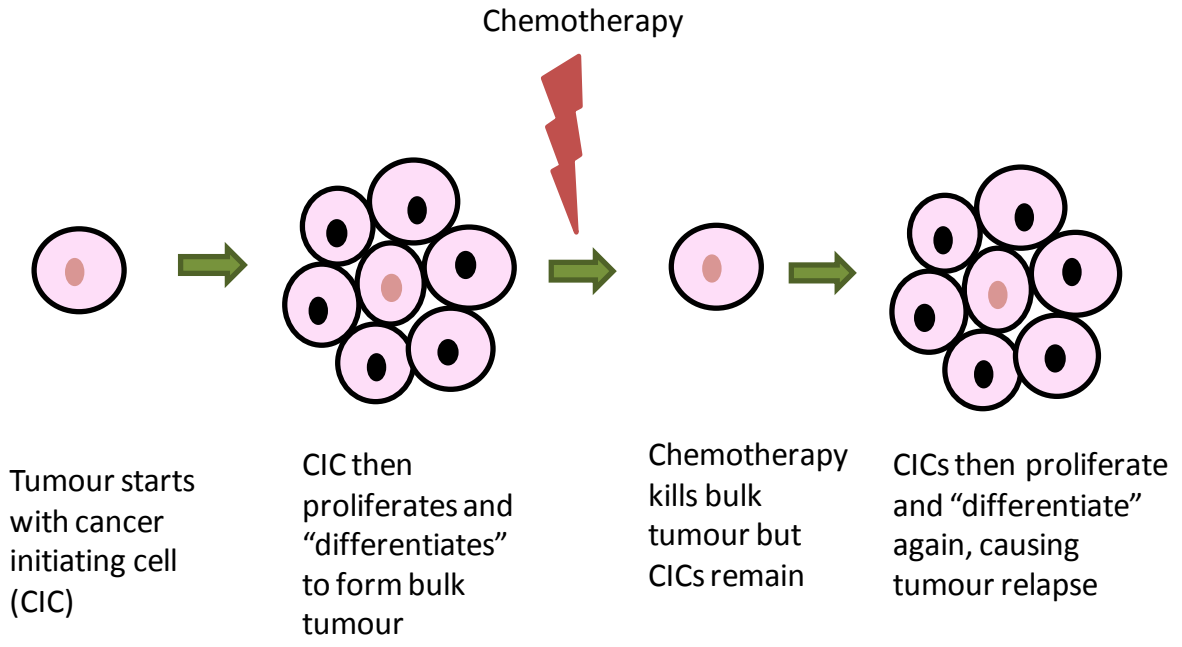

Figure 1.3: Cancer initiating cell model

high expression of genes characteristic of adipose and basal epithelial cells (such as *CD36* and glycerol-3-phosphate dehydrogenase 1 (*GPDH1*)) (Perou et al., 2000, Sørlie et al., 2001) (see table 1.1).

1.1.7 Breast cancer initiating cells

One model for the development of cancer is the "Cancer Initiating Cell (CIC) model" (see figure 1.3) (Al-Hajj et al., 2003b). CICs are a small sub-population of the total tumour, but are highly tumourgenic compared to the rest of the tumour cell population. Breast CICs are characterised by high CD44 expression, low CD24 expression, and high expression of Alcohol dehydrogenase 1 (ALDH1) (Ricardo et al., 2011). CICs are 50 times more tumourgenic than unsorted cells (Al-Hajj et al., 2003a). Similar to normal stem-cells, CICs have been shown to undergo self-renewal, as they can form 3D mammosphere structures from single cell

suspensions. CICs also show limited “differentiation”, as CICs will form tumours with phenotypically diverse populations (Ponti et al., 2005, Al-Hajj et al., 2003a).

Markers for breast CICs, such as ALDH1, as well as the gene signature for $CD44^{high}/CD24^{low}$ cells have been shown to be predictors for poor clinical outcome (Ginestier et al., 2007, Liu et al., 2007). Breast CICs are thought to play a major role in the recurrence of tumours, as typical chemotherapy treatments enriches for CICs, which could therefore lead to the regrowth of a more aggressive tumour (Tanei et al., 2009, Creighton et al., 2009, Velasco-Velázquez et al., 2012).

There is a relationship between EMT and CICs. Transformed breast epithelial cells which have undergone EMT, through expression of transcription factors Snail or Twist, produce a greater number of mammospheres and form a greater number of colonies in soft agar (Mani et al., 2008). This implies that induction of EMT leads to an increased number of CICs. Conversely, $CD44^{high}/CD24^{low}$ cells enriched from human mammary epithelia express increased transcript levels of mesenchymal markers, such as vimentin, n-cadherin and twist, and a decreased amount of e-cadherin mRNA, compared to $CD44^{low}/CD24^{high}$ cells (Mani et al., 2008, Creighton et al., 2010). This relationship could provide one explanation as to why markers associated with EMT are correlated with chemotherapy resistance (Farmer et al., 2009). Indeed, residual breast cancer cells surviving both chemotherapy and endocrine therapy show increased markers for both CICs and EMT (Creighton et al., 2009).

1.2 PRH protein

1.2.1 Overview of PRH

PRH (Proline-Rich Homeodomain) protein, also known as HHex (haematopoietically expressed homeobox) is a transcription factor which binds to DNA via a 60 amino acid conserved protein sequence known as the homeodomain. PRH is unusual as it is a homeodomain protein which can form homo-oligomers *in vivo* and *in vitro* (Soufi, et al., 2006). Like many homeodomain-containing proteins, PRH is involved in development processes, such anterioposterior axis formation, the development of multiple organs, and the development of vascular and blood systems in the early embryo (reviewed in Soufi and Jayaraman, 2008). PRH is also known to be expressed in the thyroid and liver tissues, and the haemopoietic compartment in adults (reviewed in Kershaw et al., 2013a). There is also increasing evidence that expression of PRH may play a role in type 2 diabetes. Single nucleotide polymorphisms (SNPs) rs1111875 and rs7923837, which are located in a region 3' to the *PRH* gene, have been shown to be significantly associated with type II diabetes (Sladek et al., 2007). PRH has also been shown to be involved in the regulation of lactating breast tissue, and there is some evidence that PRH may be disregulated in breast cancers (Puppin et al., 2006). Similar studies have also implicated disregulation of PRH as an important transcription factor in thyroid cancer and in hepatocarcinomas (D'Elia et al., 2002, Su et al., 2012).

1.2.2 PRH Structure

Human PRH is 270 amino acids long and has a calculated molecular mass of 30kDa. The homeodomain is highly conserved between species, with human and chicken homeodomains sharing 97% homology, and the mouse and human homeodomains only differing by 1 amino acid (Crompton et al., 1992). PRH contains three domains, an N-terminal domain which is 20% proline (amino acids 1-136), the homeodomain (amino acids 137-196) and an acidic C-terminal domain (amino acids 197-270) (see figure 1.4) (reviewed in Kershaw et al., 2013a).

1.2.3 The N-terminal domain

The isolated N-terminal domain of PRH forms dimers *in vitro* (Soufi, et al., 2006). It has also been shown that a PRH truncation mutant that lacks the first 46 amino acids is transcriptionally inactive, whilst this same mutant is transcriptionally active if it is fused to a dimeric GAL4 binding domain, suggesting that the N-terminal domain is critical for PRH transcriptional activity (Brickman, et al., 2000). The N-terminal dimer is partially resistant to unfolding by SDS, and has neither an alpha-helix or beta-sheet structure, but exhibits an extended and mobile structure reminiscent of Elastin (Soufi, et al 2006). The N-terminal domain also allows PRH to bind to other proteins. PRH binds to the co-repressor TLE, and amino acids 32-38 within PRH are involved in this interaction (Swingler et al., 2004). Mutation of phenylalanine at amino acid 32 abolishes the interaction with TLE, and repression by PRH at some PRH-dependent target genes (Noy, et al., 2010). The PRH N-terminus can also bind to eIF-4E and inhibit the mRNA transport activity of eIF-4E on specific

growth related mRNAs (like cyclin d1). PRH also antagonises oncogenic transformation of immortalised cell lines by eIF-4E (Topisirovic, et al., 2003). PRH has also been shown to interact with the promyelocytic leukaemia protein (PML), a transcription factor which acts as a tumour suppressor, in K562 leukaemic cells (Topcu et al., 1999).

1.2.4 The homeodomain

Homeodomains consist of a short N-terminal arm and 3 alpha-helices. The N-terminal arm and third helix are involved in recognising DNA sequences, with the N-terminal arm binding to the minor groove, and the third alpha helix making specific contacts with the DNA bases in the major groove (Gehring et al., 1994). Glutamine at position 50 and asparagine at position 51 of the PRH homeodomain have been shown to be important in the formation of PRH-DNA interactions in computational models (Jalili and Karami, 2012). The consensus DNA sequence for protein binding as determined by SELEX (systematic evolution of ligands by exponential enrichment) and DNaseI footprinting with purified PRH homeodomain and C-terminal domain is 5'-C/TA/TATAAA/G-3' (Crompton et al., 1992). However, the isolated PRH homeodomain alone recognises relatively short DNA consensus sequences, including 5'-TAAT-3', 5'-CAAG-3' or 5'-ATTAA-3' in electrophoretic mobility shift assays (Pellizzari, et al., 2000). The homeodomain is also able to repress gene transcription without binding to DNA, via interaction with the transcription factor Activator protein-1 (AP-1). AP-1 consists of dimers of either c-Fos, c-Jun, Activating transcription factor (ATF) and Jun dimerization protein (JDP) proteins. AP-1 dependent activation of genes is repressed by helix 3 of the PRH homeodomain binding to the N-terminus of c-Jun, resulting in inhibition of Fos/Jun heterodimerization (Schaefer, et al., 2001).

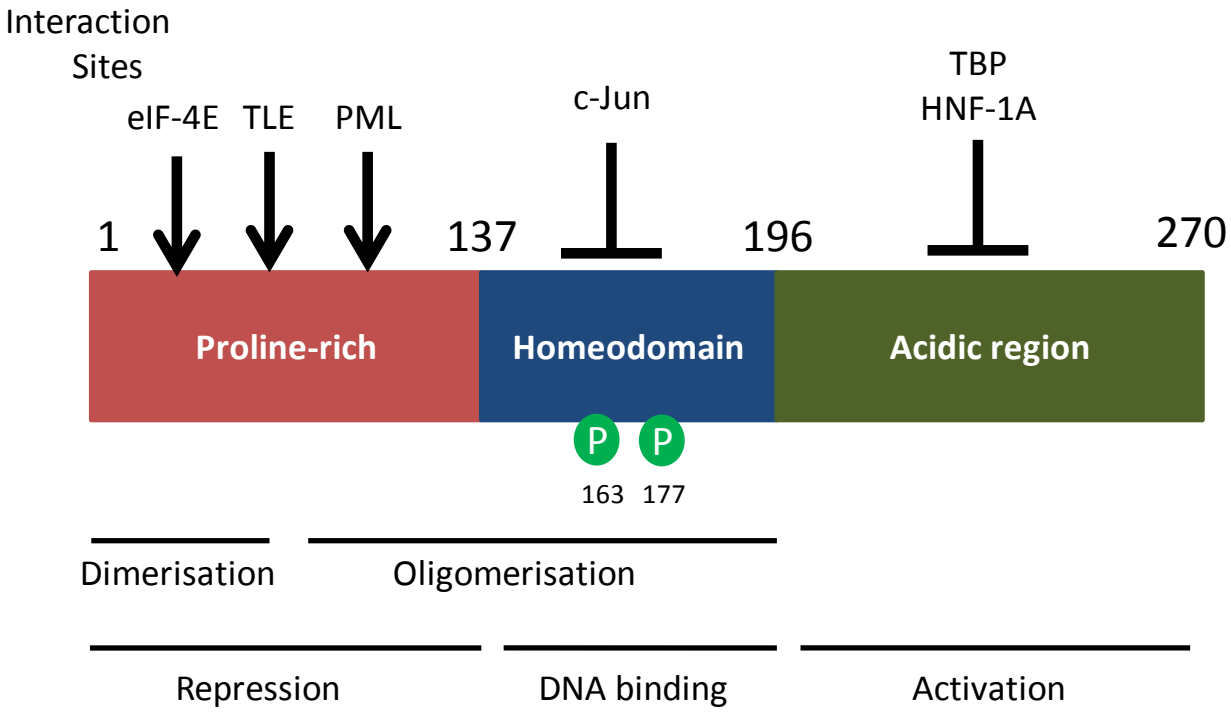

Figure 1.4: A diagram of PRH protein. This diagram shows the different domains and interaction sites of PRH with DNA and other interacting proteins (adapted from R. M. Kershaw, 2013).

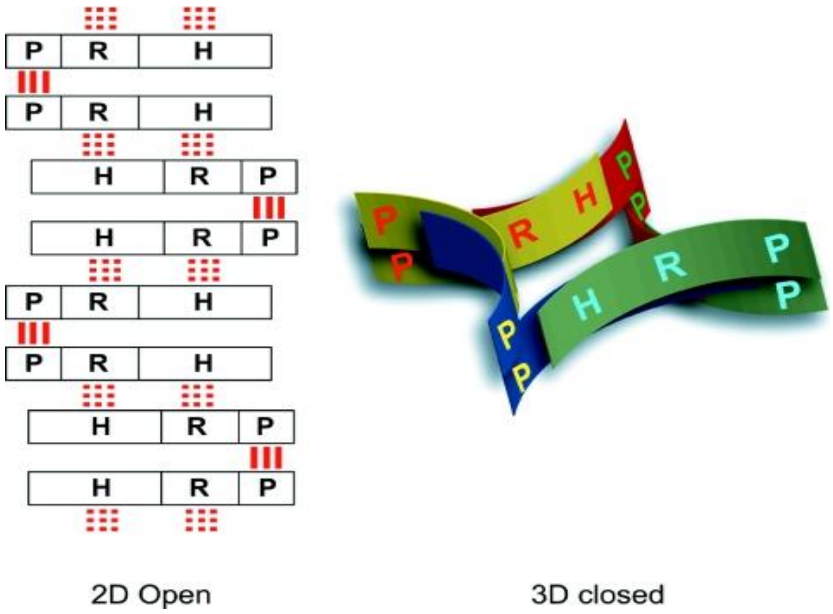

Figure 1.5: A model proposing how PRH forms octamers *in vivo*. 'P' refers to the proline-rich region, 'R' refers to the repression region, and 'H' refers to the homeodomain and C-terminal region of PRH protein (from Soufi and Jayaraman, 2008).

1.2.5 The C-terminal domain

The C-terminal domain of PRH is acidic, and acidic domains are characteristic of transcriptional activators (Triezenberg, 1995). PRH is known to activate the transcription of the bile-acid transporter *NTCP* (sodium-dependent bile acid co-transporter). It is thought that PRH activates transcription by interacting with TBP (TATA box binding protein) (Kasamatsu, et al., 2004). However, TBP-PRH interactions have also been proposed to repress transcription (Guiral et al., 2001). It has been shown that PRH binds to Hepatocyte nuclear factor-1α (HNF-1α) and stimulates the transcriptional activator activity of HNF-1α (Tanaka et al., 2005). The PRH homeodomain and C-terminal domain are required for this activity (Tanaka, et al., 2005). PRH protein without the C-terminal activation domain acts as a dominant negative mutant of PRH, with regards to its transcriptional activation activity (Kasamatsu et al., 2004).

1.2.6 Oligomerisation of PRH

In gel filtration assays, PRH elutes at a molecular weight of about 250kDa, as well as much larger molecular weight species (Soufi et al., 2006). Analytical untracentrifugation sedimentation experiments show that PRH also forms complexes of about 280 kDa, as well as larger molecular weight species (Soufi, et al., 2006). *In vivo* cross-linking experiments have shown that PRH is oligomeric, and *in vitro* cross-linking experiments have shown PRH forms homo-oligomers. Pull-down and yeast two-hybrid assays show that the N-terminal 50 amino acids of PRH are needed for dimerisation (Soufi, et al., 2006). PRH octamers have been shown to form oblate spheroids *in vitro*, with two of these octamers coming together

to form spherical hexadecameric PRH species (Soufi et al., 2010). It has been shown using dynamic light scattering experiments that the dominant PRH species *in vitro* is either a PRH octamer or hexadecamer (Shukla et al., 2012).

A model has been proposed to describe how PRH octamers form. The proline-rich dimerisation regions (hereafter known as "P" regions) self-associate with each other and form dimers. This leaves two other regions, the "R" repression region in the N-terminal domain, and the "H" region, which contains the homeodomain and the C-terminus. The "R" regions then associate with the "H" regions on another dimer, forming tetramers. This leaves two "R" regions and two "H" regions free per tetramer to interact with another PRH tetramer, resulting in a PRH octamer where there are no free regions (figure 1.5) (Soufi et al., 2006).

As stated previously, the homeodomain of PRH recognises short DNA sequences, which would make it difficult for the PRH protein to recognise its target promoters, as these sequences will occur quite frequently in the genome (once every 256 base pairs for a 4 base sequence). It has been shown that in the human goosecoid promoter, individual TAAT motifs are protected from DNaseI digestion by the PRH homeodomain, but full-length PRH protects long stretches of DNA containing multiple PRH binding motifs from digestion (Williams, et al., 2008). Since PRH exists as a homo-oligomer, and PRH binds to multiple TAAT motifs in the human goosecoid promoter, it has been suggested that the oligomeric nature of PRH allows for greater binding specificity and affinity (Soufi et al., 2010, Williams et al., 2008). Additional experiments which assess the distortion of DNA have also been carried out, and suggest that DNA is wrapped around the PRH oligomer (Williams, et al.,

2008). PRH can cause compaction of DNA *in vitro*, and this compaction is increased when multiple PRH binding sites are present (Soufi et al., 2010). A model has been proposed, whereby PRH compacts the DNA and forms nucleosome-like particles that repress transcription (Williams, et al., 2008).

1.2.7 PRH as a phosphoprotein

Human PRH binds to the β subunit of Protein Kinase CK2 (CK2), and PRH gets phosphorylated *in vivo* by CK2 on serines 163 and 177 (Soufi et al., 2009). Phosphorylation of PRH inhibits its ability to bind to DNA, thus blocking the ability of PRH to act as a transcriptional repressor (Soufi et al., 2009). A PRH phosphorylation mimic, that is a mutant protein having glutamic acid residues in place of serines at positions 163 and 177, is less tightly bound in the nucleus suggesting that phosphorylation decreases nuclear retention of PRH. Phosphorylation also leads to cleavage of PRH by the proteasome, resulting in the formation of a PRHΔC product (Noy et al., 2012c).

PRHΔC is formed when the entire C-terminal domain (amino acids 211-270) is removed, leaving the repression domain and central PRH homeodomain. PRHΔC has been shown to act as a transdominant negative regulator of PRH. Over-expression of exogenous PRHΔC leads to de-repression of *VEGFR1* transcription in K562 leukaemic cells (Noy et al., 2012c). PRHΔC is thought to exert this effect by sequestering the co-repressor TLE from full length PRH protein. Since less TLE can bind to full-length PRH, transcriptional repression by PRH at some PRH-dependent promoters is decreased (see figure 1.6). Alternatively, PRH/PRHΔC oligomers may form, blocking the function of full length PRH.

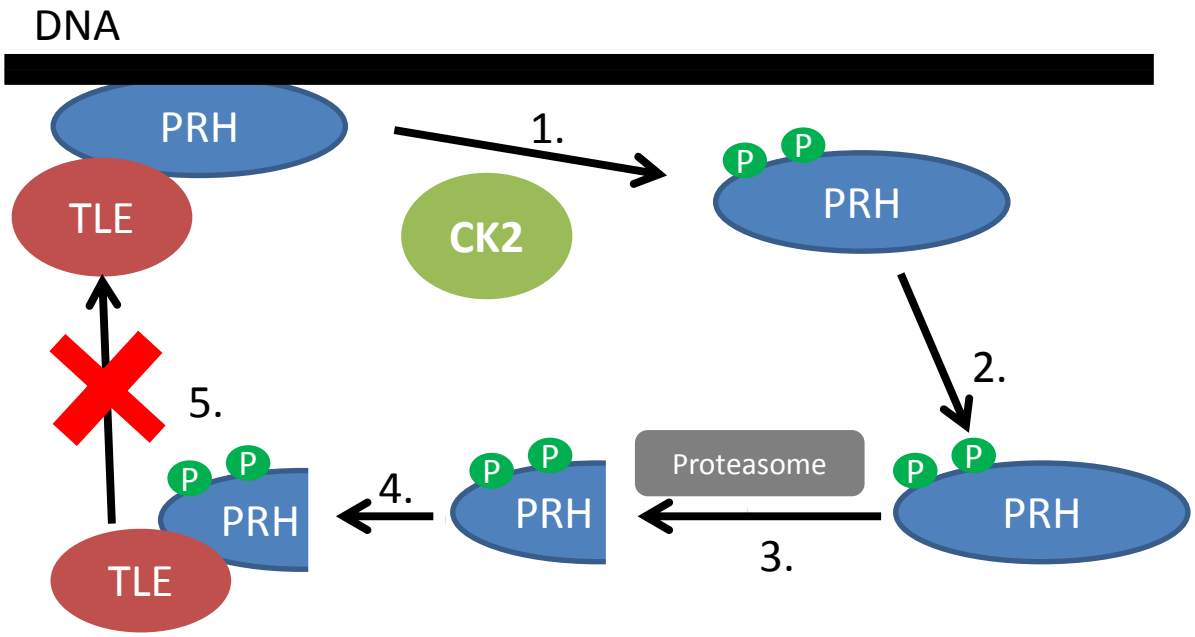

Figure 1.6: Proposed mechanism of PRHΔC-mediated regulation. 1) PRH binds to co-repressor TLE, and binds to DNA to repress transcription. 2) PRH is phosphorylated by Protein Kinase CK2, causing PRH to no longer bind to DNA and to translocate to the cytoplasm. 3) PRH is then cleaved by the proteasome, giving a truncated product with no C-terminal domain. 4) PRHΔC then binds to TLE. 5) TLE can no longer translocate to the nucleus, and hence cannot repress PRH-target genes.

1.2.8 PRH in development

PRH is required for embryonic development, and *Prh*$^{-/-}$ mice embryos die between 13.5-16.5 days *post coitum* (Martinez Barbera et al., 2000, Keng et al., 2000). PRH has also been shown to be a marker for anterior asymmetry in *Xenopus* embryos. Overexpression of PRH in these embryos causes suppression of the dorsal mesoderm, whilst expression of a mutant form of PRH (which cannot repress gene transcription) leads to anterior truncations (Brickman et al., 2000).

PRH is also required for the development of various organs (reviewed in Soufi and Jayaraman, 2008). PRH is essential for liver development, as a null-mutation of *Prh* stops

formation of the liver bud (Hunter et al., 2007). Loss of *Prh* in the hepatic diverticulum (the precursor to the embryonic liver liver), leads to a smaller and cystic liver, loss of gall bladder and bile duct, and embryonic lethality (Hunter et al., 2007). Furthermore, loss of *Prh* in the embryonic liver leads to irregular bile duct development, and polycystic liver disease in the adult mouse (Hunter et al., 2007). PRH is also required for development of the thyroid gland, as well as the pancreas (Elsalini et al., 2003, Parlato et al., 2004, Bort et al., 2004). PRH is involved in haematopoiesis, and loss of *Prh* in the haemangioblast (the precursor of both blood and endothelial cells) leads to decreased differentiation into haematopoietic cells, and into endothelial cells to a lesser extent (Guo et al., 2003). PRH levels are high in haematopoietic stem cells, and PRH expression generally decreases during the differentiation process, with the exception of granulocytes (Manfioletti et al., 1995, Jayaraman et al., 2000).

1.2.9 PRH as an inhibitor of proliferation and survival

PRH is known to be a regulator of cell proliferation. Overexpression of PRH in myb-ets (E-twenty six) transformed chicken blastoderm cells inhibits their transformation and proliferation (Jayaraman, et al., 2000). As mentioned previously, PRH can repress proliferation by inhibiting eIF-4E dependent cyclin d1 mRNA nucleocytoplasmic transport in U937 leukaemic cells (Topisirovic, 2003). PRH also induces apoptosis (a form of programmed cell death) in K562 leukemic cells, by repressing genes encoding components of the VEGF signalling pathway (VSP) (Noy, et al., 2010). Forced expression of PRH also suppressed proliferation of embryonic stem cells, while PRH knockout embryonic stem cells showed enhanced proliferation compared to wild-type stem cells (Kubo, 2005), although this has not

always been observed (Guo et al., 2003). In keeping with the growth inhibitory properties of PRH, knockout of PRH has been shown to increase survival by decreasing apoptosis by 75% in the endocardial cushion of mouse embryos (Hallaq et al., 2004).

PRH has also been suggested to be a negative regulator of hepatocyte proliferation during liver development. PRH is sequestered into the hepatocyte cytoplasm by binding to CD81 (a transmembrane protein which regulates cell proliferation and motility) during peak hepatocyte proliferation (Bhave et al., 2013). PRH has also been shown to be a negative regulator of proliferation in solid cancer cells, decreasing hepatocarcinoma growth in xenograft models (Su et al., 2012).

As mentioned previously, PRH transcriptional activity and stability is regulated by CK2. CK2 is a kinase that promotes tumourgenesis in many cancers, including mammary cells (Romieu-Mourez et al., 2001). It does this by phosphorylating a variety of proteins, which leads to increased activity of oncoproteins and a decrease in tumour suppressor protein activity (reviewed by Ahmed et al., 2002). It has been demonstrated that CK2 can influence K562 leukaemic cell survival through phosphorylation of PRH (Noy et al., 2012c). Inhibition of CK2 by inhibitors of upstream kinases, that indirectly decrease CK2 activity, leads to a reduction in cell survival. For example, dasatinib/imatinib are inhibitors that block the fusion tyrosine kinase protein BCR-ABL found in chronic myeloid leukaemia (CML) cells, and dasatinib also blocks Src kinases (Rix et al., 2007). BCR-ABL phosphorylates CK2, which promotes CK2 kinase activity (Heriche and Chambaz, 1998). Treatment of the CML K562 cell line with dasatinib results in inhibition of BCR-ABL, decreased phosphorylated PRH, and decreased cell number (see figure 1.7) (Noy et al., 2012a). The effect of dasatinib on cell number was

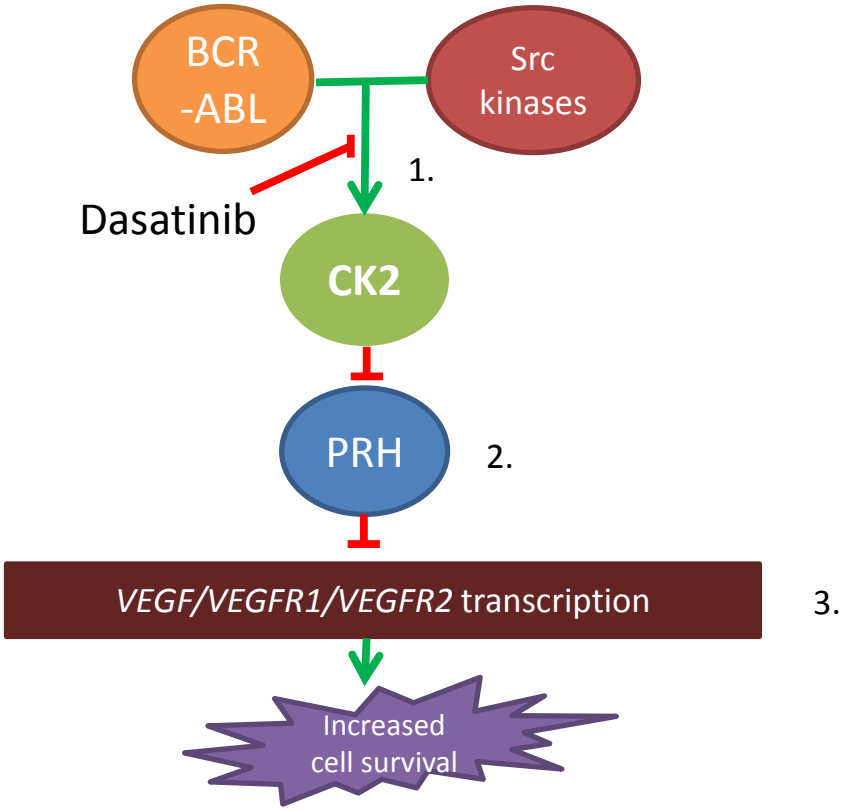

Figure 1.7: Model of PRH misregulation in CML. 1) BCR-ABL and Src kinases phosphorylate protein kinase CK2, activating its protein kinase activity. 2) CK2 phosphorylates PRH, so that PRH can no longer bind to DNA. 3) Phosphorylated PRH can then no longer repress *VEGF, VEGFR1* and *VEGFR2* transcription, leading to an increase in cell survival (adapted from Noy, et al., 2012a).

reduced when PRH expression was knocked down using *PRH* shRNA (Noy et al., 2012b). The implication of this work is that PRH expression is important for inhibition of survival by dasatinib in leukaemic cells, and that reagents that block CK2 activity will affect PRH activity and cell proliferation/survival (Noy et al., 2012b). This illustrates the importance of PRH to the control of cancer cell proliferation, survival and tumour growth.

1.2.10 PRH as an oncogene

Forced expression of PRH can also act as an oncoprotein in T-cell lineages. Overexpression of PRH in transgenic mice results in increased immature myeloid cell proliferation (Mack et

al., 2002). Furthermore, mice which had been injected with bone marrow cells overexpressing PRH developed tumours from a precursor T cell population (George, et al., 2003). Additionally, it has been shown that PRH overexpression leads to an increase of thymocyte self-renewal (Curtis and McCormack, 2010). Interestingly, induction of T cell acute lymphoblastic leukaemia by the *LMO2* (LIM domain only 2) oncogene, leads to upregulation of PRH expression (Curtis and McCormack, 2010). Taken together, these results show that PRH can act as an oncogene depending on the context.

1.2.11 PRH and cell migration

PRH has been shown to be involved in regulating migration and invasion of cells. Atrioventricular explants (from the developing heart) of *Prh* knockout mouse embryos showed a greater number of collagen-invasive cells (Hallaq et al., 2004). Furthermore, overexpression of PRH in human umbilical vein endothelial cells led to decreased cell migration and decreased invasion of these cells through Matrigel (extracellular matrix secreted from murine sarcomas) (Nakagawa et al., 2003). Overexpression of PRH also decreased expression of matrix metalloproteinase-1 (*MMP1*) (Nakagawa et al., 2003), which has been shown to play a role in tumour cell invasion, by degrading components of the extracellular matrix (reviewed in Duffy et al., 2000).

1.2.12 PRH and cancer

Misregulation of PRH protein has been associated with cancer. Expression of a *PRH-NUP98* transgene was shown to be necessary for disease induction in an acute myeloid leukaemia

(AML) patient (Jankovic et al., 2008) This is thought to occur by the PRH-NUP98 fusion protein activating transcription of genes normally targeted for repression by wild-type PRH (Jankovic et al., 2008). It has been shown that PRH is mislocalised in breast and thyroid tumours; PRH expression in normal breast and thyroid tissue is both nuclear and cytoplasmic, whereas its nuclear localisation is reduced in breast and thyroid carcinomas, suggesting there is a decrease in the transcription factor activity of PRH in these diseases (Puppin et al., 2006, D'Elia et al., 2002). It has also been shown that in hepatocarcinomas, PRH expression is significantly higher in more differentiated tumours, which tend to be less aggressive (Su et al., 2012). Taken together, this suggests that in a variety of tumour cell types, reduction of PRH activity is correlated with increased tumourgenesis.

1.2.13 PRH and breast cancer

In normal breast cells, it has been reported that PRH protein is expressed in both the nucleus and cytoplasm (Puppin et al., 2006). In breast tumour cells however, PRH is predominantly cytoplasmic, and this finding was used to suggest that PRH may no longer act as a transcription factor in breast tumour cells (Puppin et al., 2006). In MCF-7 luminal breast tumour cells, it was reported that PRH is sequestered by the nucleolus, and thus cannot act as a transcriptional repressor in this cell type (Puppin et al., 2006), however this hypothesis was not tested in this study. Moreover, knockdown of PRH in MCF-7 cells leads to an increase in cell number, and de-repression of genes in the VSP, suggesting that at least some endogenous PRH must still be active in the nucleus of MCF-7 cells despite the predominantly nucleolar localisation previously reported (Noy et al., 2010).

1.3 Potential PRH target genes that are involved in breast cancer

Several microarray studies with *Prh*$^{-/-}$ cells and PRH protein overexpression studies have identified genes that are perturbed by manipulation of PRH activity in specific contexts (Nakagawa et al., 2003, Guo et al., 2003, Kubo et al., 2010). The following genes and proteins have been shown to be affected by PRH expression in certain contexts, and are known to be relevant to breast cancer and cancer progression.

1.3.1 VEGF and VEGF receptors

PRH has been shown to affect the VEGF signalling pathway (VSP) in human umbilical vein endothelial cells (HUVECs) (Guo et al., 2003). One of the ligands of this pathway, VEGF-A, is part of a family of VEGF-related proteins, which includes VEGF-B, VEGF-C, VEGF-D and PIGF (Phosphatidylinositol-glycan biosynthesis class F protein). These proteins have been shown to be involved in embryonic angiogenesis and lymphangiogenesis (Mandriota et al., 2001). *VEGF* is alternatively spliced, and at least 9 different isoforms have been discovered in humans, with VEGF-A_{165} being the dominant isoform (Harris et al., 2012, Ferrara et al., 2003). VEGF-A acts to activate angiogenesis by binding to the receptors VEGF receptor 1 and 2 (VEGFR-1 and VEGFR-2), as well as the co-receptors Neuropilin-1 and Neuropilin-2 (NRP1 and NRP2) (Gille et al., 2001, Herzog et al., 2011, Gluzman-Poltorak et al., 2000). VEGFR-2 is the major mediator of angiogenesis, whilst VEGFR-1 seems to have a more context dependent-role depending on the cell type (Ferrara et al., 2003). However, NRP1 and NRP2 have very small cytoplasmic domains, and thus cannot transduce signals when ligand binding occurs. NRP1 can bind to VEGF-A_{165}, which can then form complexes with VEGFR-2,

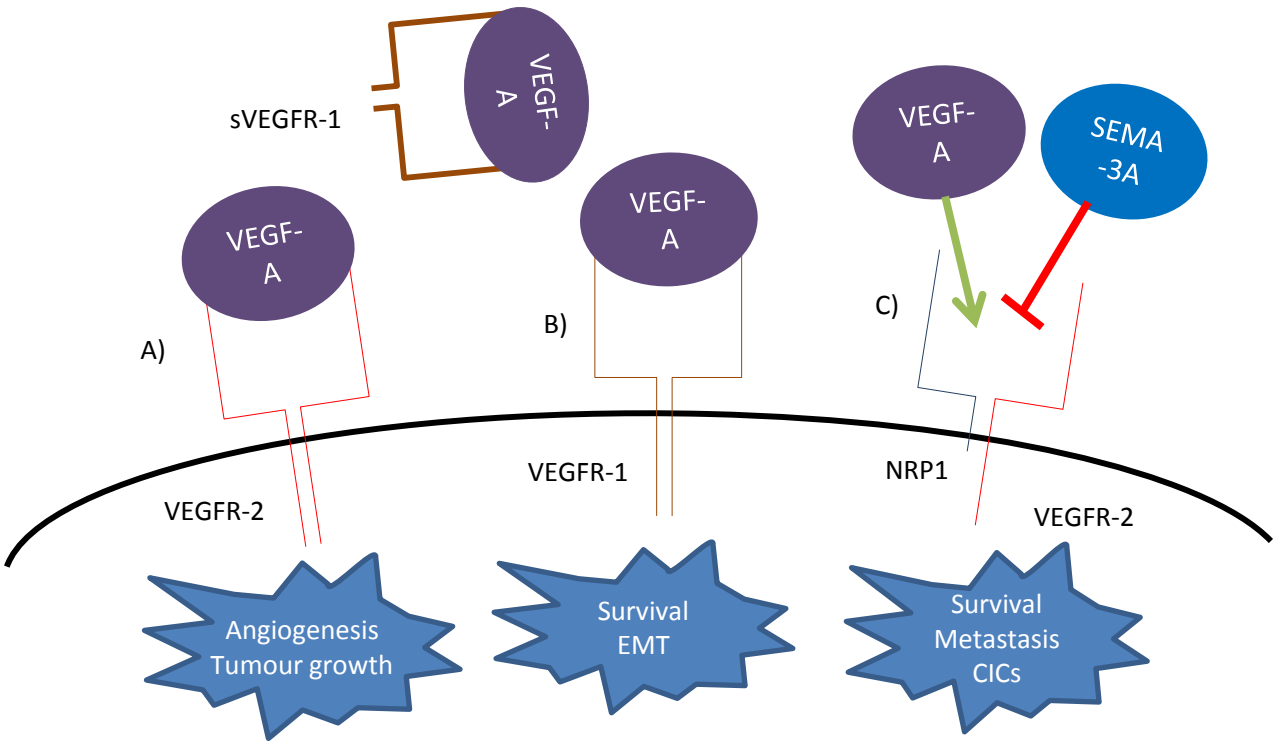

Figure 1.8: VEGF signalling pathway. A) VEGF-A binds to a VEGFR-2 homodimer, which signals to activate angiogenesis in endothelial cells, and tumour growth in epithelial cells. B) VEGF-A binds to a VEGFR-1 homodimer, which signals to activate survival and EMT in epithelial cells. Soluble VEGFR-1 (sVEGFR-1) sequesters VEGF-A ligand, inhibiting VEGF-A signalling. C) VEGF-A binds to a NRP1/VEGFR-2 heterodimer, activating survival, metastasis and production of CICs. This pathway is inhibited by SEMA-3A (Semaphorin-3A) (adapted from Kowanetz et al., 2006).

which results in increased VEGF-A binding to VEGFR-2 (see figure 1.8) (Mamluk et al., 2002, Soker et al., 2002). VEGFR-3, along with its ligand VEGF-C, has also been shown to be upregulated in breast carcinomas, and are involved in the formation of lymphatic vessels in breast tumours (Valtola et al., 1999, Skobe et al., 2001). See figure 1.8 for an overview of VEGF signalling.

Angiogenesis is the formation of blood vessels from pre-existing blood vessels. It is a process which is vital during embryonic development, as well as during wound healing. VEGF-A has been shown to induce proliferation of vascular endothelial cells in response to hypoxia, and this is mediated in part through activation of the transcription factor HIF-1α (Forsythe et al., 1996, Shweiki et al., 1992). Since angiogenesis also plays a vital role in tumour progression,

inhibition of angiogenesis (and therefore VEGF-A) has been a major field in cancer therapeutics in the last decade, and has led to FDA (U.S. Food and Drug Administration) approved therapies such as bevacizumab (Avastin), sorafenib (Nexavar) and sunitinib (Sutent).

Importantly, VEGF signalling is also associated with non-angiogenic functions in many tumour cells, for example it plays a role in cell proliferation, survival and migration. MT mice (which spontaneously develop mammary tumours) overexpressing VEGF showed tumours with increased cell proliferation and anti-apoptotic activities (through a decreased BAX/BCL-2 ratio) (Schoeffner et al., 2005). Furthermore, *Vegf* conditional knockout mice showed decreased cell proliferation, through increased accumulation of cells in the G1 phase of the cell cycle (Schoeffner et al., 2005). Knockdown of VEGF expression in metastatic breast cancer cells also promoted apoptosis, via signalling through NRP1 and the PI3-kinase signalling pathway (Bachelder et al., 2001). Conversely, VEGF-A expression increased Heparin and Fibronectin mediated migration of breast cells (Miralem et al., 2001), and increased breast carcinoma invasion, through upregulation of the chemokine receptor CXCR4 (Bachelder et al., 2002). Taken together, these experiments show that VEGF-A plays an important role in breast cancer cell survival, migration and invasion.

The receptors in the VEGF pathway also play roles in increasing cell survival, proliferation and migration. Treatment of breast tumour xenografts with an anti-VEGFR-1 antibody led to a decrease in tumour growth (Wu et al., 2006b). Knockdown of VEGFR1 in metastatic MDA-MB-231 breast cancer cells lead to decreased tumour growth and metastasis in nude mice models (Ning et al., 2013). Treatment of chemotherapy-resistant tumours in xenograft

models with an anti-VEGFR-2 antibody inhibited growth of the primary tumour (Klement et al., 2002). Taken together, this evidence suggests a role for VEGFR-1 and VEGFR-2 in breast tumour growth.

A peptide which blocked VEGF binding to the NRP1 co-receptor increased apoptosis of MDA-MB-231 breast cancer cells (Barr et al., 2005). Knockdown of neuropilin-1 expression by siRNA, as well as inhibiting NRP1 function by using an anti-NRP1 antibody, inhibited mammosphere formation of MDA-MB-231 cells (Glinka et al., 2012). This shows that VEGF receptors can also affect cell proliferation and survival independent of angiogenic pathways.

VEGF-A, VEGFR-1 and VEGFR-2 expression have all been shown to be markers for decreased overall survival in breast cancer (Linderholm et al., 2000, Ghosh et al., 2008). As mentioned earlier, overexpression of PRH led to the repression of VEGFR-1, VEGFR-2 and NRP1, and stopped VEGF-mediated proliferation, migration and invasion in endothelial cells (Nakagawa et al., 2003). Repression of *VEGFR2* in these cells was shown to involve PRH binding to GATA-2, and hence prevent GATA-2 mediated activation of transcription of the *VEGFR2* gene (Minami et al., 2004). PRH also regulates these genes in other contexts, for example, VEGF-A protein levels are also 2-3 fold higher in 9-14 day old *Prh*$^{-/-}$ mice embryos (Hallaq et al., 2004). Sequestration of VEGF-A by soluble VEGFR-1 in these mice inhibited PRH-mediated EMT (Hallaq et al., 2004). Forced expression of PRH in mouse ES cells led to the repression of *VEGFR2* expression (Kubo et al., 2005). PRH has also been shown to regulate *VEGF*, *VEGFR1* and *VEGFR2* mRNA expression in both K562 leukaemic cells, and in MCF-7 breast cancer cells (Noy et al., 2010). Furthermore, this repression occurred by PRH forming a complex with the co-repressor TLE, and binding directly to the promoters of these genes

(Noy et al., 2010). This repression by PRH is inhibited by CK2, which phosphorylates PRH and prevents it binding to the *VEGFR1* promoter (Noy et al., 2012c, Noy et al., 2012b).

1.3.2 SATB1

In *Prh*$^{-/-}$ embryoid bodies, special AT-rich binding protein 1 (*SATB1*) transcript expression is upregulated, suggesting that PRH directly or indirectly regulates *SATB1* expression (Guo, et al., 2003). SATB1 is a nuclear protein, and acts as a global regulator of gene expression. It binds to base-unwinding regions in the DNA, and forms a cage-like structure, that recruits chromatin-remodelling enzymes to regulate gene expression. SATB1 expression is significantly associated with higher tumour grade and poorer prognosis (Han et al., 2008a, Patani et al., 2009). Knockdown of SATB1 in MDA-MB-231 cells causes a decrease in growth and invasiveness *in vitro* and *in vivo*, whilst causing a restoration in cell polarity and anchorage-dependent growth (Han et al., 2008b). Overexpression of SATB1 in SKBR3 cells causes increased tumour growth and lung metastases (Han, et al., 2008). SATB1 is also known to upregulate many metastasis-associated genes (like *HER2*), whilst down-regulating many tumour-supressor genes (like e-cadherin) (Han, et al., 2008).

1.3.3 Endoglin

Overexpression of PRH in human umbilical vein endothelial cells (HUVECs) leads to a decrease in invasion and migration of these cells (Nakagawa et al., 2003). Western blotting showed that the Endoglin protein is significantly upregulated in PRH overexpressing HUVECs (Nakagawa et al., 2003). Endoglin is a type III TGF-β receptor, meaning that it can bind the

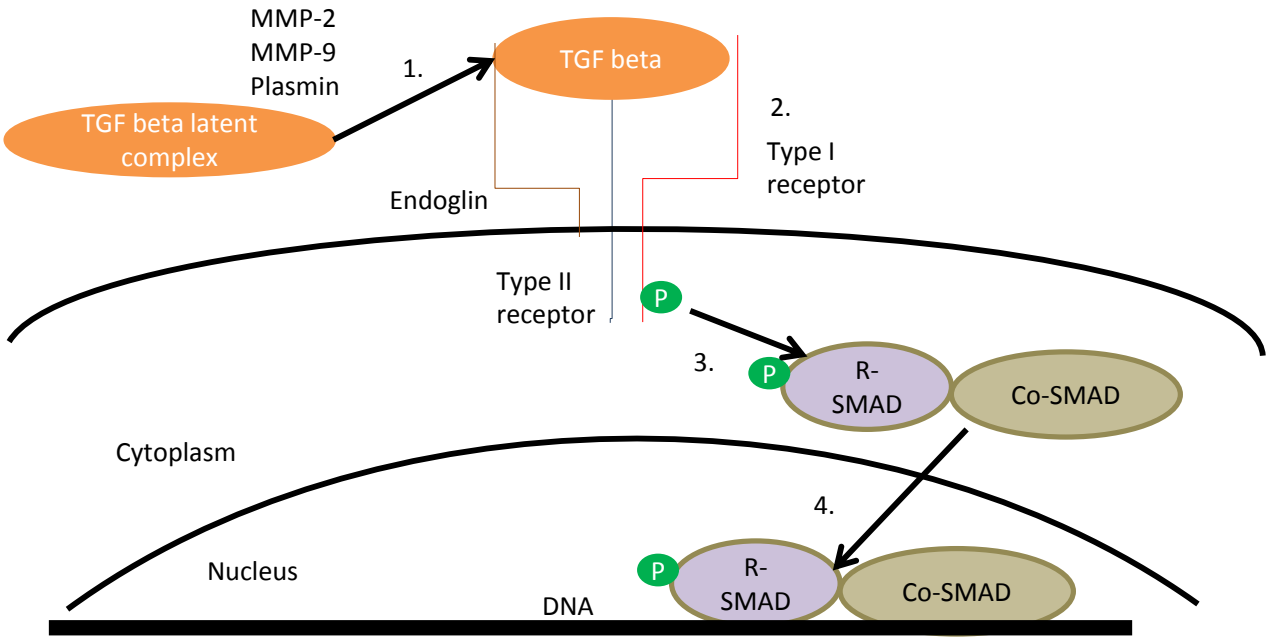

Figure 1.9: Mechanism of TGF-β signalling. 1) The TGF-β complex is activated by MMP-2, MMP-9 or plasmin. 2) TGF-β binds to a type II receptor (and Endoglin, depending on the context) which causes the phosphorylation of a type I receptor. 3) This causes phosphorylation of a R-SMAD (regulator-regulated SMAD) protein, which causes the formation of a dimeric R-SMAD:co-SMAD (common-mediator SMAD) complex. 4) This complex then translocates to the nucleus, activating the transcription of target genes (adapted from Massagué et al., 2012).

TGF-β ligand, but lacks a kinase domain, so that it cannot signal to downstream pathways by itself (Guerrero-Esteo et al., 2002). Endoglin is expressed at high levels in endothelial cells (Alt et al., 2012). TGF-β has been shown to act as a suppressor of tumour growth in endothelial cells, however TGF-β can also increase cell invasiveness and migration in a number of contexts (reviewed in Bierie and Moses, 2006). See figure 1.9 for a overview of TGF-β signalling.

Mutations in endoglin are responsible for Hereditary Hemorrhagic Telangiectasia (HHT), a disease characterised by telangiectasia (spider veins) on the mucosa and skin, frequent nose bleeds and arteriovenous malformations in the liver, lungs and brain (Gallione et al., 1998). Endoglin expression is upregulated in proliferating endothelial cells, and is thought to play a role in angiogenesis by modulating TGF-β signalling pathways (Dijke et al., 2008). Endoglin

exists in three isoforms, L-Endoglin (the long form), S-Endoglin (the short form, which differs from the long form by 33 amino acids), and a soluble form of Endoglin (Bellón et al., 1993, Hawinkels et al., 2010). Interestingly, in rat myoblast cells, increased expression of L-Endoglin increased cell proliferation, whilst increased expression of S-Endoglin reduced cell proliferation (Velasco et al., 2008). Tumour-bearing mice treated with an oral DNA vaccine, coding for murine endoglin, suppressed metastasis and had increased survival, compared to tumour-bearing mice injected with a control vaccine (Lee et al., 2006), suggesting that Endoglin is expressed and important in proliferating tumour endothelial cells.

Endoglin has seemingly dual roles in breast cancer, independent of its role of tumour angiogenesis. Soluble Endoglin levels have been found to be elevated in breast cancers, and breast cancer patients with increased plasma Endoglin levels have decreased overall survival (Vo et al., 2010). However, breast tumours which are positive for Endoglin expression significantly correlate with improved overall survival and metastasis-free survival (Henry et al., 2011). Therefore, Endoglin may be a positive or negative marker for breast cancer survival, depending on whether the Endoglin is in the soluble or membrane bound form.

Endoglin appears to suppress or enhance the invasive phenotype of breast cancer cells depending on the context. Oxmann et. al. found that Endoglin was overexpressed in MDA-MB-231 metastases, compared to parental tumours (Oxmann et al., 2008). This study also found that the high Endoglin expressing cells migrated and invaded more than low-expressing endoglin cells, and that Endoglin overexpression led to an increase in MMP-1 and MMP-19 levels (Oxmann et al., 2008). In contrast, Henry et. al. found that downregulation of Endoglin in HER2-overexpressing MCF-10A cells led to an increase in cancer cell invasion

(Henry et al., 2011). Furthermore, this study found that MDA-MB-231 cells which had been transfected with endoglin complementary DNA significantly reduced breast cancer colonisation of the lung compared to controls (Henry et al., 2011). This study also found that the effects on Endoglin in these experiments were independent of Smad signalling, which is a pathway involved with TGF-β activation (Henry et al., 2011). These seemingly contradictory results could be due to TGF-β signalling having different effects in different cells types, depending on how transformed they are (Bierie and Moses, 2006). Endoglin seemed to inhibit invasion and metastasis in parental MDA-MB-231 cells in (Henry et. al. 2011), whilst the effects of Endoglin increasing invasiveness of breast cancer cells was seen in brain metastases with MDA-MB-231 cells in (Oxmann et. al 2008), and were selected to be a more "transformed" cell than the cells used in (Henry et. al. 2011).

1.3.4 TP53

TP53 is a gene that can be regulated by PRH in hepatocarcinoma cells, since overexpression of PRH in these cells leads to decreased expression of p53 compared to control cells (Su et al., 2012). However, it is not known whether this regulation is direct or indirect. P53 is largely thought of as a "guardian of the genome", due to the role it plays in regulating the cellular response to stress, such as DNA damage, telomere erosion and aberrant expression of oncogenes (Horn and Vousden, 2007, Walerych et al., 2012). In unstressed cells, p53 has a relatively-short half life, as it is targeted for degradation by the proteasome by the E3 ubiquitin-ligase mouse double minute homolog 2 (MDM2) (Honda et al., 1997). However, when cells undergo cytotoxic stress, this leads to phosphorylation of p53 in the N-terminal domain by a number of kinases, causing stabilisation of the protein (Tibbetts et al., 1999,

She et al., 2000). This allows p53 to form a tetramer, which binds to DNA and acts to regulate of transcription of p53 target genes. P53 target genes encode proteins that regulate the cell cycle, cell survival and proliferation (reviewed in McLure and Lee, 1998).

TP53 is the most commonly mutated gene in cancer overall, being mutated in approximately 31% of all cancers but it is only mutated in approximately 23% of breast cancers (Forbes et al., 2011). *TP53* is more frequently mutated in basal and *HER2* amplified breast tumours, which are the most aggressive forms of breast cancer (34% and 22% respectively) (Curtis et al., 2012). *TP53* mutations also correlate with lymph node-positive and higher-grade breast cancers, leading to a worsening prognosis (Curtis et al., 2012). Together these studies show that *TP53* mutations are associated with increased breast cancer aggressiveness.

P53 has been shown to be a regulator of breast cancer cell invasion, and a regulator of EMT. Zhang et. al showed that expression of p53 R248W, R175H and R273H mutants in MCF-10A immortalised mammary cells led to the formation of irregular and multiacinar spheroids (described later), decreased expression of E-Cadherin and β-Catenin, and increased expression of Snail, Slug and Twist, which taken together suggest the cells are undergoing EMT (Zhang et al., 2011). Chang et. al. showed that knockdown of wild-type *TP53* in MCF-12A cells led to an decrease in E-Cadherin expression and enhanced ZEB1 expression, which are markers of EMT, via *miR-200c* (Chang et al., 2011). It was also shown by Nielsen et. al. that wild-type p53 also inhibits EMT, via inhibition of transcription of the micro RNA *miR-155* (Neilsen et al., 2013).

As has been discussed previously, the concepts of EMT and cancer initiating cells (CICs) are closely related. Therefore, it is of no surprise to discover that p53 also affects the stem cell population of mammary tumours. In murine mammary tumours, there are a greater number of stem-cells from *Tp53* knockout mice compared to control mice, as determined by limiting dilution transplantation (Cicalese et al., 2009). *Tp53* knockout stem-cells also have an increased frequency of symmetric division, and increased levels of the stem-cell marker nanog (Cicalese et al., 2009). P53 knockdown also led to an increase in the $CD44^{high}/CD24^{low}$ compartment in normal breast epithelial MCF-12A cells (Chang et al., 2011).

1.3.5 Goosecoid

PRH has been shown to be a direct transcriptional repressor of goosecoid in *Xenopus* ES cells (Brickman et al., 2000). PRH has also been shown to bind to the goosecoid promoter, as determined by chromatin immunoprecipitation (ChIP) and luciferase assays in human K562 leukaemic cells (Williams et al., 2008, Soufi et al., 2010). Therefore, it is of interest to note whether PRH has any effect on the expression of goosecoid in human breast cells.

Goosecoid is a homeodomain-containing transcription factor, involved in mammalian and Xenopus development. Injection of goosecoid mRNA in the ventral side of Xenopus embryos leads to the formation of a twinned body axis (Cho et al., 1991). As EMT is involved in both development of the embryo and in tumour metastasis, it was hypothesised that Goosecoid may be involved in tumour metastasis as well (Hartwell et al., 2006). Overexpression of Goosecoid led to increased cell motility of the immortalised human mammary epithelial cell line (HMECs), increased expression of EMT markers in HMECs, and resulted in increased

metastasis of MDA-MB-231 cells to the lungs in mouse xenograft experiments (Hartwell et al., 2006, Taube et al., 2010). Furthermore, Goosecoid expression was increased by TGF-β signalling in HMECs (Hartwell et al., 2006). Goosecoid expression was also found to be elevated in ductal breast carcinomas, compared to patient-matched normal breast tissue (Hartwell et al., 2006), however expression was not found to be a prognostic marker of clinical outcome (Taube et al., 2010).

1.3.6 Endothelial cell-specific molecule 1 (ESM1)

ESM1 expression is downregulated by PRH overexpression in HUVEC cells by direct binding of PRH to the *ESM1* promoter (Cong et al., 2006). Also, In E10.5 $Prh^{-/-}$ mouse embryos, *Esm1* expression was 11 fold greater compared to E10.5 $Prh^{+/+}$ embryos (Cong et al., 2006). Therefore, as PRH can repress ESM1 expression, it is of interest to determine whether it represses ESM1 in breast cells.

ESM1 (also known as Endocan), is a protein which is strongly expressed in the endothelial cells of the lungs (Lassalle et al., 1996). ESM1 is overexpressed in clear cell renal cell carcinoma, and in gastric cancer (Leroy et al., 2010, Liu et al., 2010). ESM1 and VEGF show similar expression patterns in renal cell carcinomas, and it has been proposed that ESM1 could play a role in VEGF-induced angiogenesis (Aitkenhead et al., 2002). ESM1 was shown to be a marker for poor prognosis in breast cancer patients (van't Veer et al., 2002), although no correlations were found between ESM1 expression and breast cancer grade, stage or ER/PR/HER2 status (Congyun et al., 2008).

1.4.2 Cell lines used in this study

In this study, experiments will be carried out predominantly using three cell lines, MCF-10A, MCF-7 and MDA-MB-231 cells. MCF-10A cells are an immortalised cell line, which arose spontaneously from a normal diploid mammary epithelium (Soule et al., 1990b). MCF-10A cells do not undergo anchorage-independent growth in Matrigel, nor do they form tumours in nude mice (Soule et al., 1990b). MCF-10A cells do not show *HER2* amplification, express wild-type p53, and unlike other immortalised cell lines, do not contain the SV40 T antigen (Merlo et al., 1995, Soule et al., 1990b). MCF-10A cells form acinar structures, when grown in 3D culture, which are phenotypically similar to mammary glandular structures (Debnath et al., 2003b). These acini are growth arrested, and contain a hollow lumen, due to the apoptosis of cells lacking contact with the basement membrane (Debnath et al., 2003a). Therefore, MCF-10A cells represent a good model for normal untransformed breast cells. They do however have some cytogenetic abnormalities, although not as many as MCF-7 and MDA-MB-231 cells (Soule et al., 1990b).

MCF-7 cells are a cell line derived from pleural effusion from a breast cancer patient (Brooks et al., 1973). They have a luminal epithelial phenotype, and they are positive for both ER and PR, although they do not have amplified *HER2* expression, and they express wild-type p53 (Brooks et al., 1973, Nagle et al., 1986, Subik et al., 2010, Fan et al., 1995). Their karyotype shows that MCF-7 cells have a mean chromosome number of 88 (Soule et al., 1973). MCF-7 cells are tumourgenic in nude mice, but only with supplementation with 17β-oestradiol (Seibert et al., 1983). As MCF-7 cells express high levels of E-cadherin, low levels of Vimentin, and in Matrigel are weakly invasive and form spherical colonies, it is thought that

MCF-7 cells represent a more “epithelial-like” phenotype with respect to EMT (Lacroix and Leclercq, 2004b).

MDA-MB-231 cells are derived from a pleural effusion from a breast cancer patient, and they have a near-triploid karyotype, containing between 60-70 chromosomes (Cailleau et al., 1974). They do not express ER, PR or have amplified *HER2* status, and they have a basal like phenotype (Lacroix and Leclercq, 2004a). MDA-MB-231 cells express a mutated form of p53 (R280K), which promotes cell survival in this cell-type (Hui et al., 2006, Roger et al., 2010). MDA-MB-231 cells are tumourgenic in nude mice, and do not require supplementation with 17β-oestradiol (Cailleau et al., 1974). As MDA-MB-231 cells are highly invasive, form stellate colonies in Matrigel, express low levels of E-Cadherin and high levels of Vimentin, it is thought they represent a “mesenchymal-like” cell with regards to EMT (Lacroix and Leclercq, 2004b).

1.4 Aims of my project

PRH is a known regulator of cell proliferation and migration in various cell types; however whether PRH regulates the growth of normal breast or breast cancer cells has not been studied extensively. The first aim of this thesis is to determine whether there is a correlation between *PRH* mRNA or PRH protein expression levels with breast tumourgenesis. To do this *PRH* mRNA expression will be examined in a database, where gene expression microarray data has been correlated with breast cancer subtype and prognosis. We will also examine the expression levels of PRH protein, its phosphorylation status, stability and sub-cellular

localisation in a variety of breast cell lines. The second aim of this thesis is to determine whether overexpression and knockdown of PRH has any effect on cell proliferation and survival in MCF-10A, MCF-7 and MDA-MB-231 cells. Thirdly, the effect of PRH on breast cell migration and invasion will also be examined. Finally, the effect of PRH on the transcription of several candidate genes relevant to breast cancer and EMT will be analysed in each of these cell lines to determine whether regulation of these genes by PRH occurs in breast cells, and whether this control is deregulated in breast cancer cells. Selected genes will also be analysed for direct or indirect regulation by PRH.

MATERIALS AND METHODS

2. Materials and methods

2.1 Data-mining the GOBO database

Data mining from the GOBO database is described in (Ringnér et al., 2011). Briefly, after loading the following URL: http://co.bmc.lu.se/gobo/gsa.pl, the Gene Set Analysis was carried out on tumour samples, using the gene set with the gene symbol "HHEX". All tumours were selected, using 3 quantiles and 10 years censoring, with the end point being overall survival and all multivariate parameters selected. For Gene Set Analysis of cell lines, the gene set with the gene symbol "HHEX" was used, and the cell line selection was "Neve et al".

2.2 Cell culture protocols

2.2.1 Adherent cell culture

MDA-MB-231, MCF-7, T47D, BT20, BT474, ZR-75-1 and HB2 cells were cultured in RPMI-1640 media (Sigma), supplemented with 10% foetal bovine serum (FBS) (Sigma) (which was heat-inactivated at 56°C for 30 minutes), 100 units/ml of penicillin and 0.1 mg/ml of streptomycin (Sigma). MCF-10A cells were grown in DMEM/F12 media (Sigma), supplemented with 5% heat-inactivated horse serum (Sigma), 20ng/µl epidermal growth factor (EGF) (Peprotech), 0.5µg/ml hydrocortisone (Sigma), 100ng/µl cholera toxin (Sigma), 10µg/ml insulin (Sigma), 100 units/ml of penicillin and 0.1 mg/ml of streptomycin (Sigma).

HEK-293 and HEK-293T cells were grown in DMEM (Sigma) with 10% FBS (Sigma) which was heat-inactivated as before, 100 units/ml of penicillin and 0.1 mg/ml of streptomycin (PAA). Cells were subcultured by diluting one in four when they reached 80% confluency. To propagate adherent cells, they were first washed with 1x phosphate-buffered serine (PBS) (Sigma). They were then treated with 1x trypsin (PAA) for 5 minutes at 37°C (apart from MCF-10A cells, which were incubated with trypsin for 20 minutes, or until cells detached). Once the cells were in suspension the trypsin was neutralised by plating the cells in the required volume of fresh media. Cells were cultured in a humidified atmosphere at 37°C and 5% CO_2. MCF-10A cells were grown in Falcon brand tissue culture flasks, whilst all other cell types were grown in Starstedt brand tissue culture flasks.

2.2.2 MTT assays

For MTT assays, approximately 5 x 10^4 cells were seeded into 16 wells each (4 wells in 4 96-well plates). After 0, 24, 48 or 72 hours, 4 wells from 1 plate for each infection was then incubated with 0.5 mg/ml MTT (3-(4,5-dimethylthiazol-2-yl)-2,5-diphenyltetrazolium bromide) in 200 µl RPMI for 2 hours. The formazan dye was solubilised with 200µl dimethyl sulphoxide (Fisher Scientific). The optical density was then taken for each well at 595nm.

2.2.3 Lipofectamine 2000 transfections

Lipofectamine transfections were carried out according to manufacturer's instructions. Briefly, 5µl of Lipofectamine (for 6-well transfection, 40µl for transfection in a 75cm^2 flask)

was then added to 100µl of serum-free media (750µl for a 75cm^2 flask). To another tube 2.5µg of DNA (21µg for a 75cm^2 flask) was added to 100µl of serum-free media (750µl for a 75cm^2 flask). The diluted DNA was added to the lipofectamine mixture, and was incubated for 5 minutes at room temperature. This complex was then added to the cells.

2.2.4 Cumulative growth curves

After 7 days induction with IPTG, cumulative growth curves with the lentiviral knockdown cells was set up. 1 x 10^5 cells were seeded into a 25 cm^2 tissue culture flask, and cells were counted every 6 days after replating (or cells reached 90% confluency, whichever was earlier). This process was repeated, and the cumulative cell number was then calculated by the following equation:

$$\frac{\text{(Number of cells counted in flask) x (Cumulative number of cells from previous count)}}{\text{(100,000 or the number of cells originally seeded previously)}}$$

For example:

Day 1: 100,000 cells seeded

Day 6: 1 x 10^6 cells counted, 1 x 10^5 cells seeded (Cumulative cell number: 1 x 10^6)

Day 12: 5 x 10^5 cells counted, 1 x 10^5 cells seeded (Cumulative cell number: (5x10^5 x 1x10^6 / 1 x 10^5) = 5x10^6)

Day 18: 1 x 10^6 cells counted, 1 x 10^5 cells seeded (Cumulative cell number: (1x10^6 x 5x10^6 / 1 x 10^5) = 5x10^7)

2.2.5 Mammosphere formation assay

For mammosphere formation assays, $4x10^4$ cells were plated into ultra-low adherrant 6 well plates (Corning), containing mammosphere media (see table 2.2). After 7 days of culturing at 37°C in 5% CO_2, the number of cells was quantified in each well by using a counting grid with 2mm by 2mm squares. To form secondary mammospheres, primary mammospheres were centrifuged at 350g (Eppendorf 5810R) for 5 minutes. The supernatant was decanted and the remaining mammospheres were incubated in 1x Trypsin-EDTA (Sigma) for 2 minutes. Five millilitres of cold mammosphere media was added to inactivate the Trypsin, and the cells were then centrifuged at 350g for 5 minutes. The number of single cells was counted, and $4x10^4$ cells were seeded into ultra-low adherrant 6 well plates (Corning), containing mammosphere media. The formation of secondary mammospheres was quantified 7 days later after culturing at 37°C in 5% CO_2.

2.3 Western blot protocols

2.3.1 Whole cell extracts

To make cell extracts, approximately $5x10^5$ MCF-7 or $5x10^5$ MDA-MB-231 cells were used. These cells were centrifuged at 1800g for 5 minutes at room temperature. The cell pellet was washed twice in PBS. The cells were resuspended in 150 µl of RIPA buffer (see table

2.2). The lysates were incubated on ice for 15 min and then centrifuged at 13000 rpm for 15 minutes at 4°C in a table-top microcentrifuge (Eppendorf 5424).

2.3.2 Quantification of proteins

Protein lysates were then quantified for their protein concentration. Protein Assay reagent (Bio-Rad) was diluted 1 in 5 with dH_2O, and 5µl of protein lysate was then added to 995µl of diluted Bradford solution. The optical density was then measured at 600nm using a Bio-Rad cuvette and measured using an INPLEN P300 nanophotometer. The equation used to determine the protein concentration was:

Protein concentration (µg/µl) = (OD - 0.0662)/ 0.0695

This equation was determined in the laboratory from a standard curve, as determined using set concentrations of bovine serum albumin.

2.3.3 Separation of proteins

Proteins were separated using SDS-PAGE. The resolving gel consisted of a final concentration of 1x resolving buffer (see table 2.2), 12% v/v acrylamide (Geneflow), 0.1% w/v ammonium persulphate (APS) (Sigma) and 0.12% v/v of tetramethylethylenediamine (TEMED) (Sigma). The stacking gel consisted of a final concentration of 1x stacking buffer (see table 2.2), 4.5 % v/v acrylamide, 0.1% w/v APS and 0.2% v/v of TEMED. The gel was then placed in a Bio-Rad Mini-PROTEAN electrophoresis tank filled with 1x running buffer (see table 2.2). The proteins were then loaded onto the gel after boiling with SDS gel loading

buffer (final concentration 1x) at 105°C for 5 minutes, and underwent electrophoresis at 140 V for 2 hours. Pageruler Plus protein ladder (Thermo Scientific) was also loaded onto the gel to determine the approximate protein sizes.

2.3.4 Transfer of proteins

The proteins were then transferred to a polyvinylidene fluoride (PVDF) membrane (Millipore IPVH00010). The membrane was activated by placing in methanol (Fischer Scientific) for 30 seconds, distilled water for 5 minutes, before being placed in transfer buffer for 15 minutes. The gel and the membrane were then sandwiched between two pieces of blotting paper (Whatmann 3030917), and placed in a cassette. This was placed in a Bio-Rad Mini Trans-Blot cell, which was filled with 1x transfer buffer (see table 2.2), which was kept cool using an ice pack. The proteins were then transferred at 70 V for 1 hour.

2.3.5 Detection of proteins with antibodies

The PVDF membrane was then stained with Ponceau S dye to confirm the complete transfer of proteins. The membrane was washed 5 times for 5 minutes with 1x PBS with 0.05% Tween-20 (PBS-T), and then blocked with 10% w/v milk (Tesco) in PBS-T overnight. After washing as before, the membrane was stained with the primary antibody (antibodies were diluted 1 in 5000 (unless otherwise stated), in 1x PBS-T with 3% w/v bovine serum albumin and 3mM sodium azide (Sigma)) for 1 hour. After washing, the membrane was then stained with the secondary antibody (diluted 1 in 2500 in PBS-T with 10% w/v milk) for 1 hour. The

membrane was washed and then stained with Enhanced Chemiluminescence solution (GE healthcare). Membranes were exposed to Hyperfilm (Amersham) for 2 minutes, before being developed using a Xograph developer.

2.3.6 Densitometric analysis

Densitometric analysis was carried out using ImageJ software. Briefly, an appropriate exposure (usually 2 minutes) of Western blot film was scanned, ensuring that the bands were not saturated. A box was drawn round the PRH triplet of proteins as detected by the M6 antibody, and lane plot analysis was performed. The area under the peak was then quantified. The same process was then carried out, but using the band which corresponds to Lamin C protein, to control for protein loading. The densitometry for PRH was then divided by the densitometry for Lamin C to obtain the relative band intensity.

2.3.7 Biochemical fractionations

Half a million MCF-10A, MCF-7 and MDA-MB-231 cells were used for biochemical fractionation (for Ad-PRH infected cells, fractionation was carried out 24 hours post-infection). Cells were harvested, and then pelleted by centrifuging at 11000prm (Thermo Scientific Heraeus Fresco 21). The pellet was resuspended in 150µl of fractionation buffer A (see table 2.2), and was incubated on ice for 15 minutes. The cytoplasmic membrane was disrupted by adding NP-40 (Sigma) (final concentration 1%) and vortexing for 10 seconds. The lysate was centrifuged at 4°C for 1 minute at 14000 rpm. The supernatant (post-nuclear

fraction) was removed, protein concentration was quantified, and then stored in 1X SDS-loading buffer (see table 2.2) at -20°C. The pellet (containing the nuclei) was resuspended in fractionation buffer B (see table 2.2), and incubated for 15 minutes on ice. The lysate was then centrifuged at 4°C for 1 minute at 14000 rpm. The supernatant (nuclear fraction) was then removed and stored in 1X SDS-loading buffer at -20°C. An equal percentage of nuclear and post-nuclear fractions was loaded onto a SDS-PAG electrophoresis gel, and the proteins were Western blotted as described in sections 2.3.2 - 2.3.5.

2.4 Adenovirus protocols

2.4.1 Stock adenovirus production

The virus were initially produced by Graciela B. Sala-Newby (Sala-Newby et al., 2003). The vectors pDC515 (coding for Myc-PRH, Myc-PRH N187A or no transgene) and pBHGfrt△E1,3FLP were co-transfected into HEK-293 cells. The pBHG vector contains expression casettes for the viral proteins (apart from E1 and E3), an inverted tandem repeat (ITR), a FLP recombinase and an frt sequence which is targeted by the FLP recombinase. The pDC515 plasmid contains the transgene, an ITR, the adenoviral packaging element (ψ) and an frt sequence. Co-transfection into HEK-293 cells leads to FLP producing a recombinant Ad vector, which contains the viral proteins and the transgene, but does not code for FLP. As HEK293 cells also produce viral E1 protein, the virus can replicate in this cell type. The adenovirus however cannot replicate in normal cell lines, and neither plasmid alone can produce adenovirus in HEK-293 cells. After a cytopathic effect was observed, the virus was then purified as explained in section 2.4.2.

2.4.2 Large-scale adenovirus production

To produce adenovirus, 10 x 75cm^2 flasks of HEK 293 cells were infected with stock adenovirus at a MOI of 2 in serum free DMEM for 2 hours, before returning the cells to their normal growth media. After a cytopathic effect was observed (usually 2-3 days), cells were harvested and resuspended in 7ml PBS. Cells were lysed by freezing in liquid nitrogen for 2 minutes, and thawing at 37°C for 5 minutes. This freeze-thaw process was repeated 3 times. The cell lysate was purified on a caesium chloride (CsCl) gradient using Beckmann 14 x 95 mm tubes by adding 2ml of 1.45 g/ml of CsCl, 2ml of 1.32 g/ml of CsCl, 2ml of 40% glycerol, and then the cell lysate in that order. The tube was then centrifuged for 18 hours at 32000 rpm using a Beckmann SW40 rotor, with no brake for deceleration. The purified virus was then visible as a band between the two CsCl layers. The virus was taken up by a 19G needle, and then placed in a Slide-a-Lyzer (Thermo scientific, 3500 MWCO, 0.5-3ml capacity, catalogue number 66330) for dialysis in adenovirus dialysis buffer (see table 2.2) for two hours, then in fresh dialysis buffer again for two hours, before dialysing overnight with fresh dialysis buffer with 10% glycerol.

2.4.3 Adenovirus titration

To titre the adenovirus, a modified version of the Clontech Adeno-X rapid titer protocol was used. Serial 10-fold dilutions of virus were made (starting from 10^{-2} to 10^{-7}), and 100µl from each dilution was used to infect 5x10^5 HEK 293 cells, which were then seeded in 1 well of a 12 well plate. The cells were left to grow in DMEM with 10% FBS. After 48 hours the media was aspirated off, and the cells were fixed by adding 1ml of methanol and leaving at -20°C

for 10 minutes. The cells were washed 3 times with PBS containing 1% w/v bovine serum albumin, and then incubated for one hour at 37°C with a murine anti-Hexon antibody (Abcam) diluted 1/2000 in PBS with 1% BSA. After washing again 3 times in PBS with 1% BSA, the cells were incubated for one hour at 37°C with horseradish peroxidase conjugated goat anti-mouse IgG antibody (Santa Cruz Biotech) diluted 1/500 in PBS with 1% BSA. After washing 3 times with PBS plus 1% BSA, the DAB staining kit (Vector laboratories) was used to visualise infected cells. The titre was determined by the following equation:

$$\frac{\text{(infected cells/field) x (fields/well)}}{\text{Volume virus (ml) x dilution factor}}$$

2.4.4 Adenovirus infection

For the adenovirus infection the adenovirus used is described in (Soufi and Corinne Smith, 2006). One million MCF-10A, MCF-7 or MDA-MB-231 cells were infected with either empty adenovirus or Myc-PRH containing adenovirus at a multiplicity of infection (MOI) of 50. Cells were then plated straight away in 2 x 75cm^2 flasks in RPMI as before (but containing only 2% heat-inactivated FBS, 5x10^5 cells in each flask). Cells were then counted using a haemacytometer and trypan blue exclusion dye (Sigma) before being used for protein extraction, RNA extraction, cell cycle analysis or Annexin-V staining after 2 or 4 days.

2.5 Lentivirus protocols

2.5.1 Generating inducible knockdown lentiviruses

To produce lentiviruses, five million HEK-293T cells were seeded into a 75cm^2 tissue culture flask and left overnight, so that they would reach a confluency of over 50%. Cells were transfected using Lipofectamine 2000 (Invitrogen), with 7µg each of plasmids psPAX2 (containing GAG and POL), pMD2.G (containing ENV) and the corresponding pLKO plasmid containing the shRNA of interest. The media was replaced after 24 hours, and the media containing the lentivirus was harvested 2 and 3 days post-transfection. The lentivirus was purified from the media by ultracentrifugation, using 14x95mm polyallomer centrifuge tubes (Beckmann), at a speed of 16600 rpm using a SW40 rotor. The supernatant was poured off and the pellet was left on ice for 2 hours, before being resuspended in the remaining supernatant (approximately 100µl).

2.5.2 Generating inducible knockdown cell lines

To produce IPTG-induceable knockdown cell lines, cells were infected with 20µl of purified lentivirus (this translates to an approximate MOI of 0.1, i.e. 10% of the cells will be selected for using puromycin). The media was replaced after 24 hours, and 48 hours post-infection infected cells were selected for, by culturing cells in 0.5µg/ml puromycin (Sigma) for 7 days. Uninfected cells were used as a negative control for the selection process, and there were

no viable cells after 7 days. After selection shRNA expression was induced by incubating the cells in 1mM IPTG for 7 days. Knockdown of PRH protein was then confirmed using Western blotting.

2.6 Antibody staining protocols

2.6.1 Immunofluorescence and confocal microscopy

To carry out immunofluorescence, firstly $5x10^5$ cells were seeded onto a 22x22 mm Surgipath premier cover glass, which was pre-sterilised with 70% ethanol. Cells were then left overnight to attach to the cover glass. The cells were washed 3 times with PBS, and were fixed using 4% w/v formaldehyde for 10 minutes. After washing with PBS 3 times, the cell membrane was then permeabilised using 0.2% triton diluted in PBS, and being placed on ice for 15 minutes. The cells were incubated with 0.5% w/v SDS for 5 minutes on ice, for antigen presentation. The coverslips were washed four times with PBS, and were blocked by incubating with 3% bovine serum albumin for 20 minutes at room temperature. After washing three times with PBS, the cover slips were incubated with the relevant primary antibody, which was diluted 1 in 200 in 3% bovine serum albumin in PBS (apart from M6 antibody which was diluted 1 in 1000), for 1 hour in the dark at room temperature. After washing 3 times with PBS, the relevant secondary antibody was diluted 1:200 in 3% bovine serum albumin in PBS, and was then placed on the cover slip for 1 hour at room temperature in the dark. After washing twice with PBS, cells were incubated with TO-PRO-3 (Invitrogen), diluted 1 in 1000 in PBS, for 10 minutes at room temperature. The cover slips

were then placed onto a microscope slide using Immumount (Thermo Scientific), and each coverslip was then sealed using clear nail varnish. Images were then taken using a Leica TCS SP2 confocal microscope, using a 63x objective immersed in oil and a numerical aperture of 1.4. The excitation laser wavelength was 633nm for TO-PRO-3, and was 488nm for FITC and 543nm for TRITC.

2.6.2 Bromodeoxyuridine assay

For bromodeoxyuridine (BrdU) assays, 5 x 10^5 cells were plated onto a 6-well plate, and were left to attach overnight. Cells were then incubated with 10μM BrdU (Sigma) for 6 hours. The media was removed, and cells were then washed with PBS. Cells were fixed with 4% w/v formaldehyde for 10 minutes at room temperature. Cells were washed three times with PBS before the cell membrane was permeabilised using 1% v/v triton in PBS. Cells were washed in PBS, before endogenous peroxidase activity was blocked by incubating the cells in 3% v/v H_2O_2 (Sigma) freshly diluted in distilled water for 5 minutes at 4°C. Cells were then washed twice in PBS, before the DNA double strands were denatured by incubating with 2M HCl for 30 minutes at 37°C. Cells were washed in PBS, and cells were incubated in murine anti-BrdU antibody (Sigma), diluted 1 in 500 in 1% w/v bovine serum albumin, 10% v/v horse serum in PBS overnight at 4°C. Cells were then washed three times before incubating with biotinylated horse anti-mouse IgG (Vector Laboratories), diluted in 1% w/v Bovine serum albumin in PBS for 30 minutes at room temperature. Cells were washed twice in PBS, before being incubated with Extravadin-peroxidase (Sigma), diluted in 1% w/v bovine serum albumin in PBS for 30 minutes at room temperature. Cells were then washed twice, before being stained with 3,3'-diaminobenzidine (DAB) solution (consisting of 1 DAB gold and 1

DAB silver tablet (Sigma), diluted in 5ml distilled water) for 10 minutes at room temperature. The percentage of positive to total number of cells was then counted using an inverted microscope at 100x magnification.

2.7 DNA protocols

2.7.1 Preparation of competent *Escherichia coli (E. coli)* XL-1 blue cells

XL-1 blue *E. coli* cells were inoculated into 5ml of LB broth (Sigma) and incubated into a shaking incubator at 200rpm at 37°C for 16 hours. 0.5ml of this culture was then diluted into 50ml of LB broth, and incubated at 37°C until the cells were in the exponential phase of growth (determined by an OD of >0.5 and <1 at 650nm). The culture was kept at 4°C for 10 minutes, before centrifugation at 4000 rpm for 5 minutes at 4°C (Thermo Scientific Heraeus Fresco 21). The pellet was resuspended in 25ml of sterile 0.1M $CaCl_2$, and was incubated at 4°C for 20 minutes. This suspension was centrifuged at 4000 rpm at 4°C for 5 minutes, and the pellet was resuspended very gently in 2ml of 0.1M $CaCl_2$. Glycerol was added to the cell suspension, to give a final concentration of 40% glycerol. This was aliquotted into 100µl per Eppendorf tube, and stored at -80°C.

2.7.2 Transformation of XL-1 blue *E. coli* cells

To transform XL-1 blue cells, 50ng of plasmid was mixed with 100µl of XL-1 blue cells, and was left to incubate on ice for 20 minutes. The cells were placed in a waterbath set at 42.5°C for 90 seconds, and were then placed on ice for 2 minutes. Following this cells were recovered by adding 1ml of LB broth, and incubating the cells at 37°C for 45 minutes. The cell cultures were then centrifuged at 13000 rpm in a tabletop centrifuge (Eppendorf 5424), for 30 seconds. The supernatant was discarded, and the remaining cells were spread on an LB agar plate (LB broth + 1.5% w/v Bacteriological agar), containing 50µg/ml ampicillin. Plates were incubated at 37°C overnight.

2.7.3 Purification of plasmid DNA

Plasmid DNA was purified using the QIAGEN maxi prep kit (QIAGEN 12163) according to manufacturer's instructions. Briefly, one colony from the agar plate was inoculated into 5ml of LB broth containing 50µg/ml ampicillin for 8 hours at 37°C, shaking at 300 rpm. 0.1ml of this starter culture was diluted into 100ml of LB broth, and left to grow overnight at 37°C, shaking at 300 rpm. The bacterial cells were centrifuged at 4000 rpm (Eppendorf 5810 R). The cells were resuspended in 10ml buffer P1. The cells were lysed by adding 10ml of buffer P2, inverting the tube 5 times, and leaving at room temperature for 5 minutes. The reaction was neutralised by adding 10ml of buffer P3, inverting 5 times, and incubating on ice for 20 minutes. The lysate was filtered using Whatmann filter paper (Catalogue number 1441 150).

After equilibrating a QIAGEN-tip 500 by flowing 10ml of buffer QBT through the tip, the filtered supernatant was then loaded onto the QIAGEN-tip. The QIAGEN-tip was then washed with 60mls of buffer QC, and the DNA was then eluted from the tip using 15ml of buffer QF. The DNA was precipitated by adding 10.5ml of isopropanol, and centrifuging at 4000 rpm at 4°C for 1 hour (Eppendorf 5810R). The DNA pellet was washed with 5ml of 70% ethanol, and centrifuged again at 4000 rpm at 4°C for 1 hour (Eppendorf 5810R). The pellet was then left to air dry for 15 minutes, and finally resuspended in 100µl TE buffer.

2.7.4 Phenol:chloroform:isoamylalchohol (PCI) extraction and DNA precipitation

The bottom layer of the phenol:chloroform:isoamylalcohol (25:24:1) mixture was added in equal volume to the DNA solution, and was vortexed for 30 seconds. This mixture was centrifuged at 13000 rpm (Eppendorf 5424) for 5 minutes, with the resulting upper layer carefully removed. Sodium acetate was added (pH 5.2) to give a final concentration of 0.3M, and also 50µg of glycogen and 2.5 volumes of ice-cold 100% ethanol. After vortexing for 30 seconds, the solution was incubated at -20°C for 10 minutes, and was then centrifuged at 13000 rpm at 4°C for 10 minutes. The supernatant was poured off and the pellet was washed with 1ml 70% ice cold ethanol. This was centrifuged at 13000 rpm at 4°C for 10 minutes, with the resultant pellet being air-dried for 15 minutes. The pellet was resuspended in the appropriate volume of TE buffer.

2.8 Quantitative PCR protocols

2.8.1 RNA extraction

RNA was extracted from cells using a Bioline ISOLATE II RNA mini kit. For details see manufacturer's instructions. Briefly, $5x10^5$ cells were pelleted, and resuspended in 450 µl of lysis buffer R, which was then incubated for 3 minutes at room temperature. This was transferred to spin column R1, and centrifuged at 10000g for 2 minutes (Eppendorf 5424). An equal volume of 70% ethanol was added to the filtrate, and was placed into spin column R2. This was then centrifuged at 10000g for 2 minutes. 500µl of wash buffer AR was added to the column, and was centrifuged at 10000g for 1 minute. 700µl of wash buffer BR was added to the column, and was centrifuged at 10000g for 1 minute. The collection column was centrifuged at 10000g for 3 minutes, to remove any residual alcohol. The RNA was eluted, by adding 30µl of nuclease free water to the spin column, and then spinning at 6000g for 1 minute. The RNA concentration was then quantified using a NanoDrop.

2.8.2 Complementary DNA production

To produce the reaction mixture, 0.5µg of RNA was added to a final concentration of 1mM dNTPs and 20ng/µl random hexamer primers (Thermo Scientific), to a final reaction volume of 12µl. This solution was then incubated at 65°C for 5 minutes. To this reaction, Superscript III reverse transcriptase (Invitrogen) was added (to a final concentration of 10U/µl), 1x First Strand buffer (Invitrogen), Ribolock RNase inhibitor (Thermo Scientific) (to a final concentration of 10 units/µl) and dithiothreitol (DTT) (Invitrogen) to a final concentration of

10mM, giving a final reaction volume of 20µl. This reaction was incubated at 25°C for 10 minutes, 42°C for 90 minutes, and finally 72°C for 10 minutes. The final cDNA concentration was then quantified using a NanoDrop.

2.8.3 Quantitative PCR

Quantitative PCR was performed by using SYBR-green as a fluorescent dye, using a final reaction composition of: 100ng cDNA template, 1x Sensimix SYBR sensimix no ROX (Bioline), 200nM forward primer and 200nM reverse primer (final reaction volume was 15µl) (Primers were ordered from MWG Eurofins). The reaction was placed in a Corbett Research RG-3000 Rotorgene thermocycler, using the following thermal parameters: 95°C for 10 minutes, 45 cycles of 95°C for 15 seconds, 60°C for 20 seconds (55°C for *GAPDH*, and 62°C for *VEGFA*), and 72°C for 5 seconds. A melting step of between 72°C and 95°C was then carried out (hold at 72°C for 45 seconds, then inclining by 1°C for 5 seconds thereafter), to determine whether one specific PCR product was formed. Each biological replicate was carried out as a technical triplicate. The data were analysed using Rotorgene 6 Software (Corbett Research, Rotorgene RG-3000). *GAPDH* was used as the internal control (unless stated otherwise). Results for relative expression ratios were calculated according to the Efficiency Calibrated Mathematical Model (as described in (Pfaffl, 2001a). Briefly, the following equation was carried out for each biological replicate:

$$E^{Ct}\ (\text{GAPDH}) \,/\, E^{ct}\ (\text{Gene of Interest})$$

The log of this equation was then taken, and a statistically significant difference was determined between control and knockdown/overexpression of PRH using a two-tailed Student's t-test (heteroscedasticity or homoscedasticty was determined using an F-test).

2.9 Flow cytometery protocols

2.9.1 Cell cycle analysis

Approximately 5 x 10^5 cells were centrifuged at 3000 rpm (Thermo Scientific Heraeus Fresco 21) and resuspended in 300µl RPMI media. IGEPAL and propidium iodide was added to a final concentration of 1% and 50µg/ml respectively. The sample was then put through a Beckton Dickson FACSCalibur flow cytometer, and analysed using FloJo software, after gating out dead cells using a FSC vs. SSC plot, which identifies debris/dead cells based on morphology.

2.9.2 Annexin-V apoptosis assay

Approximately 5 x10^5 cells were centrifuged at 3000 rpm (Thermo Scientific Heraeus Fresco 21) and resuspended in 100µl binding buffer (see table 2.2). 5µl of Annexin-V was added (BD Biosciences) and 5µl of 50µg/ml propidium iodide (Sigma), before incubating for 20 minutes in the dark. Another 200 µl of binding buffer was then added. The sample was then put through a Beckton Dickson FACSCalibur flow cytometer, and analysed using FloJo software, after gating out dead cells using a FSC vs. SSC plot.

2.9.3 CD24/CD44 staining

To analyse CD24/CD44 expression, 1 x 10^5 cells were resuspended in 100µl of PBS. Cells were stained with 5µl of CD24-FITC (BD Biosciences) and 5µl of CD44-TRITC (BD Biosciences), and were left on ice in the dark for 15 minutes. Cell staining was analysed using a FACSCalibur flow cytometer (BD Biosciences), using laser channels FL1 and FL3. Analysis was carried out using FloJo software.

2.10 Migration and invasion assays

2.10.1 Transwell migration assay

Transwell migration assays were set up as follows; 4x10^4 cells were seeded into the upper chamber of a 8µm transwell insert (Greiner Bio-One), in 200µl growth media containing only 2% fetal calf serum (for MDA-MB-231 and MCF-7 cells), or growth media lacking EGF (for MCF-10A cells). The transwell was inserted into a 24-well plate, and the lower chamber contained 1ml of appropriate growth media, containing all supplements for each cell line. After either 24 or 48 hours at 37°C in 5% CO_2 (dependent on the cell line, see chapter 5), the upper and lower chambers were washed three times with PBS, and cells were then fixed with 2% w/v formaldehyde, which also contained 2µg/ml bisbenzimide to stain the cell nuclei. After washing three times with PBS, the membrane of the transwell chamber was cut

out using a scalpel, and was placed onto a microscope slide. The slide was then sealed using a coverslip (Surgipath), Vectamount (Vector Laboratories) and clear nail varnish. The number of cells was then counted in three fields on the upper and lower parts of the membrane, using a Zeiss Axioplan 2 fluorescent microscope, at 200x magnification under UV light. The number of cells on the lower part of the membrane was then divided by the total number of cells, to give the percentage of migrated cells.

2.10.2 Matrigel invasion assay

Matrigel (BD Biosciences) was thawed by storing overnight at 4°C. Matrigel was then diluted 1 in 2 in serum-free media, and 50µl of the diluted Matrigel was pipetted into 8µm transwell inserts (Grenier Bio-One), which were inserted into 24 well plates. The plates were kept at 37°C for two hours to allow the Matrigel to set. 4 x 10^4 cells were seeded into the upper chamber in 200µl growth media containing only 2% fetal calf serum (for MDA-MB-231 and MCF-7 cells), or no EGF (for MCF-10A cells). After either 24 or 48 hours at 37°C in 5% CO_2 (dependent on the cell line, see chapter 5), the Matrigel was removed using a cotton bud. The upper and lower chambers were then washed three times with PBS, and cells were then fixed with 2% w/v formaldehyde, which also contained 2µg/ml bisbenzimide to stain the cell nuclei. After washing three times with PBS, the membrane of the transwell chamber was cut out using a scalpel, and was placed onto a microscope slide. The slide was then sealed using a coverslip (Surgipath), Immumount (Thermo Scientific) and clear nail varnish. The total

number of cells which had reached the transwell membrane was then quantified using a Zeiss Axioplan 2 fluorescent microscope, at 50x magnification under UV light.

2.10.3 Scratch wound assay

The day before scratch wound assays were to be carried out, $1x10^6$ cells were plated into a 6-well plate, so that the cells would be 100% confluent on the day of the assay. Twenty four hours later, the media was aspirated off, and a black horizontal line was drawn on the back of the 6-well plate. Three vertical scratches were then made with a P200 pipette tip, and excess cells were washed off with PBS. The media was replaced with media containing 1mM hydroxyurea, to prevent cell proliferation. Images were taken at each scratch above and below the black horizontal line, using an AMG Evos XL core Amex 1200 microscope on 100x magnification. Images were taken at 6 and 24 hours post wounding, and the area of each scratch was quantified using ImageJ software. The area of the scratch at either 6 or 24 hours was divided by the area of the scratch at 0 hours, to determine the percentage wound closure.

2.11 Mouse xenograft assay

The day before tumour cell injection, $8x10^7$ MCF-7 cells were infected with either Ad-PRH or Ad, at a multiplicity of infection of 50. Twenty four hours later, cells were harvested and

resuspended at a concentration of $5x10^7$ cells/ml. 100µl of cells ($5x10^6$ cells) were injected into each mammary fat pad of a 6 week old Balb/c female nude mouse, so that 8 mice were injected with cells containing Ad-PRH or Ad (16 mammary fat pads each). Four mice were also injected with MCF-7 cells which were not infected with adenovirus (8 mammary fat pads), and therefore 20 mice in total were used in this experiment. Mice were also had 0.72mg 17β-oestradiol tablets 60 day release (Innovative Research of America) tablets surgically implanted subcutaneously in their dorsal side. Tumour size was measured using callipers three times per week, and tumour volume was determined using the ellipsoid formula 0.5 x length x width x width (Euhus et al., 1986). Mice were then sacrificed when the tumours reached Home Office limits for tumour size.

2.12 Plasmids

pMUG1 Myc-PRH

This plasmid expresses a fusion protein consisting of an N-terminal Myc 9B11 epitope fused to amino acids 7-270 of human PRH (as described in Bess et al., 2003a).

pEGFP-PRH

This plasmid was created by inserting the PRH cDNA from a pBlueScript clone into the KpnI and EcoRI sites of pEGFP-C1 (as described in Desjobert et al., 2009).

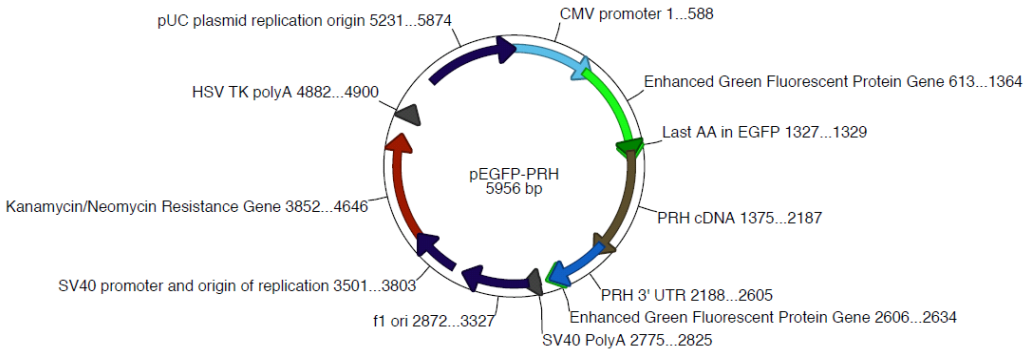

Figure 2.1: Schematic of the EGFP-PRH plasmid.

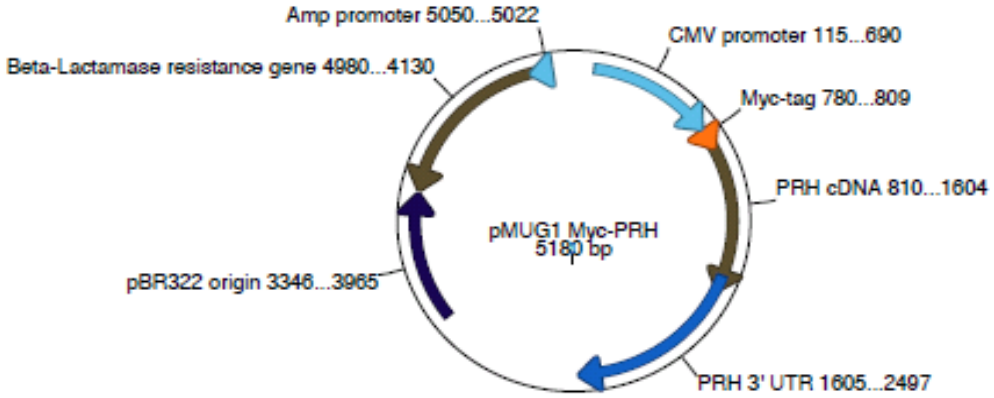

Figure 2.2: Schematic of the pMUG1 Myc-PRH plasmid.

pEGFP-C1

This plasmid expresses an enhanced green fluorescence protein. Commercially available from Clontech.

pLKO-puro-IPTG-3xLacO (PRH and control shRNA)

These constructs were obtained from Sigma. The DNA sequence for PRH shRNA knockdown is CTGTGATCAGAGGCAAGATTT (Clone ID TRCN0000274008), whilst the control sequence targets no known mammalian gene. The vector has a Woodchuck Hepatitis Post-Transcriptional Regulatory Element (WPRE), allowing for enhanced transgene expression. The vector also codes for LacI repressor protein, which binds to the three LacO sequences present in the human U6 promoter when no IPTG is present. IPTG, when present, binds allosterically to LacI protein, changing the conformation of the LacI so it can no longer bind to LacO sequences, and hence allows expression of the shRNA.

psPAX2

This vector was obtained from Addgene. This vector expresses a variant of the human HIV Gag and Pol proteins, needed for lentivirus production.

pMD2.G

This vector was obtained from Addgene. This vector expresses the VSV-G envelope protein from the vesicular stomatitis virus, needed for lentivirus production.

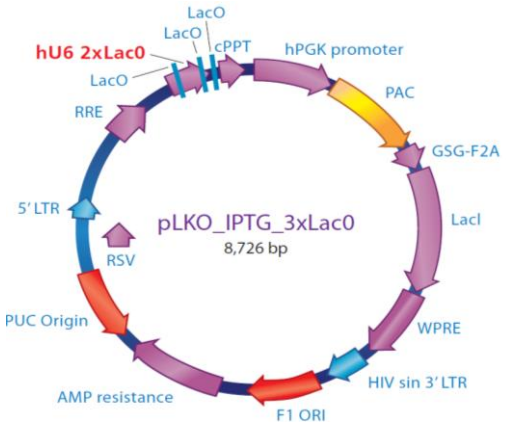

Figure 2.3: Schematic of the pLKO_IPTG_3XLacO plasmid.

Name	Description
cppt	Central polypurine tract
hPGK	Human phosphoglycerate kinase eukaryotic promoter
PAC	Puromycin N-acetyl-tranferase
WPRE	Woodchuck Hepatitis Post-Transcriptional Regulatory Element
SIN/LTR	3' self inactivating long terminal repeat
f1 ori	f1 origin of replication
AMP resistance	Ampicillin resistance gene for bacterial selection
PUC origin	pUC origin of replication
5' LTR	5' long terminal repeat
Psi	RNA packaging signal
RRE	Rev response element
LacI	Lac Repressor
GSG-F2A	Gly-Ser-Gly foot-and-mouth disease virus IRES 2A
RSV	Respiratory syncytial virus promoter

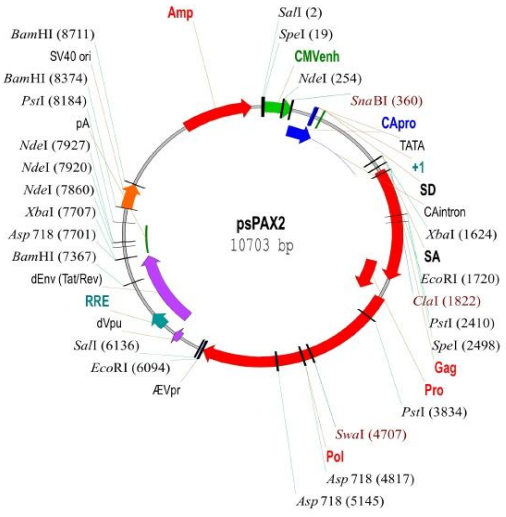

Figure 2.4: Schematic of the pSPAX2 plasmid.

Name	Description
Amp	Ampicillin resistance
CMVenh	Cytomegalovirus enhancer
CApro	Chicken beta-actin promoter
Gag	HIV Gag
Pro	HIV Pro
Pol	HIV Pol
RRE	Ribosomal response element
pA	Rabbit beta-blobin poly adenylation signal
SV40 ori	SV40 origin of replication
SD	Splice donor
SA	Splice acceptor
CA intron	Chicken beta-actin intron
AEVpr, dVpu, dEnv	Inactivated genes from HIV genome

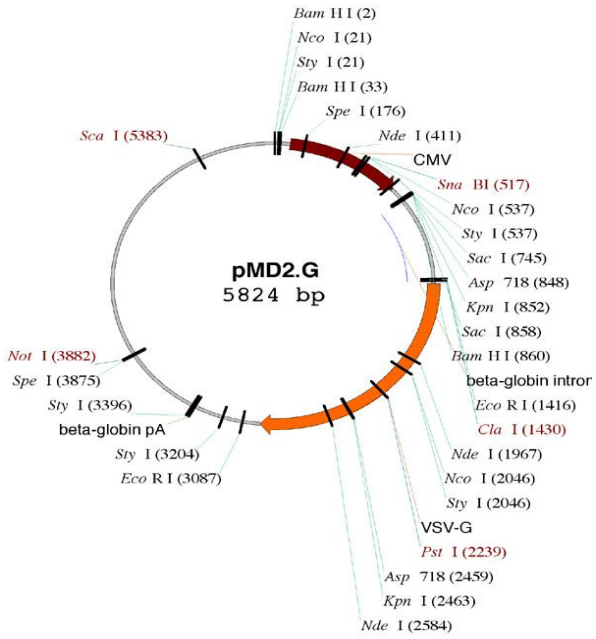

Name	Description
CMV	CMV promoter
VSV-G	Vesicular stomatitis Indiana virus G envelope protein
Beta-globin pA	Chicken beta-globin poly adenylation site

Figure 2.5: Schematic of the pMD2.G plasmid.

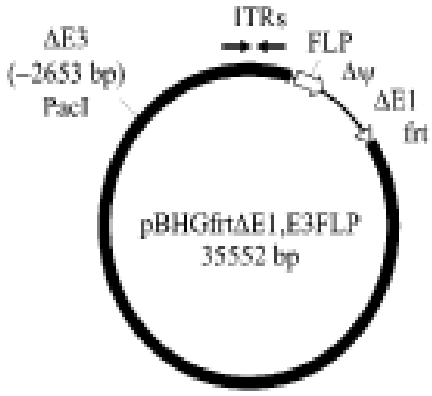

Name	Description
ITR	Inverted tamdem repeat
FLP	FLP recombinase
frt	Flippase recombination target
Δψ	Deletion – adenoviral packagine element
ΔE1, E3	Deletion- adenoviral E1 and E3 proteins

Figure 2.6: Schematic of the pBHGfrtΔE1,E3FLP plasmid.

pDC515

This vector is the viral shuttling vector, which is used for adenovirus production. For Ad (empty virus), the empty vector was used (i.e. did not code for any transgene). To produce Ad-PRH and Ad-PRH N187A, the coding regions from the pMUG1-PRH and pMUG1-PRH N187A plasmid described in (Noy et al., 2010) was excised using restriction endonucleases EcoRI and BamHI, blunted with micrococcal nuclease and ligated into pDC515 (as described in Palmer and Ng, 2008).

pBHGfrt△E1,3FLP

This vector codes for the viral proteins (minus E1 and E3) (as described in Palmer and Ng, 2008).

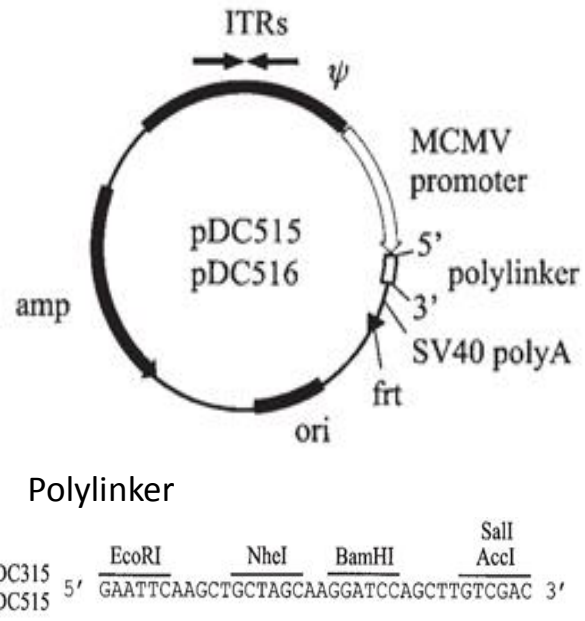

Name	Description
ITR	Inverted tamdem repeat
MCMV promoter	Maize chlorotic mottle virus promoter
SV40 polA	SV40 polyadenylation signal
frt	Flippase recombination target
Ori	Origin of replication
amp	Ampicillin resistance gene

Figure 2.7: Schematic of the pDC515 plasmid. To produce Ad-PRH and Ad-PRH N187A, the coding regions from the pMUG1-PRH and pMUG1-PRH N187A plasmid (described in Noy et al., 2010) was excised using restriction endonucleases EcoRI and BamHI, blunted with micrococcal nuclease and ligated into pDC515. The vector is as described in Palmer and Ng 2008.

2.13 Reagents and solutions

Table 2.1 – List of reagents

Reagent	Code
17β-Oestradiol tablets (0.72mg, 60 day release)	Innovative research of America SE-121
5-Bromo-2'-deoyuridine (BrdU)	Sigma B5002
Acrylamide (30%)	Geneflow A2-0074
Agarose	Sigma A9539
Ammonium persulphate	Sigma A3678
Anisomycin	Sigma A9789
Annexin-V	BD Biosciences 550474
Bacteriological Agar	Sigma A5306
Bisbenzimide	Sigma B1155
Bovine serum albumin	Sigma A2153
Bromophenol blue	Sigma B8026
Caesium chloride	Sigma 289329
Calcium chloride	Sigma C4901
Cholera Toxin	Sigma C8052
DAB (SIGMAFAST DAB with metal enhancer)	Sigma D0426
Dimethyl sulphoxide	Fischer BP231
Dithiothreitol (DTT)	Sigma D9779 Invitrogen 18080-044
DMEM:F12	Sigma D8737
DNA 100 base pair ladder	New England Biolabs N3231S
DNA loading biffer (comes with ladder)	New England Biolabs N3231S
dNTP mastermix	Invitrogen 10297018
Dulbecco's modified Eagle's medium (DMEM)	Sigma D5796
Dynabeads Protein A	Invitrogen 10001D
Enhanced Chemiluminescense solution	GE Healthcare RPN2106
Epidermal Growth Factor	Peprotech AF-100-15
Ethanol	Fischer Scientific BP2818
Ethylene glycol-bis(2-aminoethylether)-N,N,N',N'-tetraacetic acid (EGTA)	Sigma E3889
Ethylenediaminetetraacetic acid (EDTA)	Sigma E5134
Fetal Bovine Serum	Sigma F7524
First strand buffer (comes with Superscript III)	Invitrogen 18080-044
Formaldehyde (37%)	Fischer Scientific BP531
Glycerol	Fischer Scientific G30
Glycine	Sigma G8898
Glycine	Sigma 241261
Glycogen	Calbiochem CAS 9005-79-2
Hanks' Balanced Salt Solution	Sigma H6648

Reagent	**Code**
Heparin	StemCell Technologies 07980
HEPES	Sigma H3375
Horse Serum Heat Inactivated	Sigma H1138
Human Insulin Solution	Sigma I9278
Hydrochloric acid (33%)	Sigma H1758
Hydrocortisone	Sigma H0888
Hydrogen peroxide (30%)	Sigma 216763
Hydroxyurea	Sigma H8627
Igepal CA-630	Sigma I8896
Immumount	Thermo Scientific 9990402
Isopropanol	Sigma I9516
Isopropyl β-D-1-thiogalactopryanoside (IPTG)	Bioline 37036
LB Broth	Sigma L3152
Lipofectamine 2000	Invitrogen 11668
Magnesium chloride	Sigma M8266
MammoCult Basal Medium	StemCell Technologies 05621
MammoCult Proliferation Supplements	StemCell Technologies 05622
Matrigel	BD Biosciences 356234
Methanol	Fischer Scientific A413
NP-40	Sigma I8896
Pageruler Plus protein ladder	Thermo Scientific SM1811
PBS tablets	Sigma P4417
Penicillin/Streptomycin (x100)	PAA P11-010
Phenol:chloroform:isoamyl alcohol 25:24:1	Sigma P3803
Ponceau S solution	Sigma P7170
Propidium iodide	Sigma P4170
Protease inhibitor tablet	Roche 04 693 124 001
Protein Assay reagent	Bio-Rad 500-0006
Proteinase K	Sigma P2308
Puromycin dihydrochloride	Sigma P8833
Random hexamer primer	Thermo Scientific SO142
REDTaq readymix PCR reaction mix	Sigma R2523
Ribolock RNase inhibitor	Thermo Scientific EO0381
RPMI-1640	Sigma R8758
Sodium azide	Sigma S8032
Sodium chloride	Sigma S9265
Sodium deoxycholate	Sigma D6750
Sodium dodecyl sulphate	Sigma L4509
Superscript III reverse transcriptase	Invitrogen 18080-044
SYBR safe DNA gel stain 10000x	Invitrogen S33102
SYBR sensimix no ROX	Bioline QT650
Tetramethylethylenediamene	Sigma T9281
Thiazolyl blue formazan [1-(4,5-dimethylthiazol-2-yl)-3,5-diphenylformazan] (MTT)	Sigma M2003
TO-PRO-3 Iodide	Invitrogen T3605

Reagent	Code
Triton X-100	Sigma T8787
Trizma base	Sigma T4661
Trypsin-EDTA (X10)	PAA L11-003
Tween-20 (Polyoxyethylene sorbitan monolaurate)	Sigma P1379

2.14 Solutions

Table 2.2 – List of solutions

Solution	Composition
Adenovirus dialysis buffer	135 mM NaCl 10mM Tris-Cl (pH 7.5) 1mM $MgCl_2$
Annexin-V binding buffer	10mM HEPES pH 7.4 140mM NaCl 2.5 mM $CaCl_2$
ChIP elution buffer	20mM Tris-Cl (pH 7.5) 50mM NaCl 5mM EDTA
ChIP lysis buffer	50mM Tris-Cl (pH 8.0) 10mM EDTA 1% SDS Protease inhibitor tablet
ChIP RIPA buffer	10mM Tris-CL (pH 8.0) 140mM NaCl 1% v/v Triton X-100 1mM EDTA 1mM EGTA 0.1% w/v SDS 0.1% sodium deoxycholate
Fractionation buffer A	20mM Tris-Cl (pH 7.5) 5mM $MgCl_2$ 1 mM DTT Protease inhibitor tablet
Fractionation buffer B	50mM Tris-Cl (pH 7.5) 500mM NaCl 1% v/v NP-40 0.1% w/v SDS Protease inhibitor tablet

Solution	**Composition**
Mammosphere media	10% v/v MammoCult Proliferation Supplements 4µg/ml heparin 0.5µg/ml hydrocortisone 100 units/ml penicillin 0.1mg/ml streptomycin In MammoCult Basal Medium
QIAGEN Buffer P1	50mM Tris-Cl (pH 8.0) 10mM EDTA (pH 8.0) 100µg/ml Rnase A
QIAGEN Buffer P2	200mM NaOH 1% w/v SDS
QIAGEN Buffer P3	3.0 M potassium acetate pH 5.5
QIAGEN Buffer QBT	750mM NaCl 50mM MOPS (pH 7.0) 15% isopropanol 0.15% Triton X-100
QIAGEN Buffer QC	1M NaCl 50mM MOPS (pH 7.0) 15% isopropanol
QIAGEN Buffer QF	1.25M NaCl 50mM MOPS (pH 7.0) 15% isopropanol
Resolving Buffer (1x)	0.1% w/v SDS 375mM Tris-HCl Final pH 8.8
RIPA Buffer	150mM NaCl 1% v/v NP-40 0.5% v/v sodium deoxycholate 0.1% v/v SDS 50mM Tris-Cl (pH7.5) Protease inhibtor tablet
Running Buffer (1x)	0.1% w/v SDS 25mM Tris 192mM Glycine
SDS gel loading buffer (1x)	50mM Tris-Cl (pH 6.8) 100mM DTT 2% w/v SDS 0.1% bromophenol blue 10% glycerol

Solution	Composition
Stacking buffer (1x)	0.1% w/v SDS 125mM Tris-HCl Final pH 6.8
TAE buffer	40mM Tris-Acetate 1mM EDTA
TE buffer	10mM Tris-Cl (pH 8.0) 1mM EDTA (pH 8.0)
Transfer buffer (1x)	10mM Tris 100mM glycine 0.05% w/v SDS 20% v/v methanol

2.1 Antibodies

Table 2.3 – List of Antibodies

Antibody	Source	Code
Anti-BrdU antibody	Murine	Sigma B2531
Anti-CD24 antibody FITC conjugated	Murine	BD 555427
Anti-CD44 antibody TRITC conjugated	Murine	BD 555479
Anti-hexon antibody	Murine	Abcam ab8249
Anti-Lamin A/C (H-110)	Rabbit	Santa Cruz Biotech sc-20681
Anti-mouse IgG biotinylated	Horse	Vector Laboratories BA-2000
Anti-mouse IgG HRP conjugated	Goat	Santa Cruz Biotech sc-2005
Anti-Myc antibody	Murine	New England Biolabs 2276
Anti-rabbit IgG HRP conjugated	Goat	Santa Cruz Biotech sc-2313
ExtrAvadin-Peroxidase	Egg white	Sigma E2886
Normal IgG	Murine	Santa Cruz Biotech sc-2025

2.16 PCR primers

Table 2.4 – List of qPCR primers

Primer		**Sequence (5' - 3')**
VEGF-A	Forward	ATC AGC GCA GCT ACT GCC ATC C
VEGF-A	Reverse	TCT CCT ATG TGC TGG CCT TGG TG
PRH	Forward	CAC CCG ACG CCC TTT TAC AT
PRH	Reverse	GAA GGC TGG ATG GAT CGG C
VEGFR-1	Forward	TGG CCA TCA CTA AGG AGC ACT CC
VEGFR-1	Reverse	GGA ACT GCT GAT GGC CAC TGT G
VEGFR-2	Forward	TTA GTG ACC AAC ATG GAG TCG TG
VEGFR-2	Reverse	TAG TAA AGC CCT TCT TGC TGT CC
GAPDH	Forward	TGA TGA CAT CAA GAA GGT GGT GAA G
GAPDH	Reverse	TCC TTG GAG GCC ATG TGG GCC AT
Goosecoid	Forward	CTT CTC AAC CAG CTG CAC TGT CG
Goosecoid	Reverse	ACT CCT CTG ATG AGG ACC GCT TC
Neuropilin	Forward	TAT TCC CAG AAG TCT GCC C
Neuropilin	Reverse	TGT CAT CCA CAG CAA TCC CA
ESM-1	Forward	TCG AGC ACT GTC CTC TTG CA
ESM-1	Reverse	GTG GAC TGC CCT CAA CAC TGT
SATB1	Forward	TGC AAA GGT TGC AGC AAC CAA AAG C
SATB1	Reverse	AAC ATG GAT AAT GTG GGG CGG CCT
Endoglin	Forward	GCC GTG CTG GGC ATC ACC TT
Endoglin	Reverse	CGC TTG CTG GGG GAA CCT GG
p53	Forward	CCT ATC CTT ACC ATC ATC ACA CTG
p53	Reverse	TTC TTC TGT ACG GCG GTC TC
E-Cadherin	Forward	GTA ACG ACG TTG CAC CAA CC
E-Cadherin	Reverse	AGC CAG CTT GAA GCG AT
Beta-actin	Forward	TCA CCC ACA CTG TGC CCA TCT ACG A
Beta-actin	Reverse	CAC CGG AAC CGC TCA TTG CCA ATG G

CHARACTERISATION OF EXOGENOUS AND ENDOGENOUS PRH IN MULTIPLE BREAST CELL LINES

3. Characterisation of exogenous and endogenous PRH in multiple breast cell lines

3.1 Introduction

This chapter will first investigate the PRH/Hhex expression data present in the Gene Expression-Based Outcome for Breast Cancer Online (GOBO) database. The GOBO database contains mRNA expression data of 1881 breast cancer patients from 11 public data sets, which have been analysed using Affymetrix U133A arrays. The database allows genes or sets of genes to be examined using Gene Set Analysis (GSA), which correlate gene expression data with Kaplan-Meier plots of overall survival, and also compares expression for a particular gene (or set of genes) to breast cancer grade and type. The GOBO database also allows expression of a single gene to be interrogated across a large set of commonly used breast cell lines. Using this database, the correlation between *PRH* mRNA expression and breast tumour grade, subtype, survival and cell line type will be evaluated. Secondly, a new monoclonal antibody raised against PRH will be characterised and then used to investigate PRH protein expression levels in a set of breast tumour cell lines. Thirdly PRH protein expression, stability and sub-cellular localisation will be investigated in three well characterised breast cell lines: a non-tumourgenic immortalised cell line MCF-10A, and in MCF-7 and MDA-MB-231 tumour cell lines (Debnath et al., 2003a, Lacroix and Leclercq, 2004a).

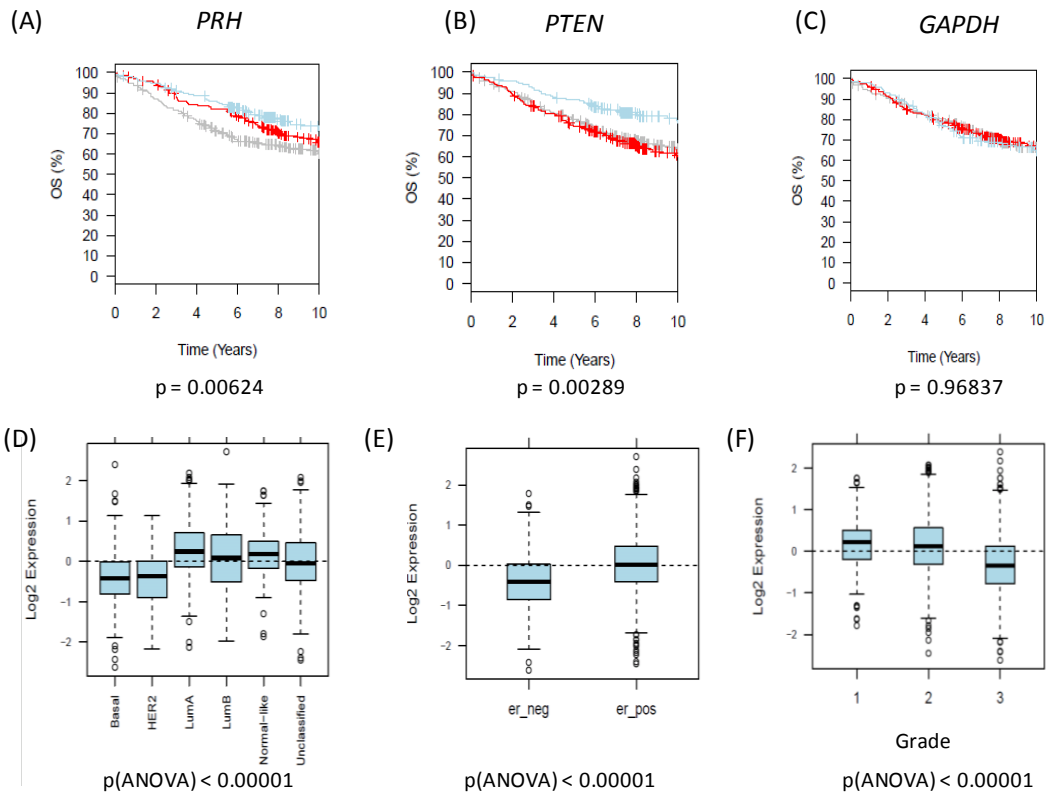

Figure 3.1. PRH is a marker for breast cancer survival. The GOBO database (Ringnér et al., 2011) was used to query the expression levels of *PRH* (A), *PTEN* (B) or *GAPDH* (C) transcript in breast tumours of 1881 patients, analysed using Affymetrix U133A arrays and na.30 gene probe set descriptions, and log2 expression values were mean centered. This was used to produce Kaplan-Meier plots for low (grey), medium (red) and high (blue) gene expression, with significance measured by Logrank test. Patients with high amounts of *PRH* transcript have significantly increased chance of overall survival than those with low amounts of *PRH* transcript. *PTEN* expression is also a positive marker for overall survival, whereas *GAPDH* is not. The GOBO database was also used to correlate *PRH* expression with breast cancer type. Figure 1 (D) shows that *PRH* expression is significantly lower in basal and *HER2* amplified cancers, and is highest in Luminal A cancers. Figure 1 (E) shows that *PRH* expression is significantly higher in ER+ breast tumours than ER- breast tumours. Figure 1 (F) shows that *PRH* expression is significantly lower in grade 3 breast tumours than in grade 1 or 2 breast tumours.

3.2 *PRH* mRNA expression correlates with increased survival

When *HHEX* (*PRH*) is queried in the GOBO database, Kaplan-Meier plots show that *PRH* mRNA expression significantly correlates with overall survival over 10 years across all breast tumour subtypes (figure 3.1 (A)). As a comparison, mRNA expression of the tumour suppressor gene *PTEN* and the housekeeping gene *GAPDH* was also queried in the same database. Increased *PTEN* transcript expression also correlates with increased overall survival, whereas *GAPDH* does not (figure 3.1 (B and C)). Interestingly *PRH* transcript

expression is significantly higher in Luminal A tumours (which are usually the least aggressive), and is significantly lower in basal and *HER2* amplified tumours (which are usually the most aggressive) (figure 3.1 (D)). Furthermore *PRH* mRNA expression is significantly higher in ER+ tumours than ER- tumours (figure 3.1 (E)), which agrees with figure 3.1 (D), as Luminal A tumours are typically ER+. When breast tumours are subdivided according to grade *PRH* mRNA expression is found to be significantly reduced in grade 3 breast tumours, compared to grade 1 or 2 tumours (figure 3.1 (F)). Grade 3 tumours are tumours which histologically have low tubule formation, increased variation in nuclei shape and size, and an increased number of mitotic cells compared to grade 1 or 2 tumours. Thus decreased *PRH* mRNA expression appears to be a significant marker for poor prognosis and more aggressive breast tumours.

3.3 Characterising the mouse monoclonal (M6) anti-PRH antibody

K562 haematopoietic cells express PRH proteins that have previously been detected using in house polyclonal antibodies (Bess et al., 2003a, Soufi et al., 2009). Limited quantities of these well characterised PRH antibodies were available for PRH protein expression studies in breast cells, and there is a lack of reliable commercially available PRH antibodies. This led to the generation of a new mouse monoclonal antibody (M6). The M6 antibody was raised against a peptide in human PRH consisting of amino acids SPFLQRPLHK (amino acids 127-136). This sequence lies 2 amino acids N-terminal to the homeodomain.

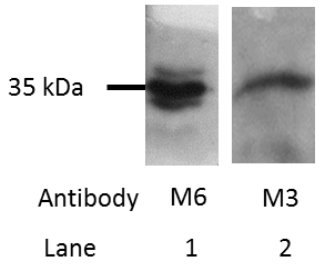

Figure 3.2: Detecting PRH in K562 cells using M6 and M3 antibodies. K562 leukaemic cell extracts (20µg) were probed with either the murine polyclonal M3 or the murine monoclonal M6 anti-PRH antibodies. M3 antibody detects a single band at 37kDa, whilst M6 antibody detects a triplet of bands at 37kDa in this cell line. This implies that one or more of the triplet of bands detected by the M6 antibody corresponds to PRH protein.

PRH protein has a predicted molecular weight of 30 kDa, but has an apparent molecular weight of 37 kDa on a SDS-PAGE gel because it is SDS resistant (Soufi et al., 2006). To determine whether the M6 monoclonal antibody recognises a 37kDa band corresponding to the PRH protein in K562 leukaemic cells, whole cell extracts were prepared and Western blotted as described in the Materials and methods section 2.3. Briefly, 20µg of protein was loaded in each lane of a SDS-PAG gel and the samples were electrophoresed to separate proteins according to size. Western blotting of the samples was performed with the M6 antibody. The cell extracts were also probed with polyclonal anti-PRH antibody (M3) for comparison. The mouse polyclonal M3 antibody was raised against a GST-fusion protein containing the N-terminal domain of PRH (Bess et al., 2003b). Figure 3.2 shows that in K562 extracts the M6 antibody (lane 1) recognises a triplet of bands at approximately 37kDa. The bands are of similar mobility to the single protein recognised by the M3 antibody (lane 2) suggesting that the M6 antibody is recognising endogenous PRH proteins in K562 cells, but that it may recognise more than one conformation of PRH, or that it may recognise PRH with different post-translational modifications.

To determine whether M6 will detect endogenous PRH in breast cells, protein extracts prepared from MDA-MB-231 cells were electrophoresed and Western blotted with M6

antibody as before. Figure 3.3 shows that the M6 antibody recognises a protein of approximately 37kDa. To confirm that this protein is PRH, MDA-MB-231 cells were knocked down for PRH expression using a lentivirus that expresses an inducible shRNA against *PRH*. Details of the method are outlined in Materials and methods section 2.5. Whole cell extracts prepared from MDA-MB-231 control and knockdown cells were Western blotted with M6 antibody and M3 antibody and with Lamin antibody. Lamin protein levels were used as a control for equal protein loading. Figure 3.3 shows that the 37kDa PRH protein is reduced in intensity in PRH knockdown cells probed with both M3 and M6 antibodies (figure 3.3). Interestingly the PRH protein is also observed as a triplet of bands of approximately 37kDa in MDA-MB-231 extracts (see figures 3.3 and 3.4). Knockdown of PRH results in a decrease in all 3 bands. In conclusion, these studies together demonstrate that the M6 antibody can recognise endogenous PRH, and that M6 antibody recognises multiple post-translational forms of PRH or multiple conformations of the PRH protein.

To determine whether M6 recognises recombinant PRH protein, MDA-MB-231 cells were transfected with Myc-PRH and GFP-PRH expression plasmids. The Myc-PRH plasmid encodes the human PRH with a Myc-tag replacing the first 7 amino acids of PRH (Swingler et al., 2004). The GFP-PRH plasmid encodes the entirety of PRH in frame with GFP, resulting in expression of a fusion protein (both plasmids were previously constructed in the laboratory and are described in Materials and methods section 4.12). Whole cell protein extracts from untransfected cells and transfected cells were Western blotted as described above. Figure 3.4 shows that as expected a protein of approximately 37 kDa corresponding to endogenous PRH is recognised in extracts from un-transfected (lane 1) and transfected cells (lanes 2 and 3). Unexpectedly there is not an additional protein band detected by the M6 antibody that

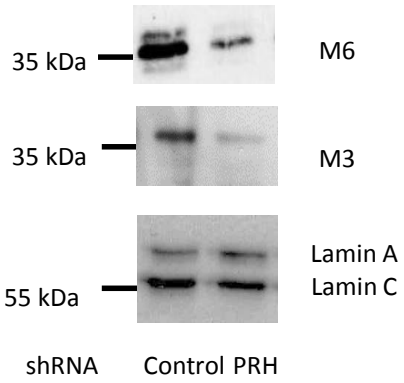

Figure 3.3: PRH knockdown can be detected by the mouse monoclonal anti-PRH antibody. MDA-MB-231 cells were infected with lentivirus coding for IPTG inducible shRNA targeting either *PRH* or a control shRNA that does not target any known mammalian gene. Selection for transfected cells was then performed 48 hours post-infection using 0.5 µg/ml puromycin; puromycin resistant mixed cell population cell lines were generated. The shRNA was induced using 1mM IPTG for 7 days in both PRH and control shRNA cell lines. Cells were then lysed and the protein was then analysed using Western blotting with M6, M3 and Lamin A/C antibodies. Representative of three experiments.

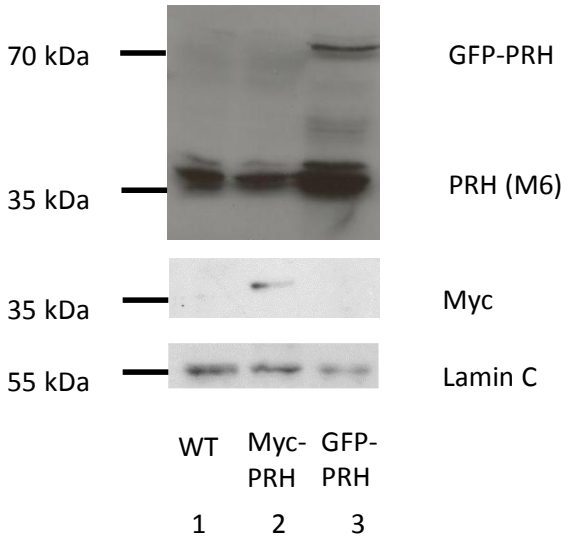

Figure 3.4: Monoclonal mouse anti-PRH antibody detects endogenous PRH and exogenous GFP-PRH. MDA-MB-231 extracts (20ug) prepared from cells transfected with Myc-PRH or GFP-PRH expression plasmids were probed using M6 antibody, Myc 9B11 monoclonal antibody and Lamin A/C rabbit polyclonal antibody. A triplet of bands appear at 37kDa in all three samples. The M6 antibody also detects a faint triplet of bands at 72 kDa (lane 3). Myc-PRH can be detected with the Myc 9B11 antibody but not the M6 antibody (lane 2). Lamin A/C was used as a control for protein loading. Representative of three experiments.

would correspond to the transfected Myc-tagged PRH protein (lane 2). Re-probing the blot with a Myc 9B11 antibody confirmed that Myc-PRH is present in the cell extract. In the GFP-PRH transfected cell extracts an additional band is detected by the M6 antibody (lane 3). This band has a mobility of 72 kDa which is in accordance with the expected size of the GFP-PRH fusion protein. This experiment was repeated several times by coworkers in the laboratory and always produced the same result. Thus it appears the Myc-PRH fusion protein is not recognised by the M6 antibody, although it does recognise the GFP-PRH fusion protein.

In conclusion the M6 monoclonal antibody recognises endogenous PRH in haematopoietic and breast cell extracts, and it can also recognise recombinant GFP-PRH. However, it is unable to detect Myc-PRH. One reason for this could be that the presence of the Myc tag at the extreme N-terminus alters the conformation of the protein, occluding the M6 epitope adjacent to the homeodomain. This may be a consequence of the octameric nature of the protein as the N-terminus of the protein is known to interact with the homeodomain and C-terminus (Soufi et al., 2006).

3.4 PRH expression in breast cell lines

To compare PRH protein and mRNA expression levels in a range of breast tumour cell lines, the *PRH* mRNA levels were first determined in breast cell lines using the GOBO database, as described previously. A description of the molecular profile of each cell type is shown in table 3.1. As can be seen in figure 3.5 (A), MDA-MB-231 cells express the highest amount of

Cell line	ER	PR	HER2	Original tissue	Cell type	Form tumours in nude mice
HB2	Unknown	Unknown	Unknown	Luminal epithelial cells from milk	Epithelial	No
MCF-10A	Negative (Pilat, et al., 1996)	Negative (Hevir, et al., 2011)	Not amplified	Human fibrocystic Mammary tissue	Epithelial	No
BT20	Negative	Negative	Not Amplified	Primary breast tumour	Epithelial	Yes
BT474	Positive	Positive	Not Amplified	Primary breast tumour	Weakly-epithelial	Yes *
T47D	Positive	Positive	Not Amplified	Metastatic (PE)	Epithelial	Yes *
MCF-7	Positive	Positive	Not Amplified	Metastatic (PE)	Epithelial	Yes *
ZR751	Positive	Positive	Not Amplified	Metastatic (Ascites)	Epithelial	Yes *
MDA-MB-231	Negative	Negative	Not Amplified	Metastatic (PE)	Basal	Yes

Table 3.1: Cell lines used for PRH expression analysis. Cell lines used in figure 3.5, detailing their Oestrogen Receptor (ER), Progesterone Receptor (PR) and Human Epidermal Growth Factor Receptor 2 (HER2) status, as well as their original tissues and their ability to form tumours in nude mice (data from Lacroix and Leclercq 2004, unless otherwise stated) . * With oestrogen supplementation. PE = Pleural effusion

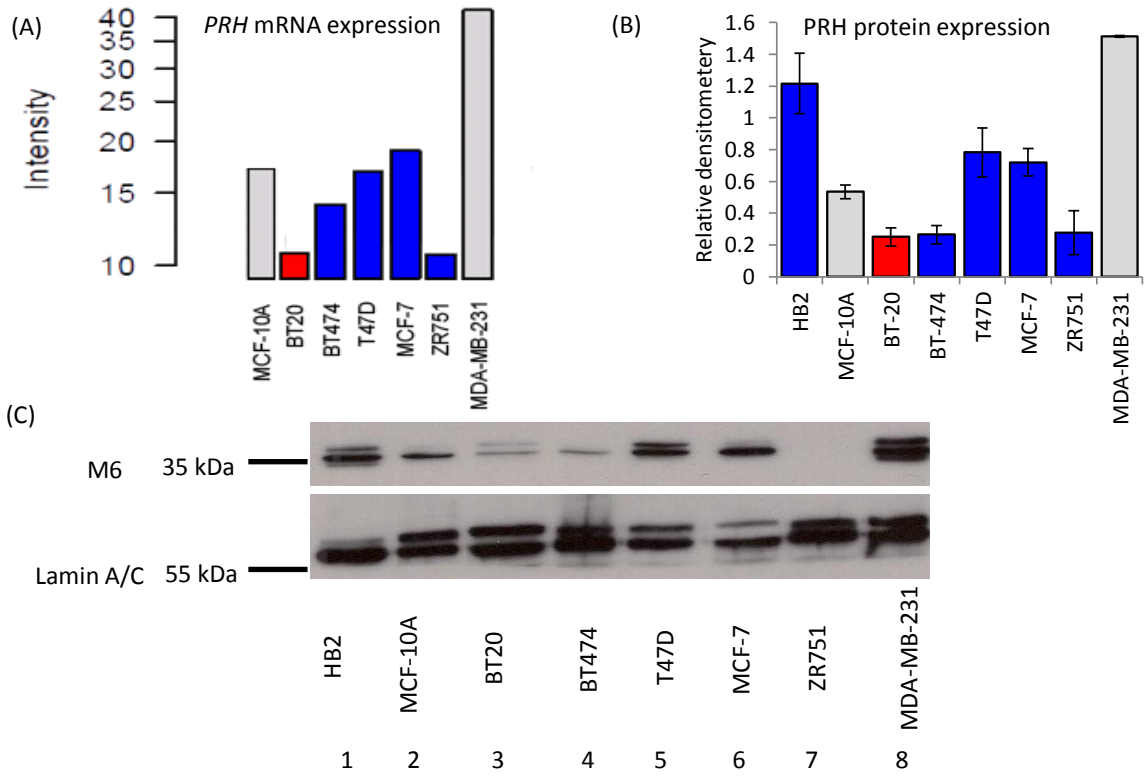

Figure 3.5: PRH expression from different breast cell lines. (A) Data from the GOBO database (Ringlér et al., 2011) was extracted, and *PRH* mRNA expression data from different breast cell lines was plotted. (B) PRH protein expression was quantified by densiometric quantification of two Western blots of cell lines using the M6 anti-PRH antibody , and Lamin C as a loading control. Grey bars and red bars refer to basal cell lines, and blue bars refer to luminal cell lines. (C) shows a representative Western Blot with 20µg of protein loaded for each cell line. Note HB2 cells are not featured in the GOBO database.

PRH transcript, whilst BT20 and ZR751 cells express the lowest amounts. Protein extracts from each of these cell lines were then Western blotted with the M6 antibody. The M6 antibody detects high levels of PRH protein expression in MDA-MB-231 cells, intermediate levels in MCF-10A, MCF-7, T47D and HB2 cells, and relatively low levels of expression in BT20, BT474 and ZR751 cells (figure 3.5 (C)). When two Western blots from two independent protein extracts taken for each cell line were quantified for PRH protein expression (as determined by the M6 antibody), using densitometric analysis and Lamin C as a loading control, the level of PRH protein expression is very similar to that observed for the *PRH* mRNA expression data from the GOBO database (figure 3.5 (B)). MDA-MB-231 cells express the most PRH, with BT20, BT474 and ZR751 cells expressing the lowest amounts. Therefore, PRH protein levels as detected by the M6 antibody correlate well with *PRH* mRNA expression data from the GOBO database. Moreover, the M6 antibody appears to be a useful antibody for investigating PRH protein in many cell lines. Additionally it can be concluded that PRH protein is expressed in normal breast cell lines and most tumour cell lines investigated.

3.5 Characterising PRH expression in MCF-10A, MCF-7 and MDA-MB-231 cells

To determine if there are differences in characterisation of PRH protein in luminal and basal cancer cells compared to normal cells, PRH protein stability and localisation was examined in MCF-10A, MCF-7 and MDA-MB-231 cells. The MCF-10A cell line represents a good model

for normal breast epithelial cell proliferation and differentiation, as it retains the ability to differentiate in a 3D culture model, where it forms acini reminiscent of breast differentiation to ducts and lobules (Debnath et al., 2003b). MCF-10A cells are not oestrogen dependent and are derived from the human fibrocystic breast epithelium (Soule et al., 1990a). Gene expression profiling of MCF-10A cells has shown that they are similar to breast cells of basal origin (Charafe-Jauffret et al., 2005). The MCF-7 tumour cell line is an ER+ and PR+ cell line of luminal origin, whereas the MDA-MB-231 tumour cell line is an ER- and PR- cell line of basal origin (Lacroix and Leclercq, 2004a).

As mentioned previously, PRH expression, stability and localisation has been characterised in human K562 leukaemic cells using in-house mouse or rabbit polyclonal antibodies. The mouse polyclonal antibody (M3) was raised against a GST-fusion protein containing the avian PRH N-terminal domain (Bess et al., 2003c). The rabbit YKN5 polyclonal antibody was raised against histidine tagged full length avian PRH protein (Soufi et al., 2009). Both antibodies specifically recognise a 37kDa band corresponding to PRH in human haematopoietic cells (Soufi et al., 2009). Western blotting experiments with extracts prepared from cells incubated with inhibitors of Protein Kinase CK2 (CK2), showed a loss of recognition of the 37kDa PRH protein with the rabbit antibody, but not with the mouse antibody (Soufi et al., 2009). Furthermore, incubation of PRH with CK2 and ATP lead to increased recognition of the phospho-protein by the YKN5 antibody, and decreased recognition by the M3 antibody (Soufi et al., 2009). Moreover, incubation of the phospho-PRH protein by Calf intestinal phosphatase (CIP) increased recognition by the M3 antibody, and decreased recognition by the YKN5 antibody (Soufi et al., 2009). Thus the mouse M3 antibody recognises hypophosphorylated PRH, whereas the YKN5 rabbit antibody

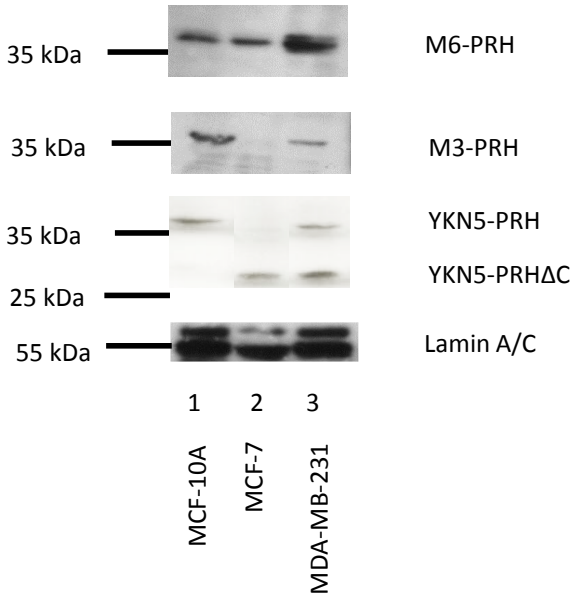

Figure 3.6: Detecting PRH in breast cell lines using M6, M3 and YKN5 antibodies. MCF-10A, MCF-7 and MDA-MB-231 cell extracts (20µg) were probed with either M6, M3 or YKN5 anti-PRH antibodies. M6 detects PRH protein in all 3 cell lines, whilst the M3 and YKN5 antibodies only detects 37kDa protein in MCF-10A and MDA-MB-231 cells. The YKN5 antibody also detects the PRHΔC product in MCF-7 and MDA-MB-231 cells. Representative of three experiments.

recognises a phosphorylation-specific conformation of PRH (Soufi et al., 2009). The rabbit antibody also recognises a truncated 27kDa phosphorylated PRH protein (PRHΔC) which plays a trans-dominant negative role over full length PRH in K562 leukaemic cells (Noy et al., 2012c). Given that the phosphorylated PRH and PRHΔC forms of PRH represent proteins that are unable to repress PRH target genes, and can block the activity of hypophosphorylated PRH in leukaemic cells, it is of interest to determine the relative amounts of these proteins in normal and tumourgenic breast cells.

To determine the endogenous levels of PRH, phosphorylated PRH and PRHΔC in MCF-10A, MCF-7 and MDA-MB-231 cells, whole cell extracts were probed with the M3, M6 and YKN5 antibodies, and also with the Lamin A/C antibody as a protein loading control. In MCF-10A cells, a 37kDa PRH protein is detected by the M6, M3 and the YKN5 antibodies (figure 3.6, lane 1) showing that PRH and phosphorylated PRH is present in this cell line. The PRHΔC

product is not detected in this Western blot, although it is detected at very low levels in some MCF-10A lysates, therefore the PRHΔC product appears to be present in MCF-10A cells at low or variable levels.

In MCF-7 cells, full length PRH protein is only detected by the M6 antibody (figure 3.6, lane 2). This suggests that the M6 antibody is more sensitive than the M3 and YKN5 antibodies, or that PRH is present in a conformation which can only be detected by the M6 antibody. The YKN5 antibody does however detect the PRHΔC product in this cell line. These results indicate that although PRH is present, little full length phosphorylated PRH is present, and most of the phosphorylated PRH is of the PRHΔC form.

In MDA-MB-231 cells, full length PRH protein is detected by the M3, M6 and YKN5 antibodies (figure 3.6, lane 3). The M6 antibody in this cell line detects a triplet of proteins at 37kDa, whilst in the other 2 cell lines it only detects a doublet (also see figure 3.5 (C)). This suggests that another conformation of PRH is present in MDA-MB-231 cells which is not present in either MCF-10A or MCF-7 cells. The PRHΔC product is also detected in MDA-MB-231 cells. Thus in MDA-MB-231 cells hypophosphorylated PRH, phosphorylated PRH and PRHΔC are present.

In conclusion PRH is present in all of the cell types tested, but unexpectedly in MCF-7 cells the PRH conformations recognised by the YKN5 and M3 antibodies are either absent or at levels below detection. MDA-MB-231 tumour cells express all forms of PRH, and express a greater amount of PRH detected by the M6 antibody compared to MCF-10A cells. An interesting finding is that the PRHΔC protein is present in both tumour cell lines, as well as in

normal cells. However, this protein appears to be expressed at a higher level relative to full length PRH in MCF-7 cells.

3.6 Characterising PRH protein localisation in MCF-10A, MCF-7 and MDA-MB-231 cells

To examine the subcellular localisation of PRH proteins detected by M6 antibody in MCF-10A cells, immunostaining with the M6 and YKN5 antibodies was carried out and proteins visualised using confocal microscopy. Insufficient M3 antibody was available for these immunofluorescence experiments. Experimental details are outlined in Materials and methods section 2.6.1 and immunostaining and confocal imaging were carried out by Emma Fallon and Dr. Rachael Kershaw. Briefly, cells were plated onto cover slips and fixed with 4% formaldehyde. The cells were then permeabilised using 0.2% triton and proteins denatured using 0.5% SDS to allow better exposure of the antibody epitopes. The cells were then incubated with the M6 or YKN5 antibodies, and secondary anti-mouse FITC conjugated antibody (for M6, λ emission 520nm) and anti-rabbit TRITC conjugated antibody (for YKN5, λ emission 572nm). Cells were also incubated with TO-PRO-3 Iodide, a DNA binding dye that was used for nuclei staining (λ emission 660nm). The fluorescence maxima for emission for the three fluorophores differ sufficiently to allow co-staining.

Figure 3.7 (A) shows that the M6 antibody (green) predominantly stains PRH in the cytoplasm, with fainter staining in the nucleus. The YKN5 antibody (red) stains for phosphorylated PRH predominantly in the nucleus, with fainter cytoplasmic staining.

Indicating that phosphorylated PRH is predominantly nuclear. TO-PRO-3 staining appears blue in the nuclei.

To further examine the subcellular localisation of PRH proteins, biochemical fractionation followed by Western blotting with PRH antibodies was carried out as described by Desjobert et al. (Desjobert et al., 2009). Briefly, $1x10^6$ cells were pelleted, and incubated in buffer containing NP-40 detergent. This lyses the cytoplasmic membrane, but does not disrupt the nuclear membrane. The nuclei were obtained by centrifugation, and the supernatant containing the post-nuclear fraction was removed and frozen. The remaining pellet was lysed using buffer containing 0.1% w/v sodium dodecyl sulphate (SDS), which disrupts the nuclear membrane. The extract was then pelleted and the supernatant which contains the soluble nuclear fraction was then frozen. An equal percentage of protein from each fraction was then loaded onto a SDS-PAG electrophoresis gel, Western blotted and probed using the M3, M6 and YKN5 antibodies. The quality of the subcellular fractionation was assessed by blotting with antibodies for the nuclear protein Lamin A/C and for the cytoplasmic protein Tubulin. The nuclear fractionation contains proteins which are tightly held in the nucleus, whilst the post-nuclear fraction contains cytoplasmic proteins as well as proteins which are not tightly held in the nucleus (Desjobert et al., 2009). Figure 3.7 (B) shows that for MCF-10A cells, PRH protein as detected by the M6 antibody is present in both the nuclear and post-nuclear fractions. The YKN5 antibody detects 37kDa phosphorylated PRH in the nuclear fraction, which is in agreement with the immunostaining. In these extracts no PRHΔC is detectable. The M3 antibody detects PRH in the post-nuclear fraction, indicating this form of PRH is either cytoplasmic or is not tightly held to the nucleus. The Tubulin and Lamin A/C antibodies indicate that the fractionation

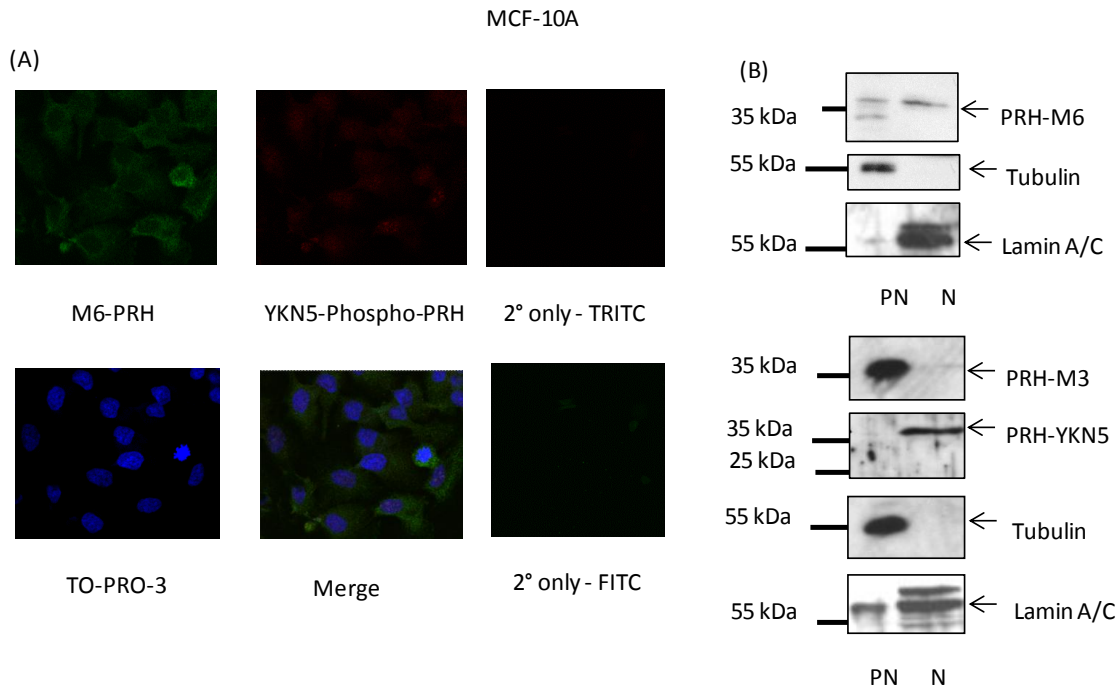

Figure 3.7: PRH localisation in MCF-10A cells. (A) MCF-10A cells were immunostained with the M6 and YKN5 antibodies, and were also incubated with TO-PRO-3 to stain for nuclei. Cells were then stained with FITC (for M6) and TRITC (for YKN5) secondary conjugated antibodies, against murine and rabbit IgG respectively. Pictures were taken at 400x magnification. (B) MCF-10A cells were biochemically fractionated into nuclear (N) and post-nuclear (PN) fractions as described in the text. The fractions were then Western blotted for PRH expression using M6, M3 and YKN5 antibodies. Lamin A/C and Tubulin antibodies were used as loading controls for nuclear and post-nuclear fractions respectively. Representative of two experiments.

was efficient. The fractionation was carried out twice independently with identical results. In summary PRH is present in the cytoplasm and nucleus of MCF-10A cells. However, the forms of PRH detected by each antibody differ in their nuclear retention properties, with full length phosphorylated PRH being tightly retained in the nuclear compartment.

Immunostaining was carried out for MCF-7 cells exactly as described above by Dr. R. Kershaw and E. Fallon. The immunostaining shows that the M6 antibody predominantly detects PRH in the cytoplasm, with very faint staining in the nucleus. The YKN5 antibody detects protein in both the nucleus and cytoplasm of the cells (Figure 3.8 (A)). Biochemical fractionation of MCF-7 cells was then carried out as described above. The YKN5 antibody detects the PRHΔC protein product alone, and this is only detected in the post-nuclear

fraction. This therefore suggests that the nuclear PRH detected by the YKN5 antibody during immunostaining is not tightly held. After fractionation the M6 antibody predominantly detects PRH in the nuclear fraction, although there is a fainter band in the post-nuclear fraction as well (figure 3.8 (B)). The M3 antibody was not used as it fails to detect PRH protein in this cell type (figure 3.6). In MCF-7 cells there is weak diffuse nuclear PRH staining and strong PRH staining appears localised in the cytoplasm, as detected by immunostaining. This is similar to the staining observed in MCF-10A cells. Unexpectedly, biochemical fractionation indicates that the PRH protein detected by M6 antibody is associated with the nuclear and tightly held protein fraction, with weaker staining in the cytoplasmic/post-nuclear protein fraction. Since there is little full length phosphorylated PRH protein in MCF-7 cells, it can be inferred that the YKN5 antibody in immunostaining is detecting the PRHΔC protein, which is present in both compartments but is not tightly held in the nuclear fraction.

In MDA-MB-231 cells, PRH protein as determined by the M6 antibody seems to be predominantly cytoplasmic as determined by immunostaining, but M6 also detects some nuclear PRH protein (figure 3.9 (A)). Therefore the distribution of PRH protein as determined by immunostaining for MDA-MB-231 cells with M6 antibody is similar to that of MCF-10A and MCF-7 cells. The YKN5 antibody detects nuclear and cytoplasmic phosphorylated PRH in immunostaining (figure 3.9 (A)). Biochemical fractionation of MDA-MB-231 cell extracts probed with the M6 antibody shows that PRH protein is predominantly retained in the nuclear fraction, although some is still present in the post-nuclear fraction (figure 3.9 (B)).

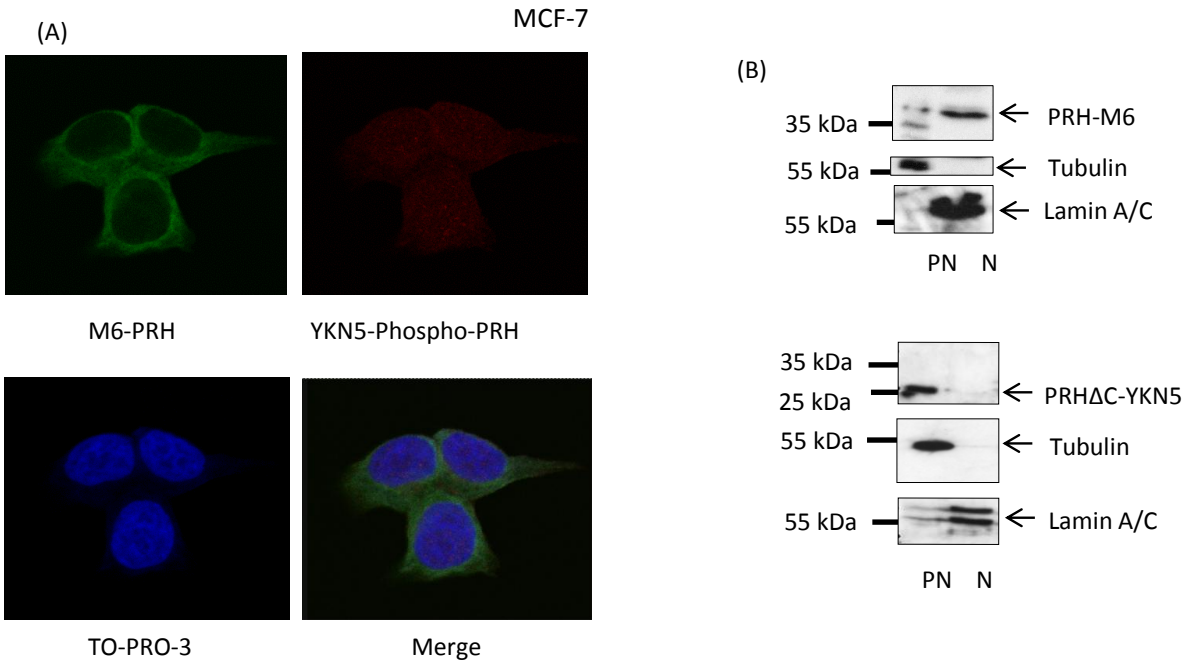

Figure 3.8: PRH localisation in MCF-7 cells. (A) MCF-7 cells were immunostained with the M6 and YKN5 antibodies, and were also incubated with TO-PRO-3 to stain for nuclei. Cells were then stained with FITC (for M6) and TRITC (for YKN5) secondary conjugated antibodies, against murine and rabbit IgG respectively. Pictures were taken at 630x magnification. (B) MCF-7 cells were biochemically fractionated into nuclear (N) and post-nuclear (PN) fractions as described in the text. The fractions were then stained for PRH expression using M6 and YKN5 antibodies. Lamin A/C and Tubulin antibodies were used as loading controls for nuclear and post-nuclear fractions respectively. Representative of two experiments.

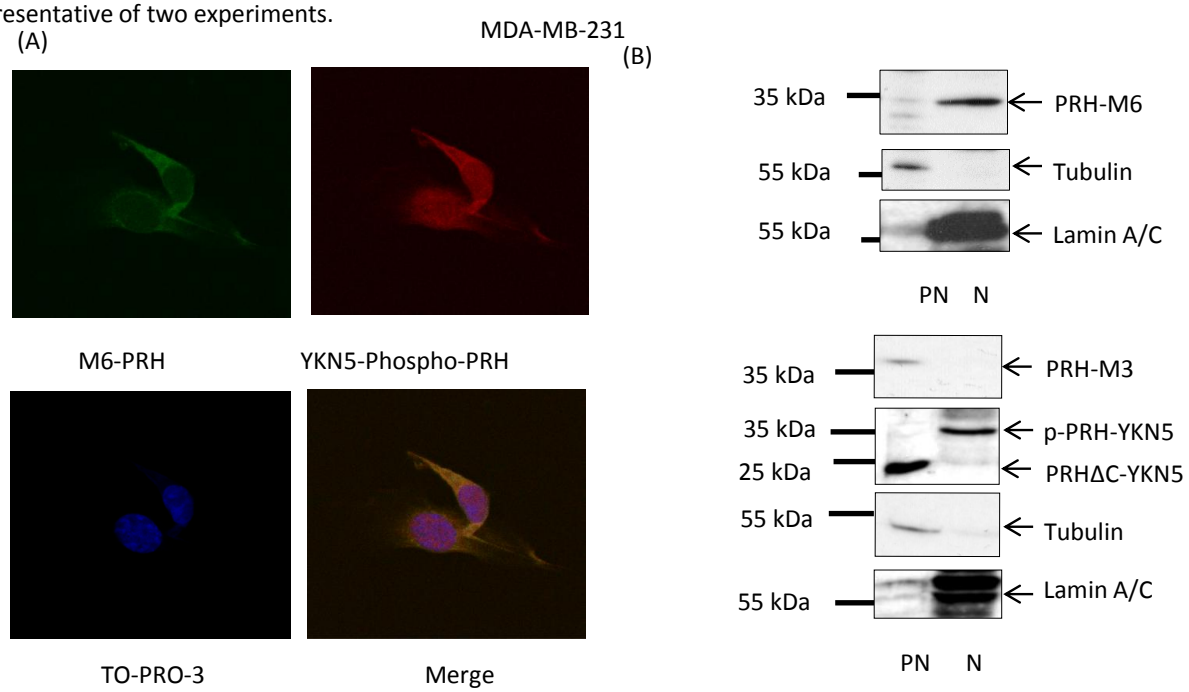

Figure 3.9: PRH localisation in MDA-MB-231 cells. (A) MDA-MB-231 cells were immunostained with the M6 and YKN5 antibodies, and were also incubated with TO-PRO-3 to stain for nuclei. Cells were then stained with FITC (for M6) and TRITC (for YKN5) secondary conjugated antibodies, against murine and rabbit IgG respectively. Pictures were taken at 630x magnification. (B) MDA-MB-231 cells were biochemically fractionated into nuclear (N) and post-nuclear (PN) fractions as described in the text. The fractions were then stained for PRH expression using M6, M3 and YKN5 antibodies. Lamin A/C and Tubulin antibodies were used as loading controls for nuclear and post-nuclear fractions respectively. Representative of two experiments.

The YKN5 antibody primarily detects 37kDa phosphorylated PRH protein in the nuclear fraction, and the PRHΔC protein product is primarily detected in the post-nuclear fraction. The M3 antibody detects full length PRH protein in the post-nuclear fraction (figure 3.9 (B)).

In summary, immunostaining in the three cell lines gave similar results when probed with the M6 antibody, which showed that PRH is predominantly present in the cytoplasm, with fainter nuclear staining. Biochemical fractionation experiments indicate that PRH proteins fractionate in a similar way in all three cell lines, and therefore there is no difference detected in PRH localisation between the non-tumourgenic MCF-10A cells and the tumourgenic MCF-7 and MDA-MB-231 cells, as detected by these assays. However, the differences between detection of PRH by M6 and M3 antibodies, as determined by Western blotting, is not likely due to sensitivity, since M3 detects PRH in the post-nuclear fraction, and M6 detects PRH in the nuclear fraction. Also, phosphorylated full length PRH is detected in MCF-10A and MDA-MB-231 cells, whilst it is present at very low levels in MCF-7 cells by the YKN5 antibody. However, the YKN5 antibody does detect PRHΔC in MCF-7 cells.

3.7 Determining the stability of PRH in MCF-10A, MCF-7 and MDA-MB-231 cells

Transcription factors are often regulated by post-transcriptional modifications or proteolytic processing. PRH protein is regulated by phosphorylation and proteosomal processing in K562 cells (Noy et al., 2012c). The product of the processing, PRHΔC, has trans-dominant activity over the transcriptional repression activity of PRH in leukaemic cells. Since the cancer cell types express phosphorylated PRH and PRHΔC at different ratios from that

observed in MCF-10A cells it was hypothesised that the three different breast cell types may have intrinsic differences in PRH stability and activity.

To assess the stability of PRH we chose to examine the stability of the PRH protein detected by the M6 antibody. MCF-7, MDA-MB-231 and MCF-10A cells were incubated with 10μg/ml of the translation inhibitor anisomycin for 8 and 16 hours, or left untreated (time 0). The cells were then lysed, protein extracts produced and Western blotted as previously described, and lysates were probed with the M6 antibody. Lamin antibody was used as a protein loading control. In MCF-10A cells, PRH protein is significantly decreased after 8 hours anisomycin treatment, and has virtually disappeared after 16 hours (figure 3.10 (A)). In MCF-7 cells, the lower mobility protein of the PRH doublet is lost after 8 hours, but the faster mobility PRH protein remains present after 16 hours anisomycin treatment (figure 3.10 (B)). In MDA-MB-231 cells, levels of expression for all PRH proteins have significantly decreased after 8 hours (figure 3.10 (C)).

As the endogenous levels of PRH protein are quite different between the cell lines, this makes it difficult to compare stability of endogenous PRH. A more useful approach would be to determine whether there is a difference in the stability of exogenous Myc-PRH, which is detected only as a single protein by the Myc antibody. Therefore, the same experiment was carried out by infecting cells with an adenovirus that expresses the Myc-PRH protein. The Ad-PRH vector and infection of each cell with Ad-PRH virus are described in Materials and methods section 2.4 and in chapter 4 section 4.2.1. Briefly, cells were incubated with an

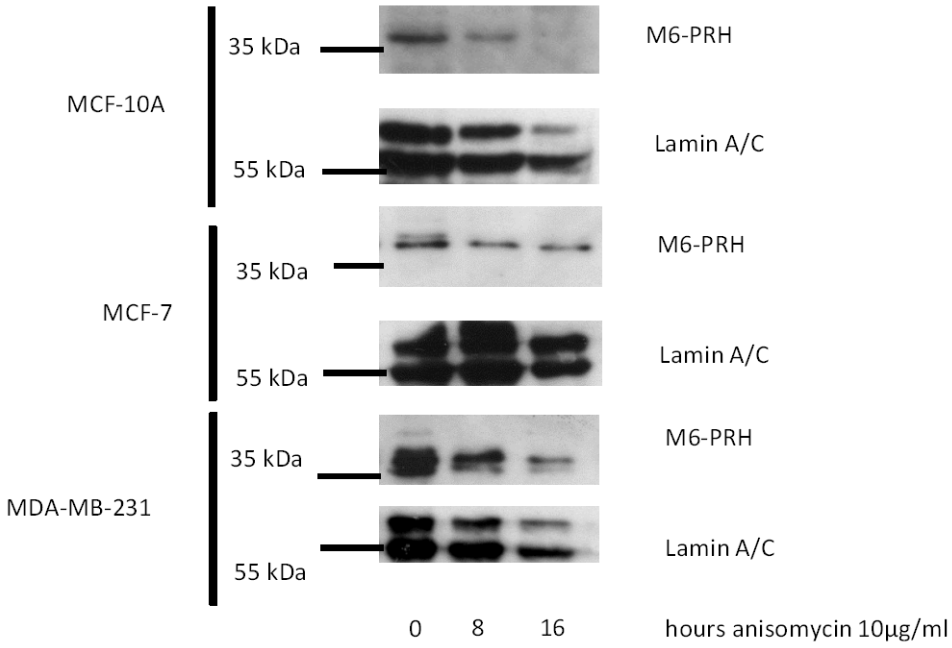

Figure 3.10: Determining the stability of endogenous PRH in breast cell lines. MCF-7, MDA-MB-231 and MCF-10A cells were incubated with 10 µg/ml anisomycin (or DMSO) for 8 or 16 hours. 20µg of cell lysate were then analysed using Western blotting and M6 antibodies. Representative of three Western blots.

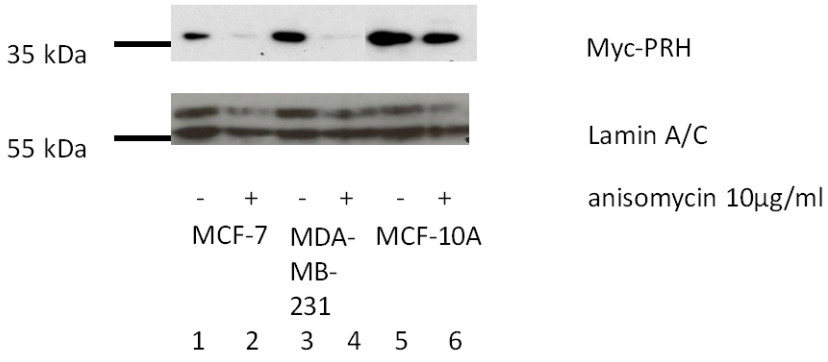

Figure 3.11: Stability of Myc-PRH in different breast cell lines. MCF-7, MDA-MB-231, and MCF-10A cells were incubated with Ad-PRH adenovirus for 24 hours, and were then incubated with 10 µg/ml anisomycin (or DMSO) for 16 hours. 20µg of cell lysate were then analysed using Western blot and the Myc 9B11 antibody. Representative of three Western blots.

adenovirus expressing Myc-PRH (Ad-PRH) at a multiplicity of infection (MOI) of 50 for 24 hours. Cells were then incubated with 10μg/ml anisomycin (or the corresponding amount of DMSO as a control) for 16 hours. Cells were then lysed, and protein extracts were produced. Myc-PRH expression was analysed using Western blotting with Myc 9B11 antibody. In MCF-7 cells, Myc-PRH is degraded after 16 hours anisomycin treatment figure 3.11, lane 2), and this also occurs in MDA-MB-231 cells (figure 3.11, lane 4). However, in MCF-10A cells Myc-PRH is still present even after 16 hours anisomycin treatment. This demonstrates that exogenous PRH is more stable in MCF-10A cells than in the two tumour cell lines.

3.8 Subcellular fractionation of Myc-PRH in MCF-10A, MCF-7 and MDA-MB-231 cells

To establish whether exogenous PRH is similar to endogenous PRH in its subcellular localisation, all three cell lines were infected with Ad or Ad-PRH for 48 hours, before biochemical fractionation. An equal percentage of nuclear and post-nuclear fraction lysate was loaded for each cell line. The fractions were then Western blotted and probed using the Myc and YKN5 antibodies (The M3 and M6 antibodies do not detect exogenous Myc-PRH). For clarity only fractions with Ad-PRH are shown. It can be seen that Myc-PRH is present in the post-nuclear fraction in all cell lines, as detected by Myc and YKN5 antibodies (figure 3.12).

Since exogenous Myc-PRH proteins in all cell lines are present in the post-nuclear fraction, the difference in stability between MCF-10A, MCF-7 and MDA-MB-231 cells cannot be accounted for by differences in subcellular localisation. Therefore, the decreased stability of

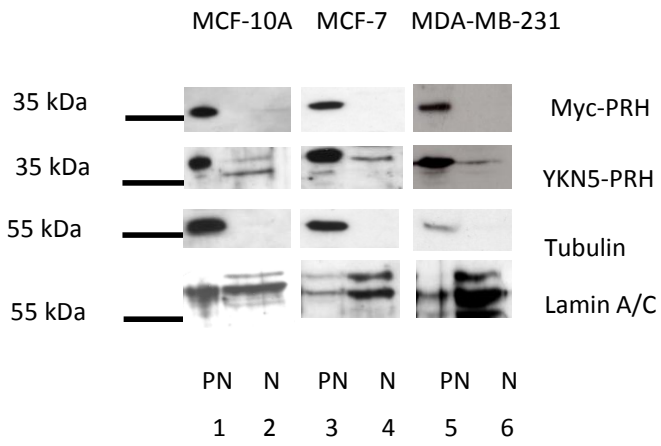

Figure 3.12: Biochemical fraction of Myc-PRH in different breast cell lines. MCF-10A, MCF-7 and MDA-MB-231 cells were infected with Ad-PRH for 48 hours. Cells were then biochemically fractionated into nuclear (N) and post-nuclear (PN) fractions as described in the text. The fractions were then stained for Myc-PRH expression using Myc 9B11 and YKN5 antibodies. Lamin A/C and Tubulin antibodies were used as loading controls for nuclear and post-nuclear fractions respectively (n=3).

exogenous PRH in tumour cell lines compared to MCF-10A cells likely reflects increased proteolytic cleavage activities of cancer cells.

3.9 Discussion

Expression of PRH protein has been shown to be clinically relevant in human cancer. For example, expression of a NUP98-PRH fusion protein (which transforms PRH from a transcriptional repressor to a transcriptional activator) has been shown to be a causative event in acute myeloid leukaemia (Jankovic et al., 2008). Here it is shown that high *PRH* mRNA expression is also clinically relevant to breast cancer, as data extracted from the GOBO database shows that *PRH* mRNA expression is positively associated with increased overall survival in breast cancer patients. Therefore, *PRH* mRNA levels are a marker for

overall survival in breast cancer, like the well known tumour suppressor *PTEN*. *PRH* mRNA expression is also generally correlated with the less aggressive forms of breast cancer, with *PRH* expression highest in ER+, Luminal A and grade 1 and 2 breast cancers, and lowest in basal, *HER2* amplified, ER- and grade 3 breast cancers.

A new M6 monoclonal antibody against PRH shows that the relative amounts of PRH protein correlate well with the relative amount of *PRH* mRNA, as determined by the GOBO database. Therefore it is concluded that the M6 antibody gives an accurate representation of *PRH* mRNA expression in breast cells. This antibody therefore may be a useful tool for further work, for example for assessing PRH protein levels in primary tumour cells, and how these levels compare with patient prognosis. It would also be of interest to determine whether this antibody shows decreased PRH staining in tumour cells compared to adjacent normal breast tissue.

It has been shown previously that PRH protein is present in both nuclear and cytoplasmic compartments in normal breast cells, whilst PRH protein is predominantly cytoplasmic in breast carcinomas (Puppin et al., 2006). Puppin et al. also showed that T47D and MCF-7 cell lines contain predominantly cytoplasmic/nucleolar PRH in immunohistochemistry experiments with an antibody against human PRH. In immunostaining experiments with M6 antibody it is shown that PRH is predominantly present in the cytoplasm in MCF-10A, MCF-7 and MDA-MB-231 cells, however some protein is also present in the nucleus of all three cell lines. Biochemical fractionation also showed that in all cell lines M6 antibody detects PRH protein in both the nuclear and post-nuclear fractions. No significant differences in

localisation of PRH protein were seen with the M6 antibody in *in vitro* fractionation experiments between non-tumourgenic MCF-10A cells and the tumourgenic cell lines MCF-7 and MDA-MB-231, as determined by these assays. However, further experiments performed by E. Fallon and Dr. R.Kershaw show that even though PRH is predominately cytoplasmic in all three cell lines, there is more tightly held nuclear PRH in MCF-10A cells compared to the tumour cells, as determined by *in situ* biochemical fractionations (R. Kershaw, E. Fallon and P.S. Jayaraman, personal communication). This finding correlates with what was seen by Puppin et. al., who showed that nuclear PRH is decreased in breast carcinomas (Puppin et al., 2006). The differences between the *in vitro* and the *in situ* fractionation experiments may have to do with the different compositions of the buffers used in the two protocols.

Next the stability of PRH protein was examined in all three cell lines. It is not easy to compare the stability of endogenous PRH protein between cell lines using the M6 antibody as the antibody detects multiple forms of the protein each of which may have a different stability and because the steady state (starting levels) of the PRH proteins detected are extremely different. For example, endogenous PRH is expressed at much higher levels in MCF-10A cells than in MCF-7 cells. Western blotting with the M6 antibody would very likely detect a small decrease in the low level of PRH protein in MCF-7 cells but would not be able to detect the same decrease in PRH protein levels in MCF-10A cells. Therefore it was thought that is would be more informative if the stability of exogenous PRH protein was examined using Myc-PRH infected cells. In both tumour cell lines exogenously expressed PRH was less stable than in normal breast cells. Decreased PRH stability could be one mechanism through which PRH activity is downregulated in tumour cells. To determine the mechanism by which PRH protein is degraded in breast tumour cells, CK2 inhibitor TBB,

proteasome inhibitor MG132 and caspase inhibitors Z-VAD-FMK were used. However, these experiments were inconclusive due to the effect these compounds have on cell viability (data not shown). Further experiments with CK2 and proteasome inhibitors will be required to investigate the mechanism responsible for the degradation of PRH in the three different cell lines. However the finding that PRH is expressed in tumour cell lines, and that its stability may be decreased in tumour cell lines is of consequence given that high PRH expression correlates with increased overall survival.

THE EFFECT OF PRH ON NORMAL AND TUMOURGENIC BREAST CELL POPULATION GROWTH

4. The effect of PRH on normal and tumourgenic breast cell population growth

4.1 Introduction

PRH has been shown to influence the proliferation of cells in a variety of cell types. In K562 leukaemic cells, over-expression of PRH leads to apoptotic cell death and decreased cell number, whilst shRNA knockdown of PRH increases cell number (Noy et al., 2010). In K562 cells this has been shown to occur through increased survival signalling via elevated expression of the *VEGF* gene and VEGF receptor genes, as a consequence of derepression of multiple genes in the VEGF signalling pathway (Noy et al., 2010). Manipulation of PRH levels in MCF-7 cells also leads to changes in cell number and modulation of expression of VEGF signalling genes (Noy et al., 2010), but the effects of PRH on cell proliferation, cell survival and VEGF signalling have not been fully analysed in this cell type. To further investigate the role of PRH in the growth of normal breast cells and breast tumour cells, the effect of exogenous PRH on cell number, apoptosis and proliferation will be determined in MCF-10A cells, MCF-7 cells and MDA-MB-231 cells. In addition the effect of knockdown of PRH on cell survival and proliferation will also be examined in the same cell lines. Finally the effect of alterations in PRH level on the expression of genes in the VEGF signalling pathway will be examined.

4.2 Effect of PRH overexpression on breast cell proliferation and survival

4.2.1 Effect of PRH overexpression on cell number

Adenoviruses were used to overexpress PRH in MCF-10A, MCF-7 and MDA-MB-231 cell lines. Adenoviruses are DNA viruses and are a useful experimental tool for transgene expression, as transfection efficiencies can reach 100% and can infect many mammalian cell types. The adenovirus which allows for exogenous PRH expression (henceforth known as Ad-PRH) contains a gene coding for the Myc-PRH fusion protein as described previously (chapter 3 section 3.3), cloned into the pDC-515 vector backbone (Soufi et al., 2006) (for plasmid map see Materials and methods section 2.12). Transgene expression is under the control of the murine cytomegalovirus (MCMV) promoter. An empty adenovirus which does not code for protein (Rad 66, referred to as Ad (Akrigg, 1992)), was used as a control, because expression of other control proteins (such as β-Galactosidase and GFP) could themselves exert effects on cell growth. To determine which multiplicity of infection (MOI) to use, MCF-7 cells were plated in 6-well plates at equal number, and infected with Ad at a MOI of 50 or 500, or left uninfected. Cells were then counted after 2 days to determine whether either viral load is toxic to cells. Figure 4.1 (A) shows that for MCF-7 cells, a MOI of 500 of control Ad reduces cell number, whilst a MOI of 50 seems to have little effect. To demonstrate that a MOI of 50 is not toxic in MCF-10A, MCF-7 and MDA-MB-231 cell lines, cells were left uninfected or infected with Ad at a MOI of 50 and equal numbers plated in 6-

well plates. Cells were counted 2 days post-infection as described previously (figure 4.1 (B)). It can be seen that at an MOI of 50 Ad has little or no effect on cell viability in all cell lines.

To determine whether infection of cells with Ad-PRH at MOI of 50 results in expression of Myc-PRH protein, MCF-10A, MCF-7 and MDA-MB-231 cells were infected with Ad and Ad-PRH. Whole cell extracts were made 48 hours post-infection, and proteins were separated by SDS-PAGE and Western blotted with Myc 9B11 antibody as described in Materials and methods section 2.3. Figure 4.2 shows that Myc-PRH is expressed in all of the cell types tested and that no expression is detected in cells infected with control adenovirus. Therefore, it was determined that an MOI of 50 was to be used for all further overexpression experiments.

To determine the effect of Myc-PRH expression on cell number for each cell line, cells were infected with Ad or Ad-PRH, and plated at equal cell number. Cell number was then counted every two days, using a haemacytometer and trypan blue for 6 days. Trypan blue staining allows the identification of viable cells as trypan blue dye is excluded from living cells (Strober, 2001). Figure 4.3 (A) shows that there are significantly fewer live Ad-PRH infected MCF-10A cells compared to Ad infected MCF-10A cells 4 days post infection. Similarly there are significantly fewer Ad-PRH infected MCF-7 cells than control Ad infected MCF-7 cells 6 days post-infection (figure 4.3 (B)). However, in MDA-MB-231 cells, there was no difference in cell number between Ad-PRH and Ad control cells after 4 days, where the cells were 90% confluent (figure 4.3 (C)). To determine whether a reduction in MDA-MB-231 cells would be

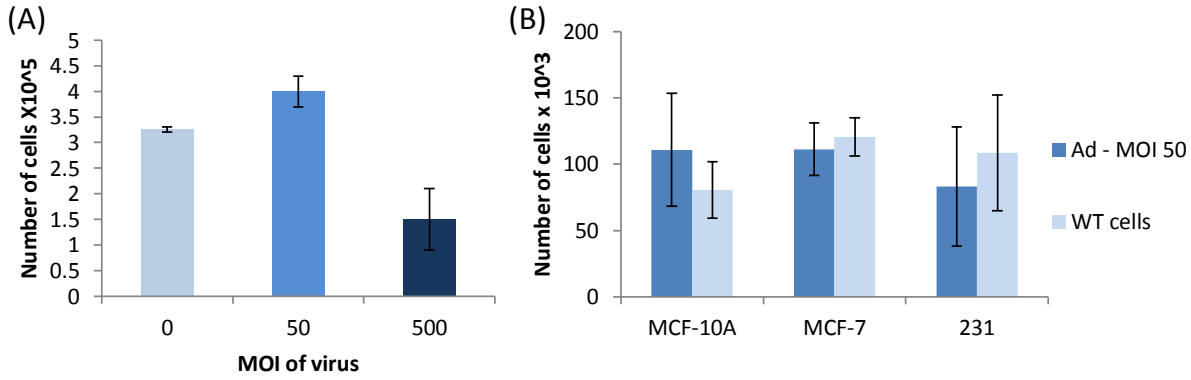

Figure 4.1: Determining a useful multiplicity of infection (MOI). (A) $1x10^5$ MCF-7 cells were uninfected, or infected with control adenovirus at a MOI of 50 or 500. Cells were then counted 48 hours later using a haemacytometer and trypan blue exclusion dye. (B) MCF-10A, MCF-7 and MDA-MB-231 cells were either uninfected or infected with Ad at a MOI of 50.

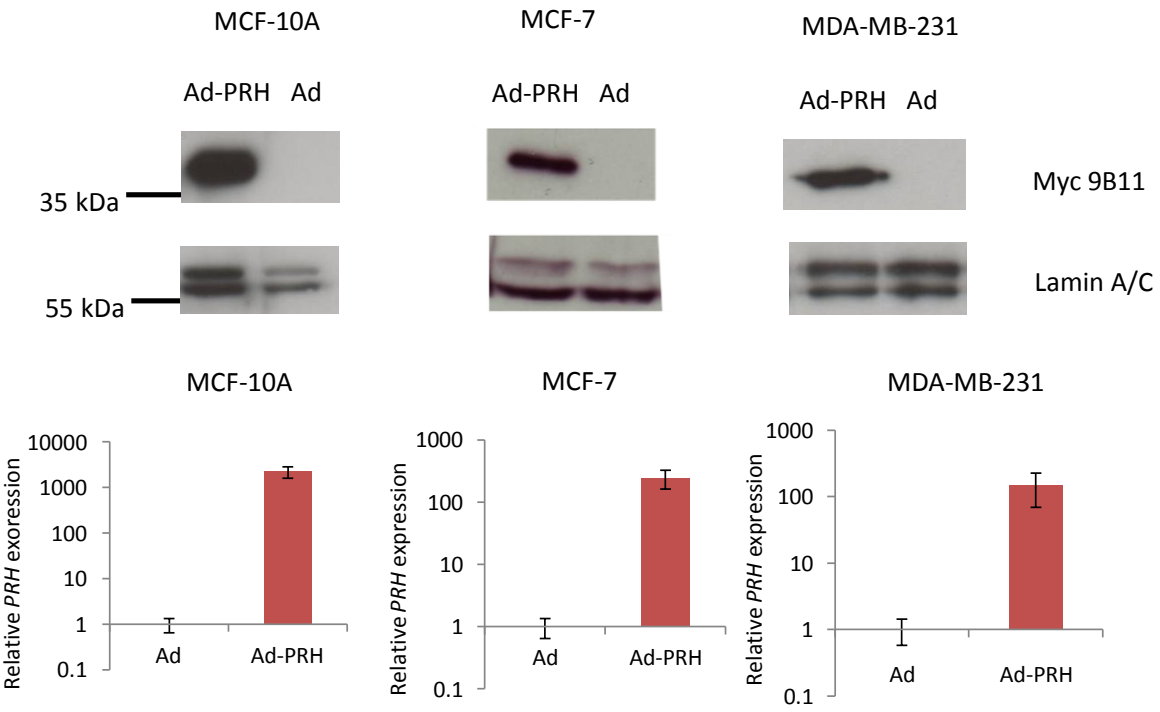

Figure 4.2: Ad-PRH infection leads to PRH overexpression. (A) MDA-MB-231, MCF-7 and MCF-10A cells were infected with control adenovirus (Ad) or PRH overexpressing adenovirus (Ad-PRH) at a MOI of 50. 20µg of protein was Western blotted using Myc 9B11 antibody to detect exogenous PRH expression. Lamin A/C was used as a loading control. (B) PRH gene expression was carried out as in Materials and methods section 2.8, and analysed using quantitative PCR, and quantified using the Pfaffl method (Pfaffl, 2001), using *GAPDH* as a housekeeping gene.

seen at a later time point, the cells were re-plated at a lower density on day 4 and counted at 8 days post-infection. The total number of cells that would have grown was calculated from multiplying the cell number at day 8 and the cell dilution at replating on day 4. Figure 4.3 (C) shows that at day 8 there is no significant difference between Ad and Ad-PRH infected cells. It can be concluded that Ad-PRH inhibits the rate of increase of the population of MCF-10A and MCF-7 cells but has apparently little effect on the rate of increase of the MDA-MB-231 cell population.

4.2.2 DNA binding is required for PRH to decrease cell number in MCF-7 cells

To determine whether the effect of ectopic PRH expression on cell number in MCF-7 cells requires DNA binding activity, cells were infected with an adenovirus expressing a mutated Myc-PRH protein. The mutated protein contains a point mutation in the homeodomain (N187A), that prevents PRH from forming PRH-DNA complexes (Desjobert et al., 2009; Soufi et al., 2010). It has also been shown that in K562 leukaemic cells, the PRH N187A mutant cannot repress transcription of the *VEGF* gene or induce apoptosis (Noy et al., 2010).

MCF-7 cells were infected with Ad, Ad-PRH or Ad-N187A adenovirus at a MOI of 50, and expression of Myc-tagged PRH protein was checked after 24 hours with the Myc 9B11 monoclonal antibody and Western blotting as described above. Figure 4.13 (A) shows that the PRH-N187A adenovirus is expressed at a higher level compared to wild-type PRH. Infected cells were counted over a period of six days post infection. Figure 4.13 (B) shows

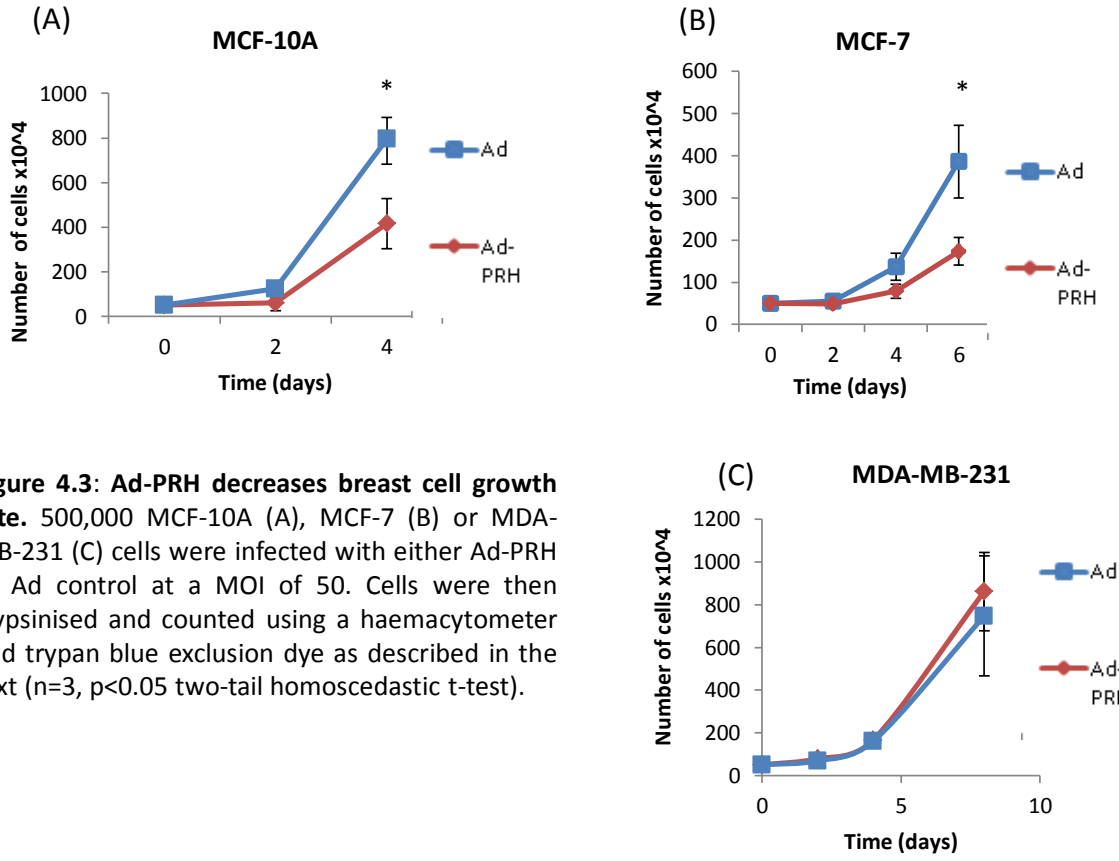

Figure 4.3: **Ad-PRH decreases breast cell growth rate.** 500,000 MCF-10A (A), MCF-7 (B) or MDA-MB-231 (C) cells were infected with either Ad-PRH or Ad control at a MOI of 50. Cells were then trypsinised and counted using a haemacytometer and trypan blue exclusion dye as described in the text (n=3, $p<0.05$ two-tail homoscedastic t-test).

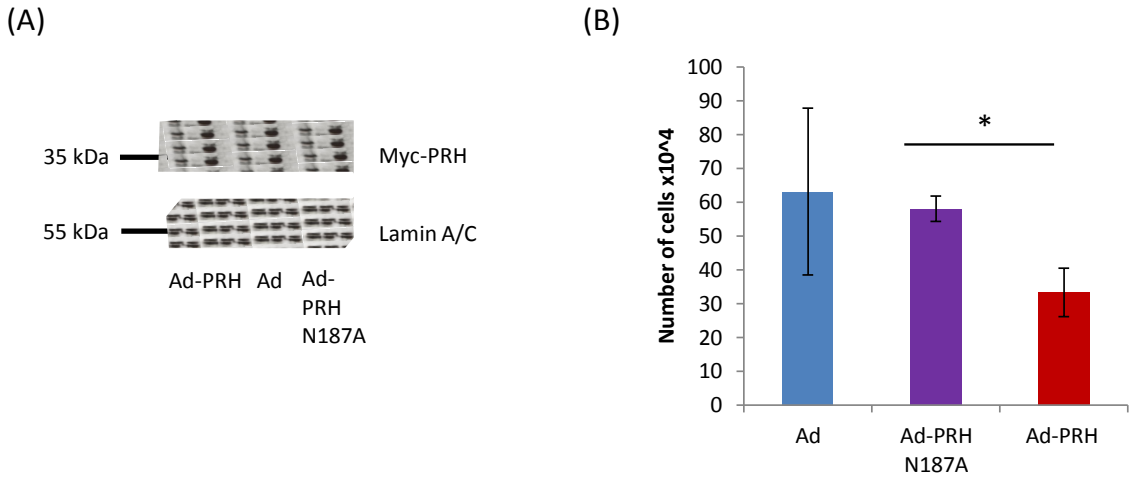

Figure 4.4: DNA binding activity is required for PRH to decrease MCF-7 cell number. (A) 500,000 MCF-7 cells were infected with either Ad-PRH, Ad-PRH N187A or Ad control at a MOI of 50. Cells were then lysed and Western blotted with the Myc 9B11 monoclonal antibody to detect exogenous PRH. (B) Cells were infected with Ad, Ad-PRH and Ad-PRH N187A viruses as before, and were plated in equal numbers in a T75 cm^2 flask. Cells were then incubated with trypsin and counted 6 days post-infection using a haemacytometer and trypan blue exclusion dye (n=3,3,3 one way ANOVA with Games-Howell post-hoc *$p<0.05$).

that the number of Ad-N187A infected cells is similar to that of Ad infected cells, whilst the number of Ad-PRH infected cells is significantly lower compared to the number of Ad-PRH N187A infected cells. Therefore, this implies that PRH needs to bind to DNA to bring about its growth inhibitory effects in MCF-7 cells.

4.2.3 Effect of PRH over-expression on apoptosis

Changes in cell number in MCF-10A and MCF-7 cells observed above could be caused by either increased cell apoptosis or decreased cell proliferation. To determine whether Ad-PRH increases apoptosis in these cell lines, co-staining of cells with propidium iodide and Annexin-V-APC conjugated protein was carried out. Both adherent and floating cells were retrieved from flasks by centrifugation. The DNA staining dye propidium iodide (PI) will only bind to the DNA of cells that do not have an intact cell membrane (Jones and Senft, 1985). Staining with PI therefore assesses the number of viable and dying cells. Phospatidylserine is normally found only in the inner cell membrane in viable cells, however when cells undergo apoptosis this protein is present in the outer membrane where it can be detected by the Annexin V-APC conjugated protein (Bret Verhoven, 1995). PI and Annexin V-APC have different fluorescence emission maxima allowing simultaneous detection of both reagents using a flow cytometer (λ617nm for PI and λ660nm for APC). Flow cytometry of cells co-stained with both PI and Annexin V-APC allows discrimination between viable cells, early and late apoptosis and cells dying through other mechanisms. Thus viable cells are cells which are not stained with either reagent, early apoptotic cells are stained with Annexin V-

APC but not PI, late apoptotic cells stain with both Annexin V and PI and cells that are dying but not apoptotic stain only with PI. The distribution of viable cells and apoptotic cells in Ad and Ad-PRH infected MCF-7 cells is shown in a scatter plot (figures 4.5 (A) and (B)). Figure 4.5 (B) shows that Ad-PRH increases the percentage of apoptotic cells from 15% to 26% in this experiment. The experiment was repeated three times and the mean and standard error are represented in figures 4.5 (C) and (D). It can be seen that two days post-infection there are slightly more apoptotic cells in the Ad-PRH population than in the control Ad population, however this change is not statistically significant (figure 4.5 (C)). However after 4 days there is a significant increase in the total number of early apoptotic cells (figure 4.5 (D)). This correlates with a significant decrease in the percentage of non-apoptotic cells detected (figure 4.5 (D)). Therefore, overexpression of PRH in MCF-7 cells causes a decrease in cell number, which can be explained at least in part by an increase in apoptosis of these cells.

In MCF-10A cells, there is no significant increase in apoptotic cells either 2 days or 4 days post infection with Ad-PRH compared to Ad (figure 4.6). This shows that the decrease in MCF-10A cell number caused by PRH overexpression in figure 4.3 is not through increased apoptosis.

MDA-MB-231 cells were also assessed, to see whether Myc-PRH had any effect on cell apoptosis. MDA-MB-231 cells were infected with Ad or Ad-PRH as described previously, and Annexin V/PI assays were carried out 2 and 4 days post-infection as described above. There

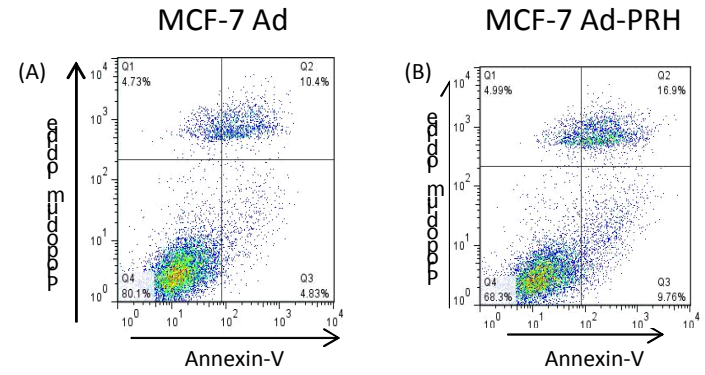

Figure 4.5: Ad-PRH increases apoptosis in MCF-7 cells. MCF-7 cells were incubated with control Ad or Ad-PRH for either 2 (C) or 4 (D) days, before being stained with 10µg/ul propodium iodide and 5µl of Annexin V-APC antibody (BD Biosciences). Cells were then analysed by flow cytometery to determine live cells (PI-, AV-), or apoptotic cells (PI-, AV+ or PI+. AV+). Representative plots are shown for Ad (A) and Ad-PRH (B) infected cells at 4 days post infection (n=3, two-tail homoscedastic t-test *p<0.05).

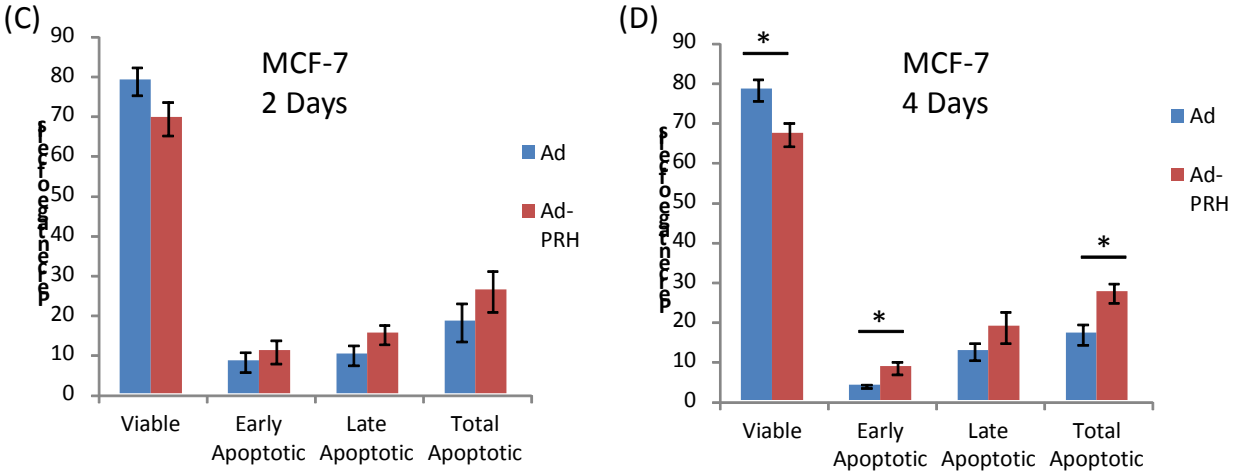

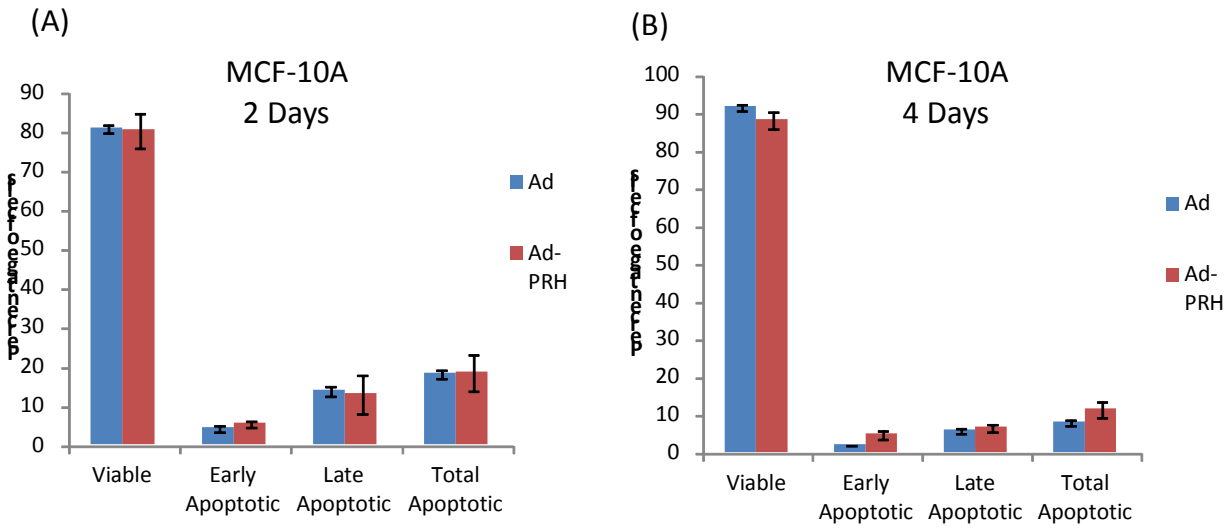

Figure 4.6: Ad-PRH does not increase apoptosis in MCF-10A cells. MCF-10A cells were incubated with control Ad or Ad-PRH for either 2 (A) or 4 (B) days, before being stained with 10µg/ul propodium iodide and 5µl of Annexin V-APC antibody (BD Biosciences). Cells were then analysed by flow cytometery to determine live cells (PI-, AV-), or apoptotic cells (PI-, AV+ or PI+. AV+) (n=3, two-tail homoscedastic t-test).

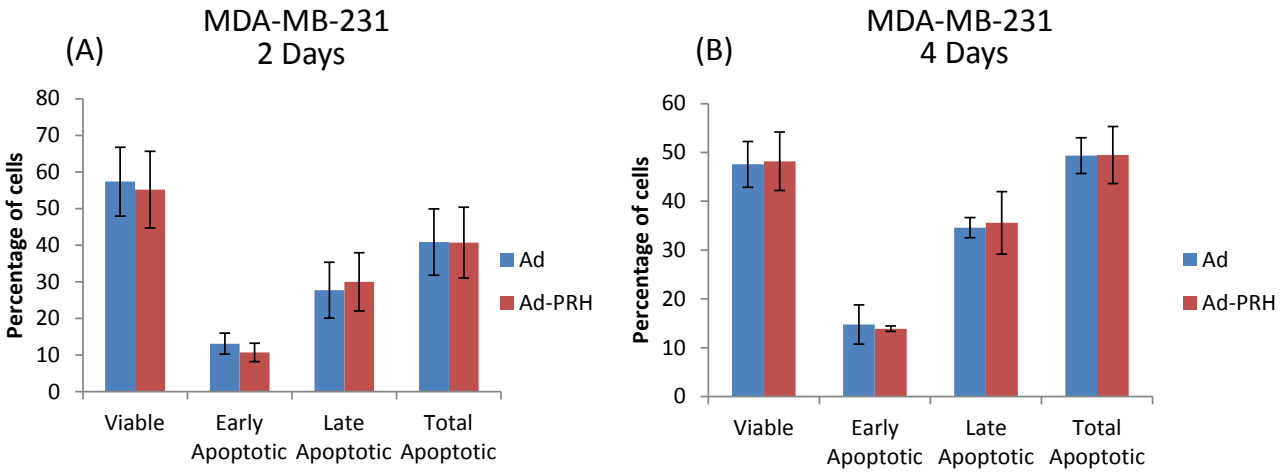

Figure 4.7: Ad-PRH does not increase apoptosis in MDA-MB-231 cells. MDA-MB-231 cells were incubated with control Ad or Ad-PRH for either 2 (A) or 4 (B) days, before being stained with 10µg/µl propodium iodide and 5µl of Annexin V-APC antibody (BD Biosciences). Cells were then analysed by flow cytometery to determine live cells (PI-, AV-), or apoptotic cells (PI-, AV+ or PI+. AV+) (n=3, two-tail homoscedastic t-test).

is no statistically significant difference between the proportions of viable, early apoptotic and late apoptotic cells at either 2 or 4 days post-infection (figure 4.7). The rate of apoptosis however is quite high in these cells (approximately 30%, compared to around 10-15% for MCF-10A and MCF-7 cells). This could be due to this cell line being particularly sensitive to trypsin, or the flow cytometery process.

4.2.4 Effect of overexpressed PRH on cell proliferation

To determine whether the decrease in cell number observed upon PRH overexpression in MCF-10A and MCF-7 cells is through alterations in cell proliferation, two assays were carried out. The first assay was a cell cycle assay, which measures the percentage of cells in each phase of the cell cycle through intensity of PI staining. During G1 phase, the cell has 2N number of chromosomes (diploid in normal human cells, although many cancer cells tend to

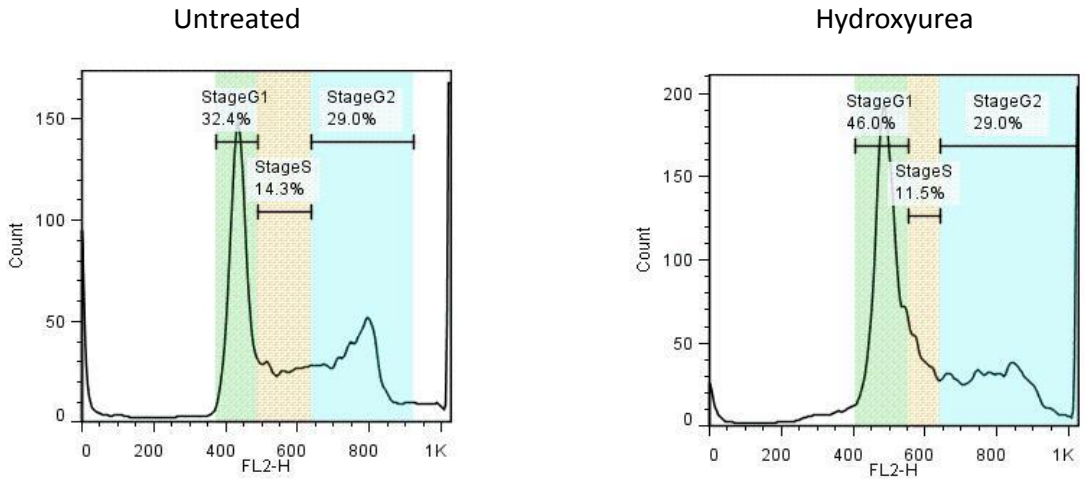

Figure 4.8: Hydroxyurea causes an increase in G1 phase. MCF-7 cells were incubated with 1mM hydroxyurea (or left untreated) for 24 hours, before being permeabilised with 1% IGEPAL, and DNA stained with 50µg/ml propidium iodide. Cells were then analysed by flow cytometery to determine cell cycle phase.

have large chromosomal abnormalities). As the cell progresses through S phase, the amount of total DNA in the cell increases until the cell has reached G2 phase, where the cell now possesses 4N number of chromosomes (tetraploid in normal human cells). Therefore, the proportion of cells at different stages of the cell cycle can be identified by DNA content (Krishan, 1977). The assay involves the incubation of cells with PI, which binds non-specifically to DNA by intercalating between the base pairs (Krishan, 1975). As PI cannot penetrate through the cell membrane, cells are first permeabilised with 1% IGEPAL. Flow cytometry is then used to differentiate cells that stain brightly with PI (G2/M) from those that stain more weakly (G1). To show that this assay can be used to examine growth arrest, that is an increase in the percentage of cells in the G1 or G2 phase of the cell cycle, MCF-7 cells were treated 1mM hydroxyurea for 24 hours. Hydroxyurea is a DNA synthesis inhibitor, that does not allow the cell to progress past S-phase, thus arresting cells in G1 (Koç et al., 2004). Figure 4.8 shows that hydroxyurea induces G1 arrest.

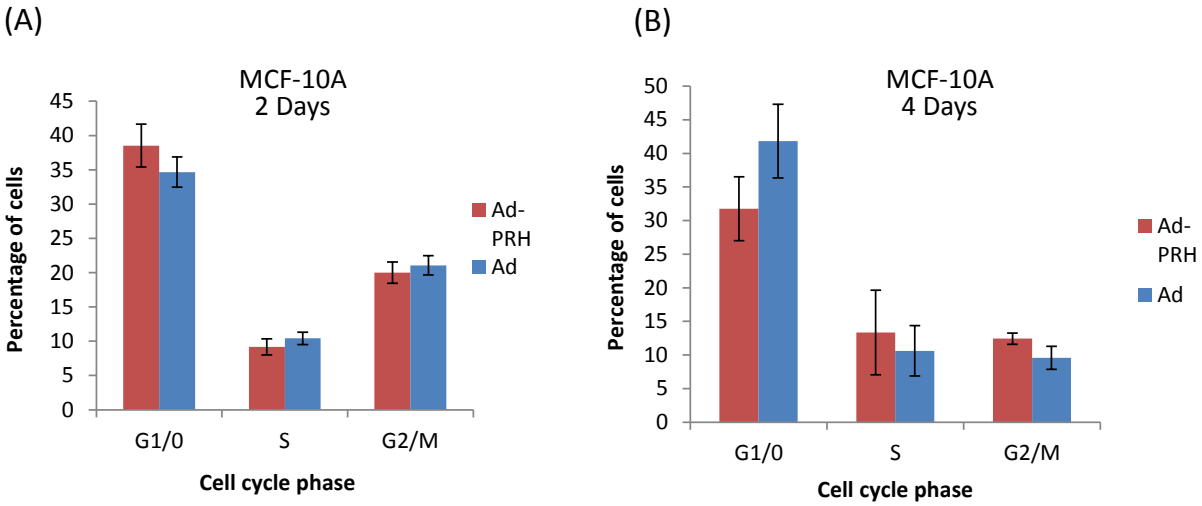

Figure 4.9: Ad-PRH does not affect cell cycle distribution in MCF-10A cells. MCF-10A cells were incubated with control Ad or Ad-PRH for either 2 (A) or 4 (B) days, before being permeabilised with 1% IGEPAL, and DNA stained with 50µg/ml propidium iodide. Cells were then analysed by flow cytometery to determine cell cycle phase (n=3, two-tail homoscedastic t-test).

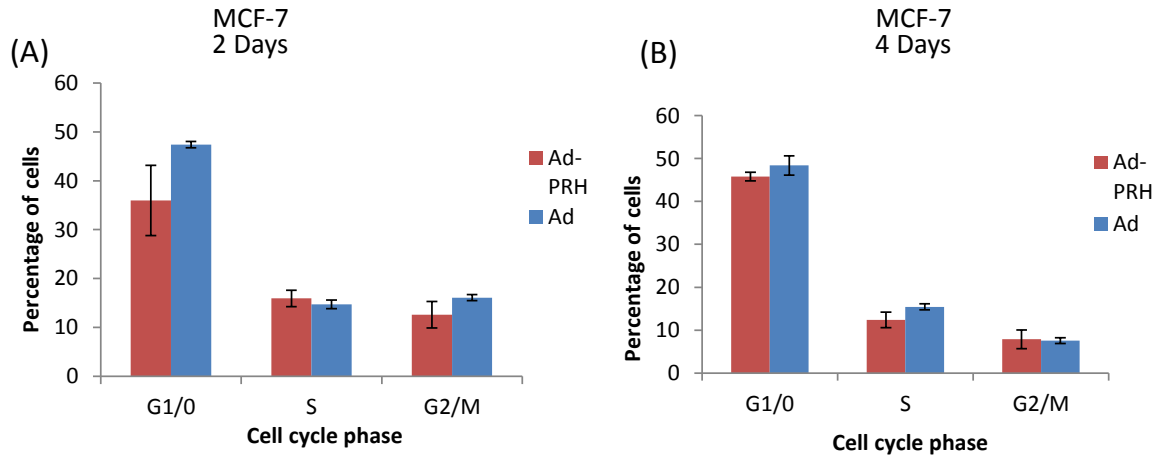

Figure 4.10: Ad-PRH does not affect cell cycle distribution in MCF-7 cells. MCF-7 cells were incubated with control Ad or Ad-PRH for either 2 (A) or 4 (A) days, before being permeabilised with 1% IGEPAL, and DNA stained with 50µg/ml propidium iodide. Cells were then analysed by flow cytometery to determine cell cycle phase (n=3, two-tail homoscedastic t-test).

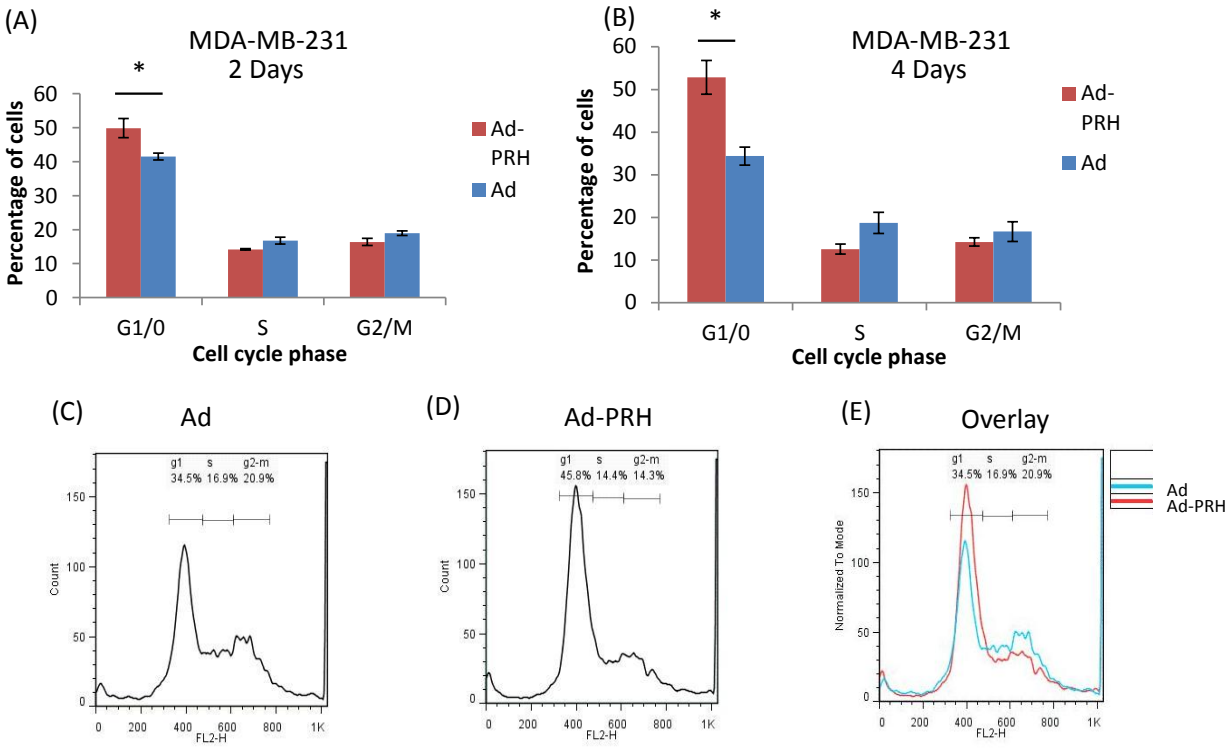

Figure 4.11: Ad-PRH increases the proportion of cells in G1 phase in MDA-MB-231 cells. MDA-MB-231 cells were incubated with control Ad or Ad-PRH for either 2 (A) or 4 (B) days, before being permeabilised with 1% IGEPAL, and DNA stained with 50µg/ml propidium iodide. Cells were then analysed by flow cytometery to determine cell cycle phase. Representative plots are shown in (C) and (D) for Ad and Ad-PRH respectively 4 days post infection, with (E) showing an overlay of the two plots (n=3, two-tail homoscedastic t-test *p<0.05).

Cell cycle staining was carried out with Ad-PRH and control Ad infected MCF-10A, MCF-7 and MDA-MB-231 cells at 2 and 4 days post-infection. In MCF-10A cells there is no significant difference in the cell cycle distribution at either 2 or 4 days post infection (figure 4.9). In MCF-7 cells, there is also no significant change in cell cycle between the Ad and Ad-PRH infected cells at either 2 or 4 days post-infection (figure 4.10). However, Ad-PRH did have a significant effect on cell cycle in MDA-MB-231 cells, as the proportion of Ad-PRH infected cells in G1 phase was increased compared to cells infected with control Ad at both 2 and 4 days post-infection (figure 4.11).

A more direct assay to measure rate of cell proliferation is the bromodeoxyuridine (BrdU) incorporation assay. BrdU is a nucleoside which can substitute for thymidine during DNA replication. Cells are incubated with 5'-bromodeoxycytidine, which is deaminated to BrdU by the cell. The incorporated BrdU is then detected by immunohistochemistry using antibodies against BrdU, and secondary or tertiary antibodies conjugated to horse radish peroxidase (HRP). When tertiary antibodies are used the signal from the primary antibody is amplified by use of a biotinylated secondary antibody. The uptake of BrdU can be quantified by scoring for HRP staining, and the rate of uptake over a defined time is used as a measure of the rate of proliferation (Hoshino T, 1985).

BrdU assays were performed as described in Materials and methods section 2.6.2. A sub-selection of slides was also blindly double-scored to ensure there was no bias in counting. In MCF-10A cells, very few cells infected with Ad-PRH incorporate BrdU, indicating that PRH significantly inhibits proliferation in MCF-10A cells (figure 4.12). Significantly, the Ad-PRH N187A mutant has no effect on MCF-10A proliferation. This demonstrates that PRH needs to bind to DNA to produce its proliferation inhibitory phenotype (figure 4.12). MCF-7 cells could not be assessed for BrdU staining, as Ad-PRH infected cells would not stay attached to the plate when plated at the densities required for this protocol. In MDA-MB-231 cells, Ad-PRH infected cells incorporate significantly less BrdU than control Ad infected cells, indicating that they are less proliferative (figure 4.13). Again, Ad-PRH-N187A had little effect on proliferation, as BrdU uptake was similar to control cells. This demonstrates that PRH needs to bind to DNA to carry out its anti-proliferative effect in MDA-MB-231 cells (figure

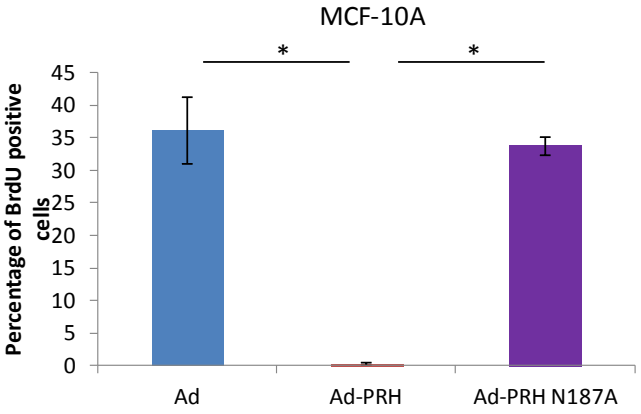

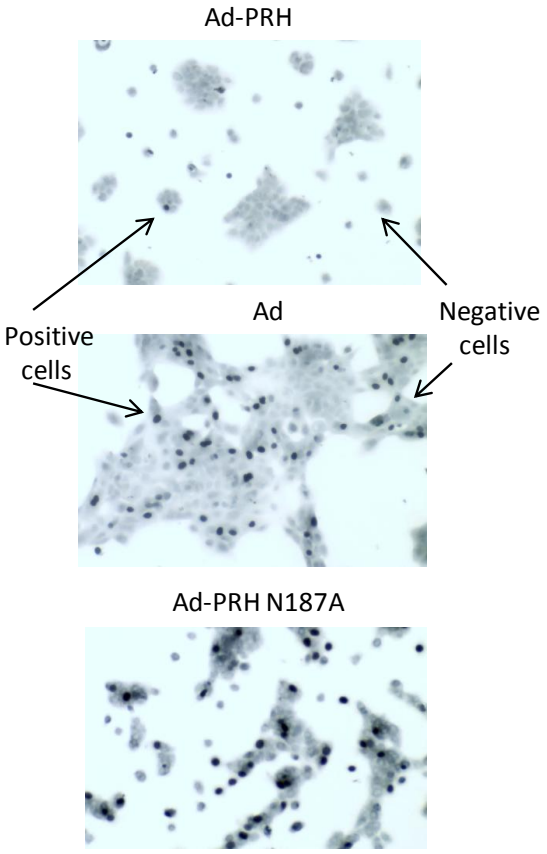

Figure 4.12: Overexpression of PRH inhibits MCF-10A proliferation as determined by BrdU staining. MCF-10A cells were infected with Ad or Ad-PRH as described previously. $5x10^5$ cells were then seeded on a 6-well plate and left for 48 hours, and were then incubated with 10µM BrdU for 6 hours. Cells were then fixed and stained for BrdU positivity as described in text (n=3,3,2, one way ANOVA with Games-Howell post-hoc *p<0.05).

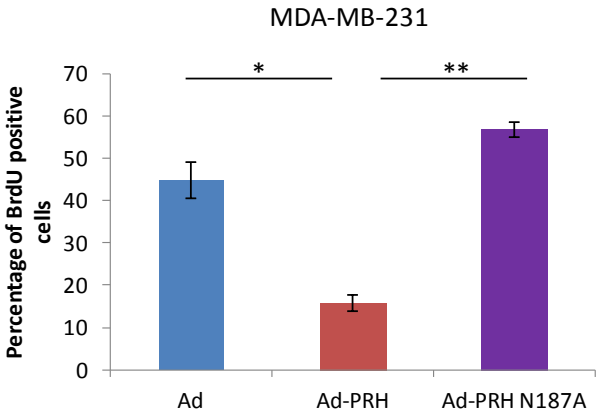

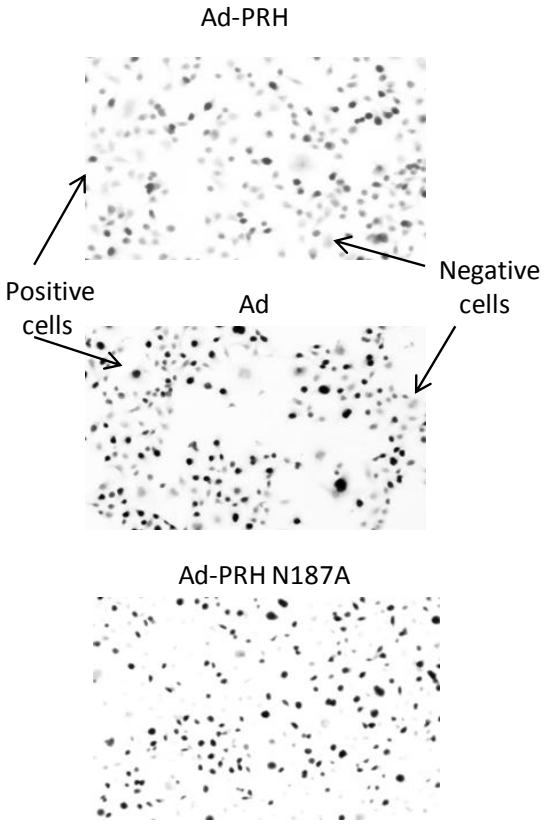

Figure 4.13: Overexpression of PRH inhibits MDA-MB-231 proliferation as determined by BrdU staining. MDA-MB-231 cells were infected with Ad or Ad-PRH as described previously. $5x10^5$ cells were then seeded on a 6-well plate and left for 48 hours, and were then incubated with 10µM BrdU for 6 hours. Cells were then fixed and stained for BrdU positivity as described in text (n=3,3,2 one way ANOVA with Games-Howell post-hoc *p<0.05 **p<0.01).

4.13). The proportion of BrdU positive cells seen in these experiments are similar to that seen in other studies (Zhang et al., 2012, Bosco et al., 2007)

To summarise, Ad-PRH infection decreases the cell number of MCF-10A and MCF-7 cells, but no change in cell number was detected in MDA-MB-231 cells. Ad-PRH infection inhibits MCF-10A proliferation as determined by BrdU assays, but no effect is seen in Annexin V/PI assays or cell cycle assays. This inhibition of cell proliferation by PRH is dependent on PRH binding to DNA. Ad-PRH infection increases MCF-7 cell apoptosis, but does not affect the cell cycle profile, and BrdU assays were not possible in this cell type. Although PRH does not appear to decrease cell number in MDA-MB-231 cells, PRH is exerting an inhibitory effect on cell proliferation. A small increase in the percentage of cells in G1 phase is observed in Ad-PRH infected MDA-MB-231 cells, and this correlates with a decrease in BrdU staining, indicating that the cells are less proliferative. This effect however may be too small to detect in cell counting assays. In conclusion, PRH overexpression inhibits cell proliferation in all three cell lines, and the effects are mediated by DNA binding.

4.3 Effect of PRH knockdown on breast cell proliferation and survival

4.3.1 Generating PRH knockdown lentiviruses

To further investigate the role of PRH in breast cell survival and proliferation, we wished to decrease PRH protein in all the cell lines through the use of small hairpin RNA (shRNA) against *PRH*. ShRNA molecules consist of 2 self-complimentary sequences between 19-29 base pairs long, one of which is homologous to the target gene, separated by an 8 nucleotide loop (Paddison et al., 2002). ShRNA is transcribed by the cell and then exported to the cytoplasm, and is then incorporated into the RNA induced silencing complex (RISC), where the shRNA is then cleaved into a guide and passenger strand. The guide strand is complementary or near complementary to the target mRNA. The target mRNA is then cleaved (in the case of perfect complementarity), or translation of the protein is inhibited (in the case of imperfect complementarity) causing decreased expression of the target protein (Wang et al., 2011).

Previous shRNA vectors used in the Jayaraman laboratory were plasmid based vectors that can integrate randomly into the genome and constitutively express the shRNA. This approach has been problematic as it has been observed in the laboratory that PRH knockdown decreases over time, possibly due to silencing of the promoter expressing the shRNA in the region where integration has taken place, and thus knockdown of PRH has disappeared before cells have grown in sufficient numbers to be assayed. Small interfering

RNA (siRNA) was also used to knockdown PRH in these breast cells, however as this produces a relatively short-term effect, no decrease in PRH protein levels could be observed using Western blotting. Presumably one reason for this is that PRH has been shown to be a relatively long-lived protein in leukaemic cells (Bess et al., 2003b), and our own studies (section 3.7) confirm this to be the case in breast cells.

Therefore, to produce cell lines which have reduced PRH expression that can be detected by Western blotting, a lentiviral plasmid vector with puromycin resistance and containing an inducible shRNA was obtained (Sigma, see figure 2.4 in Materials and methods). This plasmid also allows constitutive expression of LacI repressor protein. The shRNA is under control of a modified human U6 promoter with 3 LacO sequences. In the absence of IPTG, LacI protein binds to the LacO sequences, preventing expression of the shRNA. When ITPG is bound to LacI, the conformation of LacI changes, and LacI can no longer bind to the LacO sequences, allowing transcription of the shRNA. This plasmid can be used to produce IPTG inducible lentiviruses. These lentiviruses can also infect a greater variety of cell types then adenoviruses, including non-dividing cells (Fassati, 2006). Another advantage of this method is that lentiviruses integrate their DNA directly into the chromosome relatively efficiently, and puromycin resistant clones can be propagated, allowing efficient and stable expression of the shRNA upon induction with IPTG. In the absence of IPTG cells can be expanded in large numbers and this facilitates biochemical experiments after IPTG induction.

Firstly PRH knockdown and control lentiviruses were made. This was achieved by co-transfecting plasmids psPAX2 (expressing Gag and Pol), pMD2.G (expressing envelope protein VSV-G) and pLKO-puro-IPTG-3xLacO (expressing the shRNA) into HEK-293T

packaging cells (see Materials and methods figures 2.5-2.7 for maps). The media from these cells containing the virus was then harvested and centrifuged 48 hours later, purifying the virus (see Materials and methods section 2.5.1). To create PRH knockdown and control (shRNA coding for no known mammalian gene) shRNA polyclonal cells, cells from each cell line were infected with lentiviruses at an approximate MOI of 0.1 (see Materials and methods section 2.5.2). Infected cells were then selected 48 hours later, by incubating cells with 0.5µg/ml of puromycin for 7 days. 100% of uninfected cells die within 7 days of puromycin treatment. Puromycin resistant cells were then cultured in 1mM IPTG to induce shRNA expression.

Control and PRH knockdown MCF-7 cells were analysed for PRH protein levels using Western blotting with the M6 antibody at 2, 5 and 7 days post-IPTG induction. Figure 4.14 shows that PRH protein expression as detected by the M6 antibody is reduced after 7 days of IPTG induction compared to controls, but that at 2 and 5 days post-induction no decrease in protein is visible. Lentiviral infection of MCF-7 cells was repeated several times independently to generate 3 independent PRH knockdown and 3 independent control puromycin resistant cell lines. This protocol was repeated for MCF-10A and MDA-MB-231 cells to produce three independent PRH and control shRNA cell lines for each cell type. Figure 4.15 shows that in MCF-10A, MCF-7 and MDA-MB-231 cells, PRH expression is significantly reduced in the *PRH* shRNA cells compared to the control cells, showing that for all 3 cell lines the inducible shRNA system works effectively at 7 days post IPTG induction. In all assays described below the effects of PRH knockdown were assessed in three independent knockdown cell lines.

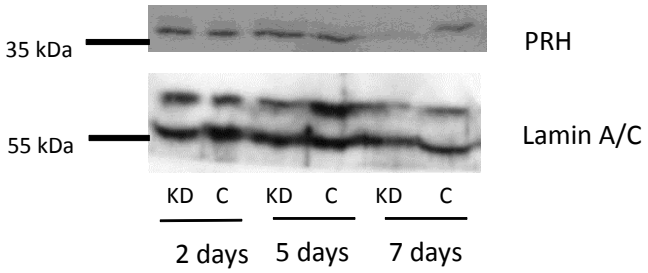

Figure 4.14: Inducible knockdown of PRH in MCF-7 cells. Cells were infected with lentivirus containing shRNA coding for either *PRH* (KD) or against no known mammalian gene as a control (C). Infected cells were then selected using 0.5µg/ml puromycin for 7 days, and shRNA expression was then induced using 1 mM IPTG. Cells were pelleted 2, 5 and 7 days post-induction, and protein was extracted and probed using Western blotting with the M6 antibody to check for successful knockdown.

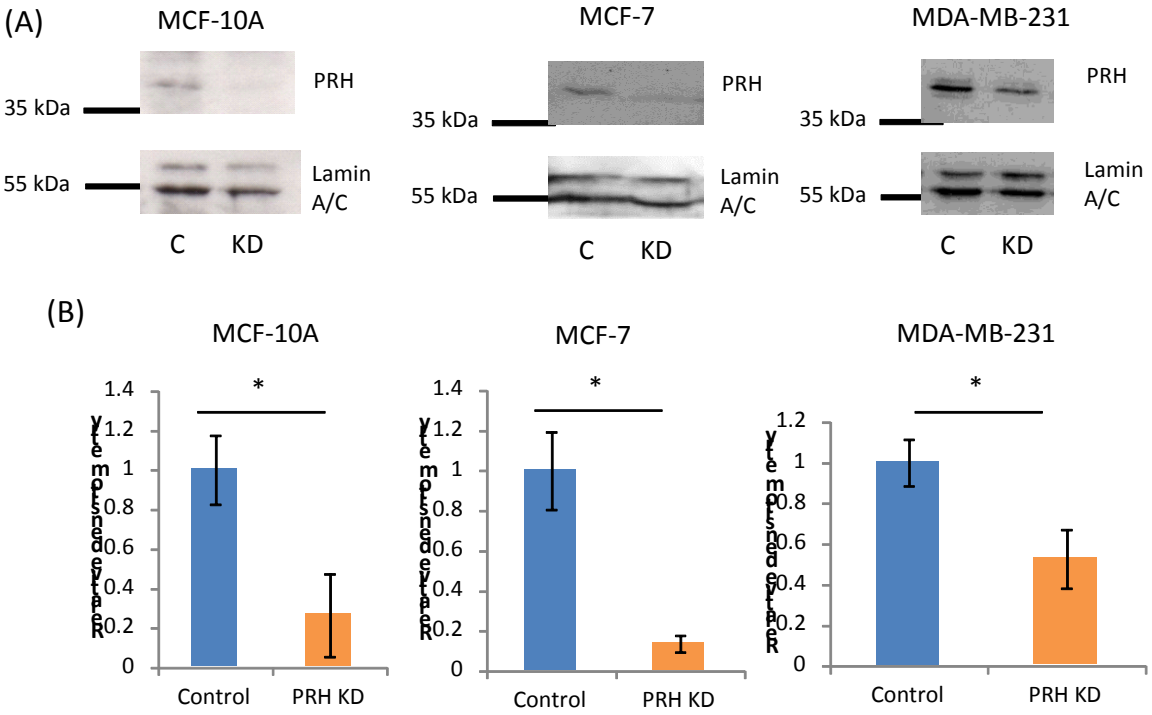

Figure 4.15: Inducible knockdown of PRH in MCF-10A, MCF-7 and MDA-MB-231 cells. Cells were infected with lentivirus containing shRNA coding for either *PRH* (KD) or against no known mammalian gene as a control (C). Infected cells were selected by incubating with 0.5µg/ml puromycin for 7 days. ShRNA expression was then induced using 1 mM IPTG. (A) Cells were pelleted 7 days post-induction, and protein was extracted, separated by SDS-PAGE and probed using Western blotting with the M6 antibody to check for successful knockdown. (B) PRH protein expression was quantified by densitometric quantification of Western blots of three independent PRH knockdown and control cell lines using the M6 anti-PRH antibody, and Lamin C as a loading control (n=3, two-tail homoscedastic t-test, *p>0.05).

4.3.2 Knockdown of PRH decreases MCF-7 cell number

To determine whether changes in the level of endogenous PRH affect breast cell growth, cell counting assays were carried out. Cumulative growth curves were then calculated by multiplying the total cell number by the cell dilution at replating. For MCF-10A cells, there was very little difference in cell number between PRH knockdown cells and controls (figure 4.16 (A)). For MCF-7 cells however, there were significantly more PRH knockdown cells than control cells (figure 4.16 (B)). Surprisingly, in MDA-MB-231 cells there were significantly less PRH knockdown cells than control cells (figure 4.16 (C)). To confirm these results 3-(4,5-Dimethylthiazol-2-yl)-2,5-diphenyltetrazolium bromide (MTT) assays were carried out. MTT assays measure the number of metabolically active cells, because the MTT compound is converted into an insoluble coloured formazan by the mitochondria of the cells. This product is dissolved in DMSO and can be measured by the absorption of the product at a wavelength of 600nm. The coloured formazan is proportional to the number of viable cells present, within a linear range (see Materials and methods section 2.2.2) (Mosmann, 1983). Using this assay, no difference in viable cell number was observed between knockdown and control cells in MCF-10A cell lines (figure 4.17 (A)).

MCF-10A cells are grown with high amounts of horse serum, as well as insulin, epidermal growth factor and cholera toxin. Thus they show a requirement for many growth factors. It was hypothesised that the high level of growth factor signalling could be masking any effect of PRH loss on the growth of this cell line. To determine whether PRH affected MCF-10A cell

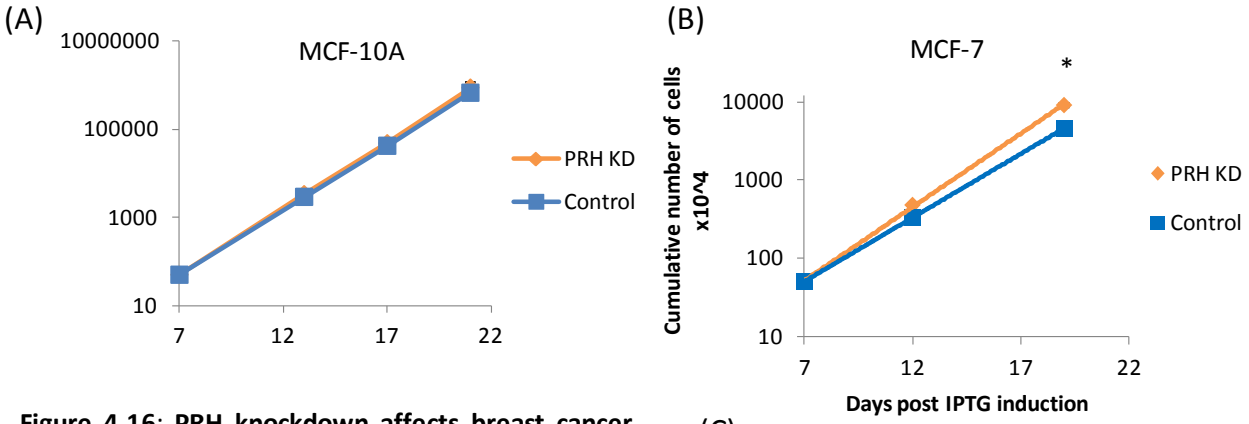

Figure 4.16: **PRH knockdown affects breast cancer cell number, but not normal MCF-10A growth rates.** Cell counting assays were carried out with PRH knockdown and control MCF-10A (A), MCF-7 (B) or MDA-MB-231 (C) cells. ShRNA expression was induced by incubating cells in 1mM IPTG for 7 days. $1x10^5$ cells were then plated in a $25cm^2$ flask, and cells were then counted 5 days after seeding. Cells were then replated and the process repeated, and the cumultive cell number was then determined by multilplying the number of cells counted by the dilution of cells at seeding. (n=3, *p<0.05 two-tail homoscedastic t-test).

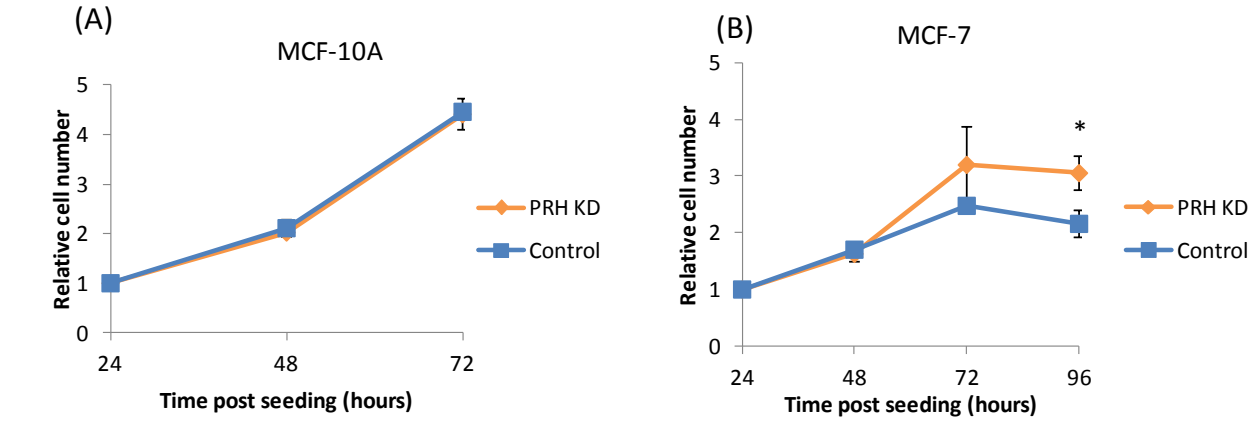

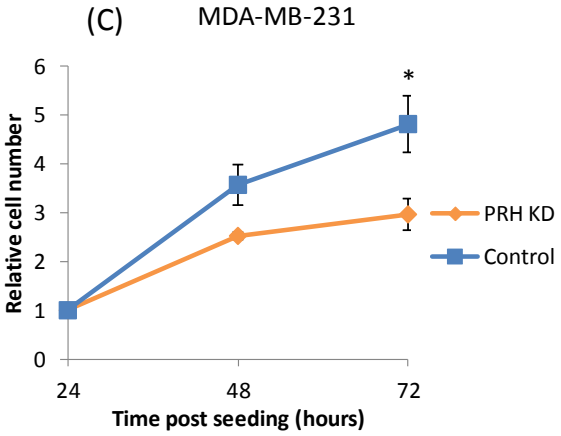

Figure 4.17: PRH knockdown affects breast cancer cell number, but not normal MCF-10A cell number. MTT assays were carried out with PRH knockdown and control MCF-10A (A), MCF-7 (B) or MDA-MB-231 (C) cells. Cells were induced as in figure 4.16. 2,000 cells were then seeded into a well in a 96-well plate in quadruplicate for each time point. After 24, 48, 72 and 96 hours (for MCF-7 cells), cells were incubated with 500 µg/ml 2-MTT for 2 hours, and the MTT crystals were then dissolved with DMSO and the optical density was then read at 600nm. (n=3, p<0.05 two-tail homoscedastic t-test).

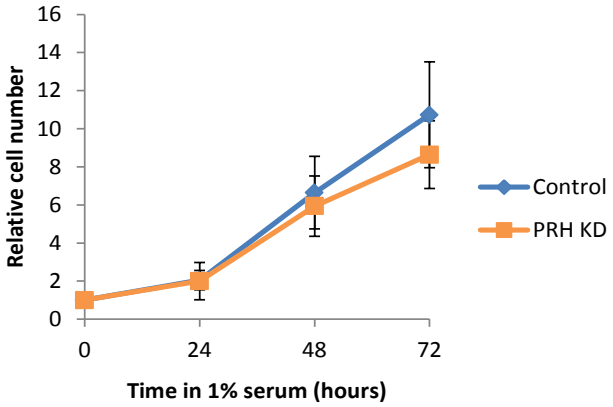

Figure 4.18: PRH knockdown does not affect MCF-10A cell number in 1% serum. MTT assays were carried out with PRH knockdown and control MCF-10A cells, which were set up and induced as in figure 4.17, but with reduced horse serum content (1% instead of 5%). After 24, 48 and 72 hours, cells were incubated with 500 µg/ml 2-MTT for 2 hours, and the MTT crystals were then dissolved with DMSO and the optical density was then read at 600nm (n=2) .

number in sub-optimal growth conditions, the MTT assay was repeated as described above, but cells were cultured in media containing 1% horse serum rather than 5% horse serum. However, there was still no difference between PRH knockdown and control cell number in these conditions (figure 4.18), thus PRH knockdown appears to have little effect on the rate of increase of the MCF-10A population.

In contrast, there were significantly more viable cells in MCF-7 PRH knockdown cell lines compared to controls at 72 hours post plating, in agreement with the results of cell counting experiments (figure 4.17 (B)). However in MDA-MB-231 cells, there were significantly fewer viable cells in the PRH knockdown cell lines compared to control cell lines (figure 4.17 (C)). Again this is in agreement with the results of cell counting experiments.

4.3.3 Effect of PRH knockdown on cell cycle

To investigate whether the effects of PRH knockdown observed in each cell line are a result of a change in cell proliferation or cell death, cell cycle and BrdU assays were carried out. MCF-10A control and PRH knockdown cells were induced for 7 days with IPTG and then plated into a 6 well plate. Twenty four hours later cells were analysed for DNA content by flow cytometery as described earlier. As expected MCF-10A control and PRH knockdown cells showed no significant difference in the percentage of cells in each phase of the cell cycle (figure 4.19 (A)). However, when MCF-7 control and knockdown cells were similarly induced and analysed a significant shift in the G1 peak was observed (figures 4.19 (B) and 4.20). This could be due to an increased proportion of S-phase cells, or it could be due to increased amount of propidium iodide staining the cells. Further experiments need to be carried out to determine whether there is an increased amount of S-phase cells, or whether this result is an artefact. Finally under similar induction and assay conditions, the MDA-MB-231 control and PRH knockdown cells show little difference in distribution of cells in each stage of the cell cycle profile (figure 4.19 (C)). This is unexpected as it was observed that population growth for PRH knockdown MDA-MB-231 cells is slower than control cells. However, cell cycle assays only show if there are alterations in the distribution of cells, but do not measure the rate of proliferation. Thus BrdU assays were employed to determine whether decreased cell number was a consequence of alterations in the rate of proliferation.

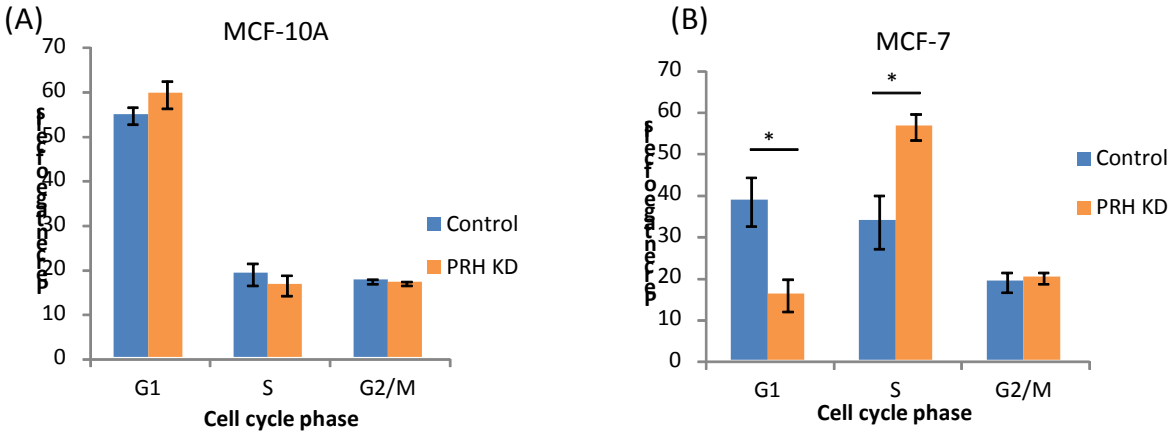

Figure 4.19: Knockdown of PRH affects MCF-7 but not MCF-10A or MDA-MB-231 cell cycle distribution. MCF-10A (A), MCF-7 (B) and MDA-MB-231 (C) cells were infected with lentivirus and induced as described in figure 4.16. $5x10^5$ cells were then seeded on a 6-well plate and left for 24 hours, before being lysed with 1% IGEPAL, and DNA stained with 50µg/ml propidium iodide. Cells were then analysed by flow cytometery to determine cell cycle phase (n=3, *p<0.05 two-tail homoscedastic t-test).

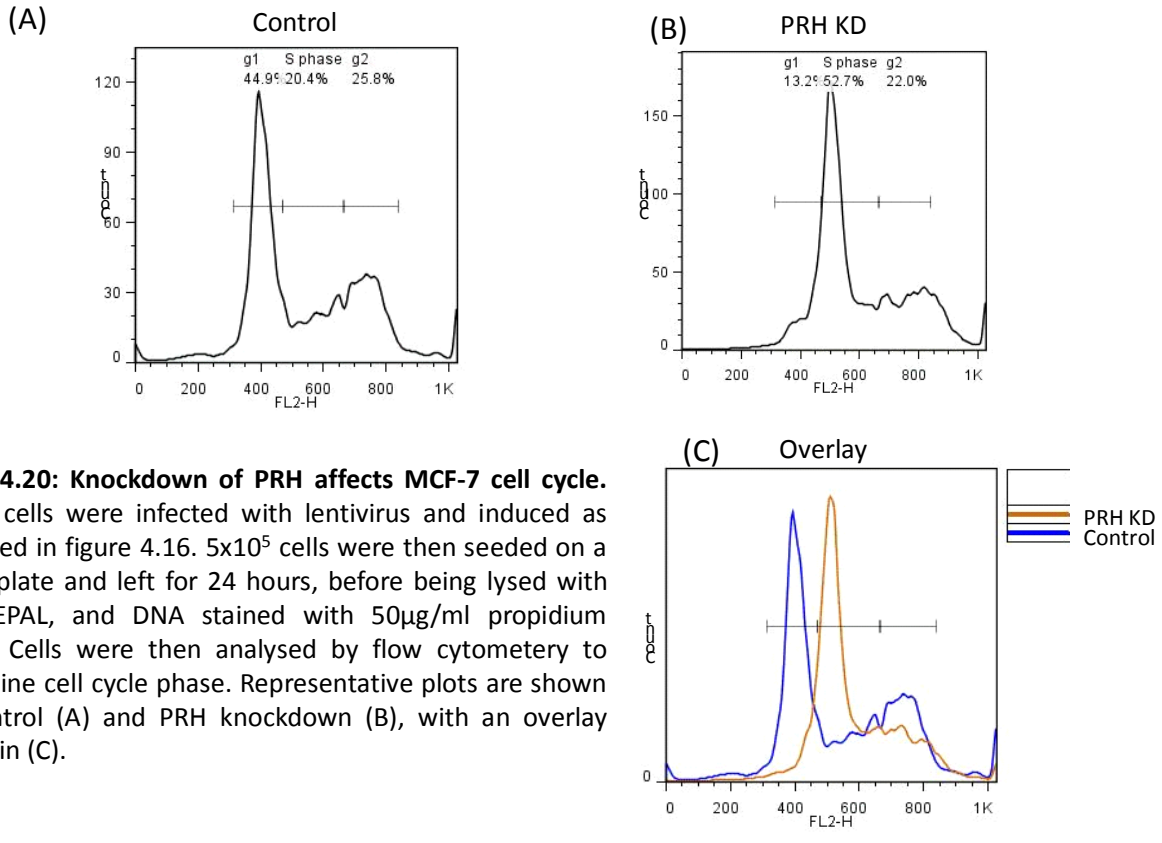

Figure 4.20: Knockdown of PRH affects MCF-7 cell cycle. MCF-7 cells were infected with lentivirus and induced as described in figure 4.16. $5x10^5$ cells were then seeded on a 6-well plate and left for 24 hours, before being lysed with 1% IGEPAL, and DNA stained with 50µg/ml propidium iodide. Cells were then analysed by flow cytometery to determine cell cycle phase. Representative plots are shown for control (A) and PRH knockdown (B), with an overlay shown in (C).

4.3.4 Effect of PRH knockdown on cell proliferation

To determine whether PRH affects the rate of cell proliferation in these cell types, BrdU assays were carried out as previously described. MCF-10A control and PRH knockdown cells were induced for 7 days with IPTG and then plated into a 6 well plate. After 24 hours, cells were incubated in media containing 10mM BrdU for 6 hours, before the cells were fixed and immunostained using a monoclonal BrdU antibody (see Materials and methods section 2.6.2). The percentage of BrdU positive cells was then counted in three fields for each knockdown and control cell line. PRH knockdown had no effect on the number of MCF-10A BrdU positive cells (figure 4.21), in agreement with the lack of difference seen in the cumulative growth curves and MTT assays seen in figures 4.16 and 4.17 respectively. PRH knockdown in MCF-7 cells significantly increased the percentage of BrdU positive cells in PRH knockdown cells compared to controls (figure 4.22), indicating that knockdown of PRH in this cell type increased the rate of cell proliferation. In contrast, PRH knockdown significantly reduced the proportion of BrdU positive MDA-MB-231 cells compared to Control cells, demonstrating that rate of cell proliferation is decreased (figure 4.23).

4.3.5 Knockdown of PRH has no effect on cell apoptosis

To determine whether the differences in cell growth in the knockdown cells are also a result of differences in cell apoptosis, PI/Annexin V co-staining assays were carried out. For each cell type, control and PRH knockdown cells were induced with IPTG for 7 days. Cells were

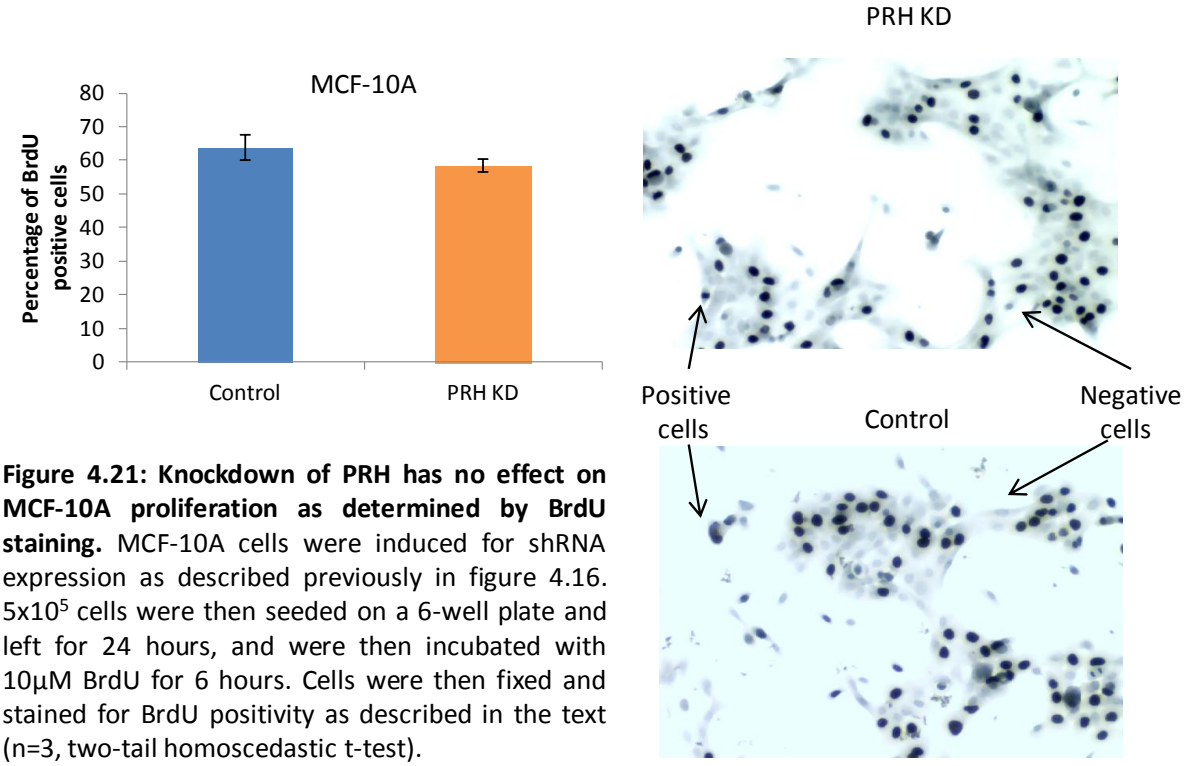

Figure 4.21: Knockdown of PRH has no effect on MCF-10A proliferation as determined by BrdU staining. MCF-10A cells were induced for shRNA expression as described previously in figure 4.16. $5x10^5$ cells were then seeded on a 6-well plate and left for 24 hours, and were then incubated with 10µM BrdU for 6 hours. Cells were then fixed and stained for BrdU positivity as described in the text (n=3, two-tail homoscedastic t-test).

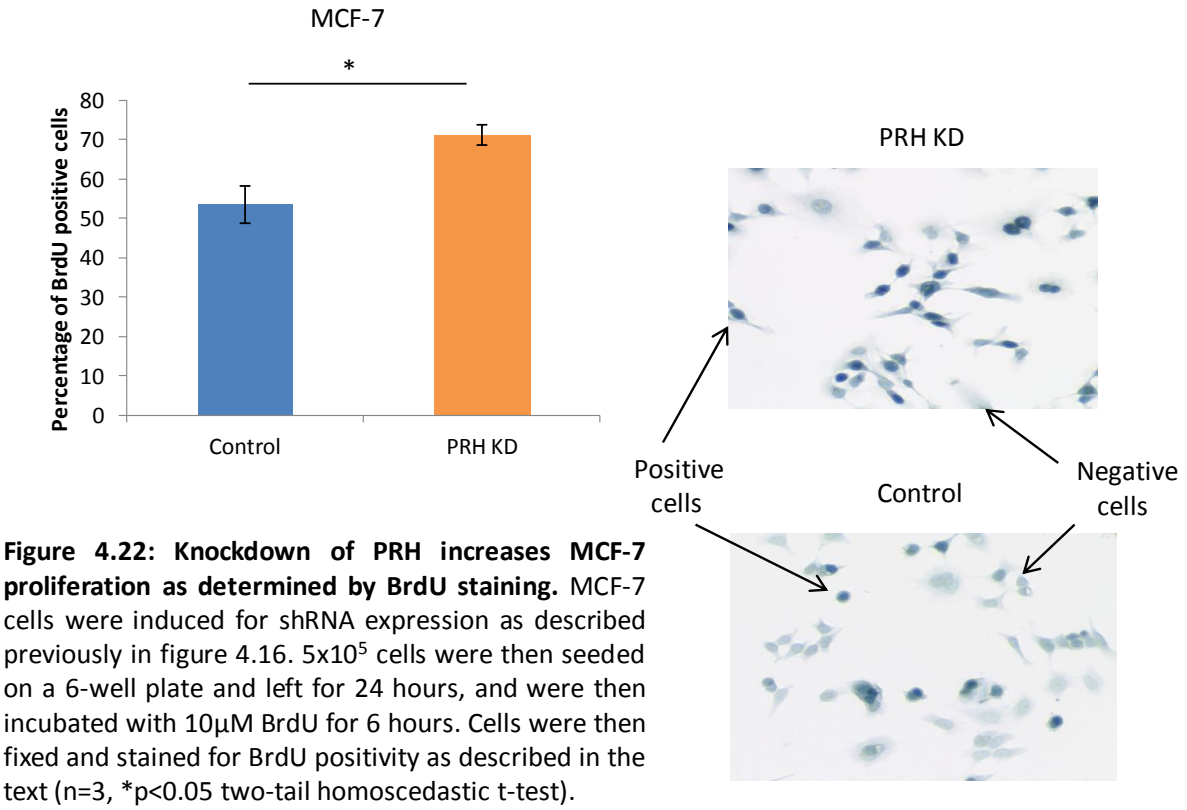

Figure 4.22: Knockdown of PRH increases MCF-7 proliferation as determined by BrdU staining. MCF-7 cells were induced for shRNA expression as described previously in figure 4.16. $5x10^5$ cells were then seeded on a 6-well plate and left for 24 hours, and were then incubated with 10µM BrdU for 6 hours. Cells were then fixed and stained for BrdU positivity as described in the text (n=3, *p<0.05 two-tail homoscedastic t-test).

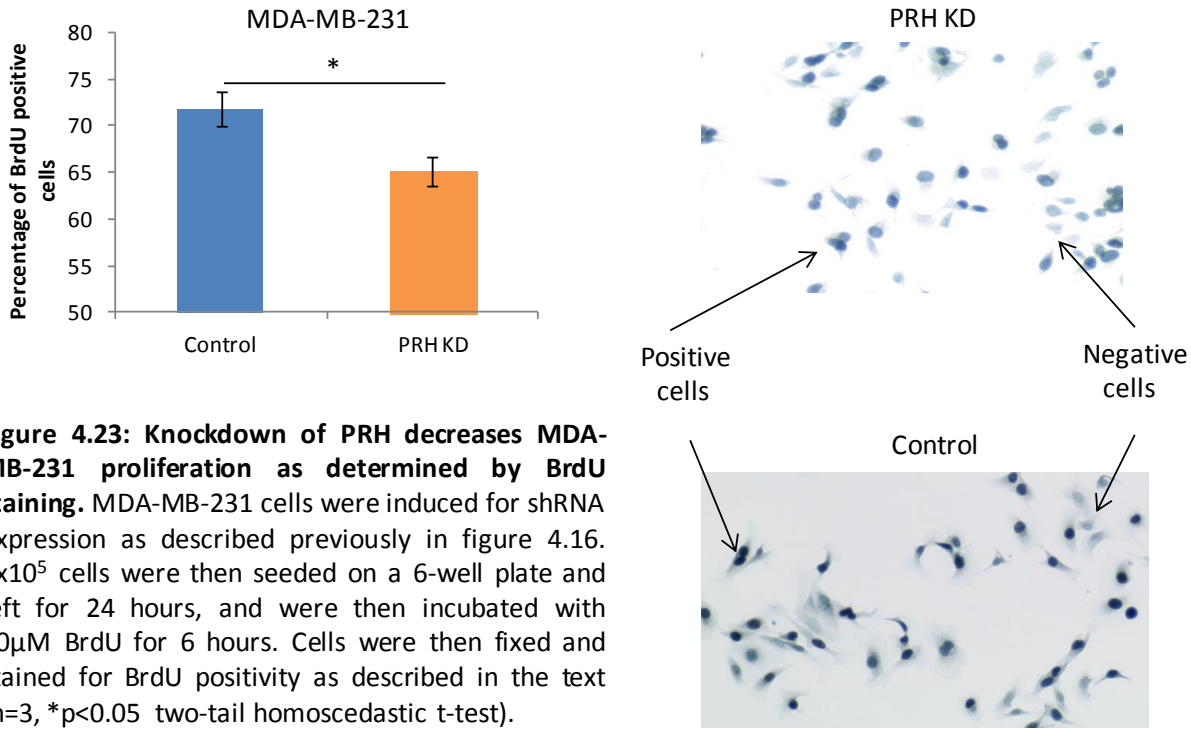

Figure 4.23: Knockdown of PRH decreases MDA-MB-231 proliferation as determined by BrdU staining. MDA-MB-231 cells were induced for shRNA expression as described previously in figure 4.16. $5x10^5$ cells were then seeded on a 6-well plate and left for 24 hours, and were then incubated with 10µM BrdU for 6 hours. Cells were then fixed and stained for BrdU positivity as described in the text (n=3, *p<0.05 two-tail homoscedastic t-test).

then plated into a 6 well plate at a density of $5x10^5$ cells per well, and 24 hours later the assays were performed in the same way as described previously. There was no effect of PRH on apoptosis in MCF-10A, MCF-7 or MDA-MB-231 cells (figure 4.24).

To summarise, loss of PRH in MCF-10A cells had no observable affect on cell number. Loss of PRH in MCF-7 cells leads to an increase in cell number, and this occurred through increased cell proliferation measured in BrdU and cell cycle assays. Surprisingly, loss of PRH in MDA-MB-231 cells leads to a decrease in cell number and proliferation, as determined using BrdU assays.

The results of PRH overexpression and knockdown are summarised in tables 4.1 and 4.2.

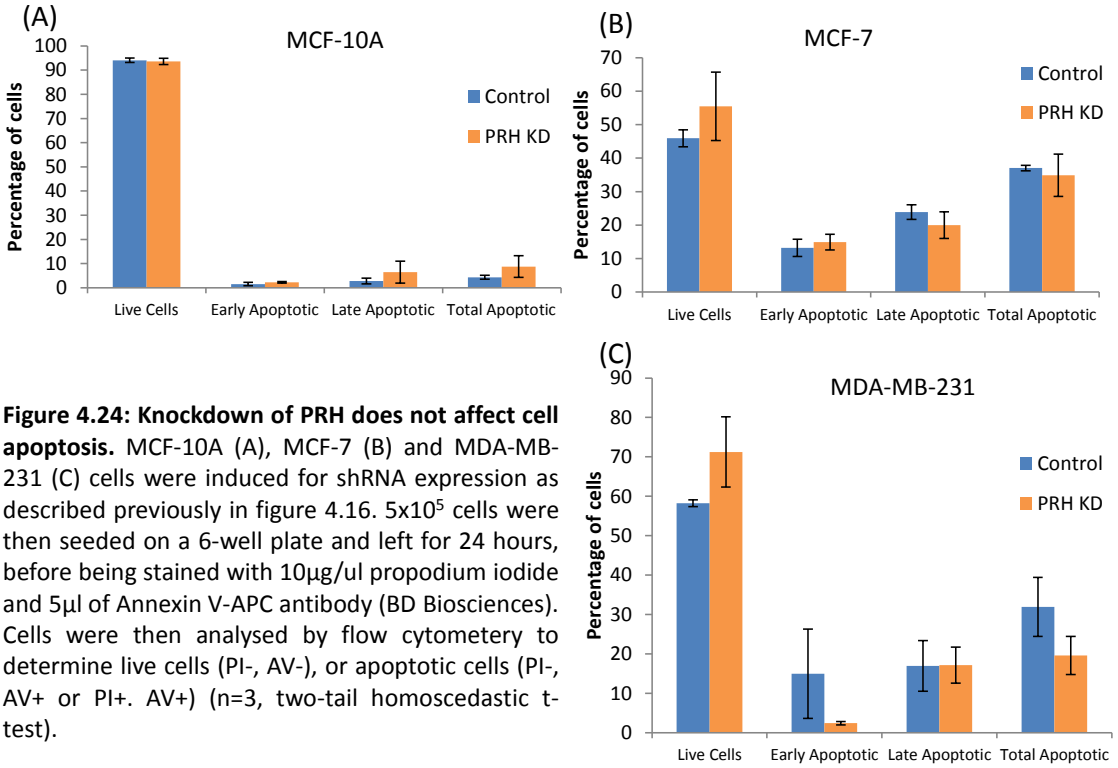

Figure 4.24: Knockdown of PRH does not affect cell apoptosis. MCF-10A (A), MCF-7 (B) and MDA-MB-231 (C) cells were induced for shRNA expression as described previously in figure 4.16. $5x10^5$ cells were then seeded on a 6-well plate and left for 24 hours, before being stained with 10µg/ul propodium iodide and 5µl of Annexin V-APC antibody (BD Biosciences). Cells were then analysed by flow cytometery to determine live cells (PI-, AV-), or apoptotic cells (PI-, AV+ or PI+. AV+) (n=3, two-tail homoscedastic t-test).

4.4 PRH and regulation of VEGF signalling genes

4.4.1 Gene expression analysis of VEGF signalling genes

Changes in cell proliferation and cell survival can both be mediated by VEGF signalling in endothelial and leukaemic cells (Noy et al., 2010, Nakagawa et al., 2003). In breast tumours VEGF acts in an autocrine manner, as well as in a paracrine manner on endothelial cells (Weigand et al., 2005). Microarray studies have identified many genes as targets for regulation by PRH (Nakagawa et al., 2003, Kubo et al., 2010). Genes from the VEGF signalling pathway (VSP) are direct targets of PRH in leukaemic cells, and are involved in promoting

PRH overexpression	MCF-10A	MCF-7	MDA-MB-231
Cell number	Decrease in viable cells	Decrease in viable cells	No change
Cell cycle	No change	No change	Increase in G1
BrdU	Decrease in cell proliferation	Not assessed	Decrease in cell proliferation
Apoptosis	No change	Increased apoptosis	No change

Table 4.1: Summary of the effect of PRH overexpression in MCF-10A, MCF-7 and MDA-MB-231 breast cell lines.

PRH knockdown	MCF-10A	MCF-7	MDA-MB-231
Cell number	No change	Increase in viable cells	Decrease in viable cells
MTT	No change	Increase in viable cells	Decrease in viable cells
Cell cycle	No change	Apparent decrease in G1 phase and increase in S phase	No change
BrdU	No change	Increased proliferation	Decreased proliferation
Apoptosis	No change	No change	No change

Table 4.2: Summary of the effect of PRH knockdown in MCF-10A, MCF-7 and MDA-MB-231 breast cell lines.

cell survival (Noy et al., 2010). Therefore, one possibility is that PRH alters the growth of breast tumour cells by directly binding and regulating the expression of VEGF signalling genes. The effect of PRH on the expression of VSP target genes was assessed in both tumour cells lines and MCF-10A cells using quantitative real-time PCR. For all knockdown experiments, control and PRH knockdown cells were pelleted 7 days after IPTG induction. RNA extraction and cDNA synthesis was carried out as described in Materials and methods section 2.8. PCR reactions were then set up using a mastermix containing SYBR green (which binds non-specifically to double stranded DNA), as described in Materials and methods section 2.8.3. The Ct and efficiency of the reaction was then calculated for the gene of interest and the *GAPDH* housekeeping gene unless otherwise stated, and the relative expression ratios were determined using the Pfaffl method (Pfaffl, 2001b). Statistical analysis was carried out using two-tailed Student's t-test according to Materials and methods section 2.8.3.

For MCF-10A cells, overexpression of PRH significantly represses the *VEGFA* transcript (figure 4.25 (A)). Expression of VEGF Receptors *VEGFR1*, *VEGFR2* and *NRP1* mRNA is also lower in the Ad-PRH infected cells but this decrease is not statistically significant in the three biological repeats (figure 4.25 (A)). For the PRH knockdown MCF-10A cells, there is no significant difference in expression of *VEGF*, *VEGFR2* or *NRP1* mRNA between knockdown and control cells (Figure 4.25 (B)). The *VEGFR1* transcript is expressed in these cells, but the transcript is at a low expression level and not reproducibly detected. Therefore quantitative PCR for *VEGFR1* mRNA was not possible with these samples. In summary, there appears to be little regulation of VSP genes by endogenous PRH in normal MCF-10A cells. However, in

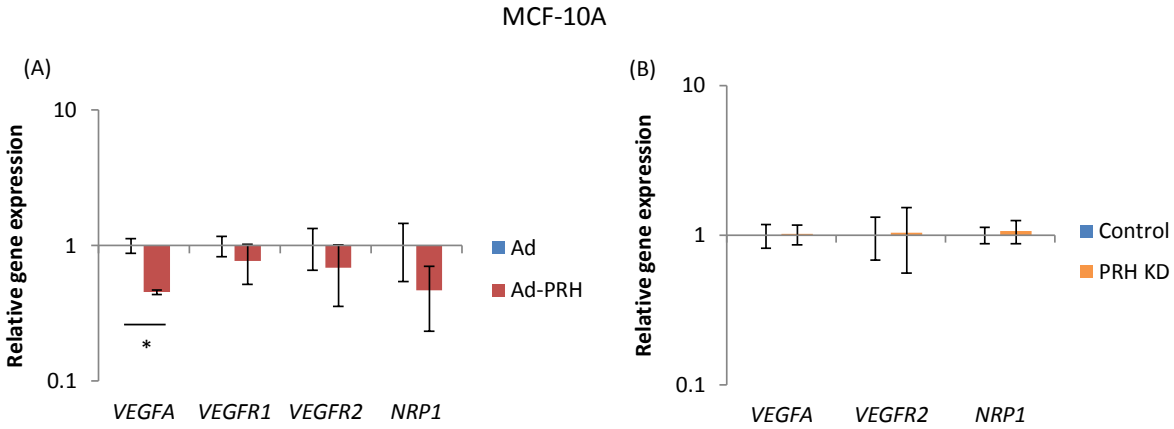

Figure 4.25: The effect of PRH on gene expression of VEGF signalling genes in MCF-10A cells. (A) MCF-10A cells were infected with either Ad or Ad-PRH at a MOI of 50 for 48 hours. Cells were then pelleted and RNA was extracted using a Bioline ISOLATE II kit, and complementary DNA was then synthesised. Gene expression was analysed using quantitative PCR, and quantified using the Pfaffl method (Pfaffl, 2001), using *GAPDH* as a housekeeping gene. (B) The same process was repeated but with PRH knockdown cells, which were induced for shRNA expression as previously described, however beta-actin was used as a housekeeping gene as *GAPDH* expression was too variable in these experiments (n=3, *p<0.05, two-tail homoscedastic t-test).

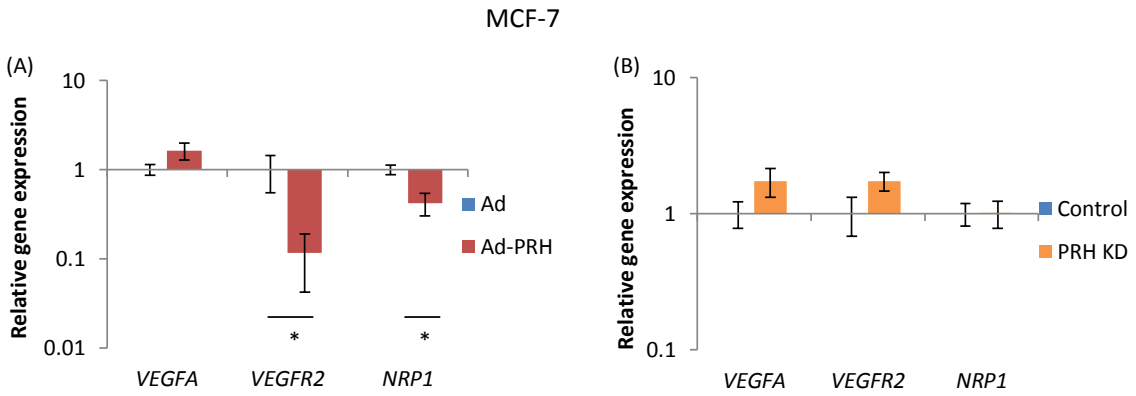

Figure 4.26: The effect of PRH on gene expression of VEGF signalling genes in MCF-7 cells. (A) MCF-7 cells were infected with either Ad or Ad-PRH at a MOI of 50 for 48 hours. Cells were then pelleted and RNA was extracted using a Bioline ISOLATE II kit, and complementary DNA was then synthesised. Gene expression was analysed using quantitative PCR, and quantified using the Pfaffl method (Pfaffl, 2001), using *GAPDH* as a housekeeping gene. (B) The same process was repeated but with PRH knockdown cells, which were induced for shRNA expression as previously described (n=3, *p<0.05, two-tail homoscedastic t-test).

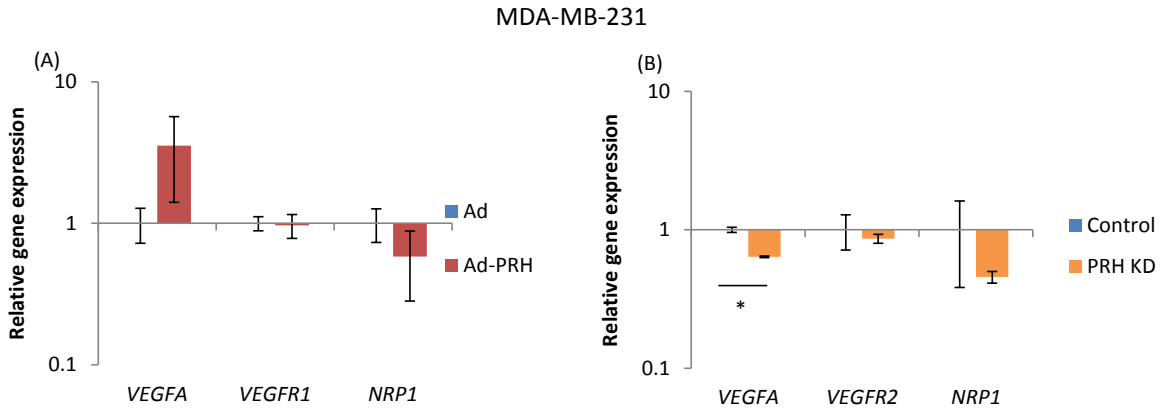

Figure 4.27: The effect of PRH on gene expression of VEGF signalling genes in MDA-MB-231 cells. (A) MDA-MB-231 cells were infected with either Ad or Ad-PRH at a MOI of 50 for 48 hours. Cells were then pelleted and RNA was extracted using a Bioline ISOLATE II kit, and complementary DNA was then synthesised. Gene expression was analysed using quantitative PCR, and quantified using the Pfaffl method (Pfaffl, 2001), using *GAPDH* as a housekeeping gene. (B) The same process was repeated but with PRH knockdown cells, which were induced for shRNA expression as previously described (n=3, *p<0.05, two-tail homoscedastic t-test).

overexpression experiments exogenous PRH may be able to bind at *VEGFA* promoter regions and effect some repression. Additional repeats will be required to achieve statistical significance at promoters of VEGF receptors/co-receptors. However it is possible that elevated PRH expression is modestly repressing several genes in the VSP.

For MCF-7 cells, PRH over-expression causes a significant repression in *VEGFR2* and *NRP1* mRNA expression (Figure 4.26 (A)). In the same experiment, *VEGFA* mRNA expression shows an apparent 50% increase in Ad-PRH infected MCF-7 cells, however this change is not statistically significant. Again *VEGFR1* mRNA is not expressed at a high enough level to be analysed by qPCR. In the PRH knockdown MCF-7 cells, *VEGF* and *VEGFR2* mRNA expression was almost two-fold higher than in control cells, but this change is not statistically significant when statistical analysis is carried out for three independent knockdown cell lines (figure 4.26 (B)). Previous experiments with a different shRNA knockdown in MCF-7 cells do

show a statistically significant increase in *VEGFA* and *VEGFR2* mRNA expression in MCF-7 cells (Noy et al., 2010). Therefore it is possible that if more cell lines had been assayed three times this change might have been statistically significant. There is no change in *NRP1* expression levels. Overexpression of PRH does show repression of VSP genes *VEGFR2* and *NRP1*, however the *VEGFA* gene does not seem to be regulated by PRH. One reason for this lack of repression at the *VEGFA* gene could be the existence of a feedback loop between VEGF receptors and *VEGFA*, as reduction in VEGF receptor expression might result in the upregulation of the VEGF ligand in these cells.

For MDA-MB-231 cells, PRH overexpression did not lead to statistically significant repression or activation of any of the VEGF receptor genes. However as observed in MCF-7 cells, PRH overexpression did lead to an apparent increase in *VEGFA* mRNA expression. Moreover, in the PRH knockdown cells, there was a significant decrease in the *VEGFA* transcript (figure 4.27 (B)), suggesting that endogenous PRH increases *VEGFA* mRNA expression. However, there was no statistically significant change in mRNA expression of *VEGFR2* or *NRP1*. Therefore, PRH does not repress transcription of the VEGF receptors in MDA-MB-231 cells, but rather endogenous and exogenous PRH appears to activate expression of the *VEGFA* gene.

4.5 Discussion

It has been shown previously that PRH decreases the proliferation of leukaemic cells and hepatocarcinoma Hepa1-6 cells (Noy et al., 2010, Su et al., 2012). In this chapter it is shown that over expression of PRH decreases MCF-10A cell number. Overexpression of PRH drastically decreases the rate of proliferation in MCF-10A cells; however there was apparently no effect on the cell cycle or apoptosis. Surprisingly PRH knockdown did not show a marked increase in MCF-10A cell number either by MTT or by cell counting over a 20 day time period, and there were no changes detected by cell cycle profiling or by BrdU incorporation. Additionally, growth of MCF-10A cells in sub-optimal conditions, with low serum, failed to show a difference in growth between control and PRH knockdown cells. However it remains possible that there is a modest increase in cell number that will be apparent over a longer period of time.

One reason for the lack of a phenotype on cell proliferation observed for PRH knockdown in this cell type could be that PRH activity with regards to growth suppression shows redundancy with other tumour suppressor genes. Knockdown of endogenous PRH had little effect on the expression of any of the genes in the VEGF signalling pathway, indicating that endogenous PRH may not be important for regulating this pathway in normal breast cells. Despite this, exogenous PRH was able to effect repression of the *VEGF* gene, as well as have a modest effect on the receptors (albeit not in a statistically significant fashion in this experiment). Therefore it can be concluded that although exogenous PRH protein may be

able to bind weakly at the VEGF signalling gene promoters in MCF-10A cells, endogenous PRH does not appear to regulate the VSP in these cells. This agrees with the effects of PRH on cell proliferation, for example, overexpression of PRH causes a decrease in *VEGF* mRNA expression, whereas knockdown of endogenous PRH expression has no effect on genes in the VSP, and no effect on cell number.

In MCF-7 cells, overexpression of PRH leads to a decrease in MCF-7 cell number, through increased apoptosis. It cannot be ruled out that the rate of proliferation is also decreased, as BrdU assays were not possible with these cells. Interestingly PRH overexpression also significantly downregulated mRNA expression of the VEGF receptors *VEGFR2* and *NRP1*, in agreement with experimental data previously published (Noy et al., 2010). Since repression of VSP genes leads to decreased survival signalling, which can lead to increased apoptosis in this cell type (Ge et al., 2009), it can be inferred that this may account for some of the decrease in cell number in Ad-PRH infected cells. Conversely, PRH knockdown leads to an increase in cell number, and there is a modest upregulation of *VEGFA* and *VEGFR2* mRNA expression (although this is not statistically significant). However, this increase in cell number occurs through an increase in the rate of cell proliferation rather than a decrease in cell apoptosis. Although it is likely that some of the effects of PRH on cancer cell growth are occurring via regulation of the VSP, PRH could also be exerting its growth control effects by regulating expression of additional genes outside the VEGF signalling pathway. This will be further examined in the next chapter.

In MDA-MB-231 cells, overexpression of PRH reduced cell proliferation, increasing the proportion of cells in G1, and decreasing BrdU uptake of Ad-PRH infected cells. This however

did not translate into a decrease in cell number. One reason for exogenous PRH having little effect on cell number is that Myc-PRH is more unstable in MDA-MB-231 cells than in MCF-10A cells (see section 3.7), and hence the effect of exogenous PRH on the phenotype of this cell could be short-lived, and hence not strong enough to be accurately measured in a cell counting assay. There is little effect of PRH overexpression on most VSP genes in this cell line, although there may be a modest increase in *VEGFA* transcript. Surprisingly, knockdown of PRH decreased MDA-MB-231 cell growth which is opposite to the increased population growth phenotype observed in PRH knockdown MCF-7 cells, K526 leukaemic cells (Noy et al., 2010) and in PNT-2C2 prostate cells (Y.H. Siddiqui, K.L. Gaston and P.S. Jayaraman, personal communication). In addition there is a significant reduction in *VEGF* mRNA expression in MDA-MB-231 PRH knockdown cells. This suggests that endogenous PRH may actually activate expression of the *VEGF* gene in MDA-MB-231 cells. Increased autocrine signalling through the VSP, leading to increased proliferation and invasion, may be a reason for the requirement for PRH in MDA-MB-231 cell proliferation (Bachelder et al., 2002). However, the pro-proliferative PRH phenotype is at odds with the role of PRH in MCF-7 and K562 cells where it acts as a transcriptional repressor of this gene.

In conclusion, overexpression of PRH is having significant inhibitory effects on the growth of all three cell lines. However, knockdown of PRH has very different effects in each of the three cell lines. This implies that the context in which PRH is expressed is important for determining the phenotype which PRH exerts on the cell.

THE EFFECT OF PRH EXPRESSION ON BREAST CELL MIGRATION, INVASION AND CANCER INITIATING CELLS

5. The effect of PRH expression on breast cell migration, invasion and cancer initiating cells

5.1 Introduction

The ability of cancerous cells to migrate and metastasise is of huge importance to clinical outcome, as metastasis is the cause of death for 90% of patients with solid tumours (Gupta and Massagué, 2006). Since overexpression of PRH has been shown to negatively regulate HUVEC migration and invasion (Nakagawa et al., 2003), we wished to determine whether PRH affects breast tumour cell migration and invasion. To this end, PRH was overexpressed and knocked down in MCF-7, and MDA-MB-231 cells. Since MCF-10A cells migrate very slowly and are non-invasive, only the effects of PRH knockdown were assessed in these cells.

5.2 Effect of PRH on migration and invasion of breast cells

5.2.1 Effect of PRH overexpression on the migration of MCF-7 and MDA-MB-231 cells

The movement of cells can be measured in two ways - measurement of overall cell motility, known as chemokinesis, and measurement of movement towards a chemoattractant,

known as chemotaxis. To measure the effect of overexpression of PRH on MCF-7 cell chemotaxis, scratch wound assays were performed. One million MCF-7 cells were infected with Ad or Ad-PRH as described previously, and plated in a 6-well plate and left for 24 hours, so that they were 100% confluent. A scratch was then made with a P200 pipette tip, and images were taken of the scratch at time zero. The scratch was then re-imaged 24 hours later, and the area of the scratch was quantified at both timepoints using ImageJ software. Cell proliferation was inhibited throughout the assay by incubating cells with 1mM hydroxyurea (as shown figure 4.8). The results show that overexpression of PRH decreases MCF-7 chemokinesis (figures 5.1 (A) and (B)).

To measure the effect of exogenous PRH on MCF7 chemotaxis, transwell assays were carried out. MCF-7 cells were infected with Ad-or Ad-PRH as described previously. After 24 hours 40,000 cells were then placed in the top chamber of a transwell in media containing 2% serum. The bottom chamber contains media with 10% serum as the chemoattractant. The transwell chamber contains a membrane with 8µm pores for the cells to migrate through (see figure 5.1 (C)). The cells were left for 48 hours, before washing and fixing with 2% formaldehyde. Cells on either side of the membrane were then stained with bisbenzamide to visualise their nuclei. The membrane was cut out and the percentage of migrated cells was counted in at least three fields using a fluorescent microscope at 100x magnification. Figure 5.1 (D) shows that there is a significant decrease in the percentage of Ad-PRH infected MCF-7 cells that migrate to the lower surface of the membrane compared to controls.

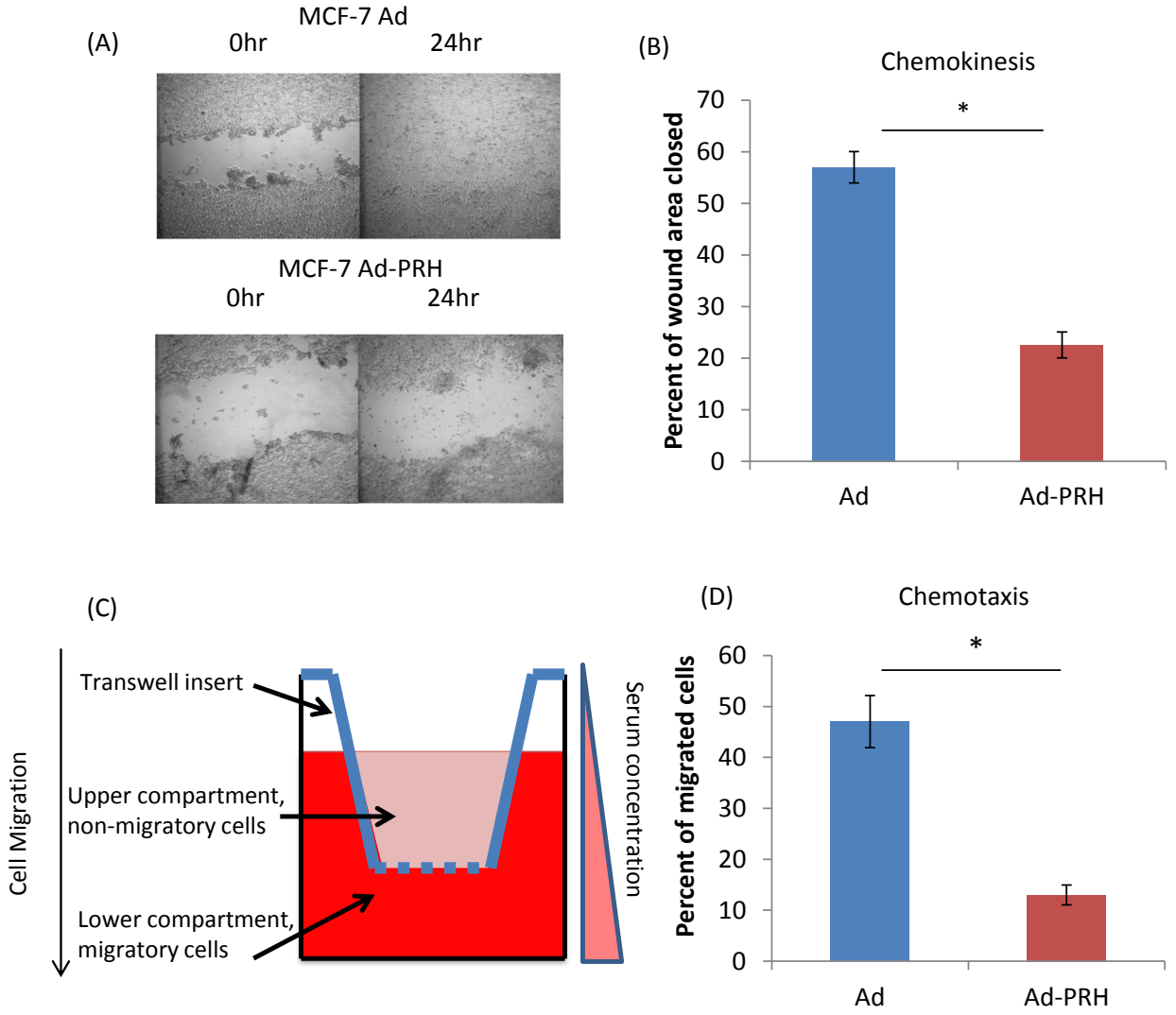

Figure 5.1: Overexpression of PRH in MCF-7 cells causes decreased migration. (A) 1 million MCF-7 cells were plated onto a 6 well plate and were infected with either Ad control (left) or Ad-PRH adenovirus (right) for 24 hours. A scratch was then created using a P200 pipette tip and pictures were taken 0 hours and 24 hours post-scratch. (B) Wound closure was then quantified using ImageJ software (n=3, *p<0.05 two-tail homoscedastic t-test). (C) MCF-7 cells were infected with Ad or Ad-PRH at a MOI of 50. 24 hours later $4x10^4$ cells were placed in an inner chamber of a transwell containing 2% serum, with the outer chamber containing 10% serum. (D) Cells were then left to migrate for 24 hours, and the number of migrated cells was quantified (n=3, *p<0.05 two-tail homoscedastic t-test).

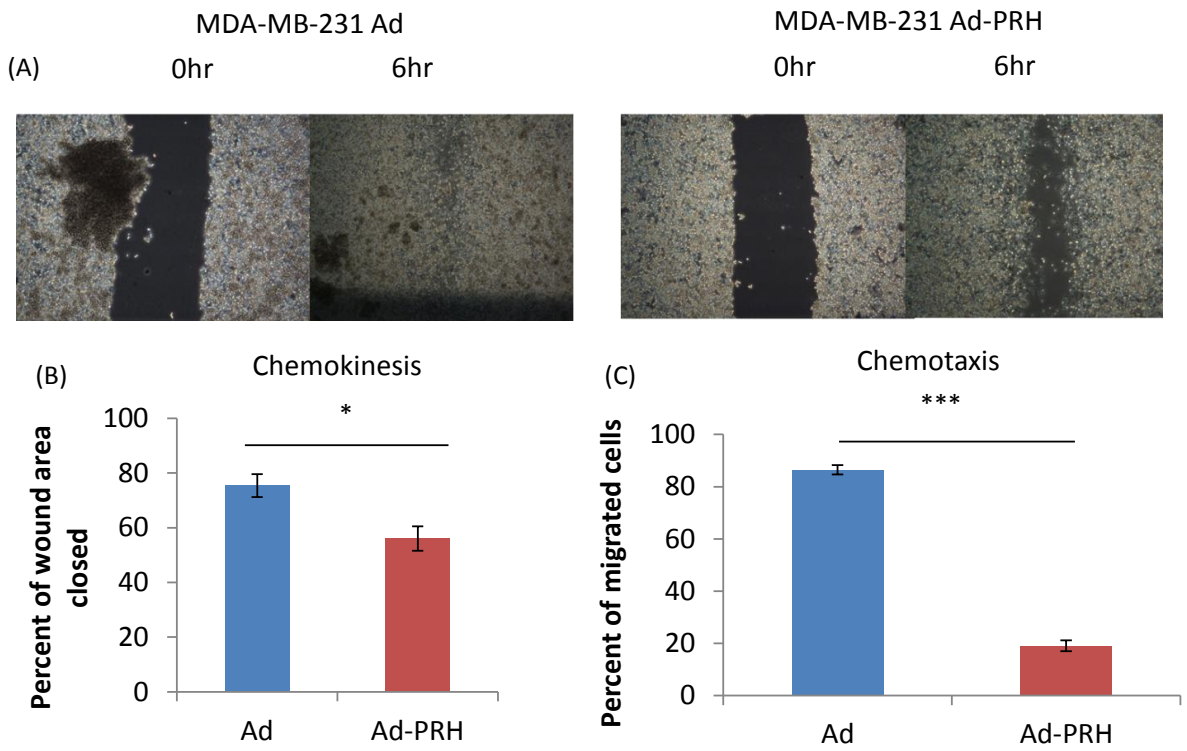

Figure 5.2: Overexpression of PRH in MDA-MB-231 cells causes decreased migration. (A) 1 million MDA-MB-231 cells were plated onto a 6 well plate and were infected with either Ad control (left) or Ad-PRH (right) adenovirus for 24 hours. A scratch was then created using a P200 pipette tip and pictures were taken 0 hours and 6 hours post-scratch. (B) Wound closure was then quantified using ImageJ software (n=3, *p<0.05 two-tail homoscedastic t-test). MDA-MB-231 cells were infected with Ad or Ad-PRH at a MOI of 50. (C) 24 hours later $4x10^4$ cells were placed in an inner chamber of a transwell containing 2% serum, with the outer chamber containing 10% serum. Cells were then left to migrate for 24 hours, and the number of migrated cells was quantified (n=3, *p<0.05 two-tail homoscedastic t-test).

To determine whether exogenous PRH affects MDA-MB-231 chemokinesis, scratch wound assays were carried out as described previously, however the assay was carried out over 6 hours rather than 24 as MDA-MB-231 cells are more migratory than MCF-7 cells. Figures 5.2 (A) and (B) shows that Ad-PRH infected MDA-MB-231 cells display less chemokinesis compared to control cells. Transwell assays were also carried out as previously described; however the assay was carried out over 24 hours rather than 48 hours. Figure 5.2 (C) shows that Ad-PRH infection significantly inhibited migration of MDA-MB-231 cells towards the chemoattractant, compared to control cells. Thus exogenous PRH inhibits the migration of both breast tumour cell types.

5.2.2 Effect of PRH knockdown in MCF-7 and MDA-MB-231 cells

To determine if endogenous PRH had effects on MCF-7 and MDA-MB-231 chemokinesis, scratch wound assays were carried out as described previously. MCF-7 PRH knockdown and control cells were induced for shRNA expression as described in the previous chapter. PRH knockdown significantly increased MCF-7 chemokinesis (figures 5.3 (A) and (B)). The effect of PRH knockdown on MCF-7 chemotaxis was also assayed, by carrying out transwell assays as previously described, over 48 hours. PRH knockdown significantly increased MCF-7 chemotaxis compared to controls (figure 5.3 (C)). The experiments were repeated in MDA-MB-231 PRH knockdown and control cells. Note that IPTG seems to decrease cell migration.

Figures 5.4 (A) and (B) show that there is little or no difference in chemokinesis between PRH knockdown and control cells. Since MDA-MB-231 cells are highly migratory, transwell assays were carried out over 6 hours. In this experiment, PRH knockdown significantly increased MDA-MB-231 chemotaxis compared to controls (figure 5.4 (C)). Thus knockdown of PRH increases chemotaxis of both breast tumour cell lines. Note that IPTG seems to decrease cell migration.

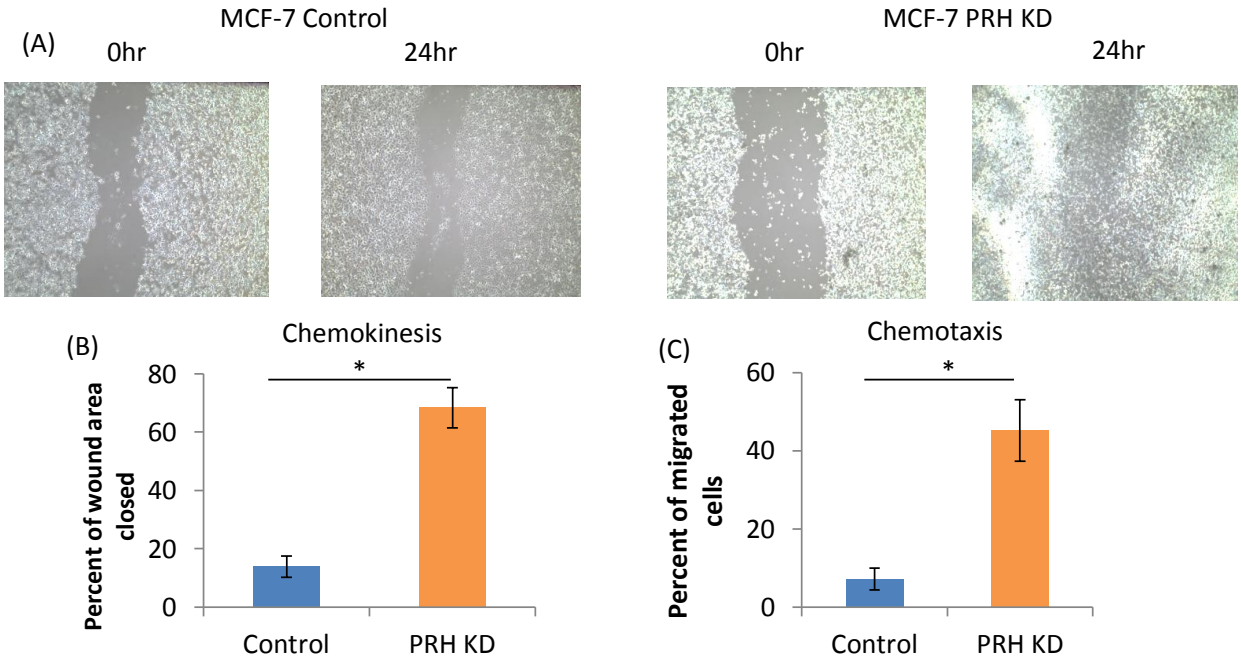

Figure 5.3: Knockdown of PRH in MCF-7 cells causes increased migration. (A) PRH or control knockdown MCF-7 cells were induced for shRNA expression as previously described. $1x10^6$ cells were then plated onto a 6 well plate and were left for 24 hours to adhere. A scratch was then created using a P200 pipette tip and pictures were taken 0 hours and 24 hours post-scratch. (B) Wound closure was then quantified using ImageJ software (n=3, *p<0.05 two-tail homoscedastic t-test). (C) $4x10^4$ cells were placed in an inner chamber of a transwell containing 2% serum, with the outer chamber containing 10% serum. Cells were then left to migrate for 48 hours, and the percentage of migrated cells was quantified (n=3, *p<0.05 two-tail homoscedastic t-test).

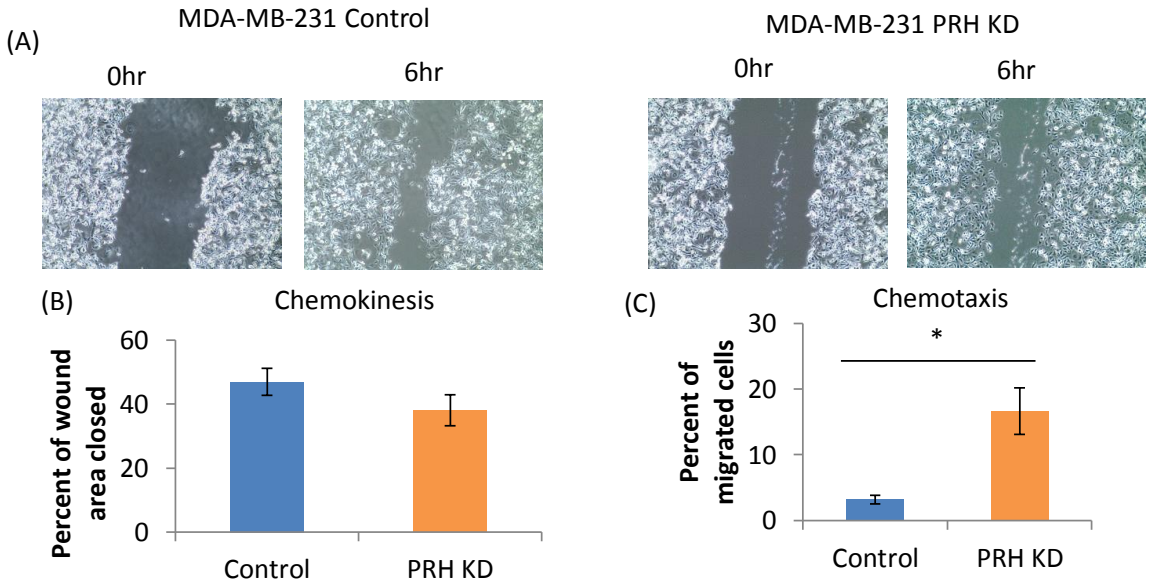

Figure 5.4: Knockdown of PRH in MDA-MB-231 cells causes decreased chemotaxis but not chemokinesis. (A) PRH or control knockdown MDA-MB-231 cells were induced for shRNA expression as previously described. $1x10^6$ cells were then plated onto a 6 well plate and were left for 24 hours to adhere. A scratch was then created using a P200 pipette tip and pictures were taken 0 hours and 6 hours post-scratch. (B) Wound closure was then quantified using ImageJ software (n=3, *p<0.05 two-tail homoscedastic t-test). (C) $4x10^4$ cells were placed in an inner chamber of a transwell containing 2% serum, with the outer chamber containing 10% serum. Cells were then left to migrate for 6 hours, and the percentage of migrated cells was quantified (n=3, *p<0.05 two-tail homoscedastic t-test).

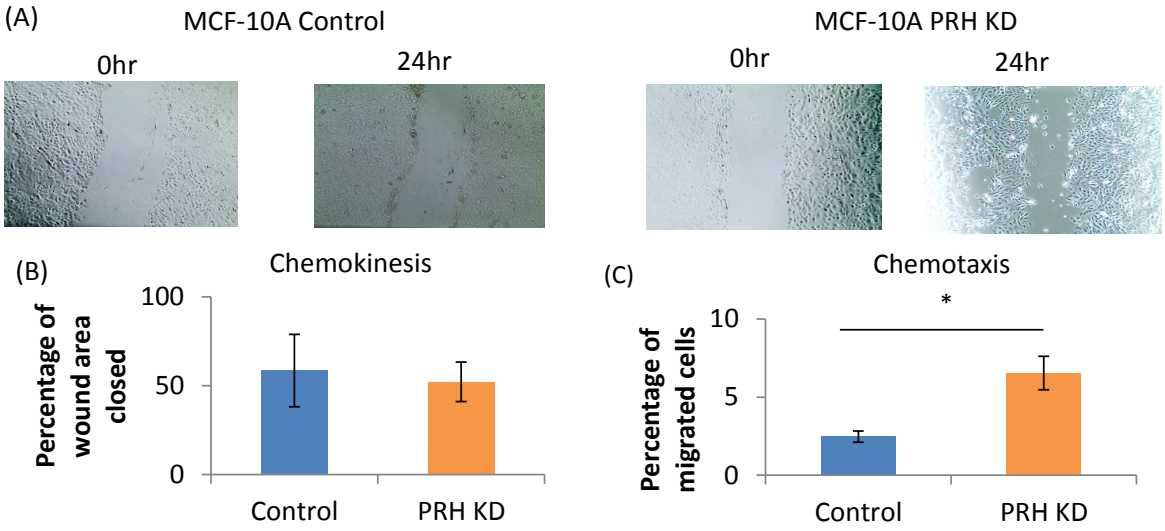

Figure 5.5: Knockdown of PRH in MCF-10A cells affects chemotaxis but not chemokinesis. (A) PRH or control knockdown MCF-10A cells were induced for shRNA expression as previously described. $1x10^6$ cells were then plated onto a 6 well plate and were left for 24 hours to adhere. A scratch was then created using a P200 pipette tip and pictures were taken 0 hours and 24 hours post-scratch. (B) Wound closure was then quantified using ImageJ software (n=3, *p<0.05 two-tail homoscedastic t-test). (C) $4x10^4$ cells were placed in an inner chamber of a transwell containing no EGF, with the outer chamber containing 10ng/ml EGF. Cells were then left to migrate for 24 hours, and the number of migrated cells was quantified (n=3, *p<0.05 two-tail homoscedastic t-test).

5.2.3 Effect of PRH knockdown in MCF-10A cells

To determine if endogenous PRH had effects on MCF-10A chemokinesis, scratch wound assays were carried out as previously described, with the assay carried out over 24 hours. ShRNA expression in MCF-10A cells was induced as described in the previous chapter. There was no difference in chemokinesis between PRH knockdown and control MCF-10A cells (figures 5.5 (A) and (B)). MCF-10A chemotaxis was also assayed, by carrying out transwell assays, however epidermal growth factor (EGF) was used as a chemoattractant in this case, as it has been previously shown that MCF-10A cells are migratory towards EGF in this assay (Irie et al., 2005). The assay was carried out over 48 hours, as these cells are not known to

be migratory. Figure 5.5 (C) shows that PRH knockdown significantly increased MCF-10A chemotaxis compared to controls. It can be concluded that PRH inhibits cell migration in normal breast cells, and in breast cancer cells. Note that IPTG seems to decrease cell migration.

5.2.4 PRH inhibits cell invasion

To determine whether PRH has effects on breast cell invasiveness, transwell invasion assays were performed. This assay involves coating the porous membrane with reconstituted basement membrane (Matrigel) (Albini et al., 1987). The assay assesses whether cells can produce enzymes that can degrade the extracellular matrix proteins present in the Matrigel, and then migrate across the membrane.

To determine the effects of PRH overexpression on invasion by MDA-MB-231 cells (which are known to be highly invasive), a 2-10% serum gradient was used as a chemoattractant. However infection with the control adenovirus (at a MOI of 50) decreases the invasion of MDA-MB-231 cells compared to uninfected cells. Therefore, an alternative method for overexpressing PRH in these cells was used. Cells were transfected with plasmids using Lipofectamine 2000 (experiment carried out by Dr. Rachael Kershaw). Briefly, cells were co-transfected with plasmids coding for GFP (pEGFP-C1) and a plasmid coding for Myc-PRH (pMUG1 Myc-PRH) or an empty vector plasmid (pMUG1) (for plasmid maps see Materials and methods section 4.12). Transwell invasion assays through a transwell membrane coated

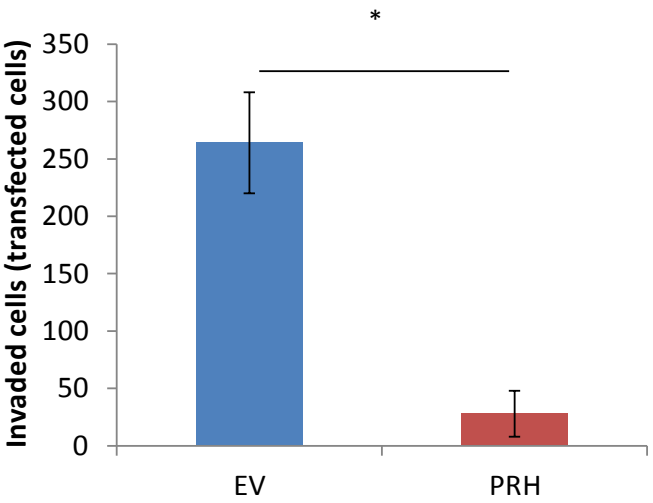

Figure 5.6: Overexpression of PRH decreases MDA-MB-231 invasion. MDA-MB-231 cells were transfected with 1.5µg of GFP plasmid and 1.5 µg of either empty pMUG1 vector (EV) or with pMUG1 vector coding for Myc-PRH (PRH). $4x10^4$ cells were placed in an inner chamber of a transwell (precoated with 50µl Matrigel) 24 hours later, containing 2% serum, with the outer chamber containing 10% serum. Cells were then left to invade for 24 hours, and the number of invasive GFP-positive cells was quantified (n=3, *$p<0.05$ two-tail homoscedastic t-test).

with Matrigel were then carried out 24 hours post-transfection, and the number of GFP positive cells that invaded through the membrane was then quantified. PRH overexpressing MDA-MB-231 cells overexpressing PRH were less invasive than control cells (figure 5.6).

MCF-10A cells are not invasive, and MCF-7 cells invade very poorly, hence the effect of overexpression of PRH could not be determined. However, it was reasoned that endogenous PRH might be inhibiting invasion in these cell types. To investigate this hypothesis, MCF-10A PRH knockdown and control cells were used. EGF was used as a chemoattractant, and cells were left to invade the transwell chamber coated with Matrigel for 48 hours, before cells were fixed and stained with bisbenzamide. Figure 5.7 (A) shows that there are significantly more invasive PRH knockdown MCF-10A cells than control cells. This suggests that the loss of PRH causes MCF-10A cells to become invasive. The invasion assay was carried out in an identical way in MCF-7 cells, apart from 10% serum being used as the chemoattractant rather than EGF. PRH knockdown also significantly increased MCF-7

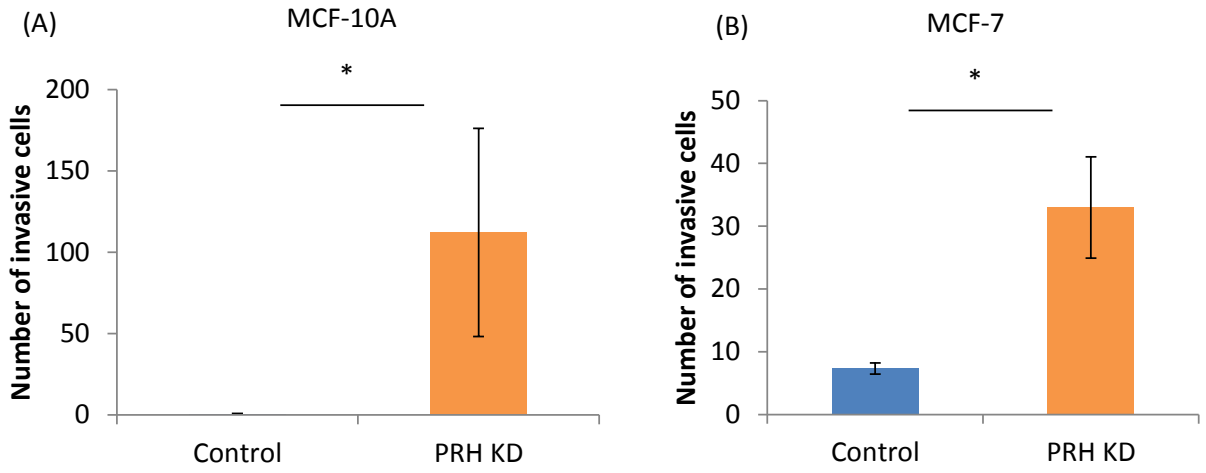

Figure 5.7: Knockdown of PRH increases MCF-10A and MCF-7 invasion. (A) IPTG inducable PRH and control shRNA MCF-10A cells were subject to transwell assays. $4x10^4$ cells were placed in an inner chamber of a transwell (precoated with 50µl Matrigel) containing no EGF, with the outer chamber containing 10ng/µl EGF. Cells were then left to invade for 48 hours, and the number of invasive cells was quantified (n=3, *p<0.05 two-tail homoscedastic t-test). (B) $4x10^4$ MCF-7 PRH knockdown and control cells were placed in an inner chamber of a transwell (precoated with 50µl Matrigel) containing 2% serum, with the outer chamber containing 10% serum. Cells were then left to invade for 48 hours, and the number of invasive cells was quantified (n=3, *p<0.05 two-tail homoscedastic t-test).

cell invasion (figure 5.7 (B)). It can be concluded that PRH inhibits invasion of immortalised breast cells and breast tumour cells.

5.3 Effect of PRH on expression of genes involved in EMT/migration/invasion

5.3.1 Gene expression analysis of genes involved in EMT/migration/invasion

To better understand the effects of PRH overexpression and knockdown on cell migration and invasion, the effect of PRH on genes that are known to be regulated by PRH in other cell types, and that are associated with migration/invasion/EMT, were analysed. PRH directly binds and represses the goosecoid (*GSC*) and *ESM1* genes within their promoter regions

(Cong et al., 2006, Brickman et al., 2000, Williams et al., 2008), and both of these genes are associated with migration or invasion. Overexpression of Goosecoid lead to increased cell motility in human mammary epithelial cells (Hartwell et al., 2006), whilst knockdown of ESM1 has been shown to decrease invasion in hepatocarcinoma cells (Kang et al., 2011). PRH is also known to regulate mRNA expression of *T53*, *SATB1* and endoglin (*ENG*) in various cell types, but the mechanism of regulation is not known (Nakagawa et al., 2003, Su et al., 2012, Guo et al., 2003). As mentioned previously in the introduction, p53 inhibits EMT in breast tumour cells (Neilsen et al., 2013), SATB1 increases migration and invasion of breast tumour cells (Han et al., 2008a), and Endoglin can inhibit or promote migration and invasion, depending on the cell type (Henry et al., 2011, Oxmann et al., 2008).

Quantitative PCR was used to assess gene expression of each of these genes, exactly as described previously in section 4.4.1 and in Materials and methods section 2.8.3. As can be see in figure 5.8, in MCF-10A cells, overexpression of PRH causes significant upregulation of endoglin, and PRH knockdown causes significant repression of this mRNA. PRH over-expression also seems to decrease e-cadherin (*CDH1*) mRNA expression two-fold, although this decrease is not statistically significant, and PRH knockdown does not affect e-cadherin mRNA expression (figure 5.8). PRH overexpression and knockdown does not affect *ESM1* or *TP53* mRNA expression in MCF-10A cells. *SATB1* and goosecoid (*GSC*) are not expressed at a high enough level in this cell type to be quantified by qPCR. These results demonstrate that endoglin transcript expression is regulated by PRH in MCF-10A cells, and that PRH is an activator of endoglin mRNA expression.

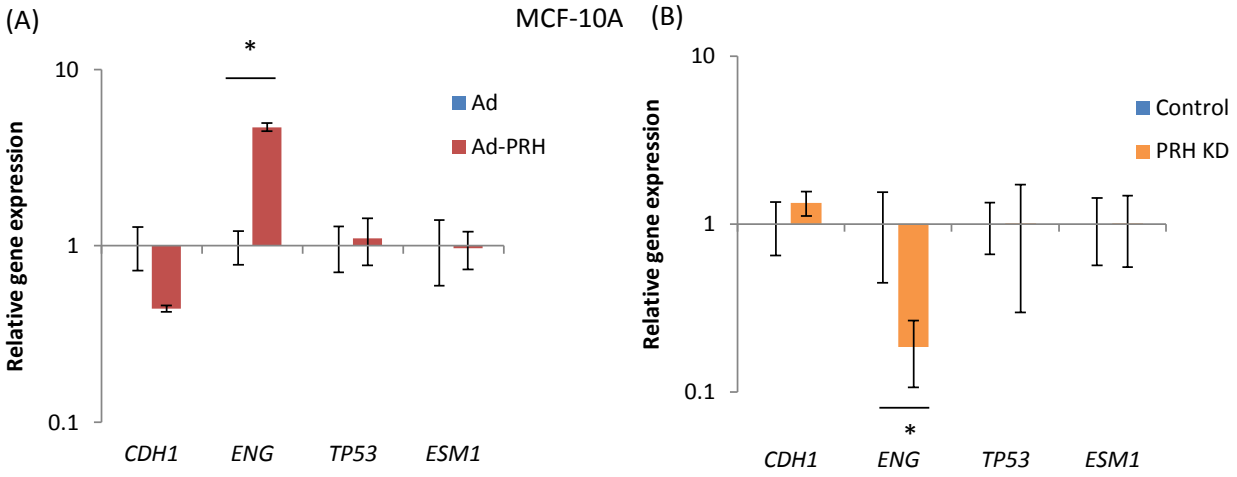

Figure 5.8: The effect of PRH overexpression and knockdown on expression of genes involved in EMT/migration in MCF-10A cells. (A) MCF-10A cells were infected with either Ad or Ad-PRH at a MOI of 50 for 48 hours. Cells were then pelleted and RNA was extracted using a Bioline ISOLATE II kit, and complementary DNA was then synthesised. Gene expression was analysed using quantitative PCR, and quantified using the Pfaffl method (Pfaffl, 2001), using *GAPDH* as a housekeeping gene (n=3, *p<0.05, two-tail homoscedastic t-test). (B) The same process was repeated but with PRH knockdown cells, which were induced for shRNA expression as previously described, however beta-actin was used as a housekeeping gene as *GAPDH* expression was too variable (n=3, *p<0.05, two-tail homoscedastic t-test).

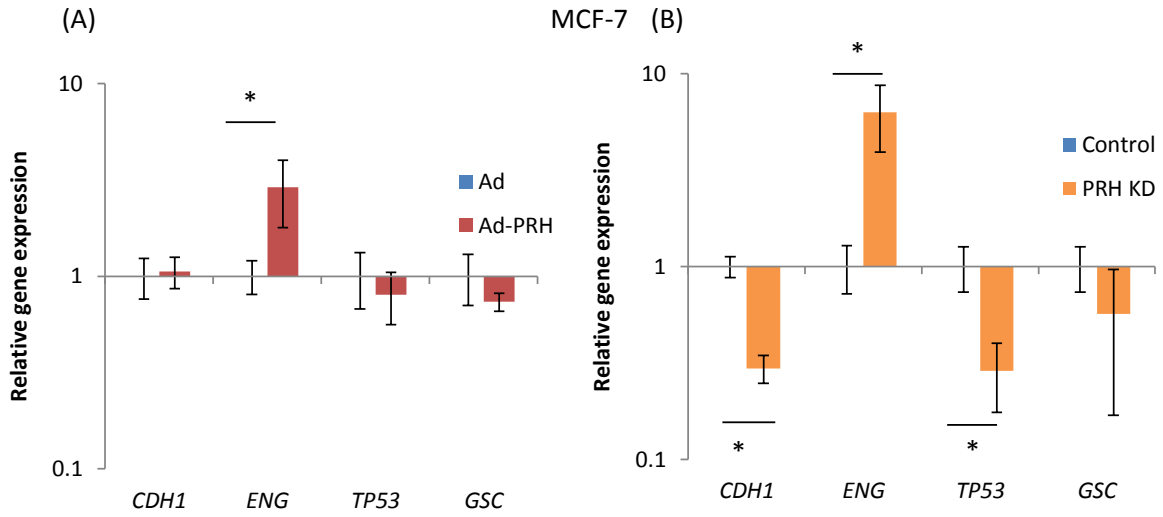

Figure 5.9: The effect of PRH overexpression and knockdown on expression of genes involved in EMT/migration in MCF-7 cells. (A) MCF-7 cells were infected with either Ad or Ad-PRH at a MOI of 50 for 48 hours. Cells were then pelleted and RNA was extracted using a Bioline ISOLATE II kit, and complementary DNA was then synthesised. Gene expression was analysed using quantitative PCR, and quantified using the Pfaffl method (Pfaffl, 2001), using *GAPDH* as a housekeeping gene (n=3, *p<0.05, two-tail homoscedastic t-test). (B) The same process was repeated but with PRH knockdown cells, which were induced for shRNA expression as previously described (n=3, *p<0.05, two-tail homoscedastic t-test).

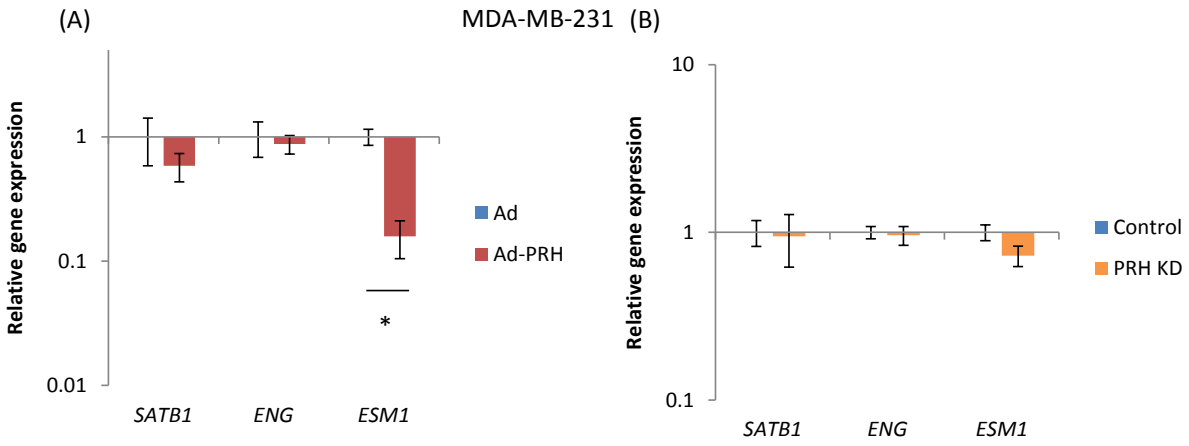

Figure 5.10: The effect of PRH overexpression and knockdown on expression of genes involved in EMT/migration in MDA-MB-231 cells. (A) MDA-MB-231 cells were infected with either Ad or Ad-PRH at a MOI of 50 for 48 hours. Cells were then pelleted and RNA was extracted using a Bioline ISOLATE II kit, and complementary DNA was then synthesised. Gene expression was analysed using quantitative PCR, and quantified using the Pfaffl method (Pfaffl, 2001), using *GAPDH* as a housekeeping gene (n=3, *p<0.05, two-tail homoscedastic t-test). (B) The same process was repeated but with PRH knockdown cells, which were induced for shRNA expression as previously described (n=3, *p<0.05, two-tail homoscedastic t-test).

In MCF-7 cells, PRH overexpression does not significantly affect *TP53*, *CDH1* or *GSC* mRNA expression (figure 5.9 (A)). However, knockdown of PRH significantly decreased *TP53* and *CDH1* expression (figure 5.9 (B)). *GSC* mRNA expression was also lower in PRH knockdown cells, although this effect was not statistically significant (figure 5.9 (B)). PRH overexpression led to increased endoglin transcript expression, which correlates with what was seen in MCF-10A cells, but unexpectedly *ENG* mRNA was also significantly increased when PRH was knocked down in MCF-7 cells. One reason for this could be that the PRH knockdown MCF-7 cells have undergone EMT, and become more tumourgenic and invasive. This is suggested by the decrease in e-cadherin and *TP53* mRNA observed, and the increased invasion of MCF-7 PRH knockdown cells. Thus regulation of this gene may be aberrant and occur through other factors, and no longer appropriately regulated by PRH in the PRH knockdown cells. *SATB1* transcript was not expressed at a high enough level at this cell type to be quantified by qPCR.

In MDA-MB-231 cells, overexpression of PRH causes a significant repression of *ESM1* mRNA expression (figure 5.10 (A)), however PRH knockdown does not cause a corresponding increase in *ESM1* transcript expression, and is in fact slightly lower (figure 5.10 (B)). PRH overexpression or knockdown did not significantly affect *SATB1* or endoglin mRNA expression in these cells (figure 5.10). *GSC*, *CDH1* and *TP53* were not assessed as their transcripts are not expressed (or mutated in the case of *TP53*) in this cell type. It can be concluded that PRH has no effect on *ENG* or *SATB1* mRNA expression, and PRH overexpression decreases *ESM1* transcript expression in this cell type.

5.4 Effect of PRH on cancer initiating cells

5.4.1 Overexpression of PRH leads to a decrease in MCF-7 mammosphere formation

In previous sections it was shown that over expression of PRH decreased MCF-7 cell number and migration, whilst knockdown of PRH increased MCF-7 cell proliferation, migration and invasion. It has been reported that MCF-7 tumour cells are a heterogeneous population, of which only a minority of cells are cancer initiating cells (Phillips et al., 2006). One technique of enriching this cancer-initiating cell (CIC) population 1000 fold is by growing cells in non-adherent conditions, and in mammosphere media, which causes the bulk cell population to die through anoikis (a form of programmed cell death when cells become detached from the extracellular matrix) (Phillips et al., 2006). This then leaves the CICs, which proliferate as spheroid mammospheres. To determine whether PRH overexpression will affect the survival

of the CIC, or will only inhibit the survival of the bulk progeny, MCF-7 cells were infected with either Ad or Ad-PRH. Infected cells were then plated into MammoCult (commercial mammosphere media) 24 hours later. The number of mammospheres formed was then counted 7 days thereafter. Ad-PRH infected cells form a reduced number of mammospheres compared to Ad infected cells (figure 5.11 (A)). To see whether this effect was permanent as would be expected if the number of CICs had been decreased, or whether this effect was transient, the mammospheres were dissociated, counted, and were replated under the same conditions to form secondary mammospheres. Ad-PRH infected cells did not show a decrease in number of secondary mammospheres compared to control cells (figure 5.11 (B)). It can be inferred from this that it is the proliferation or survival of the MCF-7 CIC progeny that is decreased but that the proportion of CICs (i.e. self-renewal of CICs) is not affected by PRH overexpression. The mammosphere formation of PRH knockdown cells was also assessed. PRH and control knockdown cells was induced with IPTG for 7 days as described previously, and cells were then plated into ultra-low adherrant plates containing MammoCult media (with 1mM IPTG added) as before. There was no significant difference in primary mammosphere number between PRH knockdown and control cells (figure 5.11 (C)). This might be expected if PRH plays no role in the self-renewal of the CIC.

$CD44^{+}/CD24^{-/low}$ have been shown to be markers for CIC's (sometimes termed cancer stem cells) and sorting MCF-7 for this population leads to identification of cells which are approximately 1000 times more tumourgenic than the rest of the MCF-7 cell population (Phillips et al., 2006). To confirm that PRH has little effect on self renewal of CIC's, Ad-PRH or Ad infected MCF-7 cells were analysed by flow cytometery 24 hours post-infection for their CD24/CD44 expression, or were plated in mammosphere media for another 24 hours

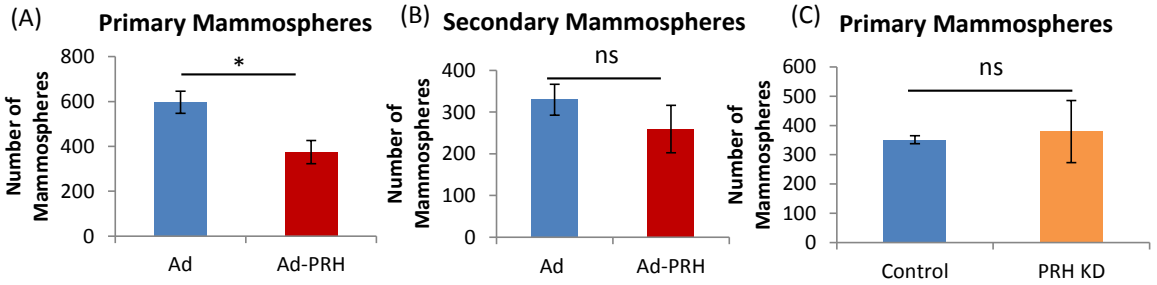

Figure 5.11: Ad-PRH decreases the number of MCF-7 mammospheres. (A) MCF-7 cells were infected with either Ad or Ad-PRH for 24 hours at a MOI of 50. $4x10^4$ cells were then plated into ultra-low adherant 6-well plates containing MammoCult media, and were left for 7 days. The number of primary mammospheres was then quantified using a counting grid (n=8, two-tail homoscedastic t-test *$p<0.05$). (B) Mammospheres were then dissociated using trypsin, and the number of cells was then quantified using a haemacytometer and Trypan blue exclusion dye. $4x10^4$ cells were then seeded in the same way as before, and the number of secondary mammospheres was then quantified (n=8, two-tail homoscedastic t-test ns=not significant). (C) PRH and control knockdown MCF-7 cells were then induced for shRNA expression as described previously, and were then plated as described above to form primary mammospheres (n=3, two-tail homoscedastic t-test *ns=not significant).

before flow cytometery analysis of their CD24/CD44 expression. Figure 5.12 shows that there is not a significant difference between the $CD44^+/CD24^{-/low}$ population of PRH overexpressed and control-infected cells at 24 hours post-infection. This time point is before infected cells are replated in non-adherrant media. The same assay was used to measure the amount of $CD44^+/CD24^{-/low}$ cells in Ad or Ad-PRH mammospheres 48 hours post-infection and after 24 hours incubation in mammosphere media. Although the proportion of $CD44^+/CD24^{-/low}$ cells was much higher in the MCF-7 cell population grown for 24 hours under mammosphere conditions, there was no difference in the $CD44^+/CD24^{-/low}$ population between the Ad and Ad-PRH infected MCF-7 cells (figure 5.13). Therefore, PRH overexpression does not seem to affect the CIC population of these cells.

To determine whether the decrease in mammosphere formation by exogenous PRH was due to increased cell apoptosis, an Annexin-V-APC assay was carried out 24 hours post infection with Ad-PRH, as well as at 48 hours post infection and 24 hours after seeding into mammosphere media. Similar to results shown previously in figure 4.4, PRH increases

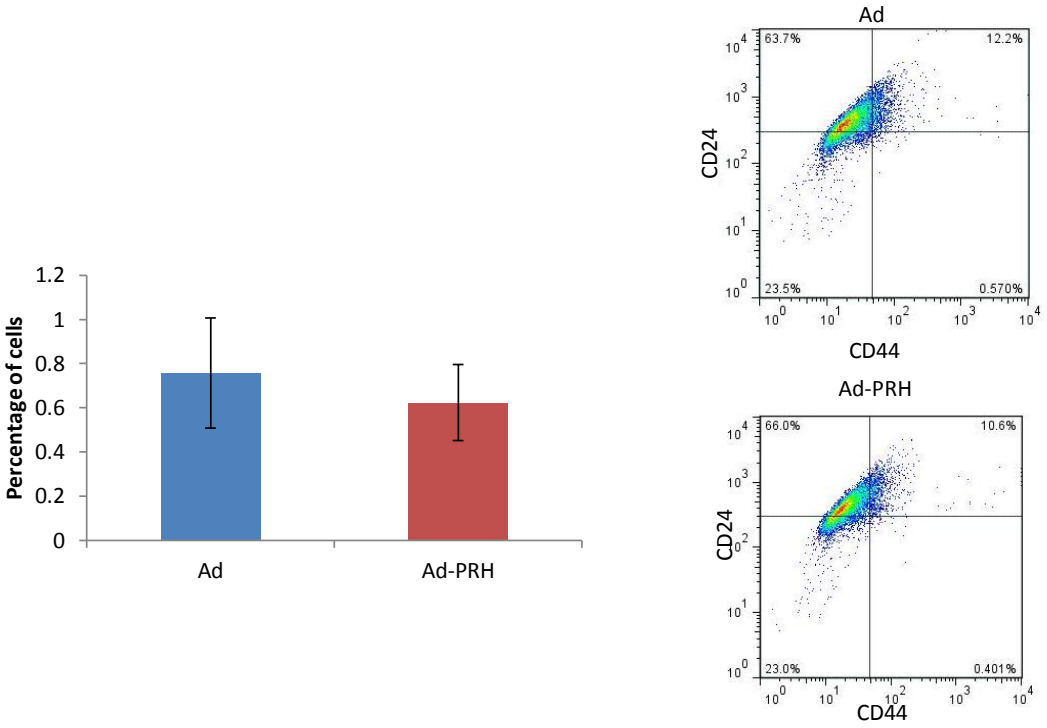

Figure 5.12: PRH overexpression does not affect the percentage of CD24^{low}CD44^{+} cells. CD24^{low}CD44^{+} cells have been shown when enriched to be markers for the mammosphere-forming sub-population of MCF-7 cells (Phillips et. al. 2006). MCF-7 cells were incubated with either control adenovirus or Ad-PRH at a MOI of 50 for 24 hours. Cells were then stained with CD24-FITC and CD44-PE for 30 minutes at 4°C before being analysed by flow cytometery (*p<0.05, n=3 two-tail homoscedastic t-test).

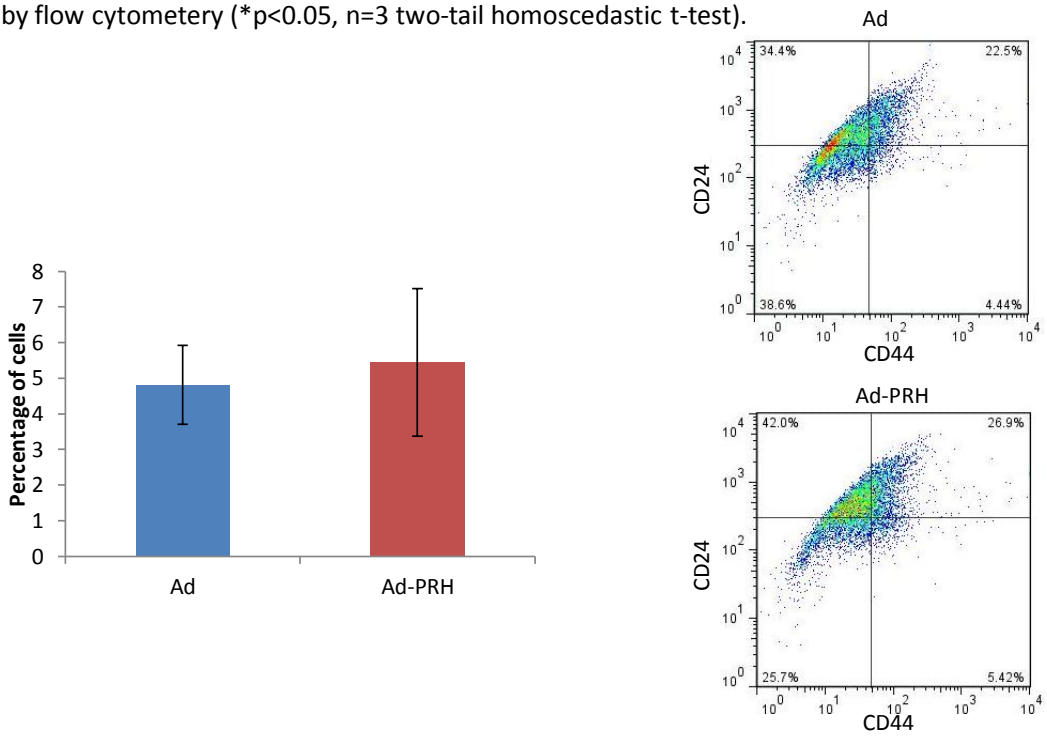

Figure 5.13: PRH overexpression does not affect the percentage of CD24^{low}CD44^{+} cells in mammospheres. MCF-7 cells were incubated with either control adenovirus or Ad-PRH at a MOI of 50 for 24 hours. Cells were then scraped and cultured in MammoCult media in non-adherrant 6-well plates for another 24 hours. Cells were then stained with CD24-FITC and CD44-PE for 30 minutes at 4°C before being analysed by flow cytometery (*p<0.05, n=3 two-tail homoscedastic t-test).

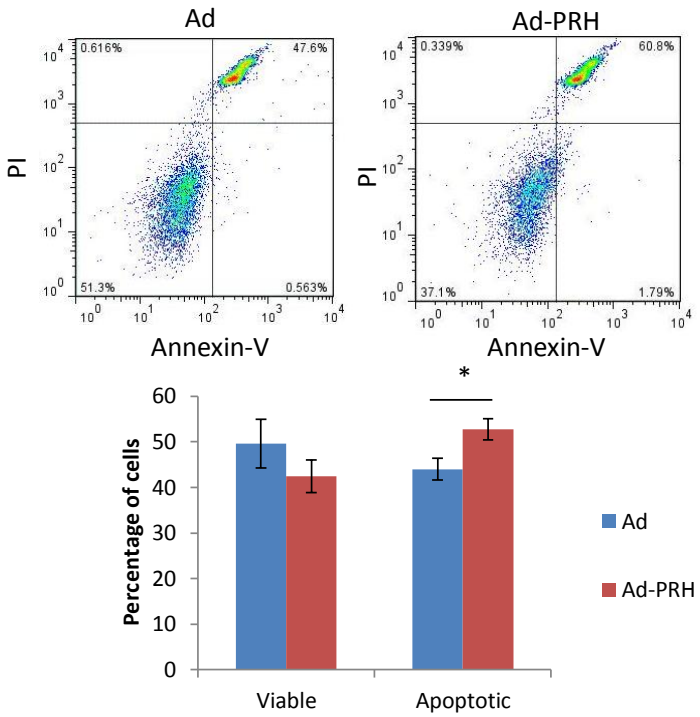

Figure 5.14: Ad-PRH increases apoptosis in MCF-7 cells. MCF-7 cells were incubated with Ad-PRH for 24 hours, before being stained with 10µg/µl propodium iodide (PI) and 5µl of Annexin V-APC antibody (BD Biosciences). Cells were then analysed by flow cytometery to determine live cells (PI-, AV-), early apoptotic (PI-, AV+) and late apoptotic (PI+. AV+) (n=3, *p<0.05 two-tail homoscedastic t-test)

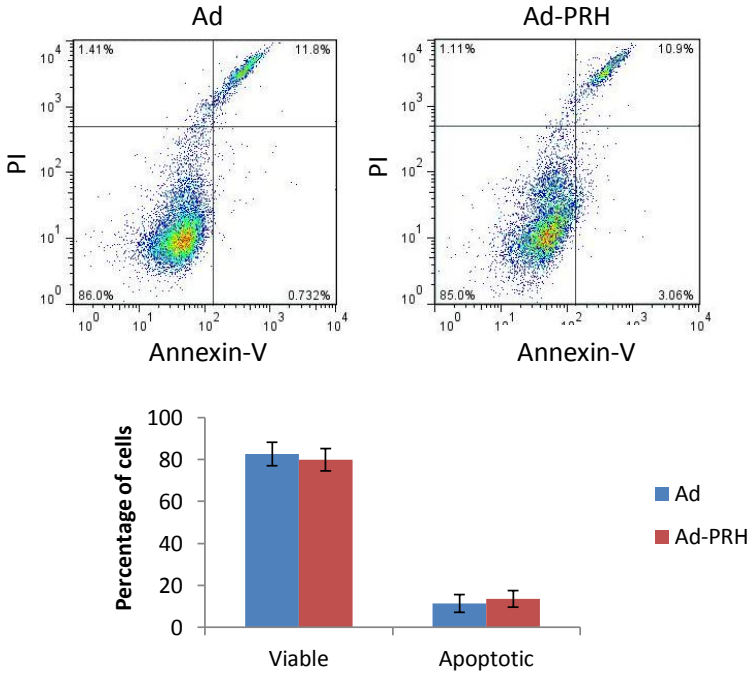

Figure 5.15: Ad-PRH does not increase apoptosis in MCF-7 mammospheres. MCF-7 cells were incubated with Ad-PRH for 24 hours. Cells were then scraped and cultured in MammoCult media in non-adherrant 6-well plates for another 24 hours. Cells were then stained with 10µg/µl propodium iodide and 5µl of Annexin V-APC antibody (BD Biosciences). Cells were then analysed by flow cytometery to determine live cells (PI-, AV-), early apoptotic (PI-, AV+) and late apoptotic (PI+. AV+) (n=3, *p<0.05 one-tail homoscedastic t-test).

apoptosis of adherent MCF-7 cells (figure 5.14). It should be noted that the particularly high number of apoptotic cells observed is likely to be due to cells needing to be detached using a cell scraper, as trypsin reduces the efficiency of mammosphere formation. The pro-apoptotic effect of Ad-PRH is lost at 48 hours post infection when the cells are cultured under mammosphere conditions for 24 hours (figure 5.15).

It is not clear exactly why a decreased number of mammospheres were observed when PRH is overexpressed. The effects of PRH on mammosphere formation occur either predominantly through the increased apoptosis of MCF-7 cells prior to plating in mammosphere media, or through decreased proliferation of cells within the mammosphere population during the 7 day mammosphere assay. Unfortunately, BrdU proliferation assays were not possible, due to the low cell number and the three-dimensional growth of mammospheres, making quantification difficult. In conclusion, these experiments show that PRH overexpression decreases the number of bulk cancer cells but not the proportion of CICs. This decrease may be either through increased apoptosis occurring before cells are plated in MammoCult media, or through a decrease in the proliferation rate during the 7 day mammosphere assay.

5.4.2 PRH increases MCF-7 tumour growth *in vivo*

Although PRH does not decrease CIC in MCF-7 cells, our studies suggest that PRH overexpression can decrease the growth of the bulk MCF-7 cancer cells. In addition our studies show that PRH overexpression decreases the migratory properties of MCF-7 cells. To

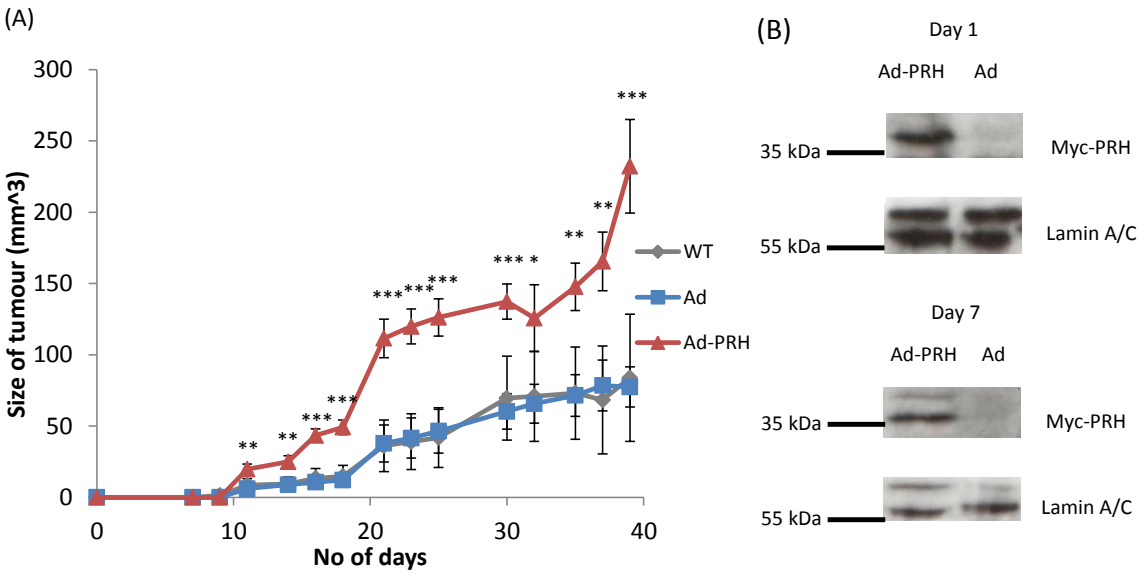

Figure 5.16: Ad-PRH increases MCF-7 tumour size *in vivo*. (A) MCF-7 cells were infected at a MOI of 50 with Ad-PRH, control adenovirus or with no virus for 24 hours. 5 million cells were then injected into each mammary fat pad of a female Balb/c nude mouse. Tumour size was then measured using the equation 0.5 x w x h x h (n=8, *p<0.05 **p<0.01 ***p<0.001 two-tail homoscedastic t-test). (B) A sample of cells were taken before injection (day 1) and after 7 days in cell culture (day 7) to show that infection by the Ad-PRH virus was successful, and to show that Myc-PRH protein is expressed in MCF-7 cells for at least a week, by Western blotting as described previously.

assess the affect of PRH overexpression *in vivo*, xenograft experiments were carried out, whereby MCF-7 cells are injected into a murine host, and allowed to develop tumours over a 6 week period. MCF-7 cells were infected with either Ad, Ad-PRH at a MOI of 50 or left uninfected. After 24 hours cells were harvested and viable cells were counted using trypan blue exclusion dye. Approximately 5 x10^6 cells were then injected into each mammary fat pad of a female 6 week old Balb/c nude mouse, with eight mice being used for Ad and Ad-PRH infected cells. Additionally 4 mice were injected with MCF-7 cells that had not been infected with adenovirus. Each mouse was supplemented with 17β-oestradiol tablets which were inserted sub-cutaneously. 17β-Oestradiol is required to supply a high continuous dose of oestrogen in the mouse, which allows the ER-positive MCF-7 tumour to grow. Tumour size was then measured three times per week (using the modified ellipsoid formula 0.5 x length x width^2 (Euhus et al., 1986)), until the mice were culled. Unexpectedly, there is a significant increase in tumour size in mice injected with Ad-PRH infected MCF-7 cells

compared to mice injected with Ad infected or uninfected MCF-7 cells (Figure 5.16). Thus, in *in vivo* experiments PRH overexpression results in an entirely unexpected oncogenic phenotype.

5.5 Discussion

In scratch wound assays, overexpression of PRH inhibited chemokinesis by MCF-7 and MDA-MB-231 cells (MCF-10A cells were not used, as they are not migratory, and thus it would be difficult to see a further decrease in migration). Knockdown of PRH increases scratch wound closure by MCF-7 cells. However, it failed to have the same effect in MDA-MB-231 cells. One reason for this discrepancy could be because MDA-MB-231 cells are highly migratory mesenchymal cells, and thus it may be difficult to increase their migration even further. PRH knockdown also has no effect on chemokinesis in MCF-10A cells. The difference in effect of PRH knockdown between MCF-7 and MCF-10A cells could be because proteins are present which inhibit MCF-10A migration, and these are either mutated or absent in MCF-7 cells, allowing the PRH knockdown phenotype to be more easily observed.

In chemotaxis assays, in all three cell types tested (MCF-7, MDA-MB-231 and MCF-10A), knock-down of PRH expression leads to increased migration. Thus, knockdown of PRH has effects on chemotaxis in MCF-10A and MDA-MB-231 cells, even though no effects on chemokinesis can be detected. For MCF-10A cells, the enhanced chemotaxis may be observed because EGF is used as a chemoattractant. One possibility is that PRH could be

repressing expression of EGF receptor and/or signalling proteins in the EGF pathway. It should also be noted that only 7% of PRH knockdown cells migrate over 24 hours. Therefore, this increase in chemotaxis may be too small to detect in non-directional cell mobility scratch wound assays. The same could also be true in MDA-MB-231 cells. Overexpression of PRH in MCF-7 and MDA-MB-231 cells leads to decreased migration (MCF-10A cells could not be used in this assay, as they are not sufficiently migratory). In each cell type, PRH is a regulator of genes associated with migration; endoglin in MCF-10A cells, e-cadherin and endoglin in MCF-7 cells and *ESM1* in MDA-MB-231 cells. Taken together, expression of PRH is an important factor in determining the chemotactic abilities of breast cells.

Invasion assays were also carried out on PRH knockdown MCF-7 cells. More PRH knockdown cells were invasive than control cells. This shows that PRH is also an important factor in cell invasion. It is thought that as cancer cells become more invasive, they undergo an epithelial to mesenchymal transition (EMT). Therefore, it is possible that PRH is a determining factor for whether a cell undergoes EMT or not. This is further suggested by the observation that both *TP53* and e-cadherin mRNA expression is lower in PRH knockdown cells than control cells.

Unusually Endoglin transcript expression is increased when PRH expression is knocked down in MCF-7 cells, as well as when PRH is overexpressed in the same cell type. This could be due to the “dual nature” of TGF-β signalling, where TGF-β has apparently opposing effects

depending on the context in which it is acting. This is not totally surprising, as Endoglin is known to inhibit migration in less tumourgenic cell types, but can act to promote cell migration in more aggressive cell types (Oxmann et al., 2008, Henry et al., 2011). Therefore, knockdown of PRH could be transforming the MCF-7 cells into a more mesenchymal, and hence more aggressive cell type, and thus this changes the role that Endoglin plays with respect to migration. Exogenous PRH has been shown to bind directly to the *ENG* promoter in both MCF-10A and MCF-7 cells (Kershaw et al., 2013b). It could not be determined whether endogenous PRH in wild type MCF-7 cells regulates *ENG* in this way as well, as no suitable anti-PRH antibody could be found for endogenous ChIP at the endoglin promoter. It is possible that the upregulation of endoglin transcript in PRH knockdown MCF-7 cells is due to the changed morphology and more mesenchymal nature of the PRH knockdown cells (R. Kershaw and P.S. Jayaraman, personal communication).

A link has been made between EMT and CICs, whereby CIC have an more "mesenchymal-like" phenotype, suggesting that EMT leads to the production of more CICs (Mani et al., 2008). Therefore, it could be hypothesised that if knockdown of PRH leads to EMT in MCF-7 cells, that there may be an increase in the number of CICs. This was not found to be the case, as there was no increase in mammosphere formation in PRH knockdown cells compared to control cells. One explanation for this could be that additional factors are required for CIC self-renewal that are not needed for EMT.

The decrease in cell number when PRH is overexpressed in MCF-7 cells in both 2D and 3D cultures led to the hypothesis that overexpression of PRH would lead to a decrease in MCF-7 tumor growth in xenograft experiments. However, overexpression of PRH in these cells surprisingly led to an increase in MCF-7 xenograft growth. This could be caused by a number of factors, including effects on the host immune system, the effects of hypoxia, high oestrogen levels *in vivo* and PRH causing mesenchymal-to-epithelial transition (MET), which will be discussed further in the next chapter.

GENERAL DISCUSSION

6. General discussion

This thesis demonstrates that PRH plays an important role in regulating cell proliferation, survival and the migratory phenotypes shown by breast cancer cells. Moreover, this thesis provides evidence that PRH is a regulator of cell invasion and that PRH can influence the expression of key genes involved in the epithelial-to-mesenchymal transition. These findings provide a possible explanation for the association between PRH expression and breast cancer prognosis.

6.1 PRH and patient prognosis

In chapter three, interrogation of a database that correlates gene expression profile with breast cancer prognosis showed that decreased *PRH* mRNA expression in breast cancer patients correlates with decreased overall survival (Ringnér et al., 2011). Interestingly, PRH mRNA is poorly expressed in the basal and HER2+ subtypes, which are the most aggressive forms of breast cancer. PRH transcript expression is also observed to be significantly decreased in grade 3 breast cancers, which are the least differentiated cancer cell type. This is a similar result to that seen in hepatocarcinoma patients, where PRH protein expression is significantly lower in the least differentiated tumours (Su et al., 2012). Taken together, these studies indicate that *PRH* mRNA expression could function as a novel marker for breast cancer survival.

6.2 PRH protein levels, localisation and modifications in different breast cell lines

This thesis demonstrates that PRH protein is found in most of the normal and tumourgenic breast cell lines tested in this study. The amount of PRH protein detected by the M6 antibody correlates with the *PRH* mRNA levels in the corresponding cell lines, as measured in microarray studies (Ringnér et al., 2011). Therefore, just as *PRH* mRNA could function as a marker for overall survival for breast cancer, the M6 anti-PRH antibody could also be used as a marker for breast cancer prognosis. Interestingly, the other anti-PRH antibodies used (M3 and YKN5) detect different forms of PRH, which are expressed at quite different levels in each cell type. The significance of this is not fully understood, and requires further investigation into the nature of the post-translational modifications and oligomerisation state of the PRH protein. It is of interest to note that the truncated PRHΔC product is expressed at high levels in both MCF-7 and MDA-MB-231 tumour cells. This product has been shown to act in a dominant negative way over full length PRH in leukaemic cells (Noy et al., 2012c). It is likely that the presence of PRHΔC will also influence the activity of full-length PRH in breast tumour cells, and therefore measurement of full length PRH levels may not be a good indicator of the amount of transcriptionally active PRH levels in the cell. Additional studies examining the role of PRHΔC in influencing PRH or TLE activity in breast cancer cells would be useful. For example, TLE proteins are negative regulators of Wnt signalling (Daniels and Weis, 2005), therefore it would be of interest to investigate whether PRHΔC activates Wnt signalling by sequestration of TLE protein in breast cancer cells.

Subcellular fractionation and staining with the M6 antibody showed that the localisation of PRH is predominantly cytoplasmic in both the non-tumourgenic and tumourgenic cell lines. However, further *in situ* fractionation experiments showed that even though PRH is predominantly cytoplasmic in MCF-10A cells there appears to be significantly more tightly held nuclear PRH in MCF-10A cells compared to MCF-7 and MDA-MB-231 cells, (R. Kershaw, E. Fallon and P-S Jayaraman, personal communication). Therefore, the *in situ* subcellular fractionation experiments do correlate with the findings of Puppin et. al., who found out that nuclear PRH is reduced in breast tumour cells compared to control cells (Puppin et al., 2006). This result is not observed in *in vitro* cell fractionation experiments where retention of nuclear proteins is measured, but this could be because *in situ* fractionation and *in vitro* fractionation experiments are carried out using very different detergent conditions.

It is interesting to note that exogenous PRH stability is lower in the tumourgenic cell lines than the non-tumourgenic cell line MCF-10A. It has been shown previously in breast cancer patients that their serum levels have higher proteolytic activity compared to healthy individuals (Roth et al., 2011). Therefore, it is possible that in tumour cells PRH activity is reduced not just by a reduction in *PRH* transcript, but also by an increase in protein degradation as well. The mechanism of PRH degradation could be investigated further, using caspase and proteasome inhibitors, to see whether these affect PRH stability. The mechanism of phosphorylation of PRH is also of interest, and warrants further investigation. This could be achieved by disrupting the activity of CK2 (either by using CK2 inhibitors such as DMAT/TBB, or by siRNA knockdown of a CK2 subunit) and determining whether this affects phosphorylated PRH levels in breast cells. The mechanism of regulation of PRH

activity will certainly be of significance if PRH protein levels prove to be an indicator of tumour prognosis.

6.3 PRH and cell growth

In chapter four, cell counting assays showed that exogenous PRH in MCF-10A and MCF-7 cells, significantly reduced cell number. In MCF-10A cells, this was due in part to a reduction in proliferation, as determined by BrdU assays, whilst exogenous PRH increased MCF-7 apoptosis. PRH also decreased proliferation in MDA-MB-231 cells, as determined by BrdU and cell cycle assays. Thus in all cases exogenous PRH appears to decrease cell growth.

The differences in the effect of exogenous PRH (i.e on proliferation or apoptosis) between the cell lines very likely reflects the genetic background of the cell line. For example, MDA-MB-231 cells express mutated p53 (R280K), therefore are presumably more resistant to apoptosis, whereas MCF-7 cells express wild-type p53. Differences in the levels of endogenous PRH in each cell line may also account for the apparent difference of exogenous PRH on the phenotype of each cell line This could explain why the effects of exogenous PRH are greater in MCF-7 cells (which express moderate levels of PRH) compared to MDA-MB-231 cells (which express high levels of PRH). This could occur because exogenous PRH has to compete with endogenous PRH at PRH binding sites within gene promoters/enhancers. Therefore, cells with low endogenous PRH in the cell will be more affected by exogenous PRH than cells already expressing high amount of PRH protein. Also,

the relative levels of PRH co-activators and co-repressors will vary between the cell types, which will influence PRH activity. It has been shown in K562 cells that PRH needs to bind to the co-repressor TLE to exert its transcriptional repression activity (Noy et al., 2010). Therefore, differing endogenous levels of TLE (or sequesterisation of TLE by PRHΔC, for example) could be one reason why exogenous PRH has different effects in different cell lines. Finally, genes which are quite lowly expressed in certain cell lines may not be repressed further by increased PRH, and conversely, genes which are highly expressed may not show increased expression when PRH levels are increased. Another reason that exogenous PRH has apparently different effects in each cell line could be that exogenous PRH is less stable in some cell lines. For example, Myc-PRH appears to be less stable in MDA-MB-231 cells than MCF-10A cells, and thus the effects of PRH may be more transitory in MDA-MB-231 cells, compared to non-tumourgenic MCF-10A cells. In accordance with this idea, the observed inhibition of proliferation by PRH is much greater in MCF-10A cells than in MDA-MB-231 cells, and although exogenous PRH did cause a decrease in MDA-MB-231 proliferation, this did not translate to a decrease in cell number in cell counting experiments. Therefore, the difference in PRH stability between the cell lines (possibly due to increased phosphorylation by CK2) could also lead to an apparent difference in exogenous PRH activity.

PRH has been shown to decrease proliferation of U937 lymphoma cells via a non-transcriptional mechanism (Topisirovic et al., 2003). In this cell line PRH binds to the translation factor protein eIF-4E, and inhibits nucleo-cytoplasmic transport of cyclin d1 mRNA (Topisirovic et al., 2003). However, PRH can also inhibit gene expression by directly

binding to promoters, leading to repression of gene expression (Noy et al., 2010). Since the PRH N187A DNA binding mutant failed to decrease MCF-10A and MDA-MB-231 proliferation, or to decrease MCF-7 cell number, it can be inferred that binding to eIF-4E is not significantly involved in the growth inhibitory activities of exogenous PRH in the three breast cell lines tested. Thus in all breast cell lines DNA binding activity is required for population growth inhibitory phenotypes. In MCF-7 cells at least two PRH regulated genes (endoglin and *VEGFR2*) are directly bound by exogenous PRH at the promoter region of these genes. Further experiments are needed to determine the precise mechanism(s) by which PRH regulates expression of these genes (for example, whether PRH needs to bind to TLE, or to another co-activator/repressor, to regulate genes in this cell type).

Knockdown of PRH caused three different effects in the three breast cell lines, causing no observable effect on proliferation in MCF-10A cells, increasing proliferation in MCF-7 cells, and decreasing proliferation in MDA-MB-231 cells. In MCF-10A cells it is likely that, as in other normal cell types, there are many redundant mechanisms to control cell proliferation (reviewed in Huang and Ingber, 1999). Therefore, reduction of PRH expression in itself may not be enough to increase cell proliferation, or increase expression of VSP genes. Alternatively, it is possible that the level of knockdown of PRH in this cell type was not sufficient to observe a phenotype.

In MCF-7 cells, reduction of PRH protein leads to an increase in cell number, whilst conversely overexpression of PRH results in decreased cell number, therefore in this cell line the overexpression and knockdown of PRH results generally correlate with each other. However, overexpression of PRH did not inhibit the cell cycle progression, whilst knockdown

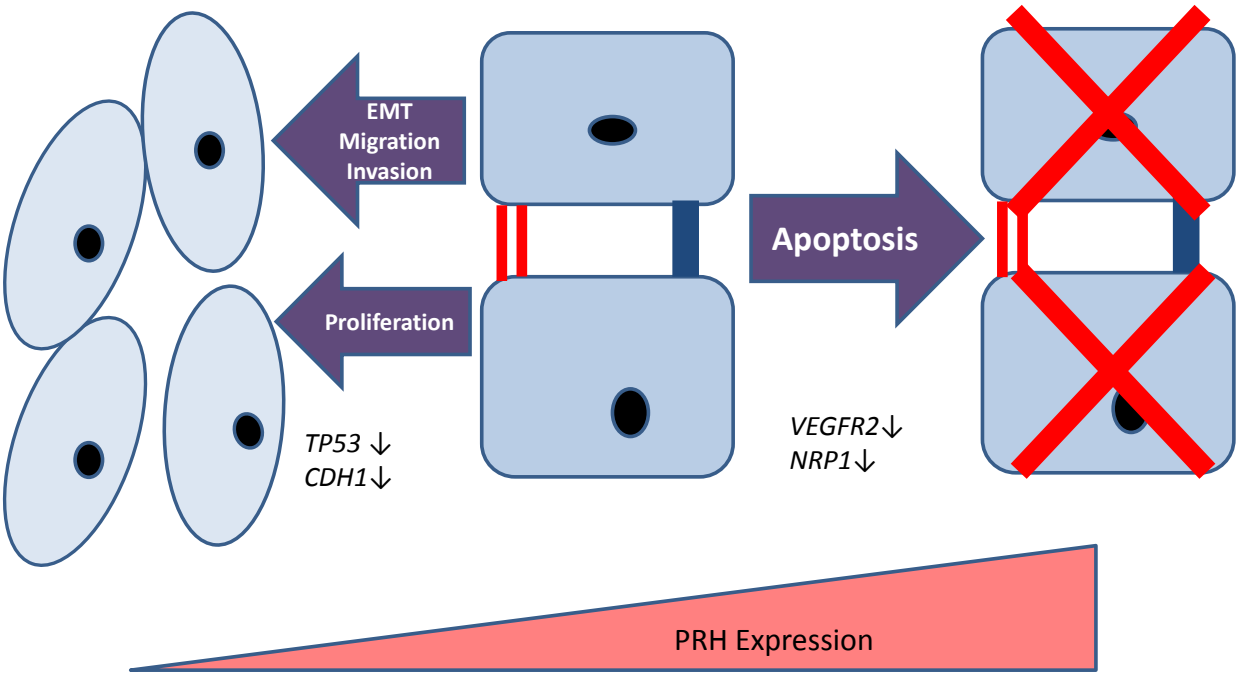

Figure 6.1: Model of PRH activity in MCF-7 cells. Reduction of PRH expression leads to EMT, and an increase in proliferation, migration and invasion. This correlates with a reduction in *TP53* and e-cadherin (*CDH1*) mRNA expression. Increased PRH leads to apoptosis of MCF-7 cells, which correlates with decreased expression of the pro-survival genes *NRP1* and *VEGFR2*.

of PRH results in faster progression through the cell cycle (through an increase in the percentage of cells in S-phase). In PRH overexpressing MCF-7 cells, increased cell apoptosis could occur through decreased autocrine signalling by VEGF signalling genes, whereas knockdown of PRH expression may have less of an effect on increasing expression of genes in this pathway, as expression levels may be near their maximal levels in this cell type. Similarly in wild-type MCF-7 cells, *TP53* transcript may be expressed at its maximal levels, preventing exogenous PRH further increasing expression of this gene. Knockdown of PRH shows that endogenous PRH does play a role in regulation of the *TP53* gene (in these cells) (see figure 6.1).

Microarray studies show that *PRH* mRNA levels are significantly lower in basal breast cancers (as seen in chapter 3). Therefore, it is unusual to find that the basal tumour cell line

MDA-MB-231 expresses relatively high levels of PRH protein compared to the other cell lines used in this study. Knockdown of PRH in MDA-MB-231 cells also leads to a decrease in cell proliferation and a decrease in *VEGF*A mRNA expression. This is unexpected, as overexpression of PRH also leads to a decrease in cell proliferation. The reason for the inconsistencies of knockdown and overexpression of PRH in these results could be that endogenous PRH activity is aberrant in this cell line, resulting in it activating genes it is known to repress in other cell lines, such as MCF-10A cells, K562 leukaemic cells and HUVECs (Nakagawa et al., 2003, Noy et al., 2010), and also resulting in PRH promoting tumour growth. This aberrant activity may be, as mentioned before, due to the expression of other mutant PRH interacting partner proteins, which alter PRH activity in this cell line. Alternatively, the endogenous PRH gene may be mutated in this cell type. Therefore, characterisation of this cell line (by RNA sequencing) could determine how the activity of endogenous PRH is altered in this cell type.

6.4 PRH in the regulation of EMT and invasion

In chapter 5, it is shown that the overall effect of PRH is that it decreases migration in all three cell types, either via overexpression or knockdown of PRH. Therefore, unlike the effect of PRH on breast cancer cell proliferation, the effect of PRH on migration appears to be more consistent and less context-dependent. Exogenous PRH expression also decreases the invasion of breast tumour cells, and knockdown of PRH increases their invasion. One explanation for the more consistent inhibition of migration/invasion, compared to the more

variable phenotype on cell growth from PRH, could be that the genes regulating migration/invasion are more tightly regulated by endogenous PRH than genes involved in regulating cell growth. Therefore, even a small decrease in PRH levels leads to increased migration and invasion. Another possibility is that cofactors regulating migration and invasion are the same in all cell types, whereas cofactors regulating growth may be different. Since loss of PRH in non-tumourgenic cells increases their invasive properties, and as metastasis is the cause of 90% of cancer deaths (Mehlen and Puisieux, 2006), increased invasion could provide an explanation for the finding that decreased PRH expression correlates with decreased survival in breast tumour patients.

Homeodomain proteins typically play a key role in the development of the embryo and the adult organs, and one process which is regulated during development is EMT (Yilmaz and Christofori, 2009, Nunes et al., 2003). Examples of homeodomain proteins that induce EMT in breast cancer cells include Paired Mesoderm Homeobox Protein 1 (PRRX1), Ladybird Homeobox 1 (LBX1), Homeobox B7 and Homeobox B9 (Wu et al., 2006a, Yu et al., 2009, Chiba et al., 2012, Ocaña et al., 2012). Therefore, it is highly likely that PRH, being a homeodomain protein mislocalised in breast cancer, can also affect EMT in breast cancer cells. In MCF-7 cells, knockdown of endogenous PRH was shown to decrease e-cadherin and *TP53* mRNA expression. As PRH knockdown also increased MCF-7 migration and invasion, it is possible that these cells may be undergoing EMT. Further evidence for this hypothesis has now been obtained in the laboratory in Western blotting experiments. Knockdown of PRH causes a decrease in E-Cadherin protein expression, and an increase in the expression of several transcription factors required for EMT (Snail, Slug and Vimentin) (R. Kershaw and

P.S. Jayaraman, personal communication). Furthermore, the morphology of the PRH knockdown cells is elongated and more mesenchymal (R.K. and P.S.J). It has previously been shown that PRH is involved in the EMT process during murine development (Hallaq et al., 2004). Taken together, this strongly suggests that PRH is involved in inhibiting EMT in MCF-7 breast cancer cells (see figure 6.1).

In MCF-10A cells, endoglin mRNA is up-regulated by PRH over-expression, and is down-regulated when PRH expression is knocked down, indicating that PRH is an activator of endoglin mRNA expression in this cell type. Surprisingly, endoglin transcript was significantly upregulated by both knockdown and overexpression of PRH in MCF-7 cells. Exogenous PRH has been shown to bind directly to the *ENG* promoter in both of these cell types, suggesting that PRH regulates *ENG* directly (Kershaw et al., 2013b). As mentioned before, PRH knockdown also appears to induce EMT in MCF-7 cells (and they acquire a more migratory and invasive phenotype). This may account for the increase in endoglin mRNA levels in MCF-7 PRH knockdown cells, whereby other factors which are upregulated during EMT activate *ENG* instead of PRH. Upregulation of Endoglin in non-tumour cells acts to inhibit cell migration, whereas upregulation of Endoglin in the more aggressive tumour cells promotes cell migration (Oxmann et al., 2008, Henry et al., 2011). This correlates with the “dual roles” that TGF-β signalling has in cancer development, inhibiting tumourgenesis in less transformed cells, and promoting tumour migration in more transformed cells (Bierie and Moses, 2006). Therefore, the transcription factors involved in the regulation of Endoglin (and TGF-β signalling) are presumably very different in the less aggressive tumours compared to the more aggressive tumour cell types.

6.5 PRH in xenografts

This thesis demonstrates that overexpression of PRH inhibits the growth of MCF-7 cells in both adherant and in mammosphere cultures, by increasing apoptosis. Moreover it shows that overexpression of PRH decreases migration of these cells. However, Ad-PRH infected MCF-7 cells are significantly more tumourgenic than Ad infected MCF-7 cells in mouse xenografts. There are many factors which could explain the discrepancies between the *in vitro* and the *in vivo* growth assays. For the tumour to be established, it must first settle in the stroma micro-environment, which is a different process from cell survival. Therefore, one possibility is that although PRH increases apoptosis of MCF-7 cells, the cells that survive are more adapted to settle in the mouse stroma. It has been suggested that cells that undergo metastasis undergo mesenchymal-epithelial transition to colonise their secondary sites (Hanahan and Weinberg, 2011). Therefore, as knockdown of PRH allows cells to undergo increased EMT in MCF-7 cells, it is possible that overexpression of PRH will lead to increased MET, allowing greater colonisation of MCF-7 cells in xenografts.

The murine immune system could also interact with the Ad-PRH infected MCF-7 cells, increasing tumourgenesis. The mice used are Balb/c nude mice, which have a mutation in the *FOXN1* gene, resulting in a dysfunctional thymus (Mecklenburg et al., 2001). This results in mice that lack T-cell activity, but maintain normal B-cell and innate immune system activity (Mecklenburg et al., 2001). Tumourgenesis is increased by inflammation, by increasing concentrations of matrix metalloproteinases (MMPs) in the stroma (leading to

increased tumour invasion), increasing reactive oxygen species (ROS) (and therefore increasing DNA damage in the tumour microenvironment) and by increasing angiogenesis, which promote epithelial tumour cell survival (Rakoff-Nahoum, 2006, Grivennikov et al., 2010). Therefore, an increase in apoptotic MCF-7 cells could lead to an increase in the inflammatory response, which in turn could make the stroma micro-environment more hospitable for tumour cells.

As mentioned previously in the introduction, VEGF receptor genes increase tumour angiogenesis, and in turn make the tumour cells less hypoxic. Also, it has been shown that primary breast tumour CICs can differentiate directly into endothelial cells, and form intratumour vessels (Bussolati et al., 2009). As exogenous PRH decreases *VEGFR2* and *NRP1* mRNA expression in MCF-7 cells, it is possible that overexpression of PRH reduces the pro-angiogenic activity of MCF-7 CICs as well. This may paradoxically allow the tumour to become more aggressive, as decreased angiogenesis may result in increased hypoxia within the MCF-7 tumour, which has been shown to lead to increased EMT (Chen et al., 2009a). Furthermore, it has been shown that anti-VEGF therapies, such as sunitinib, whilst decreasing the size of the initial tumour, frequently recur, leading to more aggressive tumours (Ebos et al., 2009). It has also been shown that anti-angiogenic agents increase the frequency of breast CICs as well (Conley et al., 2012). Therefore, inhibition of VSP genes by PRH in certain contexts could actually result in increased tumourgenesis.

6.6 Further experiments

To further determine whether PRH is pro- or anti-tumourgenic *in vivo,* the xenograft experiment could be set up in a slightly different way, by waiting approximately 2 weeks for the tumour to be established before infecting the tumour with adenovirus. Therefore, if the resulting tumours get smaller, or at least fail to increase in size, it can be shown that PRH can affect MCF-7 cell growth *in vivo,* and that the results seen previously were due to an increase in establishment of the initial tumour, rather than increased tumour growth. The experiment could also be repeated with the PRH knockdown MCF-7 cells, to determine whether this shows the opposite effect to that is seen with PRH over-expression. It would also be of interest to determine whether knockdown or overexpression of PRH can cause increased breast cancer cell metastasis *in vivo.* This has previously been achieved using highly metastatic MDA-MB-231 cells, which express GFP (Hartwell et al., 2006). This would further verify whether PRH is a repressor of tumour cell invasion, and whether this affects tumour metastasis *in vivo*.

Although it is shown that PRH directly regulates genes involved in breast cell survival and migration, the studies were limited to genes which have previously been shown to be regulated by PRH. To determine the global role of PRH as a transcription factor in the regulation of cell growth and migration, microarray analysis, RNA-sequencing and ChIP-sequencing could be carried out. This would determine whether PRH regulates genes in other pathways which are involved in cancer survival.

To conclude, PRH is an important regulator of breast cancer growth, migration, and invasion in a variety of breast cell types, and disruption of PRH activity can lead to more aggressive phenotypes.

REFERENCES

7. References

AHMED, K., GERBER, D. A. & COCHET, C. 2002. Joining the cell survival squad: an emerging role for protein kinase CK2. *Trends in cell biology,* 12**,** 226-230.

AITKENHEAD, M., WANG, S.-J., NAKATSU, M. N., MESTAS, J., HEARD, C. & HUGHES, C. C. W. 2002. Identification of Endothelial Cell Genes Expressed in an in Vitro Model of Angiogenesis: Induction of ESM-1, βig-h3, and NrCAM. *Microvascular Research,* 63**,** 159-171.

AKRIGG, G. W. G. W. A. A. 1992. Constitutive and enhanced expression from the CMV

major IE promoter in a defective adenovirus vector. *Nucleic Acids Res,* 20`**,** 2233-2239.

AL-HAJJ, M., WICHA, M., BENITO-HERNANDEZ, A., MORRISON, S. & CLARKE, M. 2003a. Prospective identification of tumorigenic breast cancer cells. *Proc Natl Acad Sci USA,* 100**,** 3983 - 3988.

AL-HAJJ, M., WICHA, M. S., BENITO-HERNANDEZ, A., MORRISON, S. J. & CLARKE, M. F. 2003b. Prospective identification of tumorigenic breast cancer cells. *Proceedings of the National Academy of Sciences,* 100**,** 3983-3988.

ALBINI, A., IWAMOTO, Y., KLEINMAN, H., MARTIN, G., AARONSON, S., KOZLOWSKI, J. & MCEWAN, R. 1987. A rapid in vitro assay for quantitating the invasive potential of tumor cells. *Cancer Research,* 47**,** 3239-3245.

ALT, A., MIGUEL-ROMERO, L., DONDERIS, J., ARISTORENA, M., BLANCO, F. J., ROUND, A., RUBIO, V., BERNABEU, C. & MARINA, A. 2012. Structural and Functional Insights into Endoglin Ligand Recognition and Binding. *PLoS ONE,* 7**,** e29948.

BACHELDER, R. E., CRAGO, A., CHUNG, J., WENDT, M. A., SHAW, L. M., ROBINSON, G. & MERCURIO, A. M. 2001. Vascular Endothelial Growth Factor Is an Autocrine Survival Factor for Neuropilin-expressing Breast Carcinoma Cells. *Cancer Research,* 61**,** 5736-5740.

BACHELDER, R. E., WENDT, M. A. & MERCURIO, A. M. 2002. Vascular Endothelial Growth Factor Promotes Breast Carcinoma Invasion in an Autocrine Manner by Regulating the Chemokine Receptor CXCR4. *Cancer Research,* 62**,** 7203-7206.

BALTIMORE, D. 2001. Our genome unveiled. *Nature,* 409**,** 814-816.

BANNISTER, A. J. & KOUZARIDES, T. 2011. Regulation of chromatin by histone modifications. *Cell Res,* 21**,** 381-395.

BARR, M. P., BYRNE, A. M., DUFFY, A. M., CONDRON, C. M., DEVOCELLE, M., HARRIOTT, P., BOUCHIER-HAYES, D. J. & HARMEY, J. H. 2005. A peptide corresponding to the neuropilin-1-binding site on VEGF165 induces apoptosis of neuropilin-1-expressing breast tumour cells. *Br J Cancer,* 92**,** 328-333.

BAUER, K. R., BROWN, M., CRESS, R. D., PARISE, C. A. & CAGGIANO, V. 2007. Descriptive analysis of estrogen receptor (ER)-negative, progesterone receptor (PR)-negative, and HER2-negative invasive breast cancer, the so-called triple-negative phenotype. *Cancer,* 109**,** 1721-1728.

BELLÓN, T., CORBI, A., LASTRES, P., CALÉS, C., CEBRIÁN, M., VERA, S., CHEIFETZ, S., MASSAGUE, J., LETARTE, M. & BERNABÉU, C. 1993. Identification and expression of two forms of the human transforming growth factor-β-binding protein endoglin with distinct cytoplasmic regions. *European Journal of Immunology,* 23**,** 2340-2345.

BESS, K., SWINGLER, T., RIVETT, A., GASTON, K. & JAYARAMAN, P. 2003a. The transcriptional repressor protein PRH interacts with the proteasome. *Biochem J,* 374**,** 667 - 675.

BESS, K. L., SWINGLER, T. E., RIVETT, A. J., GASTON, K. & JAYARAMAN, P.-S. 2003b. The transcriptional repressor protein PRH interacts with the proteasome. *Biochem. J.,* 374**,** 667-675.

BESS, K. L., SWINGLER, T. E., RIVETT, A. J., GASTON, K. & JAYARAMAN, P.-S. 2003c. The transcriptional repressor protein PRH interacts with the proteasome. *Biochemical Journal,* 374**,** 667-675.

BHAVE, V. S., MARS, W., DONTHAMSETTY, S., ZHANG, X., TAN, L., LUO, J., BOWEN, W. C. & MICHALOPOULOS, G. K. 2013. Regulation of Liver Growth by Glypican 3, CD81, Hedgehog, and Hhex. *The American Journal of Pathology,* 183**,** 153-159.

BIERIE, B. & MOSES, H. L. 2006. Tumour microenvironment: TGF[beta]: the molecular Jekyll and Hyde of cancer. *Nat Rev Cancer,* 6**,** 506-520.

BLACKWOOD, E. M. & EISENMAN, R. N. 1991. Max: a helix-loop-helix zipper protein that forms a sequence-specific DNA-binding complex with Myc. *Science,* 251**,** 1211-1217.

BORT, R., MARTINEZ-BARBERA, J. P., BEDDINGTON, R. S. P. & ZARET, K. S. 2004. Hex homeobox gene-dependent tissue positioning is required for organogenesis of the ventral pancreas. *Development,* 131**,** 797-806.

BOS, P. D., ZHANG, X. H.-F., NADAL, C., SHU, W., GOMIS, R. R., NGUYEN, D. X., MINN, A. J., VAN DE VIJVER, M. J., GERALD, W. L. & FOEKENS, J. A. 2009. Genes that mediate breast cancer metastasis to the brain. *Nature,* 459**,** 1005-1009.

BOSCO, E. E., WANG, Y., XU, H., ZILFOU, J. T., KNUDSEN, K. E., ARONOW, B. J., LOWE, S. W. & KNUDSEN, E. S. 2007. The retinoblastoma tumor suppressor modifies the therapeutic response of breast cancer. *The Journal of Clinical Investigation,* 117**,** 218-228.

BOYER, L. A., PLATH, K., ZEITLINGER, J., BRAMBRINK, T., MEDEIROS, L. A., LEE, T. I., LEVINE, S. S., WERNIG, M., TAJONAR, A. & RAY, M. K. 2006. Polycomb complexes repress developmental regulators in murine embryonic stem cells. *Nature,* 441**,** 349-353.

BRENNER, C., DEPLUS, R., DIDELOT, C., LORIOT, A., VIRÉ, E., DE SMET, C., GUTIERREZ, A., DANOVI, D., BERNARD, D. & BOON, T. 2004. Myc represses transcription through recruitment of DNA methyltransferase corepressor. *The EMBO journal,* 24**,** 336-346.

BRET VERHOVEN, R. A. S. A. P. W. 1995. Mechanisms of Phosphatidylserine Exposure, A Phagocyte

Recognition Signal, on Apoptotic T Lymphocytes. *J. Exp. Med.,* 1812**,** 1597-1601.

BRICKMAN, J., JONES, C., CLEMENTS, M., SMITH, J. & BEDDINGTON, R. 2000. Hex is a transcriptional repressor that contributes to anterior identity and suppresses Spemann organiser function. *Development,* 127**,** 2303 - 2315.

BROOKS, S. C., LOCKE, E. R. & SOULE, H. D. 1973. Estrogen Receptor in a Human Cell Line (MCF-7) from Breast Carcinoma. *Journal of Biological Chemistry,* 248**,** 6251-6253.

BROWNELL, J. E. & ALLIS, C. D. 1996. Special HATs for special occasions: linking histone acetylation to chromatin assembly and gene activation. *Current opinion in genetics & development,* 6**,** 176-184.

BUSSOLATI, B., GRANGE, C., SAPINO, A. & CAMUSSI, G. 2009. Endothelial cell differentiation of human breast tumour stem/progenitor cells. *Journal of cellular and molecular medicine,* 13**,** 309-319.

CAILLEAU, R., YOUNG, R., OLIVE, M. & REEVES, W. 1974. Breast tumor cell lines from pleural effusions. *Journal of the National Cancer Institute,* 53**,** 661-674.

CHAFFER, C. L. & WEINBERG, R. A. 2011. A Perspective on Cancer Cell Metastasis. *Science,* 331**,** 1559-1564.

CHANG, C.-J., CHAO, C.-H., XIA, W., YANG, J.-Y., XIONG, Y., LI, C.-W., YU, W.-H., REHMAN, S. K., HSU, J. L., LEE, H.-H., LIU, M., CHEN, C.-T., YU, D. & HUNG, M.-C. 2011. p53 regulates epithelial-mesenchymal transition and stem cell properties through modulating miRNAs. *Nat Cell Biol,* 13**,** 317-323.

CHARAFE-JAUFFRET, E., GINESTIER, C., MONVILLE, F., FINETTI, P., ADELAIDE, J., CERVERA, N., FEKAIRI, S., XERRI, L., JACQUEMIER, J., BIRNBAUM, D. & BERTUCCI, F. 2005. Gene expression profiling of breast cell lines identifies potential new basal markers. *Oncogene,* 25**,** 2273-2284.

CHEN, J., IMANAKA, N. & GRIFFIN, J. 2009a. Hypoxia potentiates Notch signaling in breast cancer leading to decreased E-cadherin expression and increased cell migration and invasion. *British journal of cancer,* 102**,** 351-360.

CHEN, J., IMANAKA, N. & GRIFFIN, J. D. 2009b. Hypoxia potentiates Notch signaling in breast cancer leading to decreased E-cadherin expression and increased cell migration and invasion. *Br J Cancer,* 102**,** 351-360.

CHIBA, N., COMAILLS, V., SHIOTANI, B., TAKAHASHI, F., SHIMADA, T., TAJIMA, K., WINOKUR, D., HAYASHIDA, T., WILLERS, H., BRACHTEL, E., VIVANCO, M. D. M., HABER, D. A., ZOU, L. & MAHESWARAN, S. 2012. Homeobox B9 induces epithelial-to-mesenchymal transition-associated radioresistance by accelerating DNA damage responses. *Proceedings of the National Academy of Sciences,* 109**,** 2760-2765.

CHO, H.-S., MASON, K., RAMYAR, K. X., STANLEY, A. M., GABELLI, S. B., DENNEY, D. W. & LEAHY, D. J. 2003. Structure of the extracellular region of HER2 alone and in complex with the Herceptin Fab. *Nature,* 421**,** 756-760.

CHO, K. W. Y., BLUMBERG, B., STEINBEISSER, H. & DE ROBERTIS, E. M. 1991. Molecular nature of Spemann's organizer: the role of the Xenopus homeobox gene goosecoid. *Cell,* 67**,** 1111-1120.

CICALESE, A., BONIZZI, G., PASI, C. E., FARETTA, M., RONZONI, S., GIULINI, B., BRISKEN, C., MINUCCI, S., DI FIORE, P. P. & PELICCI, P. G. 2009. The Tumor Suppressor p53 Regulates Polarity of Self-Renewing Divisions in Mammary Stem Cells. *Cell,* 138**,** 1083-1095.

CILLO, C., FAIELLA, A., CANTILE, M. & BONCINELLI, E. 1999. Homeobox Genes and Cancer. *Experimental cell research,* 248**,** 1-9.

CLYNES, R. A., TOWERS, T. L., PRESTA, L. G. & RAVETCH, J. V. 2000. Inhibitory Fc receptors modulate in vivo cytoxicity against tumor targets. *Nature medicine,* 6**,** 443-446.

COLLINS, F., LANDER, E., ROGERS, J., WATERSTON, R. & CONSO, I. 2004. Finishing the euchromatic sequence of the human genome. *Nature,* 431**,** 931-945.

CONG, R., JIANG, X., WILSON, C. M., HUNTER, M. P., VASAVADA, H. & BOGUE, C. W. 2006. Hhex is a direct repressor of endothelial cell-specific molecule 1 (ESM-1). *Biochemical and Biophysical Research Communications,* 346**,** 535-545.

CONGYUN, L., ZHENGSHENG, W. & QING, Z. 2008. Eexpression of ESM-1 in breast carcinoma and its prognostic value. *Acta Universitatis Medicinalis Anhui,* 4**,** 010.

CONLEY, S. J., GHEORDUNESCU, E., KAKARALA, P., NEWMAN, B., KORKAYA, H., HEATH, A. N., CLOUTHIER, S. G. & WICHA, M. S. 2012. Antiangiogenic agents increase breast cancer stem cells via the generation of tumor hypoxia. *Proceedings of the National Academy of Sciences,* 109**,** 2784-2789.

CONSORTIUM, T. C. E. S. 1998. Genome Sequence of the Nematode C. elegans: A Platform for Investigating Biology. *Science,* 282**,** 2012-2018.

CREIGHTON, C., CHANG, J. & ROSEN, J. 2010. Epithelial-Mesenchymal Transition (EMT) in Tumor-Initiating Cells and Its Clinical Implications in Breast Cancer. *Journal of Mammary Gland Biology and Neoplasia,* 15**,** 253-260.

CREIGHTON, C. J., LI, X., LANDIS, M., DIXON, J. M., NEUMEISTER, V. M., SJOLUND, A., RIMM, D. L., WONG, H., RODRIGUEZ, A. & HERSCHKOWITZ, J. I. 2009. Residual breast cancers after conventional therapy display mesenchymal as well as tumor-initiating features. *Proceedings of the National Academy of Sciences,* 106**,** 13820-13825.

CROMPTON, M. R., BARTLETT, T. J., MACGREGOR, A. D., MANFIOLETTI, G., BURATTI, E., GIANCOTTI, V. & GOODWIN, G. H. 1992. Identification of a novel vertebrate homeobox gene expressed in haematopoietic cells. *Nucleic Acids Research,* 20**,** 5661-5667.

CRUK. 2013. *How many different types of cancer are there?* [Online]. Available: http://www.cancerresearchuk.org/cancer-help/about-cancer/cancer-questions/how-many-different-types-of-cancer-are-there [Accessed 14/08/2013 2013].

CURTIS, C., SHAH, S. P., CHIN, S.-F., TURASHVILI, G., RUEDA, O. M., DUNNING, M. J., SPEED, D., LYNCH, A. G., SAMARAJIWA, S. & YUAN, Y. 2012. The genomic and transcriptomic architecture of 2,000 breast tumours reveals novel subgroups. *Nature,* 486**,** 346-352.

CURTIS, D. J. & MCCORMACK, M. P. 2010. The molecular basis of Lmo2-induced T-cell acute lymphoblastic leukemia. *Clinical Cancer Research,* 16**,** 5618-5623.

D'ELIA, A. V., TELL, G., RUSSO, D., ARTURI, F., PUGLISI, F., MANFIOLETTI, G., GATTEI, V., MACK, D. L., CATALDI, P., FILETTI, S., DI LORETO, C. & DAMANTE, G. 2002. Expression and Localization of the Homeodomain-Containing Protein HEX in Human Thyroid Tumors. *Journal of Clinical Endocrinology & Metabolism,* 87**,** 1376-1383.

DANIELS, D. L. & WEIS, W. I. 2005. β-Catenin directly displaces Groucho/TLE repressors from Tcf/Lef in Wnt-mediated transcription activation. *Nature structural & molecular biology,* 12**,** 364-371.

DAVIES, H., BIGNELL, G. R., COX, C., STEPHENS, P., EDKINS, S., CLEGG, S., TEAGUE, J., WOFFENDIN, H., GARNETT, M. J. & BOTTOMLEY, W. 2002. Mutations of the BRAF gene in human cancer. *Nature,* 417**,** 949-954.

DEBNATH, J., MUTHUSWAMY, S. K. & BRUGGE, J. S. 2003a. Morphogenesis and oncogenesis of MCF-10A mammary epithelial acini grown in three-dimensional basement membrane cultures. *Methods,* 30**,** 256-68.

DEBNATH, J., MUTHUSWAMY, S. K. & BRUGGE, J. S. 2003b. Morphogenesis and oncogenesis of MCF-10A mammary epithelial acini grown in three-dimensional basement membrane cultures. *Methods,* 30**,** 256-268.

DENT, R., TRUDEAU, M., PRITCHARD, K. I., HANNA, W. M., KAHN, H. K., SAWKA, C. A., LICKLEY, L. A., RAWLINSON, E., SUN, P. & NAROD, S. A. 2007. Triple-Negative Breast Cancer: Clinical Features and Patterns of Recurrence. *Clinical Cancer Research,* 13**,** 4429-4434.

DESJOBERT, C., NOY, P., SWINGLER, T., WILLIAMS, H., GASTON, K. & JAYARAMAN, P.-S. 2009. The PRH/Hex repressor protein causes nuclear retention of Groucho/TLE co-repressors. *Biochem J,* 417**,** 121-132.

DIJKE, P., GOUMANS, M.-J. & PARDALI, E. 2008. Endoglin in angiogenesis and vascular diseases. *Angiogenesis,* 11**,** 79-89.

DUFFY, M. J., MAGUIRE, T. M., HILL, A., MCDERMOTT, E. & O'HIGGINS, N. 2000. Metalloproteinases: role in breast carcinogenesis, invasion and metastasis. *Breast Cancer Res,* 2**,** 252 - 257.

EBOS, J. M. L., LEE, C. R., CRUZ-MUNOZ, W., BJARNASON, G. A., CHRISTENSEN, J. G. & KERBEL, R. S. 2009. Accelerated Metastasis after Short-Term Treatment with a Potent Inhibitor of Tumor Angiogenesis. *Cancer cell,* 15**,** 232-239.

ELSALINI, O. A., GARTZEN, J. V., CRAMER, M. & ROHR, K. B. 2003. Zebrafish hhex, nk2.1a, and pax2.1 regulate thyroid growth and differentiation downstream of Nodal-dependent transcription factors. *Developmental biology,* 263**,** 67-80.

EUHUS, D. M., HUDD, C., LAREGINA, M. C. & JOHNSON, F. E. 1986. Tumor measurement in the nude mouse. *Journal of Surgical Oncology,* 31**,** 229-234.

FAN, S., SMITH, M. L., RIVERT, D. J., DUBA, D., ZHAN, Q., KOHN, K. W., FORNACE, A. J. & O'CONNOR, P. M. 1995. Disruption of p53 Function Sensitizes Breast Cancer MCF-7 Cells to Cisplatin and Pentoxifylline. *Cancer Research,* 55**,** 1649-1654.

FARMER, H., MCCABE, N., LORD, C. J., TUTT, A. N., JOHNSON, D. A., RICHARDSON, T. B., SANTAROSA, M., DILLON, K. J., HICKSON, I. & KNIGHTS, C. 2005. Targeting the DNA repair defect in BRCA mutant cells as a therapeutic strategy. *Nature,* 434**,** 917-921.

FARMER, P., BONNEFOI, H., ANDERLE, P., CAMERON, D., WIRAPATI, P., BECETTE, V., ANDRE, S., PICCART, M., CAMPONE, M., BRAIN, E., MACGROGAN, G., PETIT, T., JASSEM, J., BIBEAU, F., BLOT, E., BOGAERTS, J., AGUET, M., BERGH, J., IGGO, R. & DELORENZI, M. 2009. A stroma-related gene signature predicts resistance to neoadjuvant chemotherapy in breast cancer. *Nat Med,* 15**,** 68-74.

FASSATI, A. 2006. HIV infection of non-dividing cells: a divisive problem. *Retrovirology,* 3**,** 74.

FERRARA, N., GERBER, H.-P. & LECOUTER, J. 2003. The biology of VEGF and its receptors. *Nature medicine,* 9**,** 669-676.

FERRARA, N., HILLAN, K. J., GERBER, H.-P. & NOVOTNY, W. 2004. Discovery and development of bevacizumab, an anti-VEGF antibody for treating cancer. *Nature reviews Drug discovery,* 3**,** 391-400.

FIDLER, I. J. 2003. The pathogenesis of cancer metastasis: the'seed and soil'hypothesis revisited. *Nature Reviews Cancer,* 3**,** 453-458.

FIEDLER, W., GRAEVEN, U., ERGÜN, S., VERAGO, S., KILIC, N., STOCKSCHLÄDER, M. & HOSSFELD, D. K. 1997. Vascular endothelial growth factor, a possible paracrine growth factor in human acute myeloid leukemia. *Blood,* 89**,** 1870-1875.

FILIPPAKOPOULOS, P. & KNAPP, S. 2012. The bromodomain interaction module. *FEBS letters,* 586**,** 2692-2704.

FLAUS, A. & OWEN-HUGHES, T. 2003. Mechanisms for nucleosome mobilization. *Biopolymers,* 68**,** 563-578.

FOLKMAN, J. 1990. What is the evidence that tumors are angiogenesis dependent? *Journal of the National Cancer Institute,* 82**,** 4-7.

FORBES, S. A., BINDAL, N., BAMFORD, S., COLE, C., KOK, C. Y., BEARE, D., JIA, M., SHEPHERD, R., LEUNG, K. & MENZIES, A. 2011. COSMIC: mining complete cancer genomes in the Catalogue of Somatic Mutations in Cancer. *Nucleic Acids Research,* 39**,** D945-D950.

FORSYTHE, J. A., JIANG, B.-H., IYER, N. V., AGANI, F., LEUNG, S. W., KOOS, R. D. & SEMENZA, G. L. 1996. Activation of vascular endothelial growth factor gene transcription by hypoxia-inducible factor 1. *Molecular and Cellular Biology,* 16**,** 4604-4613.

FUDA, N. J., ARDEHALI, M. B. & LIS, J. T. 2009. Defining mechanisms that regulate RNA polymerase II transcription in vivo. *Nature,* 461**,** 186-192.

FUTREAL, P. A., COIN, L., MARSHALL, M., DOWN, T., HUBBARD, T., WOOSTER, R., RAHMAN, N. & STRATTON, M. R. 2004. A census of human cancer genes. *Nat Rev Cancer,* 4**,** 177-183.

GALLIONE, C. J., KLAUS, D. J., YEH, E. Y., STENZEL, T. T., XUE, Y., ANTHONY, K. B., MCALLISTER, K. A., BALDWIN, M. A., BERG, J. N., LUX, A., SMITH, J. D., VARY, C. P. H., CRAIGEN, W. J., WESTERMANN, C. J. J., WARNER, M. L., MILLER, Y. E., JACKSON, C. E., GUTTMACHER, A. E. & MARCHUK, D. A. 1998. Mutation and expression analysis of the endoglin gene in hereditary hemorrhagic telangiectasia reveals null alleles. *Human Mutation,* 11**,** 286-294.

GE, Y.-L., ZHANG, X., ZHANG, J.-Y., HOU, L. & TIAN, R.-H. 2009. The mechanisms on apoptosis by inhibiting VEGF expression in human breast cancer cells. *International Immunopharmacology,* 9**,** 389-395.

GEHRING, W. J., AFFOLTER, M. & BURGLIN, T. 1994. Homeodomain proteins. *Annual review of biochemistry,* 63**,** 487-526.

GEIDUSCHEK, E. P. & TOCCHINI-VALENTINI, G. 1988. Transcription by RNA polymerase III. *Annual review of biochemistry,* 57**,** 873-914.

GHANNAM, G., TAKEDA, A., CAMARATA, T., MOORE, M. A., VIALE, A. & YASEEN, N. R. 2004. The Oncogene Nup98-HOXA9 Induces Gene Transcription in Myeloid Cells. *Journal of Biological Chemistry,* 279**,** 866-875.

GHOSH, S., SULLIVAN, C. A. W., ZERKOWSKI, M. P., MOLINARO, A. M., RIMM, D. L., CAMP, R. L. & CHUNG, G. G. 2008. High levels of vascular endothelial growth factor and its receptors (VEGFR-1, VEGFR-2, neuropilin-1) are associated with worse outcome in breast cancer. *Human Pathology,* 39**,** 1835-1843.

GILLE, H., KOWALSKI, J., LI, B., LECOUTER, J., MOFFAT, B., ZIONCHECK, T. F., PELLETIER, N. & FERRARA, N. 2001. Analysis of Biological Effects and Signaling Properties of Flt-1 (VEGFR-1) and KDR (VEGFR-2): A REASSESSMENT USING NOVEL RECEPTOR-SPECIFIC VASCULAR ENDOTHELIAL GROWTH FACTOR MUTANTS. *Journal of Biological Chemistry,* 276**,** 3222-3230.

GILMORE, T. 2006. Introduction to NF-κB: players, pathways, perspectives. *Oncogene,* 25**,** 6680-6684.

GINESTIER, C., HUR, M. H., CHARAFE-JAUFFRET, E., MONVILLE, F., DUTCHER, J., BROWN, M., JACQUEMIER, J., VIENS, P., KLEER, C. G. & LIU, S. 2007. ALDH1 is a marker of normal and malignant human mammary stem cells and a predictor of poor clinical outcome. *Cell stem cell,* 1**,** 555-567.

GLINKA, Y., MOHAMMED, N., SUBRAMANIAM, V., JOTHY, S. & PRUD'HOMME, G. J. 2012. Neuropilin-1 is expressed by breast cancer stem-like cells and is linked to NF-κB activation and tumor sphere formation. *Biochemical and Biophysical Research Communications,* 425**,** 775-780.

GLOBOCAN.

GLUZMAN-POLTORAK, Z., COHEN, T., HERZOG, Y. & NEUFELD, G. 2000. Neuropilin-2 is a receptor for the vascular endothelial growth factor (VEGF) forms VEGF-145 and VEGF-165 [corrected]. *The Journal of biological chemistry,* 275**,** 18040-18045.

GRIER, D. G., THOMPSON, A., KWASNIEWSKA, A., MCGONIGLE, G. J., HALLIDAY, H. L. & LAPPIN, T. R. 2005. The pathophysiology of HOX genes and their role in cancer. *The Journal of Pathology,* 205**,** 154-171.

GRIVENNIKOV, S. I., GRETEN, F. R. & KARIN, M. 2010. Immunity, Inflammation, and Cancer. *Cell,* 140**,** 883-899.

GUERRERO-ESTEO, M., SÁNCHEZ-ELSNER, T., LETAMENDIA, A. & BERNABÉU, C. 2002. Extracellular and Cytoplasmic Domains of Endoglin Interact with the Transforming Growth Factor-β Receptors I and II. *Journal of Biological Chemistry,* 277**,** 29197-29209.

GUIRAL, M., BESS, K., GOODWIN, G. & JAYARAMAN, P.-S. 2001. PRH Represses Transcription in Hematopoietic Cells by at Least Two Independent Mechanisms. *Journal of Biological Chemistry,* 276**,** 2961-2970.

GUO, Y., CHAN, R., RAMSEY, H., LI, W., XIE, X., SHELLEY, W. C., MARTINEZ-BARBERA, J. P., BORT, B., ZARET, K., YODER, M. & HROMAS, R. 2003. The homeoprotein Hex is required for hemangioblast differentiation. *Blood,* 102**,** 2428-2435.

GUPTA, G. P. & MASSAGUÉ, J. 2006. Cancer Metastasis: Building a Framework. *Cell,* 127**,** 679-695.

HALL, J. M. & MCDONNELL, D. P. 2005. Coregulators in nuclear estrogen receptor action. *Molecular interventions,* 5**,** 343.

HALLAQ, H., PINTER, E., ENCISO, J., MCGRATH, J., ZEISS, C., BRUECKNER, M., MADRI, J., JACOBS, H. C., WILSON, C. M., VASAVADA, H., JIANG, X. & BOGUE, C. W. 2004. A null mutation of Hhex results in abnormal cardiac development, defective vasculogenesis and elevated Vegfa levels. *Development,* 131**,** 5197-5209.

HAN, H.-J., RUSSO, J., KOHWI, Y. & KOHWI-SHIGEMATSU, T. 2008a. SATB1 reprogrammes gene expression to promote breast tumour growth and metastasis. *Nature,* 452**,** 187-193.

HAN, H., RUSSO, J., KOHWI, Y. & KOHWI-SHIGEMATSU, T. 2008b. SATB1 reprogrammes gene expression to promote breast tumour growth and metastasis. *Nature,* 452**,** 187 - 93.

HANAHAN, D. & FOLKMAN, J. 1996. Patterns and Emerging Mechanisms of the Angiogenic Switch during Tumorigenesis. *Cell,* 86**,** 353-364.

HANAHAN, D. & WEINBERG, R. 2000. The Hallmarks of Cancer. *Cell,* 100**,** 57-70.

HANAHAN, D. & WEINBERG, R. A. 2011. Hallmarks of cancer: the next generation. *Cell,* 144**,** 646-674.

HANNON, G. J. 2002. RNA interference. *Nature,* 418**,** 244-251.

HARRIS, S., CRAZE, M., NEWTON, J., FISHER, M., SHIMA, D. T., TOZER, G. M. & KANTHOU, C. 2012. Do Anti-Angiogenic VEGF (VEGFxxxb) Isoforms Exist? A Cautionary Tale. *PLoS ONE,* 7**,** e35231.

HARTWELL, K. A., MUIR, B., REINHARDT, F., CARPENTER, A. E., SGROI, D. C. & WEINBERG, R. A. 2006. The Spemann organizer gene, Goosecoid, promotes tumor metastasis. *Proceedings of the National Academy of Sciences,* 103**,** 18969-18974.

HASSIOTOU, F. & GEDDES, D. 2013. Anatomy of the human mammary gland: current status of knowledge. *Clinical anatomy,* 26**,** 29-48.

HAWINKELS, L. J. A. C., KUIPER, P., WIERCINSKA, E., VERSPAGET, H. W., LIU, Z., PARDALI, E., SIER, C. F. M. & TEN DIJKE, P. 2010. Matrix Metalloproteinase-14 (MT1-MMP)–Mediated Endoglin Shedding Inhibits Tumor Angiogenesis. *Cancer Research,* 70**,** 4141-4150.

HE, T.-C., SPARKS, A. B., RAGO, C., HERMEKING, H., ZAWEL, L., DA COSTA, L. T., MORIN, P. J., VOGELSTEIN, B. & KINZLER, K. W. 1998. Identification of c-MYC as a target of the APC pathway. *Science,* 281**,** 1509-1512.

HENRY, L. A., JOHNSON, D. A., SARRIO, D., LEE, S., QUINLAN, P. R., CROOK, T., THOMPSON, A. M., REIS-FILHO, J. S. & ISACKE, C. M. 2011. Endoglin expression in breast tumor

cells suppresses invasion and metastasis and correlates with improved clinical outcome. *Oncogene,* 30**,** 1046-1058.

HENSON, J. D., NEUMANN, A. A., YEAGER, T. R. & REDDEL, R. R. 2002. Alternative lengthening of telomeres in mammalian cells. *Oncogene,* 21**,** 598-610.

HERICHE, J.-K. & CHAMBAZ, E. M. 1998. Protein kinase CK2alpha is a target for the Abl and Bcr-Abl tyrosine kinases. *Oncogene,* 17**,** 13.

HERZOG, B., PELLET-MANY, C., BRITTON, G., HARTZOULAKIS, B. & ZACHARY, I. C. 2011. VEGF Binding to Neuropilin-1 (NRP1) is Essential for VEGF Stimulation of Endothelial Cell Migration, Complex Formation between NRP1 and VEGFR2 and Signalling via FAK Tyr407 Phosphorylation. *Molecular Biology of the Cell*.

HONDA, R., TANAKA, H. & YASUDA, H. 1997. Oncoprotein MDM2 is a ubiquitin ligase E3 for tumor suppressor p53. *FEBS letters,* 420**,** 25-27.

HORN, H. & VOUSDEN, K. 2007. Coping with stress: multiple ways to activate p53. *Oncogene,* 26**,** 1306-1316.

HOSHINO T, N. T., MUROVIC J, LEVIN EM , LEVIN VA , RUPP SM . 1985. Cell kinetic studies of in situ human brain tumors with bromodeoxyuridine

Cytometery, 6**,** 627-32.

HTUN, H., HOLTH, L. T., WALKER, D., DAVIE, J. R. & HAGER, G. L. 1999. Direct Visualization of the Human Estrogen Receptor α Reveals a Role for Ligand in the Nuclear Distribution of the Receptor. *Molecular Biology of the Cell,* 10**,** 471-486.

HUANG, S. & INGBER, D. E. 1999. The structural and mechanical complexity of cell-growth control. *Nat Cell Biol,* 1**,** E131-E138.

HUI, L., ZHENG, Y., YAN, Y., BARGONETTI, J. & FOSTER, D. A. 2006. Mutant p53 in MDA-MB-231 breast cancer cells is stabilized by elevated phospholipase D activity and contributes to survival signals generated by phospholipase D. *Oncogene,* 25**,** 7305-7310.

HUNTER, M. P., WILSON, C. M., JIANG, X., CONG, R., VASAVADA, H., KAESTNER, K. H. & BOGUE, C. W. 2007. The homeobox gene Hhex is essential for proper hepatoblast differentiation and bile duct morphogenesis. *Developmental biology,* 308**,** 355-367.

IRIE, H. Y., PEARLINE, R. V., GRUENEBERG, D., HSIA, M., RAVICHANDRAN, P., KOTHARI, N., NATESAN, S. & BRUGGE, J. S. 2005. Distinct roles of Akt1 and Akt2 in regulating cell migration and epithelial–mesenchymal transition. *The Journal of Cell Biology,* 171**,** 1023-1034.

JALILI, S. & KARAMI, L. 2012. Study of intermolecular contacts in the proline-rich homeodomain (PRH)–DNA complex using molecular dynamics simulations. *European Biophysics Journal,* 41**,** 329-340.

JANKOVIC, D., GORELLO, P., LIU, T., EHRET, S., LA STARZA, R., DESJOBERT, C., BATY, F., BRUTSCHE, M., JAYARAMAN, P.-S., SANTORO, A., MECUCCI, C. & SCHWALLER, J. 2008. Leukemogenic mechanisms and targets of a NUP98/HHEX fusion in acute myeloid leukemia. *Blood,* 111**,** 5672-5682.

JAYARAMAN, P.-S., FRAMPTON, J. & GOODWIN, G. 2000. The homeodomain protein PRH influences the differentiation of haematopoietic cells. *Leukemia Research,* 24**,** 1023-1031.

JEMAL, A., BRAY, F., CENTER, M. M., FERLAY, J., WARD, E. & FORMAN, D. 2011. Global cancer statistics. *CA: A Cancer Journal for Clinicians,* 61**,** 69-90.

JIA, H., ZHONG, C., DING, X., JIA, W., HUA, X. & ZHANG-QUN, Y. 2012. Promoter-associated small double-stranded RNA interacts with heterogeneous nuclear ribonucleoprotein A2/B1 to induce transcriptional activation. *Biochemical Journal,* 447**,** 407-416.

JONES, K. H. & SENFT, J. A. 1985. An improved method to determine cell viability by simultaneous staining with fluorescein diacetate-propidium iodide. *Journal of Histochemistry & Cytochemistry,* 33**,** 77-9.

KALLURI, R. & WEINBERG, R. A. 2009. The basics of epithelial-mesenchymal transition. *The Journal of Clinical Investigation,* 119**,** 1420-1428.

KAMMORI, M., IZUMIYAMA, N., HASHIMOTO, M., NAKAMURA, K.-I., OKANO, T., KURABAYASHI, R., NAOKI, H., HONMA, N., OGAWA, T. & KAMINISHI, M. 2005. Expression of human telomerase reverse transcriptase gene and protein, and of estrogen and progesterone receptors, in breast tumors: preliminary data from neo-adjuvant chemotherapy. *International Journal of Oncology,* 27**,** 1257.

KANG, Y., JI, N., LEE, C., LEE, H., KIM, J., YEOM, Y., KIM, D., YOON, S., KIM, J., PARK, P. & SONG, E. 2011. ESM-1 silencing decreased cell survival, migration, and invasion and modulated cell cycle progression in hepatocellular carcinoma. *Amino Acids,* 40**,** 1003-1013.

KASAMATSU, S., SATO, A., YAMAMOTO, T., KENG, V. W., YOSHIDA, H., YAMAZAKI, Y., SHIMODA, M., MIYAZAKI, J.-I. & NOGUCHI, T. 2004. Identification of the Transactivating Region of the Homeodomain Protein, Hex. *Journal of Biochemistry,* 135**,** 217-223.

KATYAL, S., OLIVER, J. H., PETERSON, M. S., FERRIS, J. V., CARR, B. S. & BARON, R. L. 2000. Extrahepatic Metastases of Hepatocellular Carcinoma1. *Radiology,* 216**,** 698-703.

KENG, V. W., YAGI, H., IKAWA, M., NAGANO, T., MYINT, Z., YAMADA, K., TANAKA, T., SATO, A., MURAMATSU, I., OKABE, M., SATO, M. & NOGUCHI, T. 2000. Homeobox Gene Hex Is Essential for Onset of Mouse Embryonic Liver Development and Differentiation of the Monocyte Lineage. *Biochemical and Biophysical Research Communications,* 276**,** 1155-1161.

KERSHAW, R. M., GASTON, K. & JAYARAMAN, P.-S. 2013a. Proline Rich Homeodomain (PRH/HHEX) protein in the control of haematopoiesis

and myeloid cell proliferation and its potential as a therapeutic target in myeloid

leukaemias and other cancers.

KERSHAW, R. M., SIDDIQUI, Y. H., ROBERTS, D., JAYARAMAN, P. S. & GASTON, K. 2013b. PRH/HHex inhibits the migration of breast and prostate epithelial cells through direct transcriptional regulation of Endoglin. *Oncogene*.

KIM, N. W., PIATYSZEK, M. A., PROWSE, K. R., HARLEY, C. B., WEST, M. D., HO, P. D. L., COVIELLO, G. M., WRIGHT, W. E., WEINRICH, S. L. & SHAY, J. W. 1994. Specific association of human telomerase activity with immortal cells and cancer. *Science,* 266**,** 2011-2015.

KIM, T.-K., EBRIGHT, R. H. & REINBERG, D. 2000. Mechanism of ATP-dependent promoter melting by transcription factor IIH. *Science,* 288**,** 1418-1421.

KLEMENT, G., HUANG, P., MAYER, B., GREEN, S. K., MAN, S., BOHLEN, P., HICKLIN, D. & KERBEL, R. S. 2002. Differences in Therapeutic Indexes of Combination Metronomic Chemotherapy and an Anti-VEGFR-2 Antibody in Multidrug-resistant Human Breast Cancer Xenografts. *Clinical Cancer Research,* 8**,** 221-232.

KOÇ, A., WHEELER, L. J., MATHEWS, C. K. & MERRILL, G. F. 2004. Hydroxyurea Arrests DNA Replication by a Mechanism That Preserves Basal dNTP Pools. *Journal of Biological Chemistry,* 279**,** 223-230.

KRISHAN, A. 1975. Rapid flow cytofluorometric analysis of mammalian cell cycle by propidium iodide staining. *The Journal of Cell Biology,* 66**,** 188-193.

KRISHAN, A. 1977. Flow Cytometry: Long-Term Storage of Propidium Iodide/Citrate-Stained Material. *Biotechnic & Histochemistry,* 52**,** 339-343.

KUBO, A., CHEN, V., KENNEDY, M., ZAHRADKA, E., DALEY, G. & KELLER, G. 2005. The homeobox gene HEX regulates proliferation and differentiation of hemangioblasts and endothelial cells during ES cell differentiation. *Blood,* 105**,** 4590 - 4597.

KUBO, A., KIM, Y. H., IRION, S., KASUDA, S., TAKEUCHI, M., OHASHI, K., IWANO, M., DOHI, Y., SAITO, Y., SNODGRASS, R. & KELLER, G. 2010. The homeobox gene Hex regulates hepatocyte differentiation from embryonic stem cell–derived endoderm. *Hepatology,* 51**,** 633-641.

KUEHNER, J. N., PEARSON, E. L. & MOORE, C. 2011. Unravelling the means to an end: RNA polymerase II transcription termination. *Nat Rev Mol Cell Biol,* 12**,** 283-294.

KULIS, M. & ESTELLER, M. 2010. 2 - DNA Methylation and Cancer. *In:* ZDENKO, H. & TOSHIKAZU, U. (eds.) *Advances in Genetics.* Academic Press.

LACROIX, M. & LECLERCQ, G. 2004a. Relevance of breast cancer cell lines as models for breast tumours: an update. *Breast Cancer Res Treat,* 83**,** 249-89.

LACROIX, M. & LECLERCQ, G. 2004b. Relevance of Breast Cancer Cell Lines as Models for Breast Tumours: An Update. *Breast Cancer Research and Treatment,* 83**,** 249-289.

LASSALLE, P., MOLET, S., JANIN, A., VAN DER HEYDEN, J., TAVERNIER, J., FIERS, W., DEVOS, R. & TONNEL, A.-B. 1996. ESM-1 Is a Novel Human Endothelial Cell-specific Molecule Expressed in Lung and Regulated by Cytokines. *Journal of Biological Chemistry,* 271**,** 20458-20464.

LEE, S.-H., MIZUTANI, N., MIZUTANI, M., LUO, Y., ZHOU, H., KAPLAN, C., KIM, S.-W., XIANG, R. & REISFELD, R. 2006. Endoglin (CD105) is a target for an oral DNA vaccine against breast cancer. *Cancer Immunology, Immunotherapy,* 55**,** 1565-1574.

LEROY, X., AUBERT, S., ZINI, L., FRANQUET, H., KERVOAZE, G., VILLERS, A., DELEHEDDE, M., COPIN, M. C. & LASSALLE, P. 2010. Vascular endocan (ESM-1) is markedly overexpressed in clear cell renal cell carcinoma. *Histopathology,* 56**,** 180-187.

LESTER, R. D., JO, M., MONTEL, V., TAKIMOTO, S. & GONIAS, S. L. 2007. uPAR induces epithelial–mesenchymal transition in hypoxic breast cancer cells. *The Journal of Cell Biology,* 178**,** 425-436.

LEVINE, M. & TJIAN, R. 2003. Transcription regulation and animal diversity. *Nature,* 424**,** 147-151.

LI, L.-C., OKINO, S. T., ZHAO, H., POOKOT, D., PLACE, R. F., URAKAMI, S., ENOKIDA, H. & DAHIYA, R. 2006. Small dsRNAs induce transcriptional activation in human cells. *Proceedings of the National Academy of Sciences,* 103**,** 17337-17342.

LI, Z., VAN CALCAR, S., QU, C., CAVENEE, W. K., ZHANG, M. Q. & REN, B. 2003. A global transcriptional regulatory role for c-Myc in Burkitt's lymphoma cells. *Proceedings of the National Academy of Sciences,* 100**,** 8164-8169.

LIFTON, R., GOLDBERG, M., KARP, R. & HOGNESS, D. The organization of the histone genes in Drosophila melanogaster: functional and evolutionary implications. Cold Spring Harbor symposia on quantitative biology, 1978. Cold Spring Harbor Laboratory Press, 1047-1051.

LINDERHOLM, B., LINDH, B., TAVELIN, B., GRANKVIST, K. & HENRIKSSON, R. 2000. p53 and vascular-endothelial-growth-factor (VEGF) expression predicts outcome in 833 patients with primary breast carcinoma. *International Journal of Cancer,* 89**,** 51-62.

LIU, N., DU, H., HU, Y., ZHANG, G.-G., WANG, X.-H. & JI, J.-F. 2010. Overexpression of endothelial cell specific molecule-1 (ESM-1) in gastric cancer. *Annals of Surgical Oncology,* 17**,** 2628-2639.

LIU, R., WANG, X., CHEN, G. Y., DALERBA, P., GURNEY, A., HOEY, T., SHERLOCK, G., LEWICKI, J., SHEDDEN, K. & CLARKE, M. F. 2007. The Prognostic Role of a Gene Signature from Tumorigenic Breast-Cancer Cells. *New England Journal of Medicine,* 356**,** 217-226.

MACK, D. L., LEIBOWITZ, D. S., COOPER, S., RAMSEY, H., BROXMEYER, H. E. & HROMAS, R. 2002. Down-regulation of the myeloid homeobox protein Hex is essential for normal T-cell development. *Immunology,* 107**,** 444-451.

MAEDA, S., KAMATA, H., LUO, J.-L., LEFFERT, H. & KARIN, M. 2005. IKKβ couples hepatocyte death to cytokine-driven compensatory proliferation that promotes chemical hepatocarcinogenesis. *Cell,* 121**,** 977-990.

MAMLUK, R., GECHTMAN, Z. E., KUTCHER, M. E., GASIUNAS, N., GALLAGHER, J. & KLAGSBRUN, M. 2002. Neuropilin-1 Binds Vascular Endothelial Growth Factor 165, Placenta Growth Factor-2, and Heparin via Its b1b2 Domain. *Journal of Biological Chemistry,* 277**,** 24818-24825.

MANDRIOTA, S. J., JUSSILA, L., JELTSCH, M., COMPAGNI, A., BAETENS, D., PREVO, R., BANERJI, S., HUARTE, J., MONTESANO, R., JACKSON, D. G., ORCI, L., ALITALO, K., CHRISTOFORI, G. & PEPPER, M. S. 2001. Vascular endothelial growth factor-C-mediated lymphangiogenesis promotes tumour metastasis. *EMBO J,* 20**,** 672-682.

MANFIOLETTI, G., GATTEI, V., BURATTI, E., RUSTIGHI, A., DE IULIIS, A., ALDINUCCI, D., GOODWIN, G. & PINTO, A. 1995. Differential expression of a novel proline-rich homeobox gene (Prh) in human hematolymphopoietic cells. *Blood,* 85**,** 1237-1245.

MANI, S. A., GUO, W., LIAO, M.-J., EATON, E. N., AYYANAN, A., ZHOU, A. Y., BROOKS, M., REINHARD, F., ZHANG, C. C., SHIPITSIN, M., CAMPBELL, L. L., POLYAK, K., BRISKEN, C., YANG, J. & WEINBERG, R. A. 2008. The Epithelial-Mesenchymal Transition Generates Cells with Properties of Stem Cells. *Cell,* 133**,** 704-715.

MARTINEZ BARBERA, J., CLEMENTS, M., THOMAS, P., RODRIGUEZ, T., MELOY, D., KIOUSSIS, D. & BEDDINGTON, R. 2000. The homeobox gene Hex is required in definitive endodermal tissues for normal forebrain, liver and thyroid formation. *Development,* 127**,** 2433 - 2445.

MCLURE, K. G. & LEE, P. W. 1998. How p53 binds DNA as a tetramer. *The EMBO journal,* 17**,** 3342-3350.

MECKLENBURG, L., NAKAMURA, M., SUNDBERG, J. P. & PAUS, R. 2001. The Nude Mouse Skin Phenotype: The Role of< i> Foxn1</i> in Hair Follicle Development and Cycling. *Experimental and molecular pathology,* 71**,** 171-178.

MEHLEN, P. & PUISIEUX, A. 2006. Metastasis: a question of life or death. *Nat Rev Cancer,* 6**,** 449-458.

MERLO, G. R., BASOLO, F., FIORE, L., DUBOC, L. & HYNES, N. E. 1995. p53-dependent and p53-independent activation of apoptosis in mammary epithelial cells reveals a survival function of EGF and insulin. *The Journal of Cell Biology,* 128**,** 1185-96.

MINAMI, T., MURAKAMI, T., HORIUCHI, K., MIURA, M., NOGUCHI, T., MIYAZAKI, J.-I., HAMAKUBO, T., AIRD, W. C. & KODAMA, T. 2004. Interaction between Hex and GATA Transcription Factors in Vascular Endothelial Cells Inhibits flk-1/KDR-mediated

Vascular Endothelial Growth Factor Signaling. *Journal of Biological Chemistry,* 279**,** 20626-20635.

MIRALEM, T., STEINBERG, R., PRICE, D. & AVRAHAM, H. 2001. VEGF (165) requires extracellular matrix components to induce mitogenic effects and migratory response in breast cancer cells. *Oncogene,* 20**,** 5511.

MIRONCHIK, Y., WINNARD, P. T., VESUNA, F., KATO, Y., WILDES, F., PATHAK, A. P., KOMINSKY, S., ARTEMOV, D., BHUJWALLA, Z., VAN DIEST, P., BURGER, H., GLACKIN, C. & RAMAN, V. 2005. Twist Overexpression Induces In vivo Angiogenesis and Correlates with Chromosomal Instability in Breast Cancer. *Cancer Research,* 65**,** 10801-10809.

MITCHELL, P. & TJIAN, R. 1989. Transcriptional regulation in mammalian cells by sequence-specific DNA binding proteins. *Science,* 245**,** 371-378.

MOCKUS, M. & HORWITZ, K. 1983. Progesterone receptors in human breast cancer. Stoichiometric translocation and nuclear receptor processing. *Journal of Biological Chemistry,* 258**,** 4778-4783.

MOORE, R. J., OWENS, D. M., STAMP, G., ARNOTT, C., BURKE, F., EAST, N., HOLDSWORTH, H., TURNER, L., ROLLINS, B. & PASPARAKIS, M. 1999. Mice deficient in tumor necrosis factor-α are resistant to skin carcinogenesis. *Nature medicine,* 5**,** 828-831.

MOSMANN, T. 1983. Rapid colorimetric assay for cellular growth and survival: Application to proliferation and cytotoxicity assays. *Journal of Immunological Methods,* 65**,** 55-63.

NAGLE, R. B., BÖCKER, W., DAVIS, J. R., HEID, H. W., KAUFMANN, M., LUCAS, D. O. & JARASCH, E. D. 1986. Characterization of breast carcinomas by two monoclonal antibodies distinguishing myoepithelial from luminal epithelial cells. *Journal of Histochemistry & Cytochemistry,* 34**,** 869-81.

NAKAGAWA, T., ABE, M., YAMAZAKI, T., MIYASHITA, H., NIWA, H., KOKUBUN, S. & SATO, Y. 2003. HEX Acts as a Negative Regulator of Angiogenesis by Modulating the Expression of Angiogenesis-Related Gene in Endothelial Cells In Vitro. *Arteriosclerosis, Thrombosis, and Vascular Biology,* 23**,** 231-237.

NEILSEN, P. M., NOLL, J. E., MATTISKE, S., BRACKEN, C. P., GREGORY, P. A., SCHULZ, R. B., LIM, S. P., KUMAR, R., SUETANI, R. J., GOODALL, G. J. & CALLEN, D. F. 2013. Mutant p53 drives invasion in breast tumors through up-regulation of miR-155. *Oncogene,* 32**,** 2992-3000.

NING, Q., LIU, C., HOU, L., MENG, M., ZHANG, X., LUO, M., SHAO, S., ZUO, X. & ZHAO, X. 2013. Vascular Endothelial Growth Factor Receptor-1 Activation Promotes Migration and Invasion of Breast Cancer Cells through Epithelial-Mesenchymal Transition. *PLoS ONE,* 8**,** e65217.

NOY, P., GASTON, K. & JAYARAMAN, P.-S. 2012a. Dasatinib inhibits leukaemic cell survival by decreasing PRH/Hhex phosphorylation resulting in increased repression of VEGF signalling genes. *Leukemia Research,* 36**,** 1434-1437.

NOY, P., GASTON, K. & JAYARAMAN, P.-S. 2012b. Dasatinib inhibits leukaemic cell survival by decreasing PRH/Hhex phosphorylation resulting in increased repression of VEGF signalling genes. *Leukemia Research*.

NOY, P., SAWASDICHAI, A., JAYARAMAN, P.-S. & GASTON, K. 2012c. Protein kinase CK2 inactivates PRH/Hhex using multiple mechanisms to de-repress VEGF-signalling genes and promote cell survival. *Nucleic Acids Research,* 40**,** 9008-9020.

NOY, P., WILLIAMS, H., SAWASDICHAI, A., GASTON, K. & JAYARAMAN, P.-S. 2010. PRH/Hhex Controls Cell Survival through Coordinate Transcriptional Regulation of Vascular Endothelial Growth Factor Signaling. *Molecular and Cellular Biology,* 30**,** 2120-2134.

NUNES, F. D., ALMEIDA, F. C. S. D., TUCCI, R. & SOUSA, S. C. O. M. D. 2003. Homeobox genes: a molecular link between development and cancer. *Pesquisa Odontológica Brasileira,* 17**,** 94-98.

OCAÑA, O. H., CÓRCOLES, R., FABRA, Á., MORENO-BUENO, G., ACLOQUE, H., VEGA, S., BARRALLO-GIMENO, A., CANO, A. & NIETO, M. A. 2012. Metastatic colonization requires the repression of the epithelial-mesenchymal transition inducer Prrx1. *Cancer cell*.

OLAUSSEN, K. A., DUNANT, A., FOURET, P., BRAMBILLA, E., ANDRÉ, F., HADDAD, V., TARANCHON, E., FILIPITS, M., PIRKER, R. & POPPER, H. H. 2006. DNA repair by ERCC1 in non–small-cell lung cancer and cisplatin-based adjuvant chemotherapy. *New England Journal of Medicine,* 355**,** 983-991.

OLAYIOYE, M. 2001. Intracellular signaling pathways of ErbB2/HER-2 and family members. *Breast Cancer Res,* 3**,** 385 - 389.

OSBORNE, C. K., YOCHMOWITZ, M. G., KNIGHT, W. A. & MCGUIRE, W. L. 1980. The value of estrogen and progesterone receptors in the treatment of breast cancer. *Cancer,* 46**,** 2884-2888.

OXMANN, D., HELD-FEINDT, J., STARK, A. M., HATTERMANN, K., YONEDA, T. & MENTLEIN, R. 2008. Endoglin expression in metastatic breast cancer cells enhances their invasive phenotype. *Oncogene,* 27**,** 3567-3575.

PADDISON, P. J., CAUDY, A. A., BERNSTEIN, E., HANNON, G. J. & CONKLIN, D. S. 2002. Short hairpin RNAs (shRNAs) induce sequence-specific silencing in mammalian cells. *Genes & Development,* 16**,** 948-958.

PAGET, S. 1889. The distribution of secondary growths in cancer of the breast. *The Lancet,* 133**,** 571-573.

PALMER, D. & NG, P. 2008. Methods for the Production of First Generation Adenoviral Vectors. *Gene Therapy Protocols.* Humana Press.

PARLATO, R., ROSICA, A., RODRIGUEZ-MALLON, A., AFFUSO, A., POSTIGLIONE, M. P., ARRA, C., MANSOURI, A., KIMURA, S., DI LAURO, R. & DE FELICE, M. 2004. An integrated regulatory network controlling survival and migration in thyroid organogenesis. *Developmental biology,* 276**,** 464-475.

PATANI, N., JIANG, W., MANSEL, R., NEWBOLD, R. & MOKBEL, K. 2009. The mRNA expression of SATB1 and SATB2 in human breast cancer. *Cancer Cell International,* 9**,** 18.

PEROU, C. M., SORLIE, T., EISEN, M. B., VAN DE RIJN, M., JEFFREY, S. S., REES, C. A., POLLACK, J. R., ROSS, D. T., JOHNSEN, H., AKSLEN, L. A., FLUGE, O., PERGAMENSCHIKOV, A., WILLIAMS, C., ZHU, S. X., LONNING, P. E., BORRESEN-DALE, A.-L., BROWN, P. O. & BOTSTEIN, D. 2000. Molecular portraits of human breast tumours. *Nature,* 406**,** 747-752.

PFAFFL, M. 2001a. A new mathematical model for relative quantification in real-time RT-PCR. *Nucleic Acids Res,* 29**,** 45.

PFAFFL, M. W. 2001b. A new mathematical model for relative quantification in real-time RT-PCR. *Nucleic Acids Res,* 29.

PHILLIPS, T. M., MCBRIDE, W. H. & PAJONK, F. 2006. The Response of CD24−/low/CD44+ Breast Cancer–Initiating Cells to Radiation. *Journal of the National Cancer Institute,* 98**,** 1777-1785.

PONTI, D., COSTA, A., ZAFFARONI, N., PRATESI, G., PETRANGOLINI, G., CORADINI, D., PILOTTI, S., PIEROTTI, M. A. & DAIDONE, M. G. 2005. Isolation and In vitro Propagation of Tumorigenic Breast Cancer Cells with Stem/Progenitor Cell Properties. *Cancer Research,* 65**,** 5506-5511.

PORTNOY, V., HUANG, V., PLACE, R. F. & LI, L.-C. 2011. Small RNA and transcriptional upregulation. *Wiley Interdisciplinary Reviews: RNA,* 2**,** 748-760.

PUPPIN, C., PUGLISI, F., PELLIZZARI, L., MANFIOLETTI, G., PESTRIN, M., PANDOLFI, M., PIGA, A., DI LORETO, C. & DAMANTE, G. 2006. HEX expression and localization in normal mammary gland and breast carcinoma. *BMC Cancer,* 6**,** 192.

RAKOFF-NAHOUM, S. 2006. Cancer Issue: Why Cancer and Inflammation? *The Yale journal of biology and medicine,* 79**,** 123.

RAMSAY, D., KENT, J., HARTMANN, R. & HARTMANN, P. 2005. Anatomy of the lactating human breast redefined with ultrasound imaging. *Journal of Anatomy,* 206**,** 525-534.

RICARDO, S., VIEIRA, A. F., GERHARD, R., LEITÃO, D., PINTO, R., CAMESELLE-TEIJEIRO, J. F., MILANEZI, F., SCHMITT, F. & PAREDES, J. 2011. Breast cancer stem cell markers CD44, CD24 and ALDH1: expression distribution within intrinsic molecular subtype. *Journal of clinical pathology,* 64**,** 937-946.

RICHARDSON, H. J. G. B. A. W. W. 1957. HISTOLOGICAL GRADING AND PROGNOSIS

IN BREAST CANCER

A STUDY OF 1409 CASES OF WHICH 359 HAVE BEEN FOLLOWED FOR 15 YEARS. *Br J Cancer,* 11**,** 359-377.

RICHMOND, T. & FINCH, J. 1984. The structure of the nucleosome core particle. *Nature (London),* 311**,** 532-537.

RINGEL, R., SOLOGUB, M., MOROZOV, Y. I., LITONIN, D., CRAMER, P. & TEMIAKOV, D. 2011. Structure of human mitochondrial RNA polymerase. *Nature,* 478**,** 269-273.

RINGNÉR, M., FREDLUND, E., HÄKKINEN, J., BORG, Å. & STAAF, J. 2011. GOBO: Gene Expression-Based Outcome for Breast Cancer Online. *PLoS ONE,* 6**,** e17911.

RIX, U., HANTSCHEL, O., DÜRNBERGER, G., RIX, L. L. R., PLANYAVSKY, M., FERNBACH, N. V., KAUPE, I., BENNETT, K. L., VALENT, P. & COLINGE, J. 2007. Chemical proteomic profiles of the BCR-ABL inhibitors imatinib, nilotinib, and dasatinib reveal novel kinase and nonkinase targets. *Blood,* 110**,** 4055-4063.

ROEDER, R. G. 1996. The role of general initiation factors in transcription by RNA polymerase II. *Trends in biochemical sciences,* 21**,** 327-335.

ROGER, L., JULLIEN, L., GIRE, V. & ROUX, P. 2010. Gain of oncogenic function of p53 mutants regulates E-cadherin expression uncoupled from cell invasion in colon cancer cells. *Journal of Cell Science,* 123**,** 1295-1305.

ROMIEU-MOUREZ, R., LANDESMAN-BOLLAG, E., SELDIN, D. C., TRAISH, A. M., MERCURIO, F. & SONENSHEIN, G. E. 2001. Roles of IKK kinases and protein kinase CK2 in activation of nuclear factor-κB in breast cancer. *Cancer Research,* 61**,** 3810-3818.

ROTH, C., PANTEL, K., MULLER, V., RACK, B., KASIMIR-BAUER, S., JANNI, W. & SCHWARZENBACH, H. 2011. Apoptosis-related deregulation of proteolytic activities and high serum levels of circulating nucleosomes and DNA in blood correlate with breast cancer progression. *BMC Cancer,* 11**,** 4.

ROY, V. & PEREZ, E. A. 2009. Beyond Trastuzumab: Small Molecule Tyrosine Kinase Inhibitors in HER-2–Positive Breast Cancer. *The Oncologist,* 14**,** 1061-1069.

SALA-NEWBY, G. B., FREEMAN, N. V., CURTO, M. A. & NEWBY, A. C. 2003. Metabolic and functional consequences of cytosolic 5'-nucleotidase-IA overexpression in neonatal rat cardiomyocytes. *American Journal of Physiology-Heart and Circulatory Physiology,* 285**,** H991-H998.

SANCHEZ, R. & ZHOU, M.-M. 2009. The role of human bromodomains in chromatin biology and gene transcription. *Current opinion in drug discovery & development,* 12**,** 659.

SCHOEFFNER, D. J., MATHENY, S. L., AKAHANE, T., FACTOR, V., BERRY, A., MERLINO, G. & THORGEIRSSON, U. P. 2005. VEGF contributes to mammary tumor growth in transgenic mice through paracrine and autocrine mechanisms. *Lab Invest,* 85**,** 608-623.

SEAL, M. D. & CHIA, S. K. 2010. What Is the Difference Between Triple-Negative and Basal Breast Cancers? *The Cancer Journal,* 16**,** 12-16 10.1097/PPO.0b013e3181cf04be.

SEIBERT, K., SHAFIE, S. M., TRICHE, T. J., WHANG-PENG, J. J., O'BRIEN, S. J., TONEY, J. H., HUFF, K. K. & LIPPMAN, M. E. 1983. Clonal Variation of MCF-7 Breast Cancer Cells in Vitro and in Athymic Nude Mice. *Cancer Research,* 43**,** 2223-2239.

SHAKUR MOHIBI, S. M., HAMID BAND, VIMLA BAND 2011. Mouse models of estrogen receptor-positive breast cancer. *J Carcinog,* 10.

SHE, Q.-B., CHEN, N. & DONG, Z. 2000. ERKs and p38 kinase phosphorylate p53 protein at serine 15 in response to UV radiation. *Journal of Biological Chemistry,* 275**,** 20444-20449.

SHUKLA, A., BURTON, N. M., JAYARAMAN, P.-S. & GASTON, K. 2012. The Proline Rich Homeodomain Protein PRH/Hhex Forms Stable Oligomers That Are Highly Resistant to Denaturation. *PLoS ONE,* 7**,** e35984.

SHWEIKI, D., ITIN, A., SOFFER, D. & KESHET, E. 1992. Vascular endothelial growth factor induced by hypoxia may mediate hypoxia-initiated angiogenesis. *Nature,* 359**,** 843-845.

SKOBE, M., HAWIGHORST, T., JACKSON, D. G., PREVO, R., JANES, L., VELASCO, P., RICCARDI, L., ALITALO, K., CLAFFEY, K. & DETMAR, M. 2001. Induction of tumor lymphangiogenesis by VEGF-C promotes breast cancer metastasis. *Nature medicine,* 7**,** 192-198.

SLADEK, R., ROCHELEAU, G., RUNG, J., DINA, C., SHEN, L., SERRE, D., BOUTIN, P., VINCENT, D., BELISLE, A., HADJADJ, S., BALKAU, B., HEUDE, B., CHARPENTIER, G., HUDSON, T. J., MONTPETIT, A., PSHEZHETSKY, A. V., PRENTKI, M., POSNER, B. I., BALDING, D. J., MEYRE, D., POLYCHRONAKOS, C. & FROGUEL, P. 2007. A genome-wide association study identifies novel risk loci for type 2 diabetes. *Nature,* 445**,** 881-885.

SLAMON, D., GODOLPHIN, W., JONES, L., HOLT, J., WONG, S., KEITH, D., LEVIN, W., STUART, S., UDOVE, J., ULLRICH, A. & ET, A. 1989. Studies of the HER-2/neu proto-oncogene in human breast and ovarian cancer. *Science,* 244**,** 707-712.

SMALLWOOD, A. & REN, B. 2013. Genome organization and long-range regulation of gene expression by enhancers. *Current Opinion in Cell Biology,* 25**,** 387-394.

SOKER, S., MIAO, H. Q., NOMI, M., TAKASHIMA, S. & KLAGSBRUN, M. 2002. VEGF165 mediates formation of complexes containing VEGFR-2 and neuropilin-1 that enhance VEGF165-receptor binding. *Journal of cellular biochemistry,* 85**,** 357-368.

SØRLIE, T., PEROU, C. M., TIBSHIRANI, R., AAS, T., GEISLER, S., JOHNSEN, H., HASTIE, T., EISEN, M. B., VAN DE RIJN, M., JEFFREY, S. S., THORSEN, T., QUIST, H., MATESE, J. C.,

BROWN, P. O., BOTSTEIN, D., LØNNING, P. E. & BØRRESEN-DALE, A.-L. 2001. Gene expression patterns of breast carcinomas distinguish tumor subclasses with clinical implications. *Proceedings of the National Academy of Sciences,* 98**,** 10869-10874.

SOUFI, A. & CORINNE SMITH, A. R. C., KEVIN GASTON AND PADMA-SHEELA JAYARAMAN 2006. Oligomerisation of the Developmental Regulator Proline Rich Homeodomain (PRH/Hex) is Mediated by a Novel Proline-rich Dimerisation Domain. *Journal of Molecular Biology,* 358**,** 943-962.

SOUFI, A. & JAYARAMAN, P.-S. 2008. PRH/Hex: an oligomeric transcription factor and multifunctional regulator of cell fate. *Biochem J,* 412**,** 399-413.

SOUFI, A., NOY, P., BUCKLE, M., SAWASDICHAI, A., GASTON, K. & JAYARAMAN, P.-S. 2009. CK2 phosphorylation of the PRH/Hex homeodomain functions as a reversible switch for DNA binding. *Nucleic Acids Research,* 37**,** 3288-3300.

SOUFI, A., SAWASDICHAI, A., SHUKLA, A., NOY, P., DAFFORN, T., SMITH, C., JAYARAMAN, P.-S. & GASTON, K. 2010. DNA compaction by the higher-order assembly of PRH/Hex homeodomain protein oligomers. *Nucleic Acids Research,* 38**,** 7513-7525.

SOUFI, A., SMITH, C., CLARKE, A. R., GASTON, K. & JAYARAMAN, P.-S. 2006. Oligomerisation of the Developmental Regulator Proline Rich Homeodomain (PRH/Hex) is Mediated by a Novel Proline-rich Dimerisation Domain. *Journal of Molecular Biology,* 358**,** 943-962.

SOULE, H., VAZQUEZ, J., LONG, A., ALBERT, S. & BRENNAN, M. 1973. A human cell line from a pleural effusion derived from a breast carcinoma. *Journal of the National Cancer Institute,* 51**,** 1409-1416.

SOULE, H. D., MALONEY, T. M., WOLMAN, S. R., PETERSON JR, W. D., BRENZ, R., MCGRATH, C. M., RUSSO, J., PAULEY, R. J., JONES, R. F. & BROOKS, S. C. 1990a. Isolation and characterization of a spontaneously immortalized human breast epithelial cell line, MCF-10. *Cancer Research,* 50**,** 6075-6086.

SOULE, H. D., MALONEY, T. M., WOLMAN, S. R., PETERSON, W. D., BRENZ, R., MCGRATH, C. M., RUSSO, J., PAULEY, R. J., JONES, R. F. & BROOKS, S. 1990b. Isolation and characterization of a spontaneously immortalized human breast epithelial cell line, MCF-10. *Cancer Research,* 50**,** 6075-6086.

STARR, D. B. & HAWLEY, D. K. 1991. TFIID binds in the minor groove of the TATA box. *Cell,* 67**,** 1231-1240.

STROBER, W. 2001. Trypan Blue Exclusion Test of Cell Viability. *Current Protocols in Immunology.* John Wiley & Sons, Inc.

SU, J., YOU, P., ZHAO, J.-P., ZHANG, S.-L., SONG, S.-H., FU, Z.-R., YE, L.-W., ZI, X.-Y., XIE, D.-F., ZHU, M.-H. & HU, Y.-P. 2012. A potential role for the homeoprotein Hhex in hepatocellular carcinoma progression. *Medical Oncology,* 29**,** 1059-1067.

SUBIK, K., LEE, J.-F., BAXTER, L., STRZEPEK, T., COSTELLO, D., CROWLEY, P., XING, L., HUNG, M.-C., BONFIGLIO, T. & HICKS, D. G. 2010. The expression patterns of ER, PR, HER2, CK5/6, EGFR, Ki-67 and AR by immunohistochemical analysis in breast cancer cell lines. *Breast cancer: basic and clinical research,* 4**,** 35.

SWINGLER, T. E., BESS, K. L., YAO, J., STIFANI, S. & JAYARAMAN, P.-S. 2004. The Proline-rich Homeodomain Protein Recruits Members of the Groucho/Transducin-like Enhancer of Split Protein Family to Co-repress Transcription in Hematopoietic Cells. *Journal of Biological Chemistry,* 279**,** 34938-34947.

SZERLONG, H. J. & HANSEN, J. C. 2010. Nucleosome distribution and linker DNA: connecting nuclear function to dynamic chromatin structure This paper is one of a selection of

papers published in a Special Issue entitled 31st Annual International Asilomar Chromatin and Chromosomes Conference, and has undergone the Journal's usual peer review process. *Biochemistry and Cell Biology,* 89**,** 24-34.

TAMM, K., RÕÕM, M., SALUMETS, A. & METSIS, M. 2009. Genes targeted by the estrogen and progesterone receptors in the human endometrial cell lines HEC1A and RL95-2. *Reproductive Biology and Endocrinology,* 7**,** 150.

TANAKA, H., YAMAMOTO, T., BAN, T., SATOH, S.-I., TANAKA, T., SHIMODA, M., MIYAZAKI, J.-I. & NOGUCHI, T. 2005. Hex stimulates the hepatocyte nuclear factor 1α-mediated activation of transcription. *Archives of biochemistry and biophysics,* 442**,** 117-124.

TANEI, T., MORIMOTO, K., SHIMAZU, K., KIM, S. J., TANJI, Y., TAGUCHI, T., TAMAKI, Y. & NOGUCHI, S. 2009. Association of Breast Cancer Stem Cells Identified by Aldehyde Dehydrogenase 1 Expression with Resistance to Sequential Paclitaxel and Epirubicin-Based Chemotherapy for Breast Cancers. *Clinical Cancer Research,* 15**,** 4234-4241.

TANG, L., NOGALES, E. & CIFERRI, C. 2010. Structure and function of SWI/SNF chromatin remodeling complexes and mechanistic implications for transcription. *Progress in biophysics and molecular biology,* 102**,** 122-128.

TAUBE, J. H., HERSCHKOWITZ, J. I., KOMUROV, K., ZHOU, A. Y., GUPTA, S., YANG, J., HARTWELL, K., ONDER, T. T., GUPTA, P. B., EVANS, K. W., HOLLIER, B. G., RAM, P. T., LANDER, E. S., ROSEN, J. M., WEINBERG, R. A. & MANI, S. A. 2010. Core epithelial-to-mesenchymal transition interactome gene-expression signature is associated with claudin-low and metaplastic breast cancer subtypes. *Proceedings of the National Academy of Sciences,* 107**,** 15449-15454.

THEVENEAU, E. & MAYOR, R. 2012. Neural crest delamination and migration: from epithelium-to-mesenchyme transition to collective cell migration. *Developmental biology,* 366**,** 34-54.

THIERY, J. P. & SLEEMAN, J. P. 2006. Complex networks orchestrate epithelial-mesenchymal transitions. *Nat Rev Mol Cell Biol,* 7**,** 131-142.

TIBBETTS, R. S., BRUMBAUGH, K. M., WILLIAMS, J. M., SARKARIA, J. N., CLIBY, W. A., SHIEH, S.-Y., TAYA, Y., PRIVES, C. & ABRAHAM, R. T. 1999. A role for ATR in the DNA damage-induced phosphorylation of p53. *Genes & Development,* 13**,** 152-157.

TOPCU, Z., MACK, D. L., HROMAS, R. A. & BORDEN, K. 1999. The promyelocytic leukemia protein PML interacts with the proline-rich homeodomain protein PRH: a RING may link hematopoiesis and growth control. *Oncogene,* 18**,** 7091.

TOPISIROVIC, I., CULJKOVIC, B., COHEN, N., PEREZ, J., SKRABANEK, L. & BORDEN, K. 2003. The proline-rich homeodomain protein, PRH, is a tissue-specific inhibitor of eIF4E-dependent cyclin D1 mRNA transport and growth. *EMBO J,* 22**,** 689 - 703.

TRIEZENBERG, S. J. 1995. Structure and function of transcriptional activation domains. *Current opinion in genetics & development,* 5**,** 190-196.

VALTOLA, R., SALVEN, P., HEIKKILÄ, P., TAIPALE, J., JOENSUU, H., REHN, M., PIHLAJANIEMI, T., WEICH, H., DEWAAL, R. & ALITALO, K. 1999. VEGFR-3 and its ligand VEGF-C are associated with angiogenesis in breast cancer. *The American Journal of Pathology,* 154**,** 1381-1390.

VAN'T VEER, L. J., DAI, H., VAN DE VIJVER, M. J., HE, Y. D., HART, A. A. M., MAO, M., PETERSE, H. L., VAN DER KOOY, K., MARTON, M. J., WITTEVEEN, A. T., SCHREIBER, G. J., KERKHOVEN, R. M., ROBERTS, C., LINSLEY, P. S., BERNARDS, R. & FRIEND, S. H. 2002. Gene expression profiling predicts clinical outcome of breast cancer. *Nature,* 415**,** 530-536.

VELASCO-VELÁZQUEZ, M. A., HOMSI, N., DE LA FUENTE, M. & PESTELL, R. G. 2012. Breast cancer stem cells. *The International Journal of Biochemistry & Cell Biology,* 44**,** 573-577.

VELASCO, S., ALVAREZ-MUÑOZ, P., PERICACHO, M., DIJKE, P. T., BERNABÉU, C., LÓPEZ-NOVOA, J. M. & RODRÍGUEZ-BARBERO, A. 2008. L- and S-endoglin differentially modulate TGFβ1 signaling mediated by ALK1 and ALK5 in L6E9 myoblasts. *Journal of Cell Science,* 121**,** 913-919.

VO, M. N., EVANS, M., LEITZEL, K., ALI, S. M., WILSON, M., DEMERS, L., EVANS, D. B. & LIPTON, A. 2010. Elevated plasma endoglin (CD105) predicts decreased response and survival in a metastatic breast cancer trial of hormone therapy. *Breast Cancer Research and Treatment,* 119**,** 767-771.

WALERYCH, D., NAPOLI, M., COLLAVIN, L. & DEL SAL, G. 2012. The rebel angel: mutant p53 as the driving oncogene in breast cancer. *Carcinogenesis,* 33**,** 2007-2017.

WANG, Z., RAO, D., SENZER, N. & NEMUNAITIS, J. 2011. RNA Interference and Cancer Therapy. *Pharmaceutical Research,* 28**,** 2983-2995.

WEIGAND, M., HANTEL, P., KREIENBERG, R. & WALTENBERGER, J. 2005. Autocrine vascular endothelial growth factor signalling in breast cancer. Evidence from cell lines and primary breast cancer cultures in vitro. *Angiogenesis,* 8**,** 197-204.

WEIGEL, N. L. & MOORE, N. L. 2007. Steroid receptor phosphorylation: a key modulator of multiple receptor functions. *Molecular Endocrinology,* 21**,** 2311-2319.

WEINBERG, R. 1991. Tumor suppressor genes. *Science,* 254**,** 1138-1146.

WILLIAMS, H., JAYARAMAN, P.-S. & GASTON, K. 2008. DNA wrapping and distortion by an oligomeric homeodomain protein. *Journal of Molecular Biology,* 383**,** 10-23.

WOOD, A. J., SMITH, I. E. & DOWSETT, M. 2003. Aromatase inhibitors in breast cancer. *New England Journal of Medicine,* 348**,** 2431-2442.

WOODWARD, W. A., STROM, E. A., TUCKER, S. L., MCNEESE, M. D., PERKINS, G. H., SCHECHTER, N. R., SINGLETARY, S. E., THERIAULT, R. L., HORTOBAGYI, G. N., HUNT, K. K. & BUCHHOLZ, T. A. 2003. Changes in the 2003 American Joint Committee on Cancer Staging for Breast Cancer Dramatically Affect Stage-Specific Survival. *Journal of Clinical Oncology,* 21**,** 3244-3248.

WU, X., CHEN, H., PARKER, B., RUBIN, E., ZHU, T., LEE, J. S., ARGANI, P. & SUKUMAR, S. 2006a. HOXB7, a Homeodomain Protein, Is Overexpressed in Breast Cancer and Confers Epithelial-Mesenchymal Transition. *Cancer Research,* 66**,** 9527-9534.

WU, Y., HOOPER, A. T., ZHONG, Z., WITTE, L., BOHLEN, P., RAFII, S. & HICKLIN, D. J. 2006b. The vascular endothelial growth factor receptor (VEGFR-1) supports growth and survival of human breast carcinoma. *International Journal of Cancer,* 119**,** 1519-1529.

YILMAZ, M. & CHRISTOFORI, G. 2009. EMT, the cytoskeleton, and cancer cell invasion. *Cancer and Metastasis Reviews,* 28**,** 15-33.

YIN, P., ROQUEIRO, D., HUANG, L., OWEN, J. K., XIE, A., NAVARRO, A., MONSIVAIS, D., KIM, J. J., DAI, Y. & BULUN, S. E. 2012. Genome-wide progesterone receptor binding: cell type-specific and shared mechanisms in T47D breast cancer cells and primary leiomyoma cells. *PLoS ONE,* 7**,** e29021.

YU, M., SMOLEN, G. A., ZHANG, J., WITTNER, B., SCHOTT, B. J., BRACHTEL, E., RAMASWAMY, S., MAHESWARAN, S. & HABER, D. A. 2009. A developmentally regulated inducer of EMT, LBX1, contributes to breast cancer progression. *Genes & Development,* 23**,** 1737-1742.

ZHANG, S., CHEN, L., CUI, B., CHUANG, H.-Y., YU, J., WANG-RODRIGUEZ, J., TANG, L., CHEN, G., BASAK, G. W. & KIPPS, T. J. 2012. ROR1 Is Expressed in Human Breast Cancer and Associated with Enhanced Tumor-Cell Growth. *PLoS ONE,* 7**,** e31127.

ZHANG, Y., YAN, W. & CHEN, X. 2011. Mutant p53 Disrupts MCF-10A Cell Polarity in Three-dimensional Culture via Epithelial-to-mesenchymal Transitions. *Journal of Biological Chemistry,* 286**,** 16218-16228.